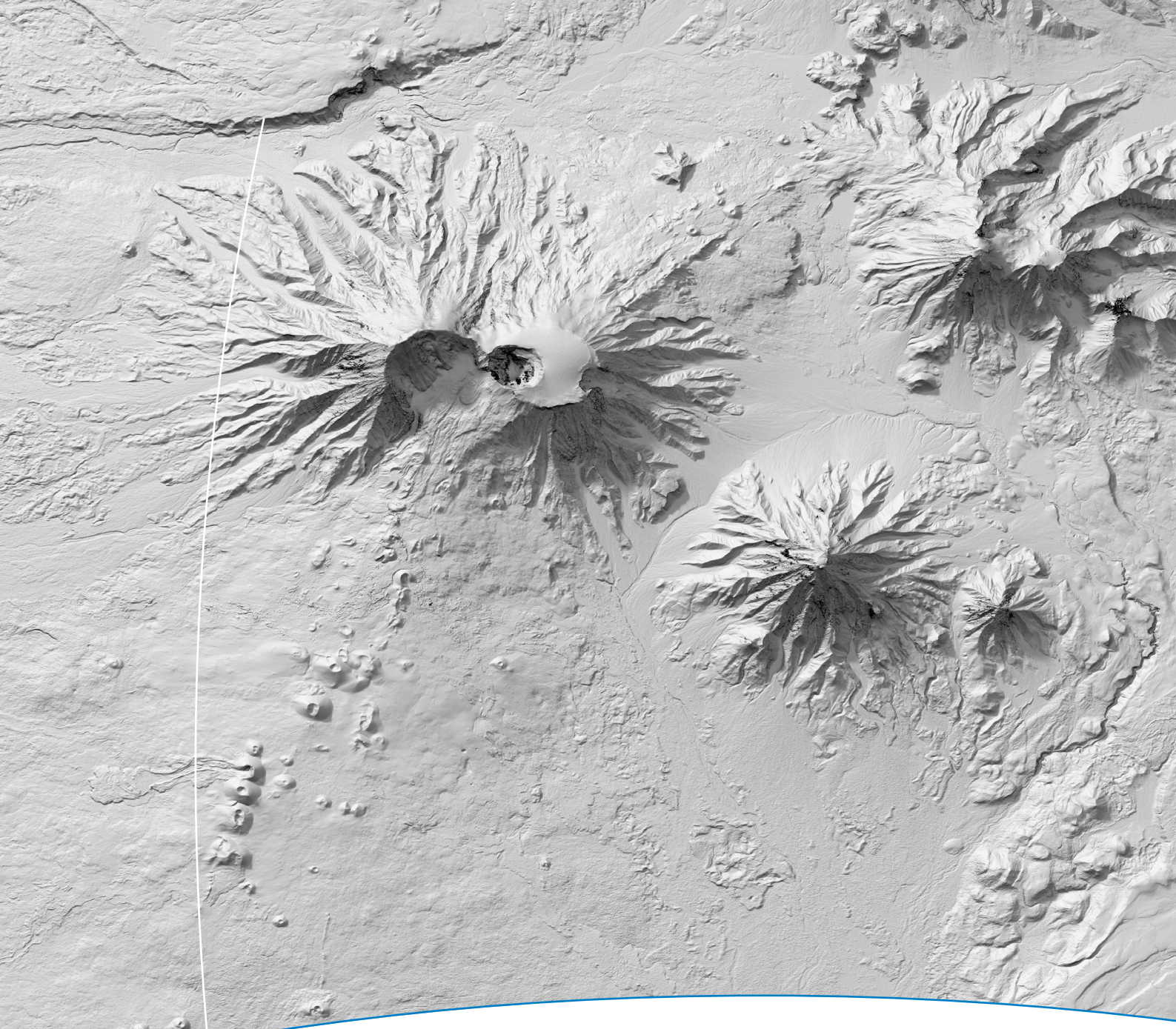

Remote Sensing Technology Institute

Institut für Methodik der Fernerkundung

Status Report 2013 – 2018

DLR

Publisher Deutsches Zentrum
für Luft- und Raumfahrt e.V.
German Aerospace Center

Institut für Methodik der Fernerkundung
Remote Sensing Technology Institute

Address Oberpfaffenhofen
82234 Weßling

Editorial Team Dr. Peter Haschberger

Printed by M & E Druckhaus, Belm

Published Oberpfaffenhofen, July 2018

www.DLR.de/EOC

Cover TanDEM-X elevation model of Kamchatka Peninsula,
Plosky Tolbachik Volcano (3058 m)

Remote Sensing Technology Institute

Institut für Methodik der Fernerkundung

Status Report 2013 – 2018

DLR

Content

Generic Processing Systems

Laboratory Infrastructure and User Services

Methods and Applications

Synthetic Aperture Radar

Optical Imaging

Spectrometric Sounding of the Atmosphere

Data Science in Earth Observation

Documentation

Foreword

The Remote Sensing Technology Institute (IMF) was founded in 2000. Together with the German Remote Sensing Data Center (DFD) it forms DLR's Earth Observation Center (EOC), the largest German institution devoted to Earth remote sensing. This IMF status report has been written in preparation for its third evaluation. It details for the scientific and engineering achievements of the institute in the period from 2013 until mid-2018. Many of the larger mission projects described have been jointly executed by IMF and DFD employing efficient task sharing.

In the five year reporting period remote sensing has undergone an unprecedentedly dynamic development. National Earth observation missions have been and are being implemented together with industry; new mission concepts have been conceived (e.g. Tandem-L); with the Sentinel satellite fleet of the European Copernicus program Earth observation has arrived at the big data era – a real game changer; private 'NewSpace' companies have launched high numbers of rapidly developed satellites and are exploring novel business models; internet giants like Google and Amazon have entered Earth observation with their cloud computing power and artificial intelligence algorithms. This was the wave of chances, challenges and opportunities we have surfed over the past five years.

Our mission is the extraction of geophysical variables, geoinformation and knowledge from remote sensing data for scientific, commercial, societal and political users – but also for our own research projects. To reach this goal we develop scientific algorithms and operational processing system solutions.

IMF's scientists and engineers have contributed to many missions at the forefront of remote sensing technology. They developed and are developing algorithms and processing systems for TerraSAR-X, TanDEM-X, Tandem-L,

EnMAP, DESIS, MERLIN, MetOp/GOME-2, Aeolus, Sentinel-2, Sentinel-5P, Sentinel-4 and Cartosat, to name just the most prominent ones. Their expertise in information retrieval from radar, optical, spectrometric and lidar data as well as their dedication to professional system implementation are widely appreciated. Today our portfolio is characterized by our involvement in almost every national and many European and international missions – an exciting perspective for the next decade.

The results presented in this report have been achieved by enthusiastic IMF scientists and engineers, supported by technical and administrative staff, to all of whom I express my sincere gratitude.

Many have contributed to the preparation of this document. I am particularly indebted to the editor-in-chief, Dr. Peter Haschberger, the core author team, Dr. Manfred Gottwald for graphics artwork, Nils Sparwasser for professional layout advice, Dr. Ramon Brcic for language check and our Controlling department.

Much of what is described in this report was achieved in close cooperation with DFD. I am very grateful to my colleague and DFD director, Prof. Dr. Stefan Dech, for his amicable and efficient cooperation.

Finally, I would like to thank all of our partners, customers and funding organizations for their collaboration and support during the past five years.

Oberpfaffenhofen, July 2018

Prof. Dr.-Ing. habil. Richard Bamler
Director
Remote Sensing Technology Institute

Introduction

Introduction

Earth Observation at DLR

Understanding the Earth system, its processes and changes, requires observation of geophysical and geobiochemical variables. Remote sensing from space is the only technology providing these measurements over large spatial and temporal extents on a regular and reliable basis. The obtained geoinformation responds to a wide variety of scientific, political, societal and economic demands from local to global scales.

DLR masters the entire system chain for satellite and airborne remote sensing: mission concepts, sensor technology, precursor experiments, information retrieval algorithms, satellite command and control, payload data reception with an international station network, data management and operational processing, value-added product development, project-oriented geoscientific research, and dedicated user services. Such a system capability is unique in Europe and is important to meet the challenges of international competition. It allows DLR – in cooperation with industry – to conceptualize, implement, operate and optimize novel Earth observation (EO) missions in a very flexible, cost-effective and quality-conscious way. Milestone missions like TerraSAR-X (the first one-meter-resolution, sub-meter-accuracy SAR system in space) or TanDEM-X (the first formation flying SAR interferometer) would not have been possible without this comprehensive approach. The flexible multi-mission concept likewise allows adaption to European large-scale missions, such as the Sentinels.

With its research portfolio, comprising methodological, geoscientific and application-oriented research, DLR contributes to solutions for the current challenges in meteorology, global change research, Earth system and environmental sciences, sustainable development, safety and security, mobility, resource management, civil engineering and urban planning. Besides its own research activities DLR is a partner to many scientific users of EO information. DLR contributes with its expertise to international science and operational organizations such as the Group on Earth Observation, the World Meteorological Organization and the Charter on Space and Major Disasters, just to name a few. Its EO portfolio makes DLR one of the most important players in the European flagship space program Copernicus, with both its operational and application capabilities.

Six institutes are the major contributors to DLR's EO program topic with the following R&D foci:

Radar and Microwaves Institute
Radar sensors and missions concepts

Institute of Optical Systems
Optical sensors and systems

Remote Sensing Technology Institute
Information retrieval from remote sensing data

German Remote Sensing Data Center
Ground segment engineering and geoscientific research

Institute of Atmospheric Physics
Lidar development, atmospheric research and models

German Space Operation Center
Satellite control and orbit determination

In March 2018 DLR's research program *Space* underwent an extensive evaluation on behalf of the Helmholtz association with the program topic *Earth Observation* receiving the highest possible grade 'outstanding'.

The main EOC building at the Oberpfaffenhofen campus.

DLR's Earth Observation Center

The Remote Sensing Technology Institute (IMF), the German Remote Sensing Data Center (DFD) and a joint controlling unit form DLR's Earth Observation Center (EOC). EOC's mission is to establish remote sensing as an indispensable tool for obtaining geoinformation relevant to global change and environmental research, planning and civil security to meet a wide range of scientific, social, economic, and national needs.

The two institutes IMF and DFD are pools of complementary expertise. Almost any larger mission or research and development project of the EOC is carried out by teams from both institutes. This has allowed a continual build-up of scientific and engineering expertise over many years that can be assembled for challenging projects in a flexible and responsive way. IMF and DFD share their responsibilities as follows:

- IMF focuses on physical and mathematical methods for algorithm and processor development to retrieve information from remote sensing data, starting from raw sensor data.
- DFD's science departments are concerned with geoscientific research as well as service development and provision.
- DFD's engineering and operations departments develop EO-specific information technologies; they develop and operate the payload data ground segment including data receiving stations and processing facilities.

This is, however, not a strict and universal separation of tasks. In adapting to the ever evolving challenges of missions and programs, the research fields of IMF and DFD have been mutually adjusted from time to time. This approach also accommodates the needs of our scientists and engineers whose commitment, enthusiasm, and initiative are the core of EOC's success.

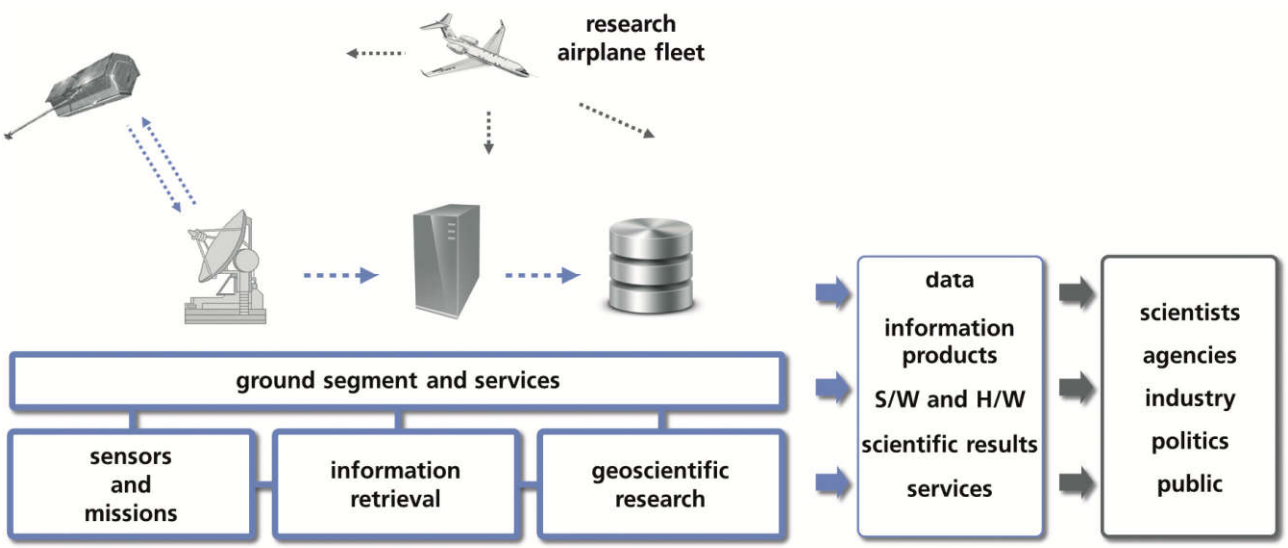

A strategic strength of DLR in EO is its end-to-end system competence which covers all elements of this scientific and engineering chain.

EOC is embedded in a wide range of international activities, for instance: We operate one of ESA's Processing and Archiving Centers as part of Europe's Copernicus program. We are partner in EUMETSAT's Satellite Application Facilities and operate the World Data Center for Remote Sensing of the Atmosphere under the auspices of the International Council of Science. We conduct ground segment functionalities for European and international customers and deploy remote sensing-based project solutions in many countries.

Finally we are responsible for all operational duties in the frame of DLR's membership in the International Charter of Space and Major Disasters.

EOC is led by a team of two directors, each of whom is assigned to lead one institute, for IMF Prof. Dr. Richard Bamler and for DFD Prof. Dr. Stefan Dech. A spokesman function alternates between the two directors in three-year intervals.

Remote Sensing Technology Institute

IMF's overarching mission is the retrieval of relevant geoinformation and knowledge from remote sensing data. Research and development are devoted to the continuous improvement of the quality and the availability of this information. We focus on three remote sensing technological fields:

– synthetic aperture radar (SAR)

– optical imaging

– sounding of the atmosphere by active and passive spectrometers

and the cross-technological topic of

– data science and artificial intelligence.

Starting from basic research on the physical principles of remote sensing and from laboratory measurements, algorithms for forward modeling, inversion and interpretation are developed and implemented as operational software systems or 'processors'. In the framework of joint projects these processors are integrated into the ground segment infrastructure of DFD or industry partners where they are operated, partially with our support. With its remote sensing expertise, the institute assists in the conceptual design of new sensors and missions. In all these algorithm and processor development lines, care is taken that the knowledge is built-up in a system-oriented and sustainable way.

Our activities are geared to current and future national and European EO missions with project periods of typically 5 – 15 years. IMF is often already involved in the first mission feasibility studies, then develops the processing systems, supports the commissioning phase, and finally provides algorithms and maintenance throughout the lifetime of the mission. Prominent examples are TerraSAR-X, TanDEM-X, Tandem-L, MetOp/GOME-2, Sentinel-5P, DESIS and EnMAP. For several of these missions IMF scientists take on the tasks of project managers. IMF complements its mission-oriented research and processor development activities with research on modern EO data analysis methods for gaining higher-level geoinformation. We see ourselves as a bridge between sensor data and users/geoscientists as well as a promoter of remote sensing in general. Therefore, we also address selected geoscientific applications for which we believe our remote sensing methods and expertise have a high impact: Geodesy, oceanography with focus on maritime safety and security, glaciology, urban mapping, traffic monitoring and autonomous driving.

Application projects are often carried out in cooperation with DFD or with external partners such as universities or Helmholtz centers.

Our research and development strategy is based on two complementary but mutually fertilizing tracks:

– The development of operational processing systems for satellite missions requires decades of expertise with a high degree of continuity of staff and evolutionary development of knowledge. The disciplines are physics, mathematics, computer science, engineering, information technology and laboratory skills.

– The invention of novel concepts and retrieval algorithms as well as the work on exploratory topics calls for an academic environment with young scientists and PhD students being given sufficient freedom of research.

IMF as a whole and each of its departments benefit from a mixture of these two cultures.

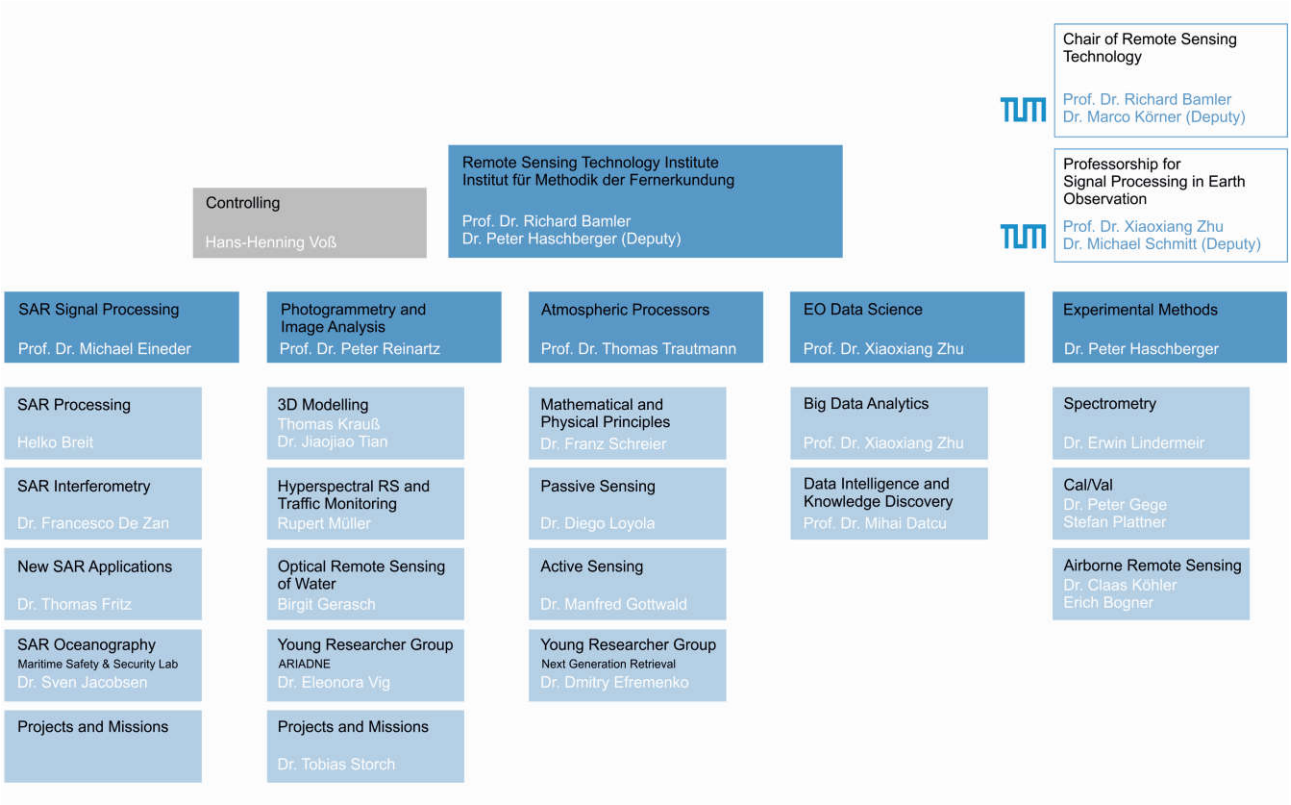

Organization of IMF (including the TUM groups, status: summer 2018). The department *EO Data Science* was established in April 2018 in response to the exciting opportunities offered by AI-based methods for EO.

Besides research and development, IMF provides services to EOC and the science community. We contribute to the DFD-hosted Center for Satellite Based Crisis Information (ZKI), operate EOC's Optical Airborne Remote Sensing and Calibration Facility and support DLR's School Lab in its task to educate and train school students and their teachers in science and engineering.

Currently IMF has 118 staff and 18 scholarship holders. It is organized into five departments of 15 – 30 employees each at the DLR campuses Oberpfaffenhofen (98), Berlin-Adlershof (8), Bremen (10) and Neustrelitz (2). Associated with IMF are two professorships at the Technical University of Munich (TUM), implemented as joint appointments: the Chair of *Remote Sensing Technology* and the Professorship for *Signal Processing in Earth Observation*. The department structure reflects the aforementioned technological fields plus a department that operates laboratories and airborne sensors.

IMF cooperates closely with several universities. Lectures, training, internships and supervision of Bachelor, Master and PhD theses are offered to students. Eleven IMF scientists are professors, honorary, guest or adjunct teaching professors or TUM Junior Fellows, i.e. they have the 'Promotionsrecht' (right to act as a first supervisor for doctoral candidates). 54 of our scientists and scholarship holders currently pursue a PhD under our supervision.

During the reporting period, we have strived for ever higher quality of our scientific work and output. Our cooperation with universities has made a considerable contribution to this continuous improvement process. We are proud of our high publication performance and an impressive series of awards and recognitions (see *Documentation* chapter).

The research and development program of IMF is subject to the program-dependent funding of the Helmholtz Association, as is the case with all DLR institutes. The majority of our activities is part of the Helmholtz program topic *Earth Observation* of the program *Space*. IMF also contributes substantially to the program *Transportation* and to a small extent to *Aeronautics*.

We finance almost half of our staff from third-party projects, the major customers and funding entities being the European Space Agency (ESA), German industry, and the Federal Ministry of Economic Affairs and Energy (BMWi).

Structure of this Report

The next chapter gives descriptions of EO missions and sensors relevant to IMF together with our roles, responsibilities and achievements therein. The *Generic Processing Systems* chapter summarizes our sensor-independent processor developments as central backbone elements of the data evaluation chain. This is followed by a depiction of our laboratory infrastructure and user services. The largest part of the report is dedicated to methods and applications for each of our four technological fields SAR, optical imaging, sounding of the atmosphere and data science. Sections close with a selection of relevant publications authored by IMF scientists. The last chapter *Documentation* concludes the report with a compilation of academic activities, awards and publications to document IMF's scientific productivity.

IMF team 'Optical Remote Sensing of Water' at DLR site Berlin-Adlershof.

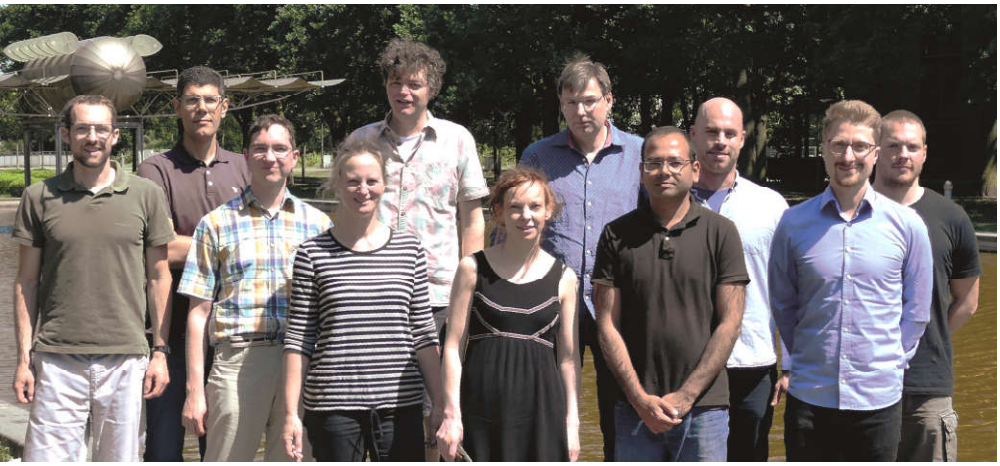

IMF team 'SAR Oceanography' at DLR site Bremen.

IMF staff at Oberpfaffenhofen (right).

web version - reduced graphics quality

Missions and Sensors

Missions and Sensors

IMF's Role in EO Missions

IMF participates in and contributes to a large number of national and international EO missions – in most cases in close cooperation with DFD. Our goal and claim is to be *the* processing system 'factory' for (almost) all national and for particularly challenging European missions, like the Sentinel series which heralds a new era of massive free and open EO data availability.

Our role in EO missions often starts with contributions to the first feasibility and concept studies, followed by the development of algorithms and operational processors and their integration into ground segments. We maintain and update the processing algorithms and support operations usually over the entire mission lifetime. For several missions we also take responsibility for project management for the PDGS (Payload Data Ground Segment) development. With our expertise in sensor signal processing we have continuously expanded our research into thematic data exploitation for selected topics, either in support of the development of new retrieval methods or in cooperative geoscientific research and application projects.

Processing system development for EO missions is the backbone of our strategy with a long-term perspective, partially far into the 2030s. Here we outline our responsibilities and developments for national, European and international missions. When our generic processors SAR-Lab, GENESIS, CATENA, UPAS and GCAPS are mentioned, the reader is referred to the *Generic Processing Systems* chapter.

Our involvement in EO missions employs three remote sensing technologies:

SAR

During the past decades Germany has maintained a strong and continuous R&D program in SAR technology and missions. Aperture synthesis techniques of SAR imaging are ever evolving and require customized and new signal processing algorithms. The coherent-wave nature of SAR allows powerful image exploitation techniques such as interferometry and tomography. IMF is strongly engaged in the conceptual definition of SAR missions, in the development of new processing methods, in operational SAR data processing in ground segments and in the exploration of new geophysical research applications. IMF's SAR activities are driven by a series of space missions initiated by the German SAR program. This program, focusing on high resolution X-band technology, brought along sophisticated new imaging modes and many other challenges and 'firsts' with each new satellite generation. But this is not the end of the story: Once in orbit, data from new SAR sensors drives the development of new processing methods and applications. IMF scientists (at that time still at DFD) have already been involved in SAR data processing since the early days of SEASAT, the first SAR satellite launched by NASA in 1978. They accompanied ESA in all European SAR missions (ERS-1/2, ENVISAT, Sentinel-1) and had leading roles in all civilian German SAR missions (SIR-C/X-SAR, SRTM, TerraSAR-X and TanDEM-X). This long-term dedication led to a high concentration of expertise in SAR processing and data analysis techniques – a solid base for the planned future missions Tandem-L and HRWS.

Optical Imaging

In optical high resolution remote sensing, Germany does not follow a dedicated mission strategy as with SAR. IMF therefore concentrated on internationally available systems like the WorldView series, Pléiades, Sentinel-2 and many more to develop its processing and data analysis capabilities. The developments range over all pre-processing levels up to dedicated high level product generation and are integrated into the generic processing system CATENA. During ESA contracts IMF e.g. developed an operational processor for the ALOS AVNIR and PRISM sensors and is responsible for validation of the Sentinel-2 level 2a products. The stereo processor for generating Digital Surface Models (DSM) from, e.g., WorldView or Cartosat data is developed to a very high automation level and has been licensed to industry for production at regional and national scales. The preparation of processing systems for the hyperspectral missions DESIS and EnMAP has been a major task for IMF in the reporting period. This includes software for calibration and radiometric, spectral, geometric and atmospheric correction. After completion, the processors will be operated at DFD for generating standardized ready-to-use image products.

Spectroscopic Sounding of the Atmosphere

The basis for our involvement in atmospheric sounding missions was laid in the 1990s when Europe placed the passive GOME sensor on the ERS-2 platform. Scientists of IMF (at that time still at DFD) invested considerable effort to provide the ERS-2 PDGS with precise and fast retrieval algorithms and processors for a range of atmospheric trace gas and cloud parameter products. This was coupled with becoming familiar with the instrument calibration characteristics, a prerequisite for accomplishing the goal of processing the raw measurement data to calibrated radiances. Since then, we have increased our expertise and reputation considerably and participated in all European atmospheric sounding missions utilizing various sensors – the past SCIAMACHY, the current GOME-2 and Sentinel-5P as well as the future Sentinel-4, Sentinel-5, Aeolus and MERLIN. With Aeolus and MERLIN, we have even expanded our expertise to active sensors employing lidar.

Formula	Species
BrO	Bromine oxide
$BrONO_2$	Bromine nitrate
CHOCHO	Glyoxal
CH_4	Methane
ClO	Chlorine monoxide
CO	Carbon monoxide
HCHO	Formaldehyde
HCl	Hydrogen chlorine
HDO	Deuterium protium oxide
HOCl	Hypochlorous acid
H_2O	Water (vapour)
$H_2{}^{17}O$	Water isotope
$H_2{}^{18}O$	Water isotope
NO_2	Nitrogen dioxide
OClO	Chlorine dioxide
OH	Hydroxyl radical
O_3	Ozone
SO_2	Sulphur dioxide

Mission/Sensor	Wavelength (nm)	Species
MERLIN	SWIR: 1645	**CH_4**
ERS-2/GOME	UV-VIS-NIR: 237 – 794	**O_3, NO_2**, H_2O, BrO, SO_2, HCHO, OClO, tropospheric O_3, tropospheric NO_2, **clouds**
ENVISAT/SCIAMACHY	UV-VIS-NIR: 215 – 1063 SWIR: 1934 – 2044 2259 – 2386	nadir: **O_3, NO_2, BrO, H_2O, SO_2, HCHO, OClO, CHOCHO, CO, CH_4, clouds, aerosols** limb: **O_3, NO_2, BrO, clouds** limb/nadir: **troposph. NO_2, troposph. BrO**
MetOp/GOME-2	UV-VIS-NIR: 240 – 790	**O_3, NO_2, H_2O, BrO, SO_2, HCHO,** OClO, CHOCHO, **tropospheric NO_2, tropospheric O_3, clouds**
Aeolus/ALADIN	UV: 355	**wind profiles, clouds, aerosols**
Sentinel-5P/TROPOMI	UV-VIS-NIR: 270 – 775 SWIR: 2305 – 2385	**O_3, SO_2, HCHO, tropospheric O_3, NO_2, tropospheric NO_2**, CO, CH_4, **clouds**, **aerosols**
Sentinel-4	UV-VIS-NIR: 305 – 775	**O_3, NO_2, H_2O, SO_2, HCHO, tropospheric NO_2, tropospheric O_3, CHOCHO, clouds,** aerosols
Sentinel-5	UV-VIS-NIR: 270 – 775 SWIR: 1590 – 1675 2305 – 2385	**O_3, NO_2, H_2O, BrO, SO_2, HCHO, OClO, CHOCHO,** CH_4, CO, **tropospheric NO_2, troposph. O_3, O_3 profiles, clouds, aerosols**

The suite of sensors used at IMF for spectrometric sounding of the Earth's atmosphere. The listed target species are those to be retrieved by the particular missions. Items in bold indicate those where IMF contributed to the operational or scientific products either in processor or algorithm development. For future missions proposed parameters are provided.

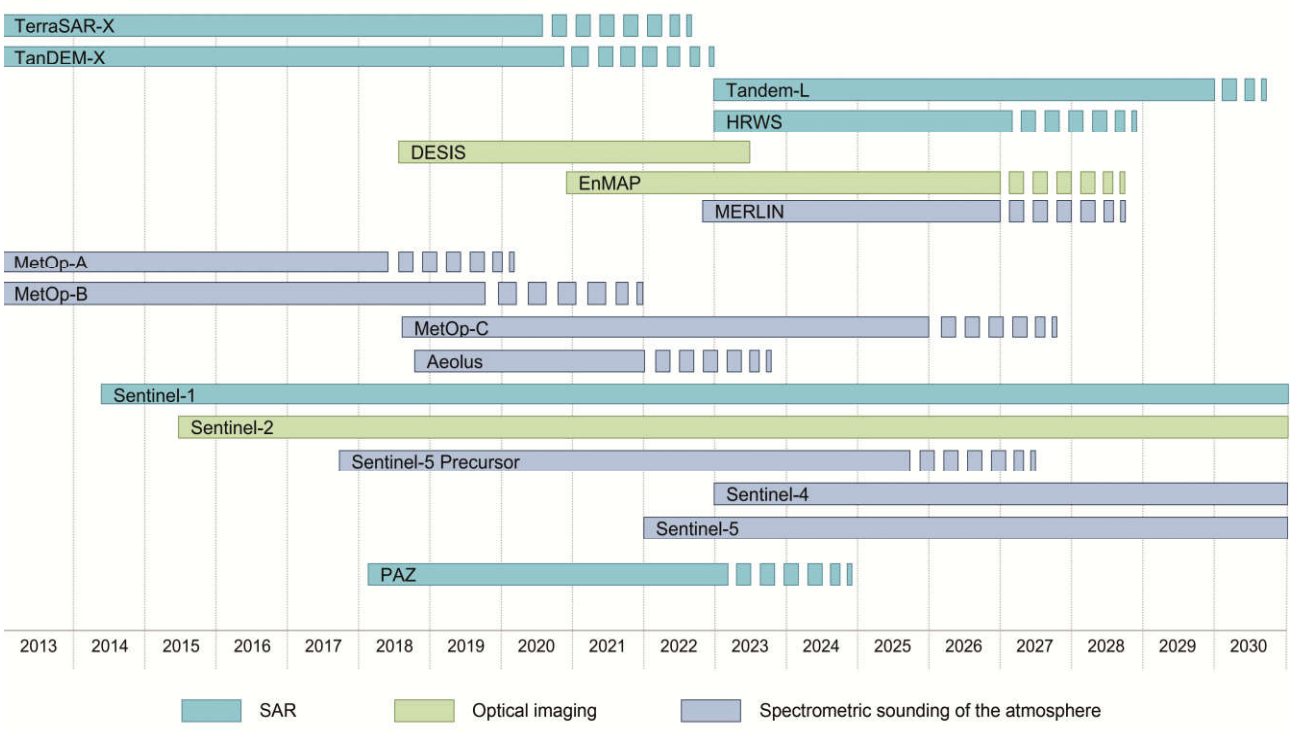

Selection of important EO missions where IMF has developed the operational processors or considerably contributed to algorithm and processor development. For the other missions see text.

National Missions

TerraSAR-X

TerraSAR-X, launched in 2007, provides high resolution SAR data to scientific and commercial users. In contrast to earlier sensors, TerraSAR-X can be freely programmed for a wide variety of operational modes such as stripmap, spotlight, ScanSAR and other experimental and even dual-channel modes. The satellite's main instrument is an advanced high resolution X-band SAR which is based on active phased array technology. This technology allows electronic beam steering and the operation of more than 10,000 possible SAR imaging modes with different resolution, polarization, incidence angle and image size. In particular, the maximum 0.25 × 0.5 m^2 resolution in staring spotlight mode and the unparalleled geolocation accuracy surpass the performance of previously available systems by an order of magnitude.

The mission was implemented in a public private partnership between DLR and the German space industry. Airbus Defence and Space (former EADS Astrium) manufactured the TerraSAR-X spacecraft and deals with commercial product service aspects. Four DLR institutes developed and operate the entire TerraSAR-X ground segment. IMF's responsibilities comprise:

- development of the complete operational SAR processing chain and the final level-1 product palette. This includes our TerraSAR-X Multi Mode SAR processor (TMSP) which is so accurately designed and so well matched to the sensor that the products surpass previous world bests in several disciplines, e.g. radiometric and geometric accuracy
- PDGS management and system engineering of the ground segment.

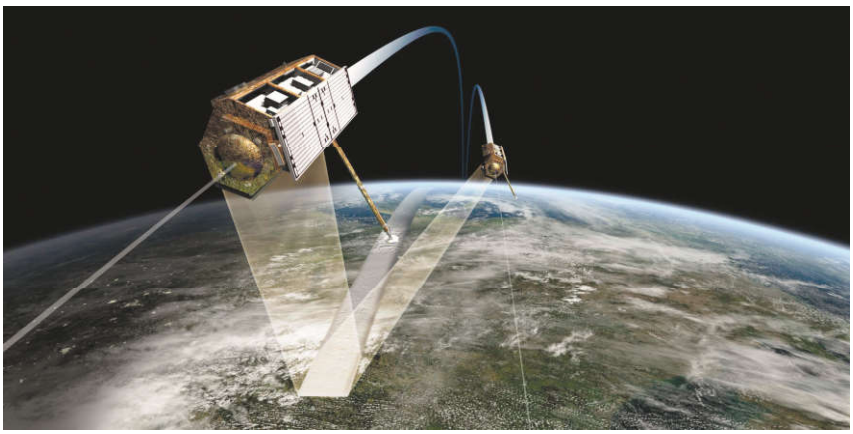

The twin-satellites TerraSAR-X (launched 2007) and TanDEM-X (2010) fly in close formation and build a bistatic interferometer for accurate 3D mapping of the Earth's surface. Due to sophisticated operation and resource management we expect them to be fully operational till about 2020, although their nominal lifetime has long been exceeded.

As a result of the high quality of TMSP, our processor became licensed for operation in the industrial TerraSAR-X Direct Access Stations worldwide.

Even during the operational phase, TMSP is being further developed and improved. For example, competition in the international market of maritime near real-time EO services necessitated faster processing chains. We responded with highly optimized workflows for SAR data, exactly balanced algorithmic tradeoffs, and thorough analysis of hidden bottlenecks. This way the throughput of the core SAR processor could be accelerated by a factor of 1.8.

The geolocation accuracy of our standard TerraSAR-X images is on the order of 0.3 m (the requirement was 1 m). Within the Helmholtz Alliance DLR@Uni we were able to further improve this absolute accuracy to 1 – 2 cm which makes SAR a geodetic measurement tool and opens up many new applications (see *SAR* chapter). We coined the term *Imaging Geodesy* for this research line and developed a new generic SAR product add-on: the SAR Geodesy Product. This product contains all necessary correction

parameters such as atmospheric propagation and Earth dynamics and thus enables users and SAR tool developers to exploit TerraSAR-X centimeter level geometric accuracy in their applications.

The success of the TerraSAR-X mission also led to the international cooperation project PAZ, where Spain procured German radar hardware elements from industry and licensed our SAR processor as a basis for their national SAR mission.

Selected publications: [30], [33]

TanDEM-X

The TanDEM-X mission is a most innovative radar mission operating as a bistatic interferometer. It is formed by TerraSAR-X and a twin satellite launched in 2010, both flying in close formation only some hundred meters apart. One satellite transmits and both synchronously receive the radar echoes. The formation flight and the cooperation of the radar systems posed numerous technical challenges which were all successfully accomplished by newly developed signal processing algorithms and estimation techniques.

The main mission goal, the generation of a global high resolution (12 m) digital elevation model, was achieved in September 2016. We were also involved in achieving many of the secondary mission goals, e.g. ocean current velocity measurements from bistatic and multi-channel experiments.

The TanDEM-X mission is financed and operated in a public private partnership like TerraSAR-X. Concerning data products, Airbus Defence and Space has taken responsibility for commercial DEM distribution while DLR handles scientific data usage. IMF's major responsibilities in this mission are:

– development of the Integrated TanDEM-X Processor (ITP) for the TanDEM-X PDGS to convert sensor bits to DEMs
– development of the customized TanDEM-X science product which is the input for all bistatic experiments (alternating bistatic, multi-polarization, etc.)
– conceptual contributions to the DEM data acquisition plan
– support calibration, validation and operations as well as conceptual evolution of the mission
– sample exploitation of data and demonstration of new geoscientific applications
– PDGS management and system engineering of the complete ground segment.

Our ITP covers the entire InSAR workflow including screening, bistatic phase synchronization, bistatic SAR focusing, interferogram generation, phase unwrapping and geocoding to a raw DEM. It is built upon the heritage of the TMSP and GENESIS processors and is optimized for the new and specific requirements of the bistatic interferometric TanDEM-X mission.

The major algorithmic challenges were:

– consistent raw DEM calibration, i.e. compensation of all internal and external effects on relative phase shifts and differential signal delays in both instruments
– unwrapping of the ambiguous InSAR phase measurements and their conversion to absolute heights based on precise knowledge of the geometric configuration.

By 2016, at least two gapless coverages of the major land surfaces were acquired and processed to raw DEMs by ITP – up to 1,000 DEMs per day. The raw DEMs were then adjusted and mosaicked at DFD to form the final global TanDEM-X DEM – a milestone in remote sensing

with benefits to all geo-related scientific disciplines and to commercial applications. The DEM was delivered to industry and from there to national and international authorities. A free version with reduced resolution (90 m) is currently being distributed by DLR. Further TanDEM-X acquisitions until the end of 2019 will be used to improve the global DEM and to produce a global change DEM, revealing changes on glaciers, forests, volcanoes and industrial areas.

Selected publications: [51], [623], [489], [400]

Tandem-L

Tandem-L is a proposed scientific SAR mission under the auspices of DLR for global and rapid monitoring of dynamic processes in the bio-, geo-, cryo- and hydrosphere. The parameters to be derived – among them seven essential climate variables – include biomass, tectonic and volcanic activities, soil moisture, ice extent and ice dynamics. The mission employs two fully polarimetric L-band SAR systems flying in formation and operating in either bistatic PolInSAR (for forest profiling) or in repeat-pass InSAR (for deformation measurement) modes. An innovative digital beamforming concept provides a mapping capacity two orders of magnitude better than TanDEM-X. Mapping of the entire land mass of the Earth can be achieved twice every eight days.

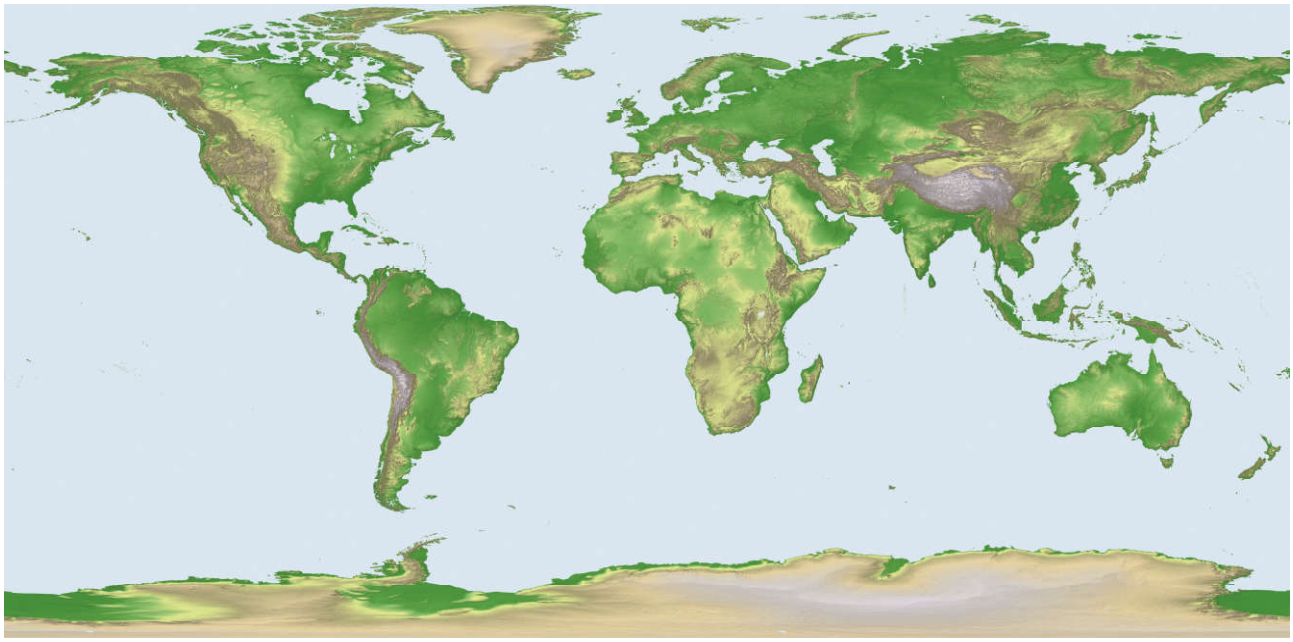

The global TanDEM-X DEM is a consistent data set covering all land surfaces with an unprecedented relative height accuracy of about 2 m and a horizontal sampling of 12 × 12 m². Between 2011 and 2015 at least two global acquisitions were collected with mountainous areas covered up to eight times. Excluding ice and forests, where radar and ICEsat laser measurements differ in penetration depth, the absolute height offset is below 1 m, a result of the outstanding calibration of the bistatic interferometric system.

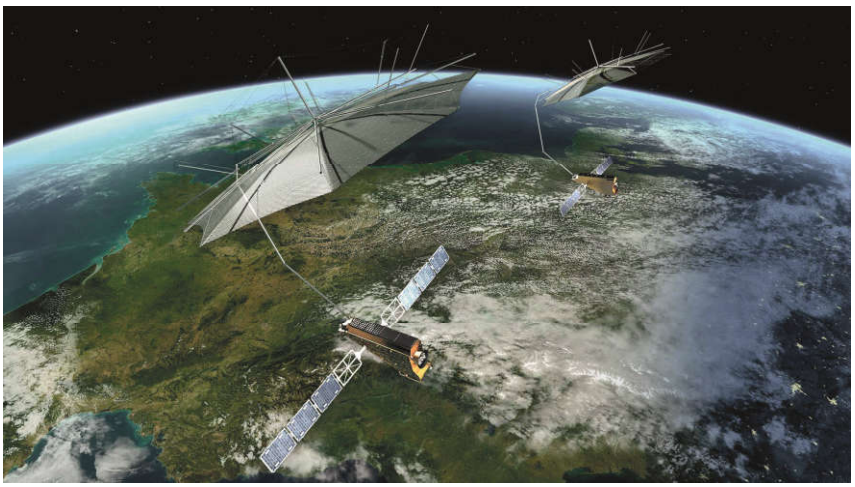

Tandem-L, a proposal for a highly innovative satellite mission for the global observation of dynamic processes on the Earth's surface with hitherto unknown quality and resolution. Thanks to the novel imaging techniques and the vast recording capacity, Tandem-L will provide urgently needed global scientific information about the bio-, geo-, cryo- and hydrosphere.

Pre-phase A studies have been conducted during the last years together with JPL and with JAXA. The essential technological concepts and the performance estimates have been finished in national phase A and B-1 studies. IMF has made significant contributions to the Helmholtz Alliance *Remote Sensing and Earth System Dynamics* in order to support algorithm development and federation of the scientific user community for Tandem-L. In this alliance we co-led the Solid Earth topic (with GFZ and LMU) and contributed to the Cryosphere (with AWI and FAU) and Hydrosphere (with GEOMAR). In this context we also developed novel correction methods for tropospheric and ionospheric signal delays, which are indispensable for meeting the high user requirements in this mission (see *SAR* chapter). Our studies were carried out in close cooperation with DLR's Microwaves and Radar Institute who initiated and led the Alliance.

Once Tandem-L is approved, IMF will be in charge of the development of all products and processors, for the operation support of a payload ground segment, for performing calibration, validation and experiments and for stimulating the scientific use of the data. The major challenges – compared to former SAR missions – are the unprecedented data rate and volume as well as the unparalleled rich and diverse product tree. We will particularly develop new higher level science products specially tailored for geotectonic, volcanologic, cryospheric and oceanographic parameter retrieval. These will be accompanied with products for biomass and forests where the algorithms are to be provided by DLR's Microwave and Radar Institute.

Selected publication: [313]

HRWS

High Resolution Wide Swath (HRWS) is a concept for a high resolution commercial X-band SAR mission based on novel concepts such as digital beamforming and elevation frequency scanning together with optional bistatic receiver satellites. Such a mission could provide both, very high resolution SAR data and regional high accuracy DEMs. IMF is investigating and contributing processing algorithms and ground segment concepts to a study currently led by Airbus Defence and Space. Our goal is to develop the HRWS processing system should the mission be implemented.

DESIS

DLR has partnered with Teledyne Brown Engineering, USA, to add the DLR Earth Sensing Imaging Spectrometer (DESIS) to Teledyne's Multi-User System for Earth Sensing (MUSES) platform on the International Space Station (ISS). The DESIS instrument will be operational in 2018 and will provide spaceborne Visible to Near InfraRed (VNIR) hyperspectral data to support scientific, humanitarian, and commercial objectives.

The DESIS instrument has been built by DLR's Institute of Optical Sensor Systems. It features 235 bands with 2.55 nm spectral resolution, covering a range

from 400 nm to 1,000 nm with 30 m spatial resolution. The pointing unit of DESIS allows a 15° forward and backward along-track view in continuous and BRDF (Bidirectional Reflectance Distribution Function) modes.

IMF's responsibilities comprise:

- project management and system engineering for the payload ground segment
- development of the processor system to generate products up to level 2a (georeferenced reflectance cubes)
- in-flight radiometric and geometric calibration on a regular basis
- scientific coordination (shared with DFD).

IMF has developed the operational processing chain to derive different types of DESIS products from tiled data takes of size 1,024 × 1,024 pixels (≈ 30 × 30 km²). An identical processing chain is licensed by IMF to Teledyne Brown Engineering running in the Amazon Cloud for commercial product generation.

DESIS level 1a products (Earth image scenes, on-board calibration measurements, dark current measurements and experimental products) will be long-term archived together with the corresponding metadata, while level 1b products (systematically and radiometrically corrected data), level 1c products (geometrically corrected data employing global references) and level 2a products (atmospherically compensated data) will be processed on demand before being delivered to the user for further value-added product generation.

DESIS will undergo extensive characterization and calibration measurements before launch and will be re-calibrated after launch by updating the calibration tables. IMF performs regular inflight calibration employing measurements of internal light sources (bank of white and colored LED lamps) and globally distributed reference sites for assessing the radiometric, spectrometric and geometric characteristics of the DESIS hyperspectral instrument in orbit.

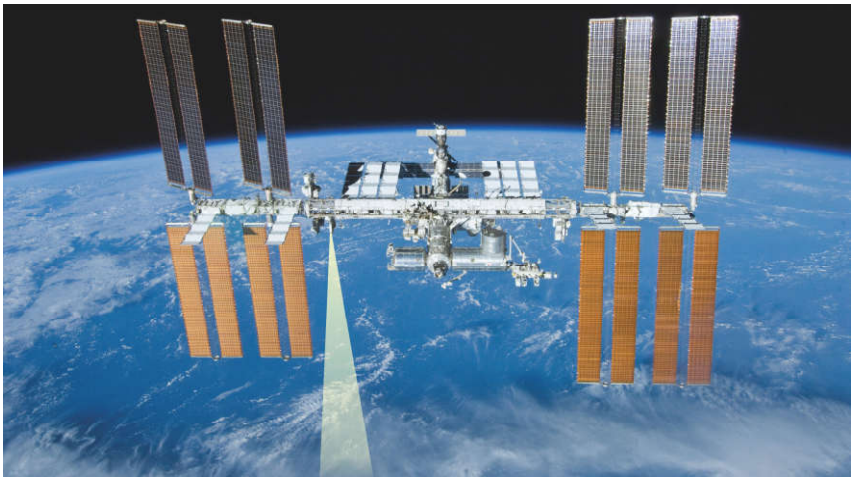

The DESIS hyperspectral camera system on the MUSES platform aboard the ISS monitors the Earth from 2018 on.

DESIS has several special acquisition modes. The off-nadir along-track capability and the forward motion compensation (continuous scanning of the same target on ground for a specific time period) allow geophysical parameters to be derived from BRDF signatures of specific targets and to validate and improve atmospheric compensation methods. We also aim to develop novel super-resolution techniques employing the rolling shutter acquisition mode. Once data are available, we will further expand our competence in the field of data fusion, in particular in connection with future instruments hosted by MUSES, and improve machine learning methods for information retrieval. Furthermore, DESIS can be regarded as a precursor to the German EnMAP mission especially since both ground segments have similar functionalities.

EnMAP

The Environmental Mapping and Analysis Program (EnMAP) establishes the first German high-resolution hyperspectral remote sensing satellite mission. It is a scientific path finder mission based on the long heritage and expertise in airborne imaging spectroscopy in Germany. The launch is scheduled for 2020.

EnMAP is driven by the need to quantify the status and processes of Earth's environments in the context of growing anthropogenic impacts. It will cover the spectral range from 420 – 2,450 nm with a spectral sampling distance varying between 5 nm and 12 nm and a spatial resolution of 30 m. Only airborne sensors such as IMF's HySpex are capable of delivering products of similar spectral performance. With its 30° tilting capability and mapping capacity of 30 × 5,000 km^2 per day in a sun-synchronous repeat orbit, EnMAP allows for frequent and global acquisitions.

The German hyperspectral satellite EnMAP forseen to be launched 2020.

The EnMAP mission is managed by DLR's Space Administration. They assigned IMF responsibility for the complete ground segment in a collaborative effort with DFD and GSOC. IMF's role comprises:

- project management of the ground segment for all mission phases
- development of the on-ground image processing chain and integration into DFD's multi-mission Data and Information Management System
- support for instrument pre-flight characterization based on IMF's Calibration Home Base (CHB)
- spectral, radiometric and geometric instrument in-flight calibration.

Our fully automatic processing chain for EnMAP includes three major components. It consists of:

- systematic and radiometric processor which corrects the raw hyperspectral image data for systematic effects and converts them to physical at-sensor radiance values based on regularly updated calibration tables
- orthorectification processor which generates map-conformal products by removing geometric distortions caused by sensor-internal geometry, thermal-influenced mounting angles, satellite motion and terrain-related influences. An improved sensor model is achieved using ground control points, which are extracted automatically from global reference images from Sentinel-2
- atmospheric correction processor which converts top-of-atmosphere radiance to ground surface reflectances.

In preparation of EnMAP we have significantly invested in building up expertise in hyperspectral data analysis.

MERLIN

The Franco-German collaborative Methane Remote Sensing Lidar Mission (MERLIN) will measure atmospheric CH_4 with unprecedented accuracy to locate anthropogenic sources. It will carry an active SWIR instrument which exploits the differential-absorption lidar technique as a novel sensor approach.

France will provide an extension of their Myriade platform together with its operations while Germany will develop the lidar instrument and all aspects of the payload. MERLIN has successfully passed the preliminary definition (phase B) and is now in its preliminary design and development (phase C). It is planned to launch the satellite in 2023 with mission duration of at least three years.

We contribute considerably to processor development and instrument performance related tasks. Our responsibilities include:

- development of the operational level 0-1b processor which delivers differential absorption optical depths from calibrated measurement data
- development of long-term monitoring (LTM), including dedicated payload command and control facilities
- implementation of a level 2 processor with algorithms developed at DLR's Institute of Atmospheric Physics (IPA).

In the past year we completed the first design for the level 0-1b processor based on our generic GCAPS system and completed the level 1b keypoint review, a major milestone in processor development. We also programmed a mock-up to estimate the computational resources needed. The amount of data for the processing was calculated from a nominal mission orbit. The result was that with three processor instances all timeliness requirements can be met.

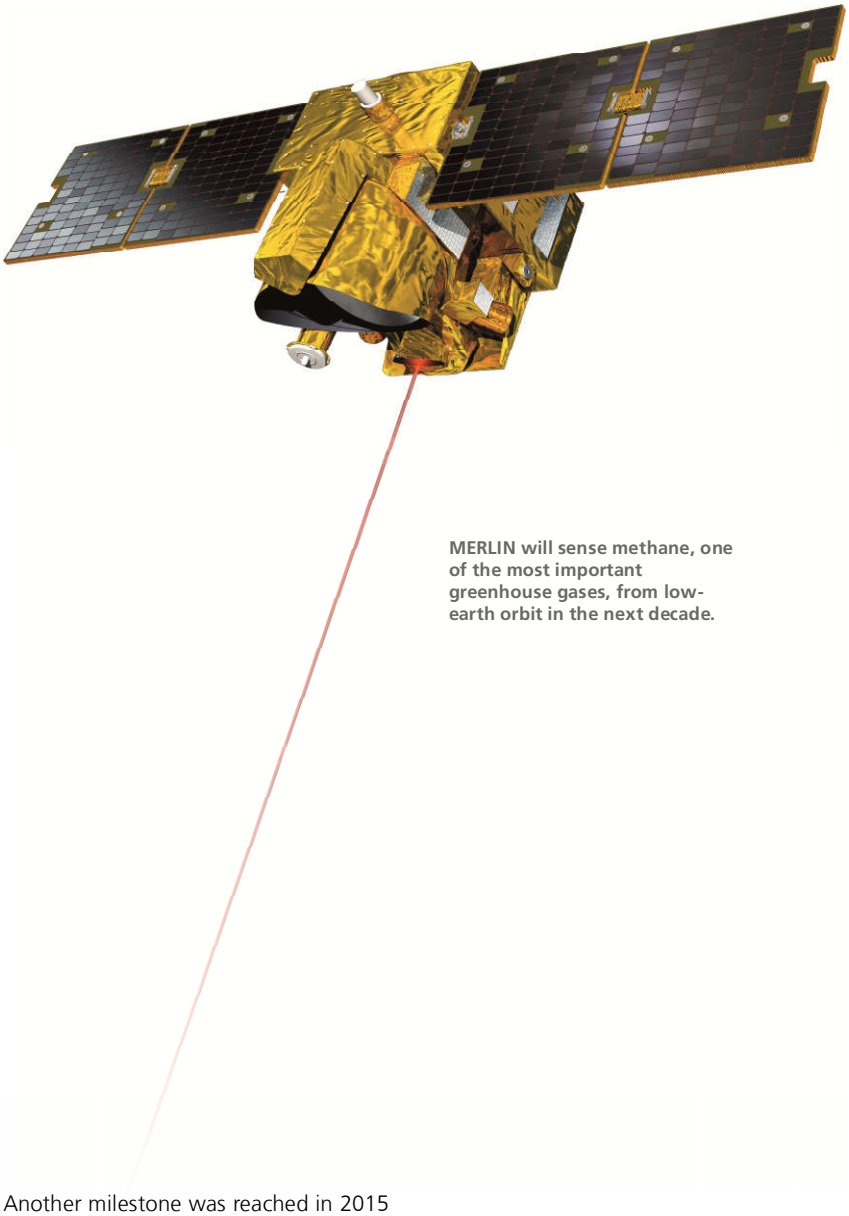

MERLIN will sense methane, one of the most important greenhouse gases, from low-earth orbit in the next decade.

Another milestone was reached in 2015 with the successful completion of the PDR review. There we outlined our strategies for how to perform the LTM task including an example model on how to track the laser pulse properties. Additional effort is being invested into the development of the user interface and actual instrument operation in collaboration with IPA and industry.

ESA, EUMETSAT and Copernicus Missions

ERS-1 and ERS-2

ESA's first EO mission ERS-1 was operational from 1991 – 2000 followed by its successor ERS-2 from 1995 – 2011. The payload of both ERS platforms included a C-band SAR. Originally designed for maritime applications, they acquired a global 20 year time series of medium resolution images that is so unique in its consistency, that it is still used as a reference for glaciology, polar research and interferometric deformation measurements over land. We used this data set to establish and validate the first European land motion consortium Terrafirma under ESA contracts. During the reporting period we generated a first ERS-1/2 ground deformation map of Germany both as a reference and in preparation for a larger national contract based on Sentinel-1 data.

ERS-2 hosted the GOME spectrometer that for the first time conducted atmospheric measurements from a European space-borne platform. During its in-orbit lifetime, IMF, in collaboration with partner institutes, developed the algorithms and processors for generation of operational near-real time, offline and reprocessed GOME level 1 and level 2 products. This work had established our expertise in spaceborne spectroscopic sounding of the atmosphere which allowed us to contribute to and win contracts for past, present and future atmospheric missions.

In GOME's post-mission phase, we have further analyzed the GOME calibration data, improved the level 1 processing algorithms and reprocessed the whole mission level 1 data on behalf of ESA. The older proprietary level 1 format was replaced with a modern design using netCDF4, and was aligned with the data structure of contemporary atmospheric sounding missions.

The data from GOME continues to be used as the reference for generating climate data records. In this context, together with Max Planck Institute for Chemistry, we developed and processed a level 2 product for a climatological water vapor record from the sensors GOME, SCIAMACHY, and GOME-2. A climatological ozone record was also derived from these sensors in the framework of the ESA Climate Change Initiative.

Selected publications: [381], [359], [31], [279], [6]

ENVISAT

ENVISAT, ESA's Earth Observation flagship mission in the first decade of the 21st century, operated successfully between 2002 and 2012. It carried, among other instruments, the spectrometer SCIAMACHY, jointly provided by Germany and the Netherlands. A large share of instrument operations and data processing tasks had been assigned to IMF in the development and in-orbit phase.

After the platform stopped functioning in April 2012, ESA and DLR initiated a phase F where measurement data was prepared for long-term preservation. This ensured full exploitation of SCIAMACHY's unique capabilities by achieving the utmost instrument calibration accuracy and even extracting new products which had not existed in the portfolio of trace gases at the beginning of the mission. We participated in tasks reflecting our more

than 15-year long involvement in the SCIAMACHY mission, particularly algorithm and processor development.

In this phase F (2012 – 2018), two new versions of the level 0-1b and level 2 processors were implemented by IMF. The level 0-1b processor was ported to our generic GCAPS framework. The product palette of the level 2 processor was extended by five new products including CHOCHO, HCHO, CH_4 together with tropospheric NO_2 and tropospheric BrO, both exploiting SCIAMACHY's unique capability of limb/nadir matching. All other retrievals could be considerably improved. In a final step we changed the format of the ENVISAT end user products from the binary, non-standard ENVISAT format to the standard, self-descriptive netCDF4 format, which is considered a prerequisite for using SCIAMACHY data products well into the future.

Selected publications: [43], [99]

MetOp

The series of three MetOp satellites defines EUMETSAT's polar Earth observation system. With MetOp-A (2006) and MetOp-B (2012) two components are presently operational. The launch of MetOp-C is currently envisaged for 2018. One of MetOp's goals is the provision of geophysical atmospheric data products for the Copernicus program well beyond 2020.

The MetOp payload includes the GOME-2 instrument, an advanced version of GOME. Its swath can reach up to 1,920 km and the spatial resolution, when the swath is reduced by a factor of two, reaches 40 × 40 km^2.

The Satellite Application Facility on Atmospheric Composition (AC-SAF, formerly Ozone Monitoring SAF), hosted by the Finnish Meteorological Institute, is responsible for providing operational atmospheric products from MetOp.

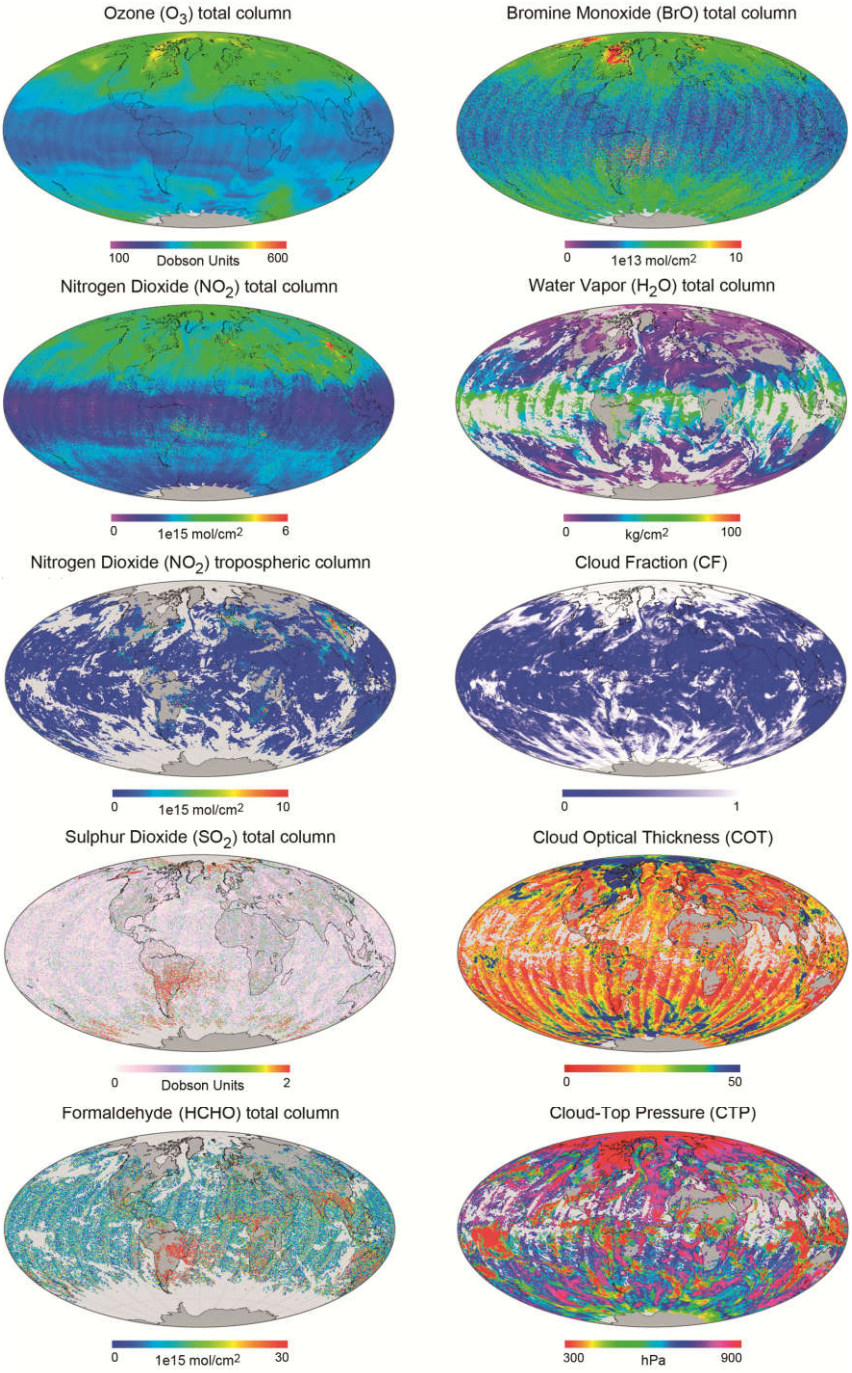

Atmospheric parameters operationally retrieved by IMF's processing system in the framework of the AC-SAF.

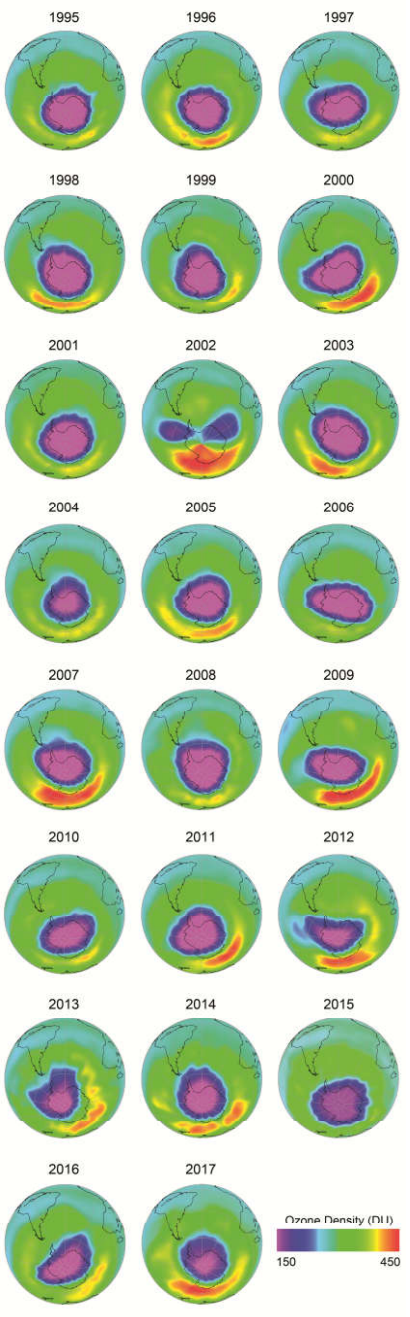

Evolution of the ozone hole over Antarctica derived from European satellite measurements (GOME, SCIAMACHY and GOME-2) between early October 1995 until 2017.

Based on experience gained over almost two decades in algorithm development and systematic operational processing of data from atmospheric sensors we constitute a considerable part of the AC-SAF which is a decentralized facility in cooperation with a European-wide network of meteorological and research organizations.

Our responsibilities include:

- development and continuous improvement of retrieval algorithms and operational processors for GOME-2 total column products
- supporting DFD for the implementation and maintenance of operational data processing and subsequent data dissemination.

In past years we developed new (tropospheric O_3, OClO, CHOCHO) and improved (O_3, NO_2, SO_2, BrO, HCHO, H_2O) trace gas and cloud parameter (fraction, albedo and height) algorithms for the two GOME-2 sensors in orbit. The operational retrieval of these products uses our well-established processor. AC-SAF services provided at EOC occur in near real-time, offline and reprocessing modes. In February 2017, a new continuous development and operations phase (CDOP-3) of the AC-SAF started. It will run until 2022. During this phase we will develop products for the third GOME-2 instrument on MetOp-C and respond to the increasing operational needs of the Copernicus Atmospheric Monitoring Service for tropospheric trace gas products from GOME-2.

Selected publications: [209], [211], [296], [261]

Aeolus

ESA's Earth Explorer mission Aeolus will provide global wind profile estimates with the goal of improving numerical weather forecasting and climate modeling. Its instrument ALADIN is based on a direct detection Doppler lidar operating in continuous mode in the UV. It is a novel design and provides an enormous challenge not only for its development but also for operating the sensor during the in-orbit phase. The instrument measures the backscattered Doppler shifted signal emitted by the laser for retrieving profiles of the line-of-sight wind velocity in the troposphere and parts of the stratosphere. The launch of the mission is planned for 2018.

IMF's responsibilities for Aeolus include development and implementation tasks:

- the Aeolus end-to-end simulator (E2S)
- operational level 0-1b and level 1b-2a processors.

This work involved participation in instrument characterization tests, comparisons with the ALADIN Airborne Demonstrator, and E2S-level 1b processor simulations. All new E2S and processor versions have been successfully tested and delivered to ESA, together with recommendations for further algorithm refinement and quality control measures.

Aeolus data will be visualized and accessed via VirES, the Virtual workspace for Earth Observation scientists, a new web-based service of ESA. We are part of the VirES development team and contribute our extensive technical and scientific Aeolus mission expertise.

All our tasks in support of the Aeolus mission occur in close collaboration with DLR's Institute of Atmospheric Physics.

Sentinel-1, launched in 2014, ensures continuity of C-band SAR data from the ERS-1/2 and ENVISAT missions.

Sentinel-1

Sentinel-1a (2014) and -1b (2016) ensure continuity of C-band SAR data from the ERS-1/2 and ENVISAT missions. The SAR on Sentinel-1, operating in four modes, has higher capabilities than its predecessor instruments on ENVISAT and ERS. Both of the Sentinel-1 satellites provide frequent global coverage. For some areas near a local ground station, products can be delivered within one hour of data acquisition.

DFD was selected to host a PAC for Sentinel-1. The data are also received at DFD data acquisition stations and via the European Data Relay Satellite System, primarily for use in the national maritime security project.

IMF is involved in ESA's SAR instrument and product calibration teams and in future will contribute to improvements of the SAR products. In a national assignment by the Federal Institute for Geosciences and Natural Resources (BGR), IMF is producing a national ground deformation map from interferometric Sentinel-1 data to be distributed to national authorities and later to the public. A first version has been delivered to BGR in 2017 and is currently being evaluated. A future European-wide Ground Motion Service is currently under discussion and IMF is seeking to contribute with its know-how.

Selected publications: [254], [116], [171]

SAOCOM-CS

SAOCOM 1A/B is a planned Argentinian L-band SAR system consisting of two satellites with launch dates in the 2018/2019 timeframe. In 2014 ESA considered augmenting the satellites with a passive companion satellite (CS) shortly after their placement into orbit. This would have allowed generation of DEMs and bi-static imagery. The following year IMF was contracted for a corresponding study into a complete ground system including algorithm design and operational processing concepts. ESA has however abandoned its CS plans after insufficient support from ESA member states.

Sentinel-2

Sentinel-2a (2015) and -2b (2017) routinely deliver high resolution optical information over all of Earth's land-masses. They complement other systems such as the Landsat series. The two satellites provide a systematic global coverage every five days and a shorter revisit time of 2 – 3 days at mid-latitudes.

The main instrument of Sentinel-2a and -2b is the optical payload MSI (Multispectral Imager) for the VNIR and SWIR spectral ranges with 13 bands providing a maximum spatial resolution of 10 m. Particularly important is its radiometric stability, together with the agreement of both MSI-A and MSI-B with MODIS and Landsat's Operational Land Imager within 1 – 2 %. The products from Sentinel-2 are used for land cover mapping, agriculture, forestry, vegetation and ecologic change monitoring and also for monitoring of water bodies.

IMF is involved in the Sentinel-2 Mission Performance Center by leading the level 2a validation. Together with DFD, we process and use Sentinel-2 data as part of the national collaborative

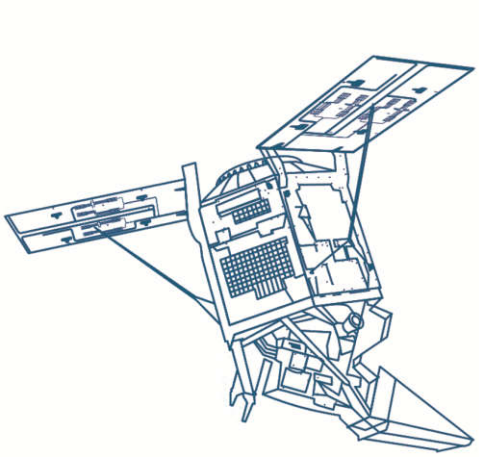

Copernicus ground segment and the CODE-DE project. Within the ESA project MAJA (MACCS-ATCOR Joined Atmospheric Correction) IMF and CNES joined forces to develop a new best-of atmospheric correction processor for Sentinel-2. The prototype has been finished and is operated at IMF and CNES using also time series to improve the results. Data are distributed freely for public use.

Sentinel-5 Precursor

The Sentinel-5 Precursor (Sentinel-5P) spacecraft, launched in 2017, delivers a key set of atmospheric composition, cloud and aerosol data products for air quality and climate applications. Sentinel-5P was developed under the overall responsibility of ESA while the sensing instrument TROPOMI, a UV-VIS-NIR-SWIR imaging spectrometer, is a joint undertaking of the Netherlands and ESA.

TROPOMI combines daily global coverage with a high spatial resolution of 3.5 × 7 km^2 and delivers 23 million measurements every day. Compared to GOME-2 this is a data volume increase by a factor of ≈100, one of the major challenges for processor development. The current Sentinel-5P product portfolio comprises operational level 2 products for O_3, NO_2, SO_2, HCHO, CO and CH_4, as well as cloud and aerosol properties. The work on these products is funded by ESA together with national contributions from the Netherlands, Germany, Belgium and Finland.

In the ground segment domain IMF has been assigned major tasks in the key areas of algorithm and processor development, while DFD hosts the operational functions of processing, archiving and data dissemination. In particular our responsibility includes:

- algorithm development for a subset of level 2 products, namely O_3 (total and tropospheric), SO_2, HCHO and cloud properties fraction, top pressure and optical thickness. They are produced by UPAS2, our generic processor, which has been integrated into the Sentinel-5P PDGS developed and operated by DFD
- co-leadership, together with KNMI, of the Sentinel-5P level 2 working group. This expert group coordinated the scientific work for developing and validating the retrieval algorithms, and the engineering work for developing the operational processors and integrating them into the PDGS during the commissioning phase of Sentinel-5P
- coordination of the level 2 Expert Support Laboratories responsible for monitoring the quality of the level 2 products, further development of the retrieval algorithms and updates of the operational processors. This occurs in the framework of the Sentinel-5P Mission Performance Center (MPC) under the auspices of ESA-ESRIN and coordinated by KNMI. The MPC is the responsible entity for algorithm and processor work during the entire routine in-orbit phase.

The first level 2 products, presented at EOC on December 1, 2017, shortly after the instrument was switched-on, already highlighted the enormous improvement in space-borne spectrometric sounding. The full suite of trace gases under our responsibility could be presented fulfilling all the challenging requirements, including timely delivery, specified spatial resolution and retrieval accuracy. It became immediately obvious that due to the high spatial resolution together with low background fine detail is clearly visible in the level 2 products[1].

[1] available at https://atmos.eoc.dlr.de/tropomi

Sentinel-5P continues our strong heritage for atmospheric missions starting with GOME, SCIAMACHY and GOME-2. The work on Sentinel-5P will, in addition, prepare us for involvement in the Sentinel-4 and Sentinel-5 missions.

Selected publications: [54], [162], [54], [36]

Sentinel-4 and Sentinel-5

Both Sentinel-4 and -5 focus on the state of Earth's atmosphere and its chemical composition. Their payloads will be implemented on operational EUMETSAT missions.

Sentinel-4, onboard the Meteosat Third Generation Sounder (MTG-S) platform, establishes a UV-VIS-NIR spectrometer in geostationary orbit with a field-of-view focused on central Europe. It will be launched in 2023 with the second spacecraft following in 2031. Sentinel-4 is particularly interesting because its position in geostationary orbit provides for hourly measurements of the air quality over Europe with a high spatial resolution of 8 × 8 km^2. This will permit the study of the diurnal variation of important atmospheric constituents in great detail.

IMF leads the Sentinel-4 level 2 project for developing the operational products for a suite of trace gases which currently comprises O_3, SO_2, NO_2, HCHO, CHOCHO, together with properties of clouds, aerosols and surfaces. The Sentinel-4 level 2 consortium consists of renowned experts in the fields of algorithm development, independent verification and processor development for UV-VIS-NIR sensors from several European countries.

Sentinel-5 will operate on the MetOp Second Generation platform in polar orbit.

The payload complement includes, among others, a UV-VIS-NIR-SWIR spectrometer. The first Sentinel-5 launch is targeted for 2022 with a design life of seven years, followed by two identical missions in 2027 and 2032. Sentinel-5 will provide atmospheric composition data with global coverage on a daily basis for air quality and climate monitoring as well as information on stratospheric ozone and solar radiation.

SO_2 plumes from the Mt. Agung (marked by red triangle) volcanic eruption in Indonesia retrieved from GOME-2 (top) and TROPOMI/Sentinel-5P data (bottom). With the new generation of atmospheric sensors employed on the Sentinel platforms an enormous increase in spatial resolution can be achieved.

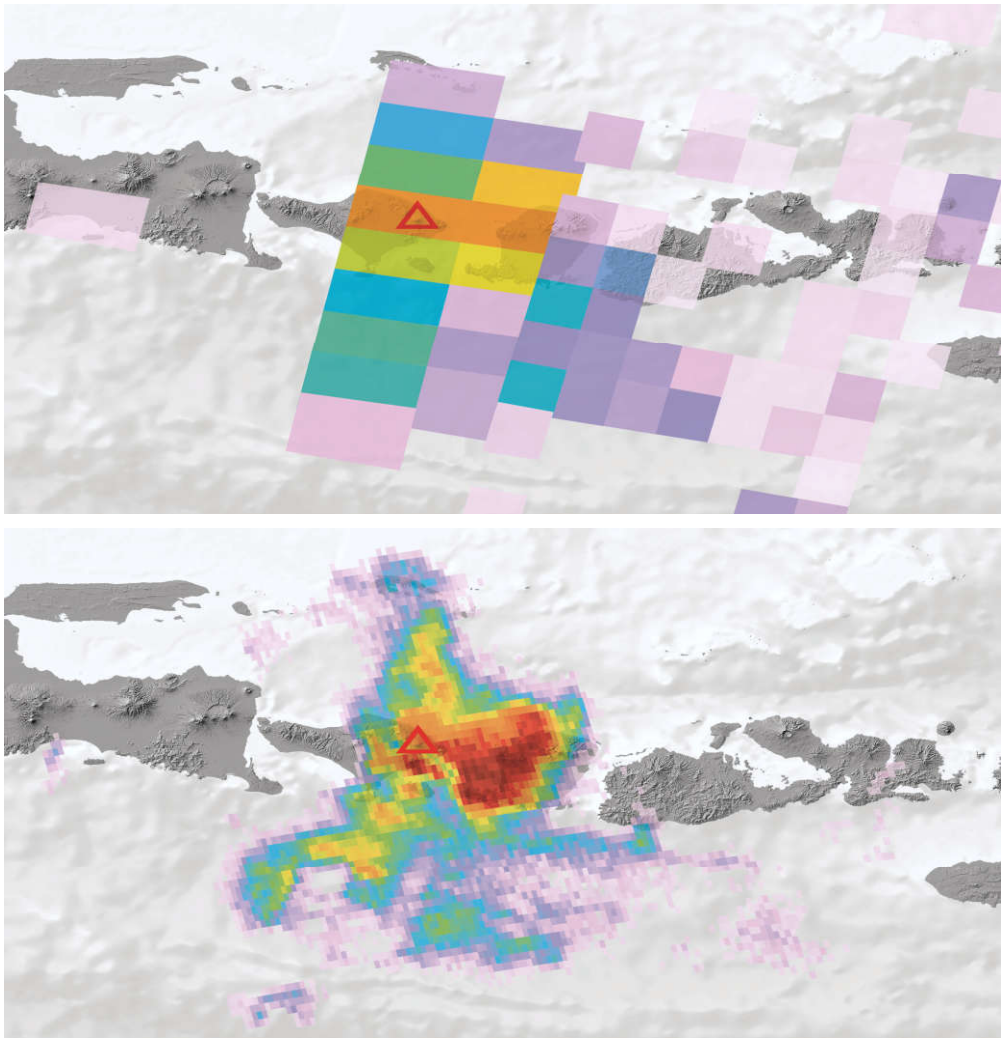

For Sentinel-5, EUMETSAT selected the consortia from IMF and Science & Technology Corporation/NL for the development of the operational processors. The products under DLR responsibility will be O_3 (total, profiles and tropospheric), NO_2 (total and tropospheric), SO_2, HCHO, CHOCHO as well as cloud properties and aerosol index and aerosol optical depth.

The hourly trace gas maps over Europe from Sentinel-4, together with the daily global coverage from Sentinel-5P and Sentinel-5, will initiate a 'golden age' for atmospheric remote sensing for the next decades. Adding data from GOME, SCIAMACHY and GOME-2 will create a unique climate data record of 50 years.

CarbonSat

CarbonSat was a proposed mission in the framework of the ESA Earth Explorer program with the goal of measuring global concentrations of carbon dioxide and methane, the two most important greenhouse gases of partially anthropogenic origin. In 2015 it was abandoned in favor of a competing EO explorer mission. During the early study phase IMF contributed to the definition of the level 0-1 processors, including the algorithms, and key aspects of instrument calibration.

Sentinel-4's field-of-view with geographic coverage area (GCA), reference area (RA) and limiting observation zenith angle (OZA).

Other International Missions

PAZ

The Spanish X-band dual-use SAR satellite PAZ, launched February 22, 2018, is strongly based on the TerraSAR-X design. The satellite is flown in the TerraSAR-X orbit and the products are highly compatible. IMF developed the PAZ operational SAR processor, licensed it to the Spanish ground segment and provides maintenance during the operational phase. After the PAZ commissioning phase both commercial and scientific users should profit from the enhanced image acquisition capacity of both missions.

Radarsat

Radarsat-1, non-operational since early 2013, and Radarsat-2 are SAR spacecraft owned and operated by the Canadian Space Agency and Radarsat International. Since 1995 they deliver C-Band SAR coverage for a wide range of applications such as the monitoring and mapping of ice, marine and land surfaces or resource management in Canada and on a global scale. In 2018 Radarsat-2 will be supplemented by the Radarsat Constellation Mission (RCM) consisting of three satellites.

Radarsat data can also be directly received and used by other nations. In order to contribute to maritime security applications over European waters, EOC receives Radarsat-2 data in Neustrelitz. Preparations for acquiring data from RCM at Neustrelitz are ongoing. In order to exploit the data of the Radarsat missions, IMF's maritime processor suite SAINT (see *Generic Processing Systems* chapter) is being extended.

ALOS and ALOS-2

The Advanced Land Observing Satellites ALOS (2006 – 2011) and ALOS-2 (2014) are owned and operated by the Japanese Space Agency JAXA.

Both ALOS and ALOS-2 carry an advanced L-band SAR. IMF extensively used the data in preparatory studies for Tandem-L and within the Helmholtz Alliance *Remote Sensing and Earth System Dynamics*.

ALOS carried two additional optical instruments, AVNIR and PRISM. As an ESA contractor, IMF has developed operational processors for both optical sensors and implemented them at ESA facilities. The main reason for this contract was the substantially higher geometric accuracy of IMF products than the standard ones. The complex processing chain includes data quality improvements through deconvolution, matching with global reference databases to improve the geolocation accuracy for consistent product families and for orthorectification. More than 500,000 scenes have been reprocessed at ESA premises to date.

Selected publications: [630], [735]

NISAR

NISAR is a joint 3-year SAR mission of NASA and ISRO to be launched in late 2021. It will carry both, an L-Band and an S-Band radar to measure land surface changes of ecosystems, ice sheets and natural hazards including earthquakes, volcanoes and landslides. Many of the NISAR science goals are in good agreement with those of DLR's Tandem-L. Therefore IMF keeps close contact with NASA/JPL to harmonize science requirements and the development of new algorithms. NISAR data may be a valuable source to develop and test Tandem-L algorithms before launch and Tandem-L may provide data continuity to NASA after NISAR.

Ikonos-2 and WorldView-1/2/3/4

The Ikonos-2 spacecraft, launched in 1999, provided civilian access on a commercial basis to optical very high resolution satellite data (1 m panchromatic and 4 m multispectral) for the first time. Even higher resolution became available with the WorldView series of satellites which were launched 2007 – 2016. DLR established a partnership with European Space Imaging EUSI, Munich, for exploiting all platforms. While EUSI covers all commercial aspects, DLR contributes its DFD ground segment facilities and engineering know-how. In exchange, some acquired data may be used for research purposes and in the framework of the Center for Satellite Based Crisis Information. We use this data for developing automatic object detection algorithms (e.g. ships, buildings, bridges). We use our CATENA processor for DSM generation and for developing methods for 3D change detection. A corresponding license has been granted to GAF AG.

Pléiades

The French Pléiades constellation, with Pléiades-1A (2011) and Pléiades-1B (2012), is a pair of optical imagers providing a very high multispectral resolution of 2 m and a panchromatic resolution of 0.5 m. It allows coverage of the Earth's surface with a repeat cycle of 26 days. Through its high agility it offers a daily revisit capability for any terrestrial location. In addition, the Pléiades constellation offers along-track triplet stereo imaging which allows the derivation of high quality DSM using our CATENA system. The same methodology development and license partnership with GAF AG applies as mentioned in the previous paragraph.

IRS-P5 (Cartosat)

In 2005, IRS-P5 of the Indian Space Research Organization ISRO, alternatively termed Cartosat, was lifted into low-Earth orbit. Its payload comprises two panchromatic cameras that were especially designed for in-flight stereo viewing in support of, e.g. cartography and terrain modeling applications. Since the mid 90's, a long-standing collaboration between DLR and ISRO ensures access to data from the IRS program. It permits acquiring raw data from IRS spacecraft at DFD and for harvesting an IRS science data pool by DLR staff. Data reception occurs in support of the remote sensing company GAF AG on the basis of a mutual cooperation agreement. This addresses the exchange of data products and software such as the IMF-developed processor for the generation of DSMs from Cartosat data (5 m GSD). We have licensed our processor to GAF AG. Up to now, large areas such as Europe and the Middle East have been processed by GAF using our software and have been commercially exploited to a large extent.

Ziyuan-3

The Chinese satellites Ziyuan ZY-3/01 and ZY-3/02 were launched in 2012 and 2016 respectively. They carry three panchromatic cameras each, one forward looking, one backward looking (each 4 m GSD) and one nadir looking (2.5 m GSD). In addition, a multispectral camera with four channels (RGB and NIR, 6 m GSD) complements the payload. The high quality data are used by IMF to produce DSMs with 5 m spacing and also serve for filling holes in DSMs derived from Cartosat DSMs. Currently we negotiate with Chinese authorities for receiving data over Germany on a regular basis, free of charge, for scientific use.

DSCOVR

The Deep Space Climate Observatory (DSCOVR) is a NOAA mission in orbit since 2015 at the Lagrangian Point L1 between Earth and the Sun at a distance of 1.5 million km. Its primary objective is to provide early warning in case of strong solar activity and, in addition, collect data for climate and atmospheric studies. Amongst the suite of payload sensors is EPIC, NASA's Enhanced Polychromatic Imaging Camera, UV-Visible imager. At IMF we use its data, covering the UV-Visible wavelength range, to retrieve cloud information over Earth's sunlit hemisphere.

SCISAT-1

Canada's SCISAT-1 has observed the Earth's atmosphere since 2003. Its mission objective is the study of trace gases in limb viewing geometry by using solar occultation. The data, collected over more than 10 years, comprise a unique repository for spectrometric sounding of the terrestrial atmosphere. We use it for investigating certain aspects of spectral analyses of the atmospheres of exoplanets.

Balloon-/Air-/UAV-borne Sensors

TELIS

TELIS, the terahertz and submillimeter limb sounder was a helium-cooled three-channel heterodyne spectrometer for trace gas measurements in the stratosphere, developed and operated by IMF with major support from SRON. The detectors consisted of a far-infrared (FIR) channel (1,790 – 1,870 GHz) and a submillimeter channel (450 – 650 GHz provided by SRON).

TELIS was part of the stratospheric balloon gondola provided by the Institute for Meteorology and Climate Research, KIT, together with the Fourier spectrometer MIPAS-B2. This TELIS/MIPAS-B2 platform was a unique chemistry mission allowing a complete coverage of all species relevant to stratospheric ozone. TELIS focused on short lived species such as OH, ClO, BrO, HCl, O_3, HOCl and HO_2.

View from 'near space' as seen by the terahertz limb sounder TELIS on its 2014 flight from an altitude of 36 km.

The last TELIS campaign, *Probing the Composition above Canada between 5 km and 35 km*, was conducted in Timmins/Canada in 2014. The main target was the bromine budget and partitioning. While MIPAS-B measured $BrONO_2$, TELIS concentrated on BrO. Preliminary results show that BrO during the daytime and $BrONO_2$ during night, between 24 and 28 km, were somewhat larger than predicted by the numerical global atmosphere-chemistry model EMAC.

The raw data from both TELIS channels was processed by us to yield radiometrically calibrated radiances together with the required auxiliary data. Our TELIS characterization efforts greatly profited from IMF's FT spectrometer BRUKER IFS 125HR.

For the retrieval of geophysical parameters, i.e. molecular concentrations, we use the PILS code developed at IMF. It is based on the GARLIC forward model and DRACULA regularization modules and is applicable for microwave to mid-IR limb emission spectra.

Due to budget restrictions we took TELIS out of operation in 2014.

Selected publications: [82], [332], [426], [785]

3K, 4k, Real-Time Camera Systems and Processors

IMF has developed several real-time camera systems and an on-board processing system for airborne monitoring of traffic and disasters since 2007. The main reason for the development was the programmatic goal to use remote sensing data for specific traffic-related mass events and to effectively monitor disaster situations in real-time from flexible airborne platforms. Several DLR-projects like the current VABENE++ project (traffic management in case of mass events and disasters) rely strongly on this system. In this project, maps of the whole dynamic situation of vehicle and pedestrian traffic as well as detailed information about the infrastructure are derived and distributed to end users.

The IMF developed the '3K' and '4k' optical sensor systems (based on COTS Canon cameras) which are fully certified on different airplanes and helicopters. A real-time image data processing chain and data distribution network to end users has been built and demonstrated. Aerial images at resolutions from 5 – 20 cm, acquired with a frequency of 2 – 5 Hz, are immediately georeferenced onboard and orthorectified on GPUs using the GPS-IMU data. For a 1,000 m flight altitude the acquisition of an area of 2.5 × 10 km^2 is possible within 2 minutes. Our recent developments were aimed at miniaturization and certification of these sensor systems on helicopters which are available to security-related authorities. In this

3K camera system for real-time airborne traffic and disaster monitoring.

context, the 4k camera, the camera system originally developed and certified for the Eurocopter BO-105, has been further improved and certified for Airbus H 135 (formerly EC 135) and H 145 helicopters. Helicopters of these types are the backbone of security authorities and organizations worldwide. Equipped with an air-to-ground C-band data link, the sensor system is capable of rapid mapping and real-time road traffic monitoring by distributing the results directly to security forces.

In recent years, we have further improved the real-time processing software and developed new real-time thematic mapping processors, e.g. a new real-time 3D processor computes high resolution DSMs within seconds directly in the aircraft and sends it to the ground station. This is relevant in cases of environmental disasters when immediate evaluation of the actual status of buildings, streets and bridges is required. Such data is also valuable for monitoring traffic in detail in urban scenarios or for generating flood maps. On the ground, orthorectified aerial image mosaics and traffic data are transferred to a DLR traffic internet portal of the Institute of Transportation Systems and the ZKI portal of DFD. After fusion with data from other sources, detailed situation and traffic monitoring can be performed by authorized users. Furthermore, human crowds can be monitored using single pedestrian tracking or crowd density estimation.

Selected publications: [368], [779]

Hyperspectral Airborne Camera HySpex

In 2012, DLR procured a HySpex sensor system from the Norwegian company Norsk Elektro Optikk. The system consists of two airborne imaging spectrometers: a VNIR-1600 for the visible and near infrared and a SWIR-320m-e covering the short wave infrared spectral domain. In combination the system continuously covers the spectral range from 0.4 – 2.5 µm with 416 channels. The spatial resolution depends on flight altitude and is thus configurable between 0.3 and 3 m.

The HySpex system serves us as:

- EnMAP and DESIS simulator for the pre-launch acquisition of test scenes before mission launch
- generator for benchmark datasets supporting our development and validation of novel multi-/hyperspectral data analysis algorithms
- platform for the development and test of advanced calibration methods for the mitigation of typical sensor artifacts such as stray light or non-linearity.

The HySpex system is intended for reference and validation measurements. It has been extensively characterized in our Calibration Home Base (CHB). In combination with the currently developed level 1 processor L0ne (see *Laboratory Infrastructure and User Services* chapter) we expect to deliver at-sensor radiance with unprecedented accuracy and traceable uncertainties.

Selected publication: [307]

Hyperspectral camera system HySpex installed on a DLR aircraft.

Hyperspectral Imager (Cubert UHD 185) operated on a commercial UAV. The system allows for hyperspectral inspection of infrastructure, traffic monitoring or vegetation health assessment.

UAV-borne Systems

Unmanned aerial vehicles (UAVs) provide a cheap and versatile platform for optical remote sensing. Cameras and scanners of various spectral ranges are readily available in sizes that fit on low cost COTS UAV systems.

IMF operates a DJI S900 UAV platform, specified for a total weight of 10 kg, which is able to carry payloads of up to 2 kg for about 20 min per battery charge. It is equipped with a universal mounting system that allows for quick replacement of the sensor payload in the field for flying multi-sensor missions. The platform can be operated manually or autonomously, following a predefined flight path.

The pool of available sensors comprises multiple cameras suitable for a variety of remote sensing applications. Each sensor is mounted on a stabilizing gimbal to compensate for movement of the UAV. Compact RGB cameras are used for traffic monitoring, infrastructure inspection or 3D visualization of buildings. Thermal cameras are used for finding fawns in meadows or the generation of 3D visualizations of the energy loss of buildings. A Cubert UHD 185 VIS/NIR hyperspectral imager is used to discriminate cars by the hyperspectral features of their paint in the domain of traffic monitoring, to detect roof or façade materials as a parameter in the context of energy efficiency studies or to assess plant health from above the canopy. Non-imaging spectrometers with high spectral resolution are flown for reflectance measurements in inland water remote sensing applications or the validation of hyperspectral satellite sensors, e.g. EnMAP.

Generic Processing Systems

Generic Processing Systems

IMF is involved in so many missions that processor development must be streamlined and made time- and cost-efficient. For our three key technology areas, we have therefore established *generic* system development lines in order to safeguard the essential expertise beyond the lifetime of single projects. This approach enables us to maintain generic solutions, advance their functionality, and at the same time increase their level of maturity. Common standards and operational stability can be achieved and enhanced in this way. Step by step, the pool of well tested, configuration-controlled and quality-assured building blocks is enlarged, which gives upcoming projects a favorable starting point. It ensures that extensive investments can not only be used by single missions but inherited by a multitude of sensors.

SAR Data

SAR-Lab/GENESIS

Complementary to the SAR sensors built by industry, IMF develops SAR and InSAR processing systems which reflect the technological evolution of national and international missions. The crucial requirement on these processing systems is to achieve SAR product quality at the theoretical limit. Furthermore, typical multi-year space projects have additional requirements such as high software documentation standards, strict version control, ECSS conformity, multi-level test procedures, high data throughput and scalability.

Our current workhorses, the TerraSAR-X Multi Mode SAR Processor (TMSP), the Integrated TanDEM-X Processor (ITP) and the Integrated Wide Area Processor (IWAP) for Persistent Scatter Interferometry (PSI) still use some algorithmic modules of the experimental SIR-X/SAR mission in 1994 and later SRTM in 2000. Since that time, one common library has been the base for all further developments such as SAR-Lab (for SAR processors) and GENESIS (for interferometric SAR processors). It is maintained by a team of IMF engineers and an external contractor and provides a powerful industry standard development environment. Its most important features are:

- parallelized code, scalable from desktop to multi-CPU computers
- thematic libraries for a wide range of tasks such as signal processing, time and orbit handling and linear algebra
- mechanisms for version control
- mechanisms for automatic documentation and library browse functions
- portability, supporting different compilers and hardware platforms in parallel.

Currently we are intensively investigating software concepts and processor deployment technologies that utilize cloud computing in preparation for future missions like Tandem-L.

SAINT

Our modular software suite SAINT bundles algorithms for maritime information retrieval from SAR data. It is used for research and development in IMF's Bremen research lab but also as the basis for operational deployments at DFD's Neustrelitz ground station. Parameters such as sea state, wind fields, oil spills, ships, icebergs and sea ice classes are currently extracted automatically and in near real-time.

TerraSAR-X staring spotlight image of Munich, June 8th, 2018. The resolution of 0.25 × 0.5 m² reveals not only urban structures but even individual objects like lamp posts or trees. Near the TUM (upper center) we arranged 26 corner reflectors to form a TUM logo on the occasion of the university's 150th anniversary.

The algorithms were initially designed for TerraSAR-X data, but have been continuously adapted to support other sensors and platforms such as Sentinel-1, Radarsat-2 and COSMO-Skymed.

More recent developments are methods for estimating underwater topography from variations in ocean wave patterns, the use of time series to derive bathymetry maps in tidal flats like the Wadden Sea and for calculating ice drift vector fields from combinations of SAR images from different sensors. These algorithms were implemented into experimental prototype processors and will be integrated into the operational data processing chain of DFD's ground station network sites after validation.

Optical Data

CATENA

In optical remote sensing IMF develops operational software processors for fully automatic and robust pre-processing (level 0, 1a, 1b) and higher level processing like atmospheric correction or DSM generation. The challenge is to turn scientific algorithms – e.g. from PhD works – into robust processors, capable of digesting thousands of images automatically in a short time. This is also a prerequisite for generating higher level products.

To be as independent as possible from individual optical sensor properties we have developed and continuously improved our generic processing chain framework CATENA. CATENA is a multi-sensor, multi-purpose processing system for data from many different optical remote sensing systems. It is mostly based on IMF-developed software modules (the XDibias system and libraries) but any other processor running under a Linux environment can be included. It is certified under ISO 9001:2015 describing all processes for developing software for CATENA and operating the system. It represents a framework of modules which can be combined into processing chains for generic project needs or general processing like automatic orthorectification, employing worldwide reference data bases of orthoimages and DEMs, or atmospheric correction of satellite imagery. Tailored software packages from CATENA have been used by IMF for developing the ground processing systems of the DESIS and EnMAP missions.

3D surface model of K2 derived from WorldView-2 data (visualization: DFD).

The general processing scheme is embedded in a sophisticated distributed grid computing framework, managing the automatic execution of the requested jobs on any set of workstations. Since it is generic by design, only new import modules have to be written for new sensors. CATENA can ingest more than 40 high and very high resolution sensor data, e.g. from Landsat, SPOT4/5, IRS-P6-LISS III/AWiFS, ALOS-AVNIR/PRISM, Sentinel-2, RapidEye, Cartosat-1, ZY-3, Ikonos, GeoEye, WorldView and Pléiades as well as NewSpace data, e.g. from Planet.

In the past years various higher level processing chains have been implemented in CATENA. These include a stereo DSM processor that automatically generates DSMs for large amounts of stereo data including geometric bundle adjustment in a short time. This is also valid for large scale airborne data acquisitions. Support for recent satellite missions, as well as spaceborne video evaluation from Planet and UAV/MAV images has recently been added.

Atmospheric correction is now supported using either the DLR PACO or the joint CNES/DLR-developed MAJA processors. Additional thematic processing chains include risk assessment for strong rain as well as the DriveMark processor for providing highly accurate georeferenced data for autonomous driving.

CATENA supports multiple grid or cloud computing platforms, including its own lightweight cluster system, as well as DFD's Data and Information Management System DIMS. The CATENA platform was further developed to support multiple modern computing platforms by allowing processors to run as Docker containers. This was tested in various environments such as Apache MESOS, Hadoop/CALVALUS and Amazon Web Services.

Atmospheric Data

GCAPS – Level 0-1

The processing of raw instrument data (level 0) to calibrated data (level 1), usually radiances, is the first step in the workflow for deriving geophysical parameters of the atmosphere. In the past two decades IMF had developed level 0-1 processors for GOME and SCIAMACHY. Both relied on instrument specific approaches. However, with several new atmospheric composition missions becoming operational, another concept was required to be able to accommodate the needs of advanced instrument designs. This led to the development of GCAPS, the Generic Calibration Processing System, featuring:

- instrument independency
- configurability of calibration chains
- independency from data formats
- usage of standard libraries
- multithreading capability.

The generic processor was realized as a configurable framework, to which calibration as well as input/output plugins can be added. GCAPS provides a lean structure with all the basic functionality needed for level 0-1 processing. Instrument-specific processors are built by coding the relevant plug-ins and defining calibration chains in a configuration file. GCAPS was adopted as the operational processor for the reprocessing of SCIAMACHY data. In this reporting period we added a generic database interface for calibration data and new output plugins for the netCDF4 data format. The flexibility of GCAPS is demonstrated by the fact that we will also use it without modifications for the operational level 0-1b processing of MERLIN data, even though the calibration procedures for the MERLIN lidar mission are very different from those for passive spectrometers.

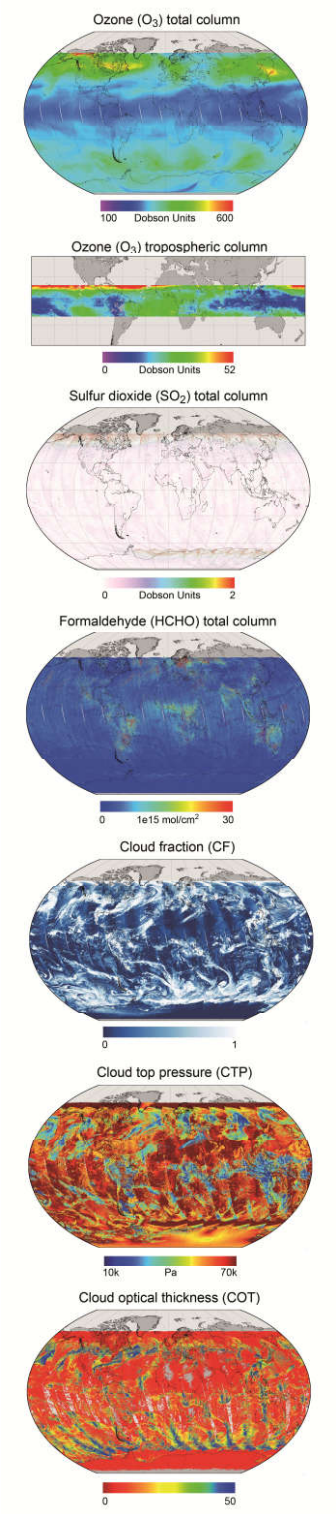

Atmospheric parameters operationally retrieved by IMF's processing system UPAS2 in the framework of the Sentinel-5P payload data ground segment.

UPAS and UPAS2 – Level 1-2

In spectrometric sounding, operational level 2 processing systems translate the theoretical basics of radiative transfer, inversion and scattering into software tools applicable for retrieving geophysical quantities from calibrated level 1 data. Their structures require flexibility because ongoing research produces new algorithms which have to be incorporated to maintain state-of-the-art performance. In the past, IMF decided to develop UPAS, the Universal Processor for Atmospheric UV-VIS-NIR Sensors as a generic multi-mission system for the retrieval of trace gases and cloud properties. Since its operational readiness back in 2004, UPAS has been continuously improved and forms the backbone level 2 atmospheric retrieval system at IMF.

In order to cope with the hundredfold increase in data volume produced by the Copernicus missions and the requirements on near real-time processing for air quality applications, a second generation of UPAS, termed UPAS2, was developed. It consists of a C++ framework with basic modules including level 1 product ingestion, level 2 algorithms and level 2 product output. All these modules use generic interfaces to assure high reusability through modularity. Considerable investment went into the requirement analysis of the design to make sure it can be used for all past, current and known future UVN spectrometer missions. The framework contains the scientific level 2 trace gas retrieval algorithms which evolve over time. The mission-specific operational processors, i.e. our deliverables, can be generated out of this generic code base. This allows the scientific community to obtain datasets from different sensors processed with an identical implementation of the level 2 algorithm. This is an important prerequisite for obtaining meaningful multi-sensor datasets over several decades as needed for climate studies.

One big challenge in the design of UPAS2 was to cope with the increased throughput rates the new missions require (GOME: 2.8×10^4 measurements per day and GOME-2: 2.1×10^5 measurements per day in contrast to Sentinel-5P: 2.3×10^7 measurements per day), with each measurement containing more than 4000 spectral points. This challenge was met by fully exploiting multiprocessor parallelization using OpenMP, considering performance in the design phase and investing in the performance analysis and optimization of complex retrieval modules and interfaces with the usually time consuming radiative transfer models. Furthermore, a user-friendly configuration concept was implemented to allow for easy configurability of processing parameters and the level 2 format. Also, support tools for converting, modifying and visualizing all kinds of data involved became part of the code base.

The excellent performance of UPAS2 was demonstrated shortly after the first Sentinel-5P/TROPOMI level 1b data became available. ESA presented the first images of Sentinel-5P during an event that took place at EOC on December 1, 2017, only a few weeks after the satellite launch. UPAS2 has been integrated into the Sentinel-5P Payload Data Ground Segment at DFD where it operationally generates products even more performant than required while providing the stability needed for any operational 24/7 system. We also plan to use the new UPAS2 for processing data from GOME-2 in the AC-SAF project, from Sentinel-4 and Sentinel-5 missions, and for reprocessing of the already completed GOME mission which provides a dataset of trace gases like O_3, NO_2, H_2O as well as cloud and aerosol properties dating back to 1995.

Laboratory Infrastructure and User Services

Laboratory Infrastructure and User Services

IMF operates several optics laboratories, introduced in the following, to support remote sensing methods development and validation.

For dedicated topics we offer our expertise and infrastructure to external users. Besides the IMF user service OpAiRS for airborne remote sensing, we contribute to the services WDC-RSAT (World Data Center for Remote Sensing of the Atmosphere) and ZKI (Center for Satellite-based Crisis Information) managed by DFD.

Spectroscopic Reference Lab

IMF operates a spectroscopic laboratory for contributing parameters with defined uncertainties to spectroscopic databases for atmospheric constituents. The facility utilizes a commercial high resolution Fourier transform spectrometer (Bruker IFS 125HR). We are the only group worldwide capable of measuring spectroscopy from the FIR to the UV spectral region.

Spectrometric reference lab

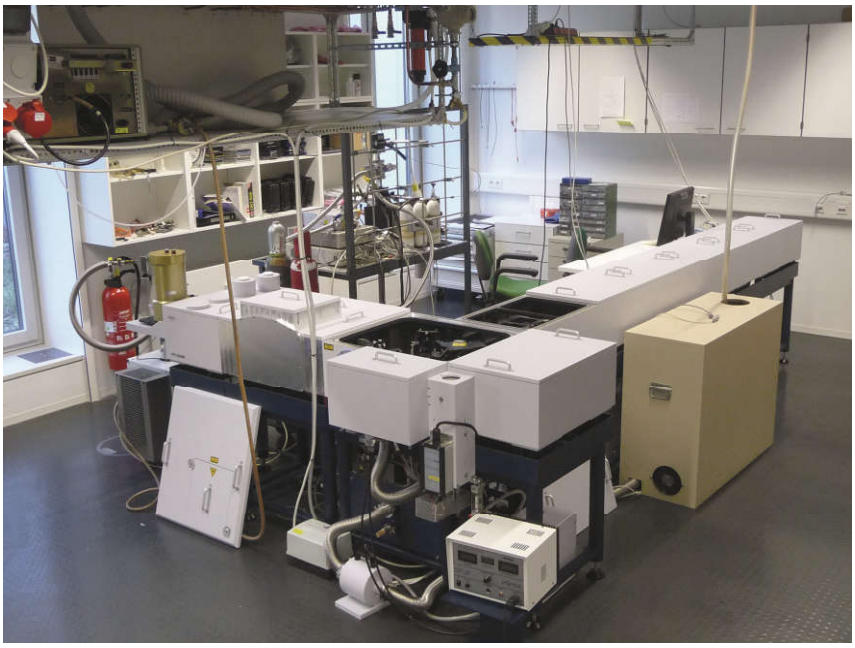

One of the key topics of our laboratory work concerns the quality of the data. Numerous sources contribute to it. Their characterization requires expertise in many fields such as instrumentation, preparation of gaseous samples and data analysis procedures. Our laboratory belongs to the few world-wide capable of providing spectroscopic data with well-defined error bars. Our team is part of the HITRAN scientific advisory committee.

For laboratory work of the highest quality, particular attention must be paid to the absorption cells. In our laboratory four cells are available, all designed at IMF. They cover a temperature range from 190 to 1,000 K and absorption path lengths from 0.16 m to 200 m. One cell is equipped with two window pairs for measuring different spectral regions such as UV/MIR or MIR/FIR for the same gas sample. A flow system and a gas handling system allow synthesis of all relevant atmospheric constituents. An 800 liter mixing chamber and calibrated pressure and temperature sensors permit generation of defined gas/air mixtures.

Software for data processing has been developed for:

- correction of instrument errors including detector nonlinearity, channeling and sample/instrument thermal emission
- line fitting
- calculation of line positions, line strengths, pressure broadening and line shifting from line fit results of multiple spectra.

The resulting certified data can be stored in an extended HITRAN database format.

Underwater Simulator

We operate an underwater environment simulator (ENVILAB) for growing phytoplankton under well-defined light, temperature and nutrient conditions. Its custom-built light source enables creation of light with well-defined spectral composition similar to natural aquatic environments. The setup opens the door for systematic studies on phytoplankton physiology and optical properties which are highly variable and cannot be represented well by single spectra from a database. Results from these measurements are fed to models that simulate the variety of reflectance spectra occurring in nature as basis for quantitative optical remote sensing.

ENVILAB is currently used for studies on the absorption and fluorescence of cyanobacteria.

Selected publication: [118]

Calibration Home Base

Since 2007 IMF has operated the Calibration Home Base (CHB), an optics laboratory built under ESA contract for the characterization of airborne hyperspectral sensors and field spectrometers in the spectral range from 350 to 2,500 nm. With its normed and traceable sources, its vicinity to the airport Oberpfaffenhofen and accessibility for large and heavy instruments, this laboratory offers a unique service in Europe for the remote sensing community. The CHB allows radiometric, spectral and geometric sensor characterization. Equipment and calibration methods are continuously upgraded and refined in cooperation with the Physikalisch-Technische Bundesanstalt (German national metrology institute). On a regular basis we perform characterization campaigns for the Swiss-Belgian airborne APEX instrument and our own sensor suite.

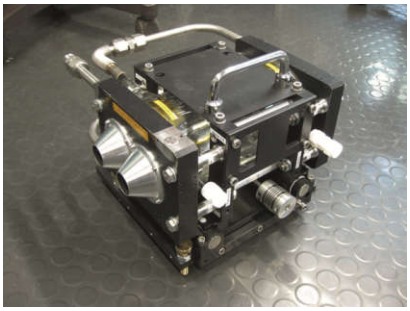

Absorption cell developed by IMF for the Bruker IFS 125HR sample compartment: absorption path 22 cm, temperature range 190 – 350 K. The cell body is a double-jacketed glass tube. Windows are mounted on stainless steel flanges coated with PFA. The window openings with baffles can be seen.

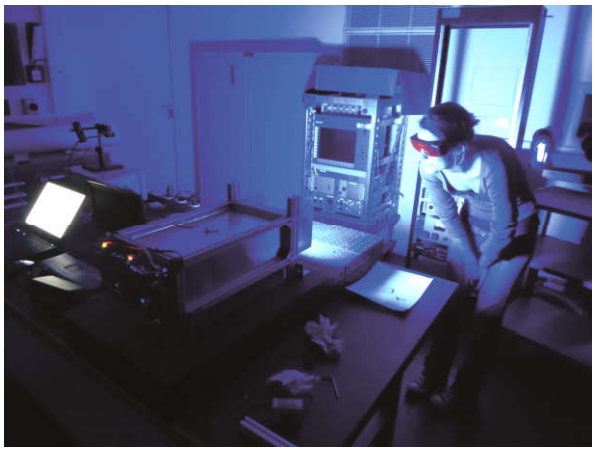

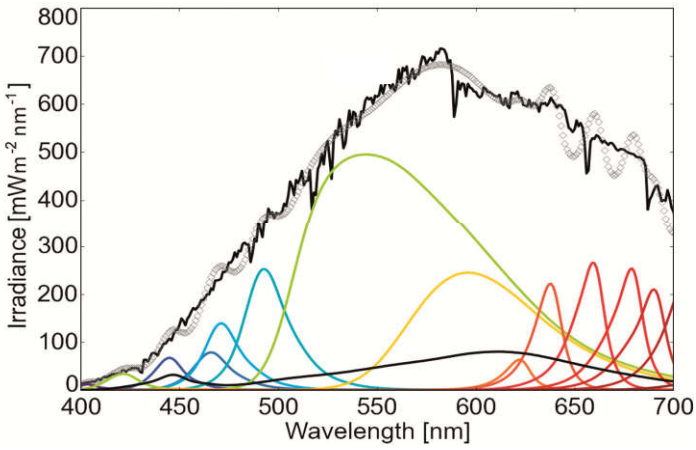

Left: ENVILAB setup: A tunable sun simulator emulates any underwater light spectrum with respect to intensity and spectral composition.
Right: Desired (black solid line) and realized (grey circles) downwelling irradiance spectra at 1 m water depth. Colored lines reflect contributions of individual LED spectra.

The CHB is a well-suited environment for developing and testing new cal/val methods for the level 0 to level 1b data processing step. For handling and evaluation of hyperspectral sensor data generated in the CHB we developed two complementary software packages:

– *ImSpeC*, written in Python, is a toolbox for the evaluation of laboratory imaging and non-imaging spectrometer data. Providing algorithms to extract relevant information in datasets of several hundred Gigabytes, ImSpeC is used for analyzing geometric, spectral and radiometric laboratory measurement data. Individual properties for each instrument pixel are retrieved and presented as 2D data maps. Due to its generic concept, we were able to license ImSpeC to industry.

– *L0ne* is a level 1 processor, which utilizes the evaluation data provided by ImSpeC. Its modular design allows it to be used with a wide range of sensors. Single processing modules, like non-linearity or radiometric response correction, can be switched off or interchanged leading to lower efforts in operation.

One focus of our work covers stray light characterization and correction. For an example application we have shown that stray light calibration can lead to a 19 % reduction of systematic errors in the level 2 data product (bathymetry). To measure ghost images and stray light effects we developed a dedicated radiance source (narrow spectral bandwidth, small divergence angle) which allows stray light characterization with a dynamic range of up to 10^8. In the subsequent calibration step ghost images are individually mapped out, corresponding signals are relocated to their origin and diffuse in-band stray light is corrected.

Besides operating the CHB for airborne imaging spectrometers it is utilized for the laboratory characterization of the satellite mission EnMAP. We support the manufacturer OHB System in characterization of spectral, geometric, radiometric and stray light instrument properties as well as traceability.

Selected publications: [881], [307], [306]

Calibration Home Base

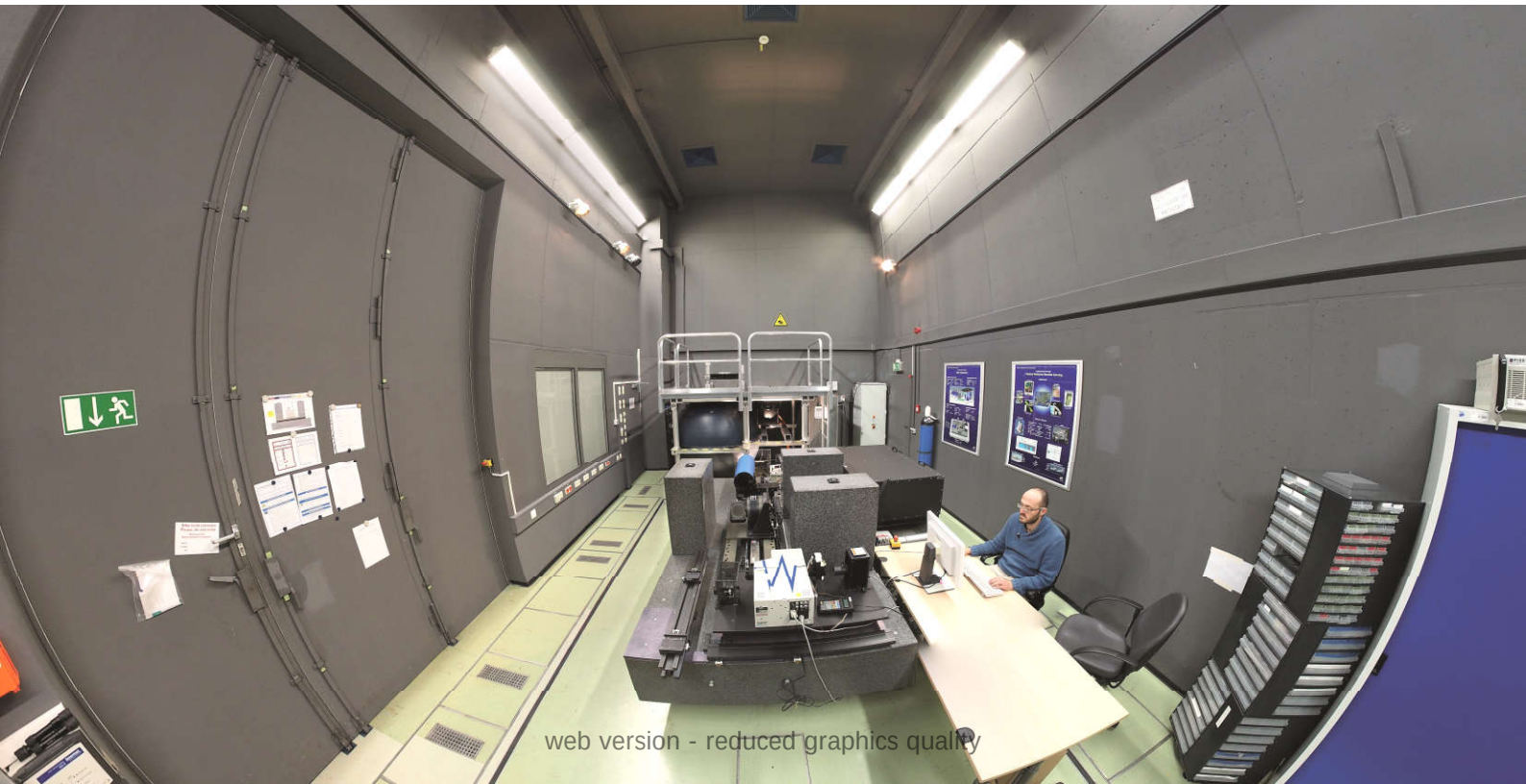

Airborne Remote Sensing

The IMF-operated user service *Optical Airborne Remote Sensing and Calibration Home Base* (OpAiRS) allows users to draw on the accumulated IMF expertise in hyperspectral remote sensing, including

- planning and execution of airborne surveys in close cooperation with DLR's research flight facility, which operates the largest airborne research fleet in Europe
- access to a suite of field and airborne sensors (HySpex) based on measurements in our Calibration Home Base
- processing of the acquired data (system corrections, orthorectification, atmospheric correction) using state-of-the-art algorithms of CATENA
- long-term data archiving in the German Satellite Data Archive of DFD.

The ISO 9001:2015 certified user service conducted 66 survey flights with a total of 182 flight hours over 42 areas of interest in the review period.

OpAiRS is actively engaged in knowledge transfer with its peers in the European Facility for Airborne Research (EUFAR).

In addition to this service we operate two high resolution optical camera systems onboard of DLR planes (*3K* system) and helicopters (*4k* system), mainly to develop and test real-time situation awareness procedures for traffic or crowd monitoring, and disaster management applications (see *Optical Imaging* chapter).

Selected publication: [907]

Areas of interest covered by IMF's airborne remote sensing activities during the review period.
blue: hyperspectral data acquisition within user service OpAiRS (sensor system HySpex)
green: test sites for situation awareness campaigns (sensor systems 3K and 4k, resp.)

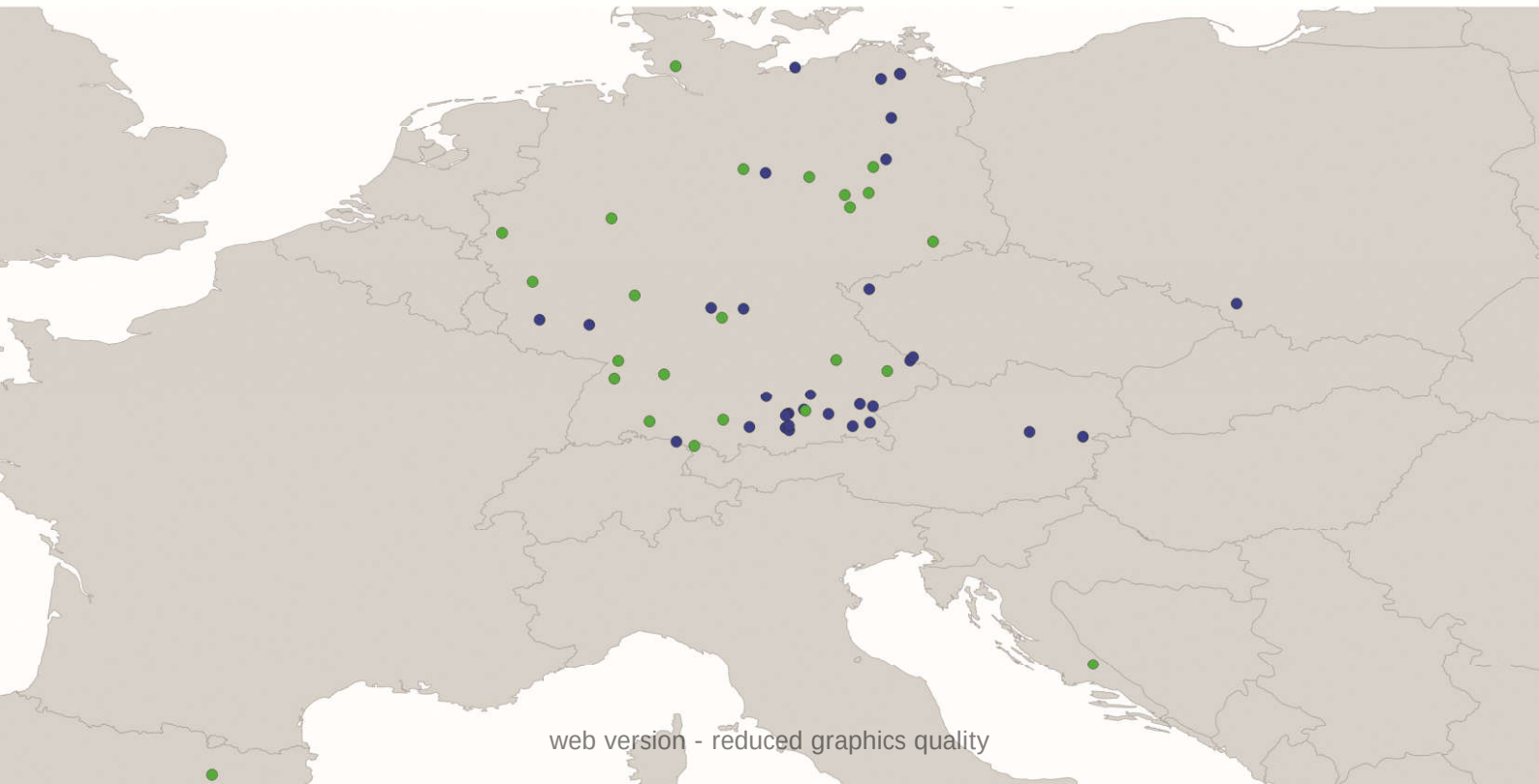

Synthetic Aperture Radar

Synthetic Aperture Radar

Our research and development activities cover the entire SAR data chain from sensor bits to geo-information products. Developments for operational missions such as the processors for TerraSAR-X and TanDEM-X are described in the chapter *Missions and Sensors*. In the following we summarize our major achievements in developing algorithms for

- **SAR focusing**
- **DEMs, glaciology and imaging geodesy**
- **SAR oceanography**
- **SAR interferometry**
- **geodetic tomographic SAR.**

While our focal point is on methods and algorithms related to SAR signal processing, we foster interaction with geoscientists and other end-users to utilize our methods for science and new applications. Additionally our research also encompasses selected geoscientific fields where an in-depth knowledge of SAR is required, e.g. SAR oceanography, volcanic and tectonic mapping, glaciology and precision mapping.

The technological readiness level of our algorithms for these activities spans the entire range from basic research to operations.

SAR Focusing

SAR processing, or focusing, means generating high resolution images from raw data acquired by a SAR sensor: the challenge is to synthesize a large aperture along the flight track by coherent summation of the echoes received by the comparatively small antenna. It is the most crucial step in the SAR data chain because it is mathematically complex, computationally expensive and it ultimately determines the quality and accuracy of the image and all higher level products in the information extraction chain. The front-end of a SAR processor must be exactly made-to-measure for a specific SAR sensor in order to account for all its peculiarities and potential aging over the years – only then can optimal image quality be guaranteed over the lifetime of a mission. The developmental challenge is to ensure that the algorithms for focusing, multi-looking and geocoding are formulated sensor-indenpendent. Efficient implementation in software, tailored to the hardware architecture, is also crucial. A processing time of hours for a single image may be acceptable in a research environment, but not in operational missions like TerraSAR-X and TanDEM-X, where more than 1,000 precision SAR images are focused daily during peak periods.

Over the last few decades the imaging capabilities of spaceborne SAR sensors have evolved from simple medium resolution stripmap systems with rather fixed settings (e.g. ERS-1/2) to high resolution phased-array multi-mode/multi-channel sensors such as TerraSAR-X and its possible successors. In line with these developments our SAR focusing algorithms have had to be substantially revised. Starting with a range-Doppler algorithm for the SIR-C/XSAR mission in the early nineties, IMF introduced an interpolation-free chirp scaling algorithm for SRTM in 2000. Later, this processor was extended by SPECAN (spectral analysis) elements for burst modes like ScanSAR, TOPSAR and sliding spotlight processing and, most importantly, merged into *one* hybrid TerraSAR-X Multi-mode SAR processor (TMSP) for the TerraSAR-X mission.

Recent algorithm developments at IMF target decimeter resolution SAR for next-generation X-band SAR systems with very long synthetic apertures and bandwidths exceeding 1 GHz.

Large scale deformation mapping project: Ground subsidence (red) and uplift (blue) map of Germany, derived from ERS-1 data. A series of similar products is currently produced from Sentinel-1 data for the German Federal Institute for Geosciences and Natural Resources (BGR).

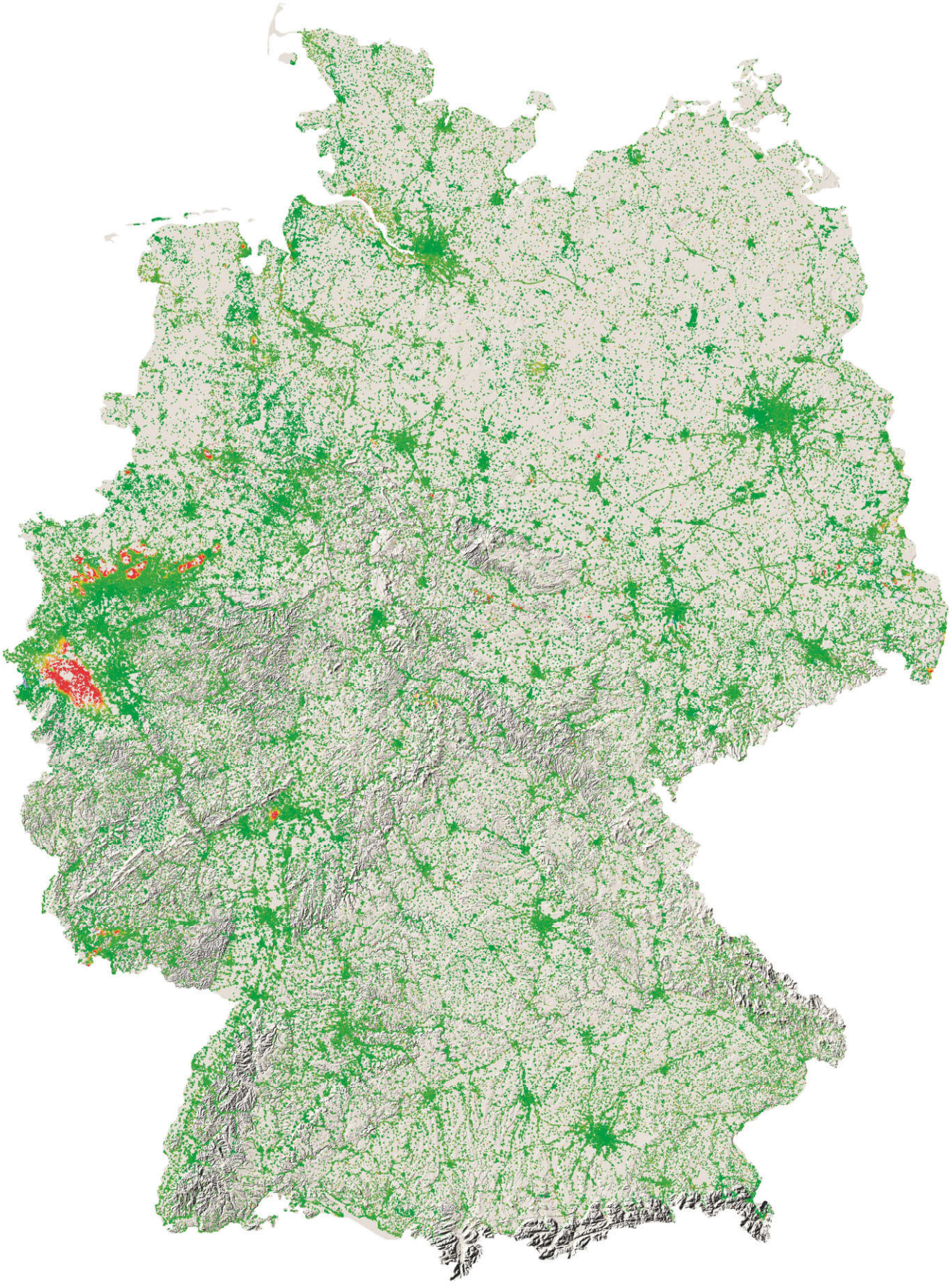

Such a new VHR algorithm has been successfully tested in a prototype SAR processor and proven to achieve a resolution better than 25 cm in both range and azimuth. Key technologies of this algorithm were then incorporated into the operational TMSP, enabling focusing at an azimuth resolution of 22 cm for TerraSAR-X's new staring spotlight mode.

Experiments with such VHR SAR focusing in combination with a geometrically calibrated autofocus have led to a new technique: 3D height determination of isolated points from a single 2D SAR image. This apparent miracle exploits the curvature of satellite orbits in combination with the very long (> 40 km) aperture of staring spotlight mode. Indeed we could demonstrate that the elevation of bright points such as concave corners on a building façade can be determined to an accuracy of approximately 10 meters from space – using a single TerraSAR-X staring spotlight image.

TerraSAR-X staring spotlight image of an eight story building. Colors represent the elevation of windows as determined from this single image by a new geometrically calibrated autofocus algorithm.

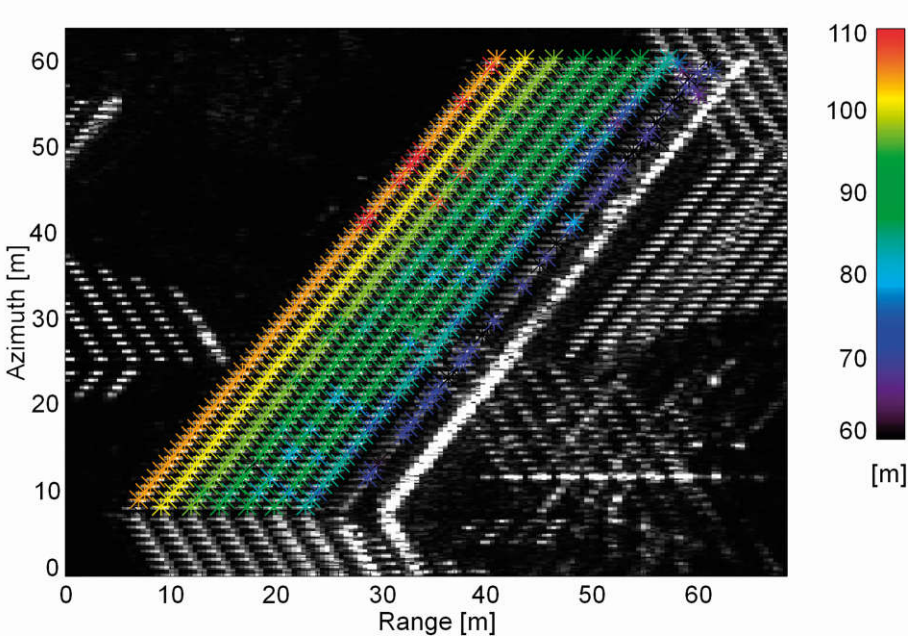

Aside from national missions we support European SAR missions (notably Sentinel-1) and projects in the fields of SAR systems, algorithm development and geometric calibration as well as the design of entire payload data ground segments (PDGS). In that context we assisted in commissioning the Sentinel-1A and -1B SAR satellites in 2014 and 2016. In 2015 we led an ESA Phase A study for the definition of a PDGS including key processing algorithms for the bistatic SAR mission SAOCOM-CS. For this mission ESA intended to launch a receive-only SAR satellite as a bistatic companion to the Argentinian SAOCOM L-band satellite. Our activities also included the definition of a PDGS to be operated as an ESA third party mission. Even though ESA decided not to implement the mission, our design and research activities continue in the context of the Tandem-L studies. Key elements are efficient SAR data workflows and systematic interferometric and tomographic processing.

After the successful launch of the Spanish PAZ satellite in February 2018, the first SAR image was successfully processed by IMF's PAZ SAR processor which had been licensed to the PAZ project in 2010. Our support for the mission has been reactivated after four years of launch delay and further developments are planned to equip direct access stations with our processor and for the synergetic use of the TerraSAR-X and PAZ systems.

Another activity, started in 2018, aims to transfer SAR processing and ship detection algorithms from the ground to space. Together with five European partners in the framework of the EC Horizon 2020 project EO-ALERT, IMF is developing an end-to-end processor running on a breadboard space hardware with the goal of delivering ship positions and weather information to users even faster than today.

Selected publications: [702], [290], [128]

SAR Geodesy Algorithms

The SAR image geometry and phase of the image pixels depend on the satellite's orbit and signal travel time, both of which can be determined very precisely. The resulting geometric range and azimuth measurement accuracy, on the order of centimeters for pixels and even millimeters for the phase, is a most powerful capability of SAR. In this chapter we report on our developments of interferometric methods for TanDEM-X terrain reconstruction and on radargrammetric methods using pixel coordinates for point positioning. We have in fact established a new discipline called *Imaging Geodesy* that combines geodetic methods from the disciplines of GNSS and SAR imaging. Furthermore we report on selected applications of our methods and data in the fields of glaciology and geodesy. Interferometric methods for time series analysis are reported in a separate chapter.

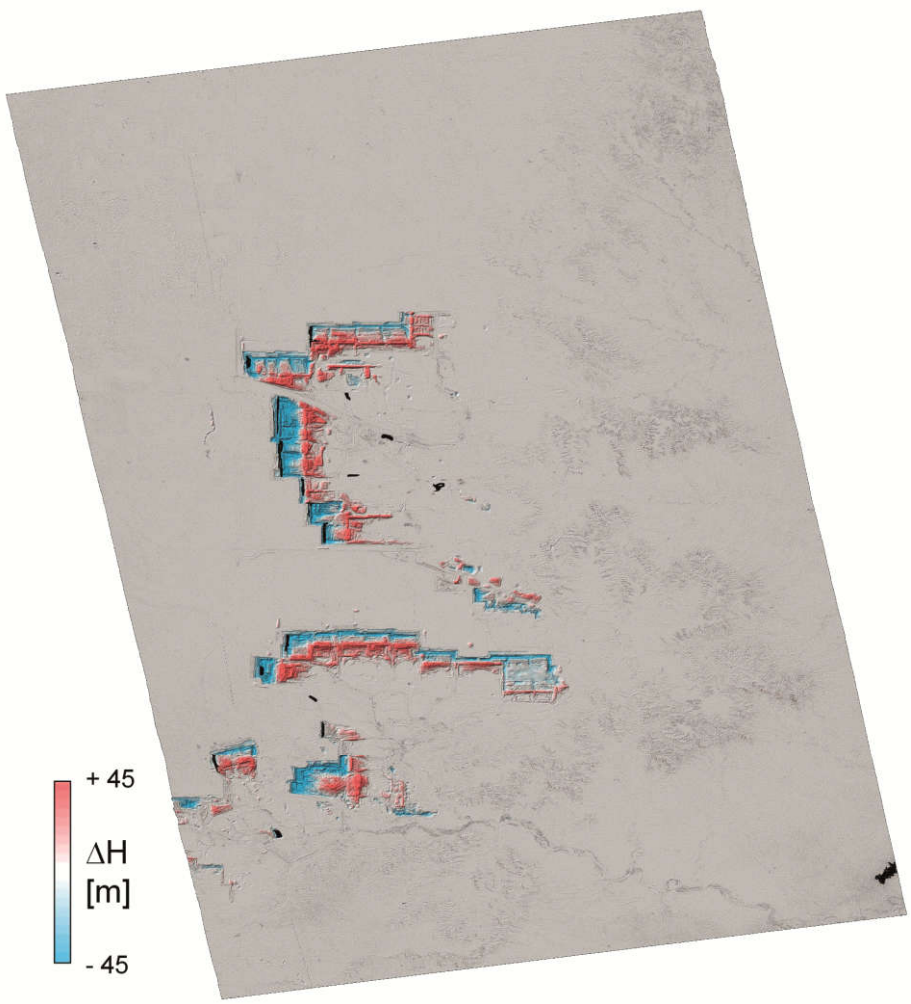

Difference between the TanDEM-X DEM (2011 – 2014) and a 2016 TanDEM-X DEM acquisition of an open pit mine in Wyoming. The horizontal resolution is 6 m and the height accuracy on bare soil is better than 0.8 m.

New Algorithms for TanDEM-X

In the reporting period, our operational Integrated TanDEM-X Processor (ITP) was extended with newly developed algorithms to solve the phase ambiguity problem in phase-to-height conversion by combining data from at least two global coverages acquired with different baselines. This major improvement was necessary for two reasons. First, to process some especially difficult large baseline data sets from the early mission phase. Second, to significantly increase the reliability of the Global DEM product completed in 2016.

After finalization of the main mission product, the Global DEM, the ITP phase unwrapping algorithms were further upgraded to generate experimental high-resolution local DEMs (HDEMs) with finer posting (6 m) and relative height errors of 0.8 m for specific areas, well below the 2 m requirement of the nominal product.

The generation of HDEMs requires new data acquisitions in specific large-baseline satellite formations requiring orbital changes that cost satellite fuel and time. We therefore developed an alternative solution based on standard mission data. Using sophisticated – unfortunately still quite time-consuming – non-local interferometric filtering approaches, we generated a number of high resolution DEM demonstration products with unprecedented detail and height accuracy (see *Data Science* chapter).

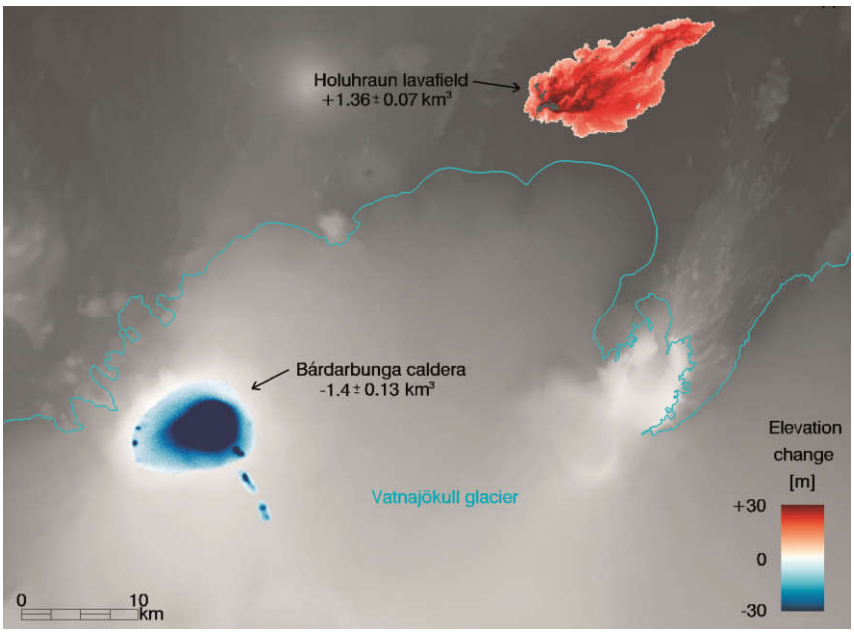

Topographical changes in TanDEM-X DEMs of the Bárðarbunga caldera and Holuhraun lava field due to the 2014/2015 volcanic unrest. The ice volume lost due to the collapsed caldera (blue) corresponds to the volume of the newly emerged lava field (red).

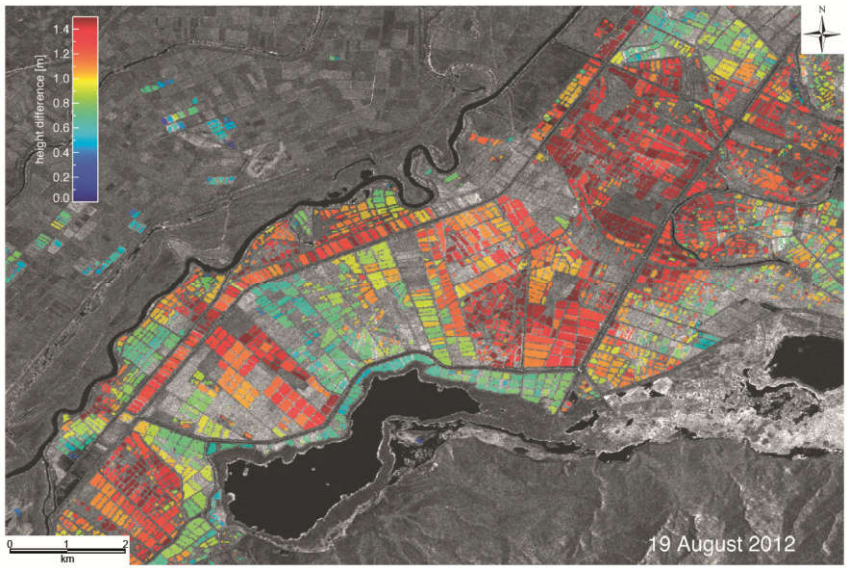

Elevation changes of rice fields in Ipsala, Turkey, monitored with multi-temporal TanDEM-X DEMs during the growing period July – September, 2012.

Since September 2017, TanDEM-X has been acquiring an additional global bistatic data set for the generation of a global elevation change layer, the *Change DEM*. Based on our refined algorithms for HDEM generation and using the existing global DEM as a reference, ITP is now able to produce a new global DEM from only one additional global coverage (compared to two and more coverages for the first version) and to analyze significant temporal height changes 'on-the-fly' in an operational way.

Prominent elevation changes observed in TanDEM-X DEMs are mostly caused by deforestation, mining, volcanic activity and glacier dynamics. An example for the latter two cases combined is shown in our study of the Bardabunga volcano 2014/2015 in Iceland. Sub-glacial eruptions caused a glacial surface subsidence above the collapsed caldera and a comparable volume gain in the nearby lava flow connected by a sub-glacial graben.

Even much smaller height changes are visible in TanDEM-X DEM time series. A spectacular example is monitoring of the growth phases of paddy rice plants, resulting in height changes of about 1.4 m within one growing season. Such unexpected signals motivate the global approach chosen for Change DEM generation in contrast to local approaches applied in areas where changes are expected such as glaciers.

Selected publications: [320], [753], [153], [37], [233], [30]

Imaging Geodesy

This technique turns a high resolution imaging radar like TerraSAR-X into a geodetic measurement device. A few radar images can capture motion fields over large areas of the Earth's surface, effectively substituting thousands of GNSS receivers.

Absolute radargrammetric Earth surface displacement measurement from space using SAR imagery is a powerful alternative to the established InSAR technique. The advantages are that true 2D information can be retrieved (InSAR provides only 1D) and *absolute* displacements determined (InSAR requires a reference point) without ambiguities (no phase unwrapping is necessary). The accuracy of radargrammetric methods is limited by the pixel resolution, object contrast, orbit accuracy, wave propagation distortion, SAR processor inaccuracies and geodetic effects. All these influences are the focus of this research topic. The basic concept was developed in the Helmholtz Alliance *DLR@Uni* project *Munich Aerospace: Hochauflösende geodätische Erdbeobachtung, Korrekturverfahren und Validierung*. Here, together with partners from TUM and DLR GSOC, we developed methods to achieve absolute radar positioning accuracy on the centimeter level.

We installed corner reflectors at the geodetic observatories Wettzell (Germany), O'Higgins (Antarctica) and Metsähovi (Finland) and developed compensation methods for reducing the overall error of absolute range measurements from decimeters to one centimeter and below. The methods include correction of dry and wet atmospheric delays using measurement data and numerical weather models, ionospheric delay, solid Earth tides, continental drift, atmospheric pressure loading and ocean tidal loading.

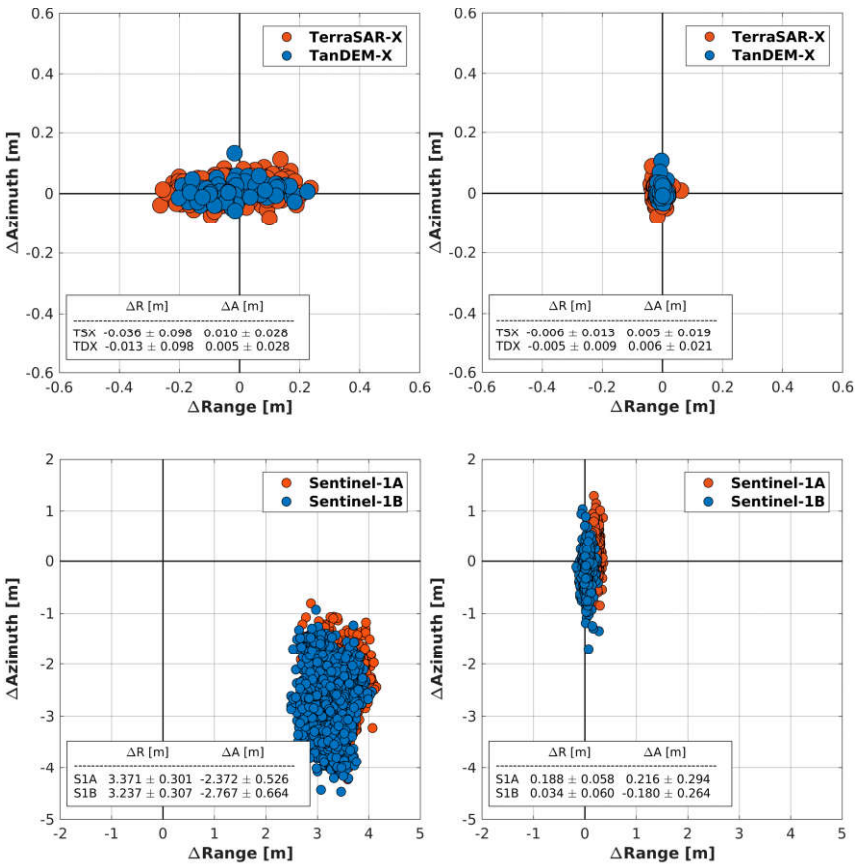

Pixel position accuracy in 2D image without (left) and with (right) our corrections for TerraSAR-X (top) and Sentinel-1 (bottom). Note that e.g. the range standard deviation is reduced by a factor of 5 for Sentinel-1 and even more for TerraSAR-X.

Today we look back on time series of more than six years for each site. Our results clearly show that we can localize an object in two-dimensional image space with 10 – 20 mm accuracy and in absolute three-dimensional space with about 5 cm accuracy.

We coined the term *Imaging Geodesy* for this research field and are now exploiting many new applications such as:

The 3D grounding position of a street lamp post in San Francisco can be determined with < 5 cm accuracy from multiple high resolution TerraSAR-X images. Thousands of such points can be found in images of urban areas.

– absolute geodynamic motion estimation
– localizing 3D ground control points for image orthorectification and precision maps
– generation of consistent reference heights for TanDEM-X elevation models.

We extended our techniques to Sentinel-1 and its new TOPS acquisition mode under an ESA contract. The results of our work have been incorporated into the calibration of these sensors and their SAR processors, leading to a geometric accuracy improvement of at least one order of magnitude.

During recent years our imaging geodesy methods have matured from experimental applications to operational use not only in our product chains but also in tailored geodesy processors for operational use with TerraSAR-X, PAZ (Spain) and Sentinel-1 (ESA).

This SAR geodesy processor generates a new type of SAR product, the *SAR Geodesy Product*. It is designed as a correction layer to conventional SAR products containing ready-to-use information layers for tropospheric and ionospheric propagation delays, for Earth dynamics and, if required, system corrections for sensor and processor. With the help of the *SAR Geodesy Product*, users can conveniently exploit 2D centimeter accuracy in standard TerraSAR-X image products and in principle also in products from other sensors such as Sentinel-1.

Concepts for the use of our techniques in industrial mapping are described in the following paragraph and in the chapter on Geodetic TomoSAR.

Selected publications: [114], [258], [262], [30], [557], [60]

Ground Control Points from Geodetic SAR Data

Supported by DLR's Technology Marketing under the Trademark Drivemark™ and by a Helmholtz Validation Fund we transferred the Imaging Geodesy scientific algorithms into a near operational processor. The purpose of this processor is to support the generation of precision maps (e.g. for automated driving) by generating highly accurate 3D reference points from SAR data. Such reference points are typically street lamps or sign posts which can also be detected in high resolution optical imagery.

Our new processor automatically generates *3D Ground Control Points* (GCPs) by searching for homologous points in stacks of stereo SAR observations, and then determining their 3D coordinates with a typical accuracy of < 10 cm. If only some of these control points can be identified in optical imagery, they can be used to significantly improve the geometric accuracy of both, the optical image and the derived thematic map.

The technique is currently being tested in cooperation with several industrial partners. The results achieved so far are so promising that our method could soon become a new contribution to precision mapping – on par with ground-based or GNSS-based methods.

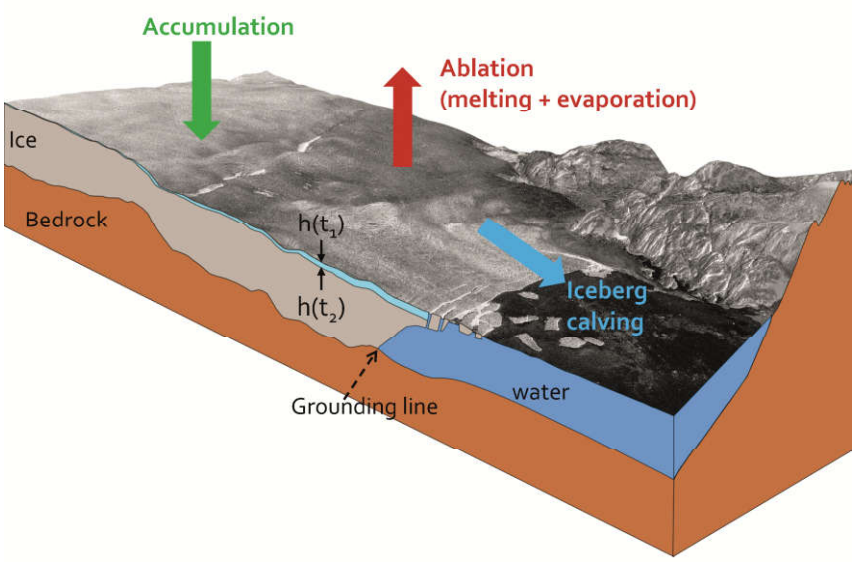

SAR can retrieve information about several mass balance contributors of a glacier: Height changes due to accumulation and ablation and calving flux.

Application of SAR Data for Glaciology

The cryosphere and its dynamics play an important role in understanding global climate change and indeed with SAR we can contribute to the characterization of several Essential Climate Variables (ECVs)[1] and to the determination of parameters for glaciers and ice sheets (area, surface elevation, ice velocity, ice mass change, calving front and grounding line).

A major application of glacier surface elevation change measurements is the determination of the total net mass balance and, hence, the induced sea level rise. Due to the relatively slow changes of glacier surface elevation, reference heights are often derived using older archived data from other missions (e.g. SRTM or ICESat).

The penetration of radar signals of different wavelengths into the dry snow is significant for the determination of the dynamics and mass balances of glaciers and ice caps, and it changes drastically with the condition of their snow covered surface. These effects have been investigated and taken into account for our extensive study of the mass losses of the North and South Patagonian Icefields. The total mass change rate of the combined area (16,984 km^2) is found to be 17.7 Gt/year, leading to a sea level rise contribution of 49 µm/year. The methods refined in this research are now applied to larger areas like the Antarctic Peninsula.

The change in elevation described above gives only bulk information about the mass balance. Other SAR-based measurements help to estimate the individual components of the mass balance and glacier dynamics, e.g. the surface velocity or the behavior of the calving front:

$$\dot{B} = \dot{B}_{ac} + \dot{B}_{ab} + \dot{B}_{cv}$$

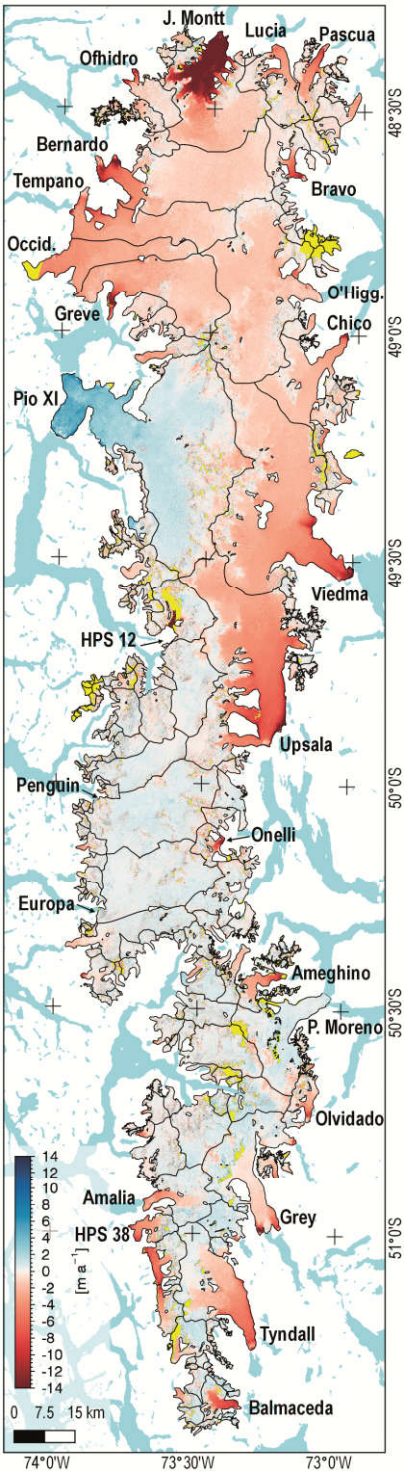

Ice elevation changes of the Patagonian ice fields between 2012 and 2016 measured with TanDEM-X.

[1] https://public.wmo.int/en/programmes/global-climate-observing-system/essential-climate-variables

where $\dot{B}$ is the total net mass balance, $\dot{B}_{ac} + \dot{B}_{ab}$ the surface mass balance from accumulation and ablation and $\dot{B_{cv}}$ the calving flux.

While accumulation and ablation cannot be determined from space, the ice velocity or calving flux can be derived from SAR and InSAR data. For this we developed highly accurate methods for velocity estimation from TerraSAR-X data using feature and speckle tracking.

Another parameter of the ice sheet ECV is the grounding line, the location of the transition where the ice resting on bedrock detaches and becomes a floating ice shelf. Its position is determined by differential InSAR processing of Sentinel-1 and TerraSAR-X data. This method has been automated and extensively applied to large glacial systems including coastal East Greenland and the main Antarctic outlet glaciers in the framework of two ESA and DFG projects. Larger marine-terminating glaciers of the Northeast Greenland ice stream are of particular interest, because they drain 16 % of the whole ice sheet into the ocean.

Calving front locations, ice surface velocity and surface elevation change derived from time series of SAR data were analyzed and indicated very different behavior of even closely neighboring glaciers. Our expertise in this field is a valuable contribution to international collaborations in the context of the ESA Climate Change Initiative.

Selected publications: [384], [608], [148], [168], [127], [16], [67]

SAR Interferometry

Advancements in Interferometric Techniques

SAR interferometry allows to measure ground deformation with sub-wavelength precision. Historically the techniques have progressed from single interferograms to algorithms based on stacks of images providing time series of deformation, like Persistent Scatterer Interferometry (PSI). More recently, Distributed Scatterer Interferometry (DSI) techniques have bridged the world of interferograms and the world of time series. These developments have been followed also in our institute from the very beginning. However, all these algorithms suffer from distortions caused by e.g. atmospheric propagation delays. Therefore, we investigated correction techniques that significantly increase the precision of the deformation products and reduce the number of acquisitions required in the stack. Some of these advancements are already in use operationally such as for the German ground deformation service. Others have been demonstrated and are an essential part of the processing concept for the future Tandem-L mission. Many of these developments were performed in the frame of the Helmholtz Alliance *Remote Sensing and Earth System Dynamics*, together with national and international scientists. Besides this strong focus on error reduction, we have supported the development of the Tandem-L mission concept with product definitions, processing concepts, and performance analyses for future products such as 3D deformation vectors or strain maps.

Tropospheric Corrections

Even though SAR imagery is mostly weather independent, propagation through the spatially varying troposphere leaves a mark in the range delays measured by SAR and the error patterns are clearly visible in SAR interferometry. While such delays constitute an interesting signal for meteorological applications, for ground deformation measurement they constitute a nuisance and corrections are highly desirable.

The starting point for our tropospheric corrections are weather models. In particular we apply ready-to-use ECMWF ERA Interim model data while also optimizing local high resolution weather models (e.g. WRF) for our purposes. The SAR signal path delays are calculated by ray-tracing and integration through a 3D atmospheric refractivity map which is calculated from pressure, temperature and humidity provided by the weather model. The derived geometric and phase corrections are helpful in several stages of SAR and InSAR processing, e.g. for very high resolution SAR focusing and for interferometric coregistration. Phase corrections in deformation mapping are particularly significant at large distances (> 100 km), where the power of the tropospheric disturbance is often 10 times larger than the desired deformation signal. Fortunately, ECMWF models are accurate enough to reduce the error variance by a factor of 4. At smaller spatial scales (< 10 km) improvements are significant if topographic variations in the scene cause a height-dependent stratification even for a spatially homogeneous troposphere.

Our extensive experience with the correction of SAR interferograms using weather models and GNSS observations has put us in a leading position in error reduction and predicting the performance of deformation products.

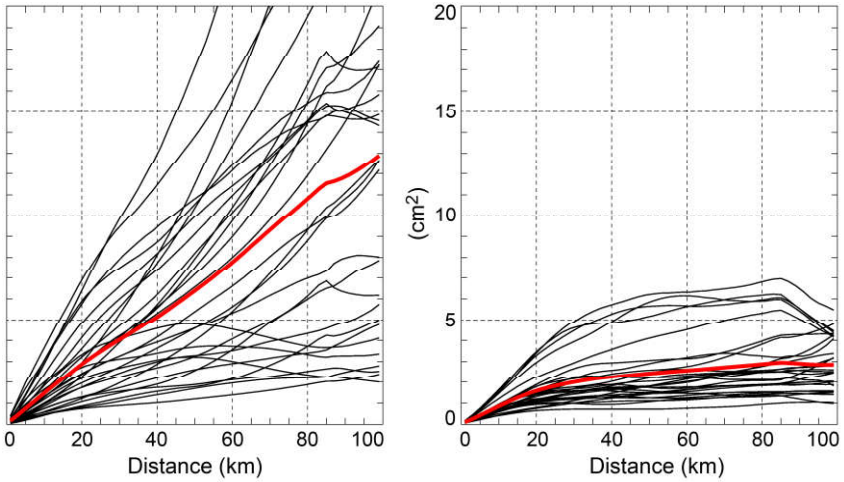

The ECMWF ERA interim weather model helps in reducing the InSAR deformation error variance by a factor of four at scales of 100 km. Shown are the error variograms before (left) and after (right) our compensation.

Based on this experience we are able to define solid observation requirements for future projects and missions (e.g. Tandem-L) in order to achieve the desired product performance.

Selected publication: [506]

Ionospheric Corrections

Not only the troposphere (< 18 km above the Earth surface) but also the ionosphere (80 – 1000 km) produces unwanted delays that must be compensated for to obtain accurate ground deformation maps. Unlike tropospheric delays, these delays are dispersive or wavelength-dependent ($\sim\lambda^2$), with longer wavelengths (e.g. ALOS, ALOS-2, SAOCOM, Tandem-L) being much more affected than shorter ones (e.g. TerraSAR-X). Available ionospheric space weather models are not sufficient for our purposes because their resolution is limited by the density of ground- and space-based GNSS receivers.

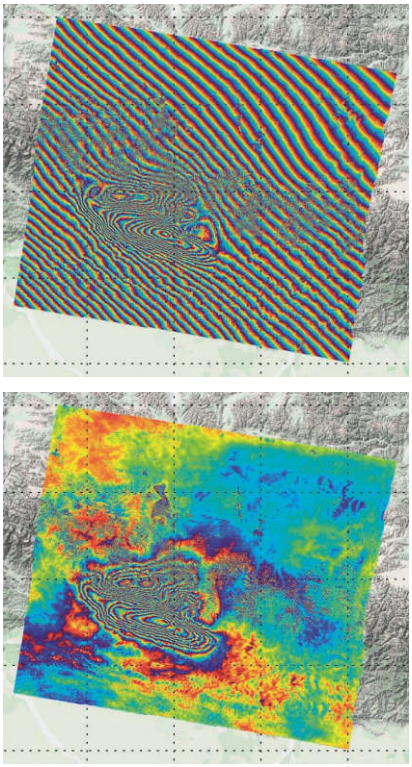

Sentinel-1 interferogram of the Nepal earthquake (2015) without (top) and with (bottom) our ionospheric correction.

Fortunately it is possible to estimate the total electron content from the SAR images themselves, exploiting the dispersive character of the ionosphere – similarly to dual-frequency GNSS. Over the course of the past few years, we have convincingly demonstrated the feasibility of the split-spectrum technique. In addition we have studied algorithms tailored to fast spatial variations of the ionosphere, apt to deal with more difficult and rare cases.

Originally the SAR community understood the importance of ionospheric corrections only for rather long wavelength L- and P-band SARs. However, during our research we clearly demonstrated the need to apply the split-spectrum technique even to Sentinel-1 C-band data. In consequence we developed algorithms for the peculiar influence of the ionosphere on TOPS mode data of Sentinel-1. Future developments will address the integration of ionospheric corrections in time series and multi-baseline workflows.

Selected publications: [207], [607], [116], [115]

Sequential Estimation for Distributed Scatterer Interferometry (DSI)

To enhance the spatial coverage of deformation products, it is necessary to include Distributed Scatterers in the estimation. These are generally natural areas (e.g. bare or vegetated surfaces) with coherence properties less than ideal. They are typically not exploited at full resolution but after adaptive or even non-local spatial averaging of the interferograms (e.g. the SqueeSAR algorithm). DSI processing performance relies on using a large number of interferograms, ideally all possible combinations from all acquisitions over a certain area. Therefore DSI processing is currently performed once all data are available and the computational effort grows roughly quadratically with the number of acquisitions involved.

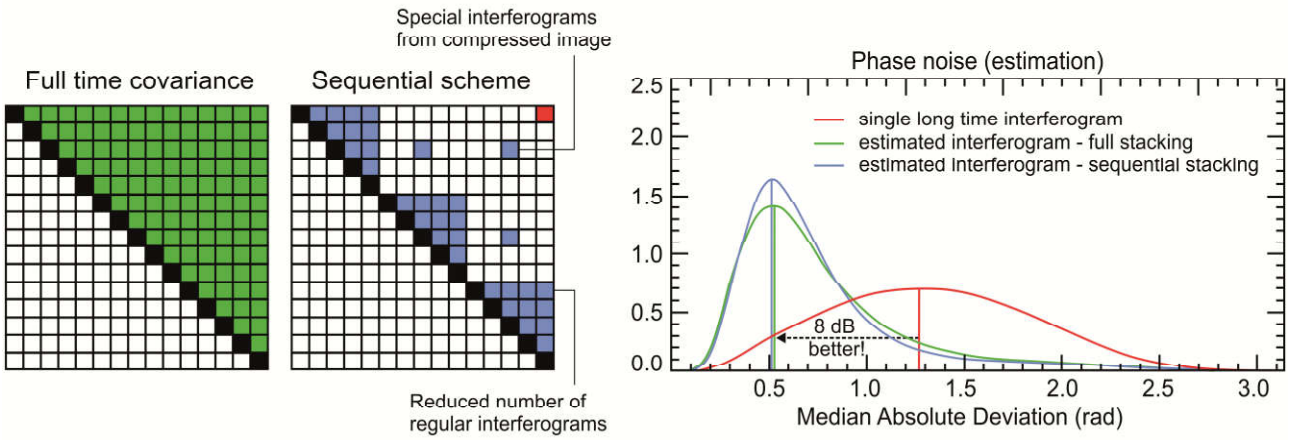

Exploiting the full covariance matrix with all possible interferograms achieves 8 dB phase noise reduction compared to a single long time interferogram. Our new sequential estimator achieves the same performance using only a fraction of the full covariance matrix – saving significant computing resources.

The ambitious goals of the Tandem-L proposal foresee the continuous acquisition and processing of all global areas subject to tectonic strain for an entire decade. Obviously available DSI techniques are impracticable for such streaming-type processing. We have therefore developed a new method to process the data sequentially during the mission, without compromising the phase estimation quality. Ordinary DSI phase estimation is performed over subsets of acquisitions, for example yearly, and successively a temporal phase connection is established between these subsets. First demonstrations have been conducted with Sentinel-1 data and they confirm the validity and performance of our method. Operationalization and verification activities are ongoing.

Selected publications: [92], [2], [750]

Closure Phases and Moisture Retrieval

Closure phases are a recent discovery in SAR interferometry: they are observed as circular phase inconsistencies in triplets of interferograms generated from three SAR images. The best understood physical mechanism able to generate significant closure phase is the variation of moisture in semi-transparent scatterers, e.g. soil. We are among the first to investigate this effect systematically. Since the effect is expected to be more significant for longer wavelengths we have started investigating the inversion of moisture levels from closure phases using ALOS-2 L-band data. Nonetheless, we have also shown the presence of closure phase inconsistencies in C- and X-band.

The evolution of soil moisture over six months estimated over Kumamoto region (Japan) from ALOS-2 closure phases. The area is 60 × 80 km² in size.

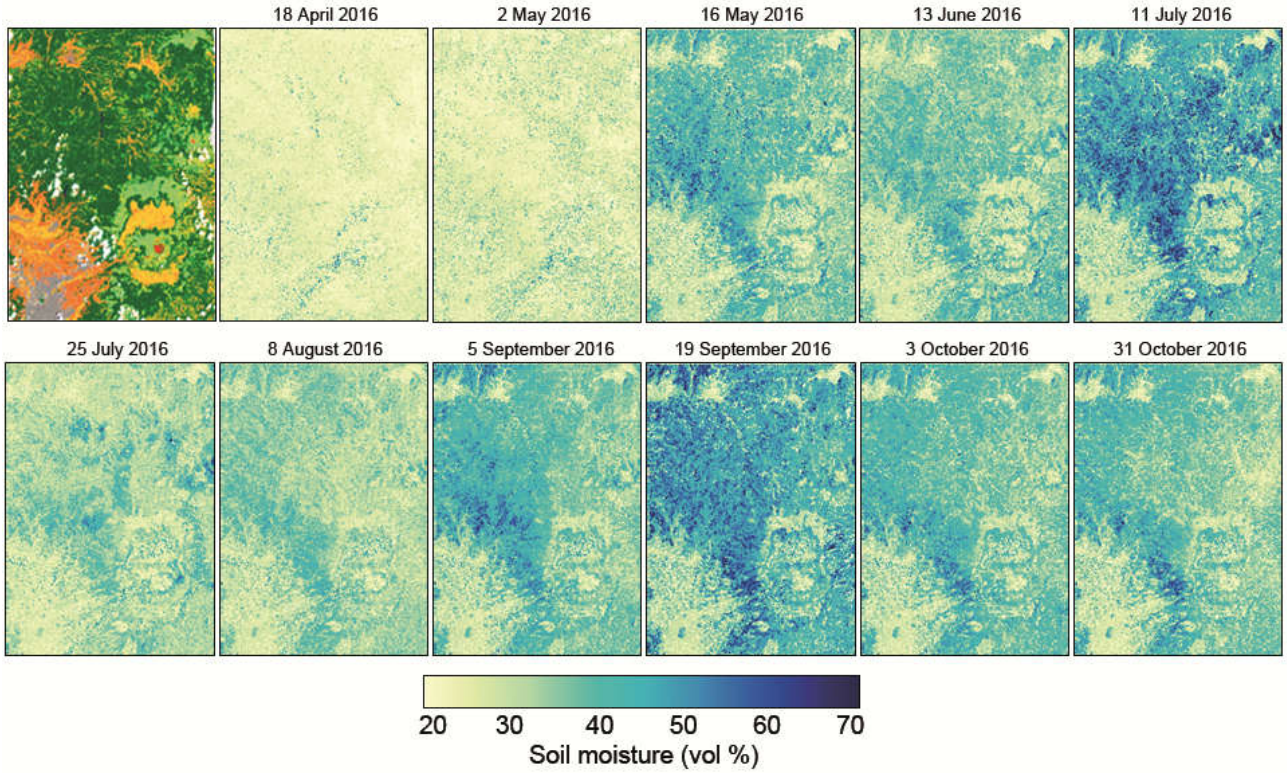

Further studies are necessary to understand the behavior of closure phases over different land covers. Surprisingly, the inversion seems to work best over forested areas, and is more difficult for agricultural surfaces. The topic is also relevant for the interferometric processing of distributed scatterers, since the presence of phase inconsistencies calls current phase history retrieval algorithms into question.

Selected publications: [350], [283]

3D Motion Reconstruction

Single line-of-sight deformation products, both single interferograms and time series, provide the projection of the ground motion onto a fixed direction and relative to a reference point. Many users and applications require full 3D motion reconstruction and higher order mechanical parameters, e.g. the retrieval of tectonic strain. In the context of Tandem-L studies we have developed first concepts for simultaneous mosaicking and 3D motion reconstruction from multiple lines of sight. From the 3D motion vectors it is possible to estimate the rotation and strain components of the deformation without ambiguity.

Strain (here: shear component) retrieval of Darwin glacier, Antarctica, reconstructed from TerraSAR-X interferograms with three different line-of-sight directions.

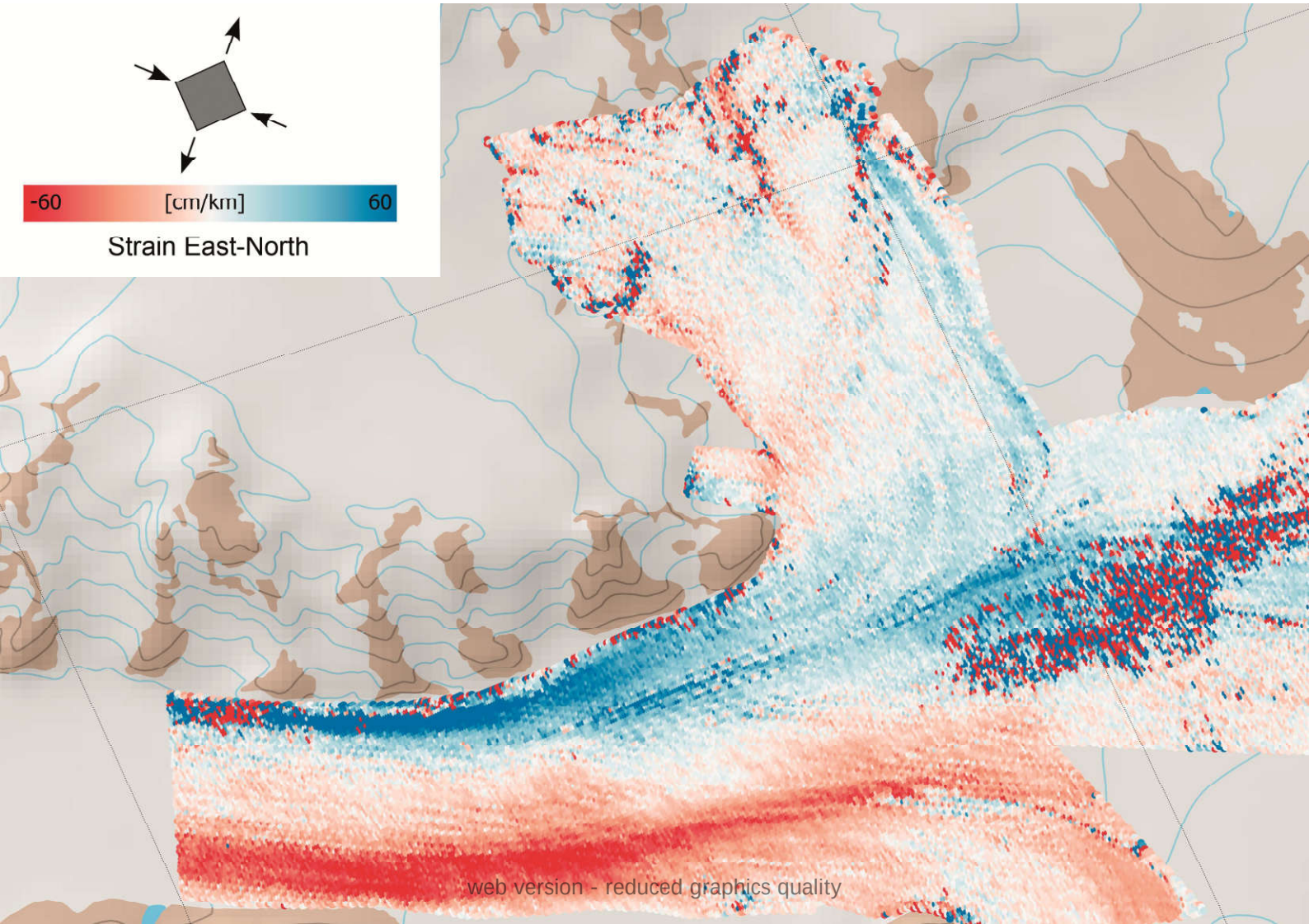

Unfortunately, current SAR missions do not routinely provide a sufficient geometrical diversity for 3D motion inversion. However, a dedicated experiment with TerraSAR-X left-looking acquisitions (in addition to ascending and descending right looking regular geometries) has provided the opportunity to reconstruct 3D motion over a deforming glacier. The experiment also provides the opportunity of testing assumptions (such as glacier flow downslope) that are normally necessary to retrieve the 3D motion when the geometric diversity is insufficient. The research results are incorporated into the Tandem-L observation and processing concepts.

Selected publications: [181], [20]

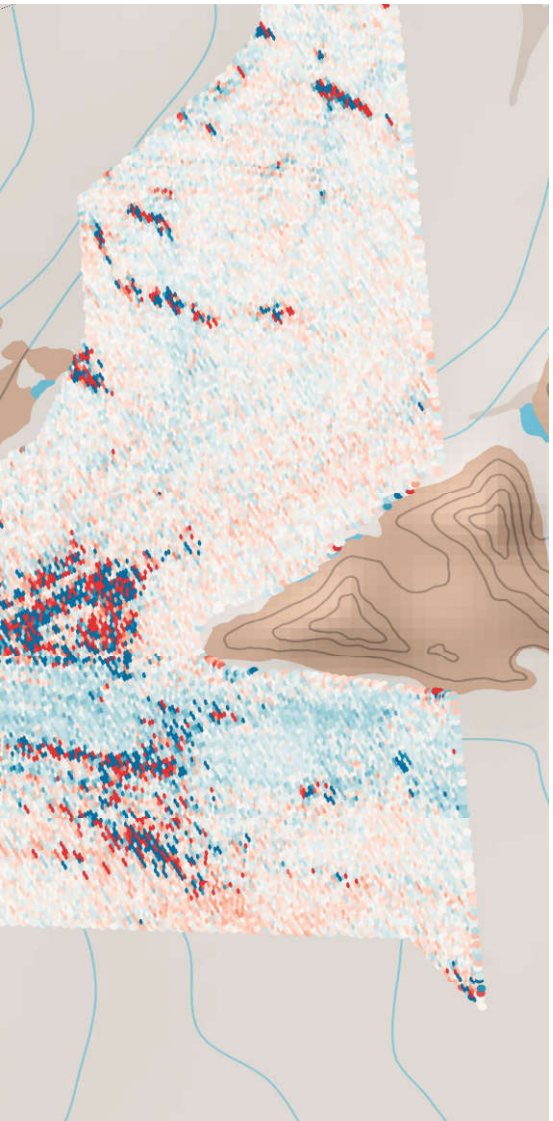

Large Scale Deformation Mapping Projects

Since the days of ERS-1, IMF's GENESIS InSAR library has been under continuous development as new sensors has been launched (TerraSAR-X, Sentinel-1, ALOS-2), sometimes with new acquisition modes (e.g. spotlight, TOPS). The development and operationalization of the Interferometric Wide Area Processor (IWAP) culminated in the generation of the nationwide PSI map of Germany for the Federal Institute for Geosciences and Natural Resources (BGR), derived from Sentinel-1 data. This project started in 2016 and will continue until 2019 with a series of updates of the deformation products (velocity and time series). For this project we applied for the first time operationally tropospheric phase correction based on ECMWF data and developed new mosaicking and GNSS-based calibration strategies to deliver a seamless product.

In mid-2016 a customised version of our processor was installed on the cloud based Geohazards Exploitation Platform (GEP) of ESA for the generation of InSAR products from Sentinel-1 acquisitions. The purpose of GEP is to demonstrate fully automated InSAR processing in order to support thematic experts monitoring earthquakes, volcanoes and floods. Since mid 2017, when a peak performance of 100 interferograms/day was reached, the service has been monitoring 40 % of all seismically active areas or 15 % of the Earth's land surface. The products, publically viewable in the GEP GeoBrowser, allow quick assessment of surface changes, most importantly any movement that occurred in the time between acquisitions – and this with centimeter precision.

SAR Tomography

Tomographic Reconstruction

Tomographic SAR inversion (TomoSAR), is the general process of reconstructing a 3D reflectivity cube of an imaged scene from multiple 2D SAR images acquired with different incidence angles, determined by the baseline distribution. Compared to medical CT, the 3D reconstruction in TomoSAR requires more complex algorithms because of the irregular and sparse sampling in the angular coordinate. TomoSAR is essentially a spectral estimation problem where for every range-azimuth pixel the reflectivity profile (and possibly its temporal variation) in the third dimension, *elevation*, must be found.

Typical applications of TomoSAR are 3D profiling of semi-transparent layers such as forest, ice or snow, as well as opaque and discrete 3D objects such as buildings and rock surfaces on mountains. During the recent years, we have been concentrating on the latter case, with particular focus on urban areas, where TomoSAR is equivalent to layover separation.

When using multi-temporal data stacks, we can not only determine the 3D position and reflectivity of objects, but also their deformation in the line of sight (sometimes called *differential* TomoSAR).

The elevation resolution and location accuracy of the tomographically reconstructed 3D objects is limited by the span and the distribution of the baselines. The narrow orbital tube of TerraSAR-X, e.g., limits the elevation resolution to about 40 m, which is much less than the 2D sub-meter resolution in the other two dimensions, range and azimuth. Therefore, one major challenge in our research was the separation of objects within this resolution limit. As a result, in the last reporting period, we developed a super-resolution technique named *SL1MMER* to distinguish two or more objects even if they are very closely located in one resolution cell. Even after several years after its invention, our SL1MMER algorithm is still state of the art in tomographic reconstruction.

SL1MMER is a compressive sensing-based algorithm. The price to pay for its high quality 3D reconstruction is the computational effort. Therefore, in this review period, together with UCLA, we developed a fast and accurate complex-valued basis pursuit denoising algorithm for super-resolving tomographic SAR. So far, we are the only group that is able to carry out compressive sensing-based tomographic reconstruction of an entire urban area from TerraSAR-X image stacks. In addition, we developed several extensions of the SL1MMER algorithm for reducing the number of images required for TomoSAR reconstruction while retaining the high accuracy. They are presented in the *Data Science* chapter.

Selected publications: [24], [337]

Staring Spotlight TomoSAR

Staring spotlight, a new mode introduced in TerraSAR in the reporting period, is characterized by an increased azimuth resolution compared to the conventional sliding spotlight. We first demonstrated the potential of this mode for TomoSAR by means of an interferometric stack with an azimuth resolution of 0.24 m. To this end, we tailored our interferometric and tomographic processors for the distinctive features of the staring spotlight mode. As a result of a first comparison between sliding and staring spotlight TomoSAR, the following was observed: The density of the staring spotlight point cloud is about five times higher and the relative height accuracy of the staring spotlight point cloud is approximately seven times higher due to the higher signal-to-clutter ratio and the lower pointwise layover probability.

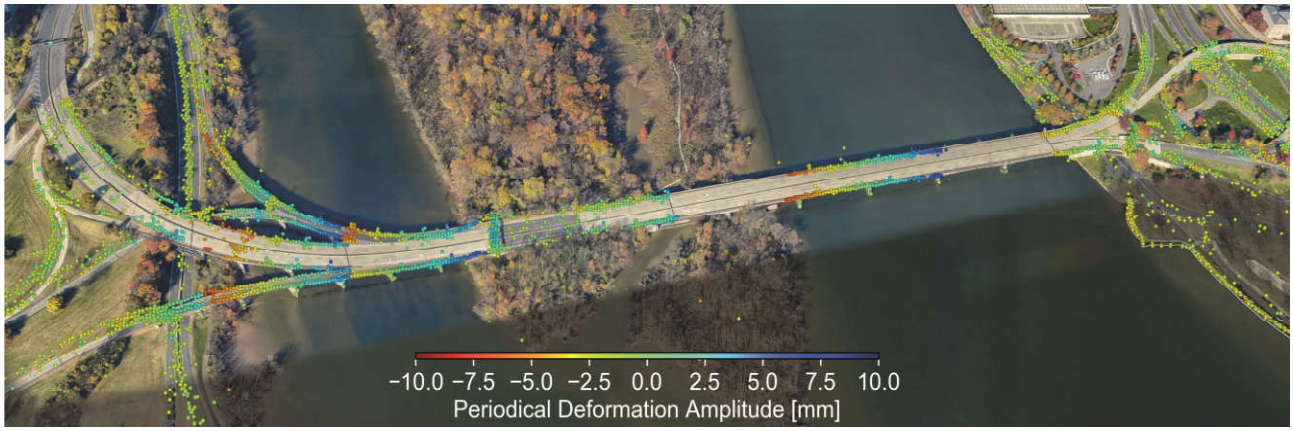

Deformation pattern of the Theodore Roosevelt Bridge in Washington, D.C., generated from a tomographic TerraSAR-X staring spotlight stack. Six percent of the reconstructed points are shown here, overlaid on the Google Earth 3D building model and color-coded by the amplitude of seasonal thermal deformation. The staring spotlight mode allows for very detailed monitoring of urban infrastructure.

3D Deformation Monitoring

SAR tomography, similar to its conventional counterparts, such as InSAR and PSI, is only capable to capture 1D deformation along the satellite's line-of-sight. We developed a method based on L1-norm minimization within local spatial cubes, to reconstruct 3D displacement vectors from TomoSAR point clouds available from, at least, three different viewing geometries. The method differs from the ones known for standard InSAR or PSI in that it benefits from the extremely high point density of TomoSAR and that it is more robust with respect to outliers due to its L1-norm minimization.

Selected publication: [223]

From TomoSAR Point Clouds to Objects

The scatterer density obtained from VHR TomoSAR is in the order of 0.6 – 1 million/km^2. The retrieved rich scatterer information from multiple incidence angles allows for the first time to generate 3D point clouds from spaceborne radar with a point density comparable to lidar. In the review period we developed a series of robust algorithms to reconstruct building façades and building roofs that can automatically run on a large scale. Very recently, we also carried out the first demonstration of 3D prismatic building model reconstruction using these spaceborne TomoSAR point clouds.

Selected publications: [399], [326], [239]

DefoSAR – TomoSAR Framework for Tandem-L

As mentioned in the *Sensors and Missions* chapter, Tandem-L is an exciting German space mission concept comprised of two satellites carrying L-band SARs. It can map the Earth surface in both high resolution and wide swath with an unprecedented accuracy. To prepare for Tandem-L, we developed the framework *DefoSAR* that is tailored for SAR tomography in urban areas using a minimum number of bistatic Tandem-L data. This novel generic framework exploits the property of data stacks, which consist of bistatic pairs (containing the undisturbed topography information) taken at different times (allowing for motion estimation).

First, the bistatic interferograms, together with geometric priors, are used for highly precise elevation estimation, requiring only a few images. These high-quality elevation estimates are then used as a deterministic prior in estimating deformation coefficients. In addition, deformation model order selection is introduced for avoiding overfitting.

As practical demonstrations, we tested our framework with TanDEM-X pursuit monostatic data. A high quality 4D TomoSAR point cloud of individual building façades can be reconstructed from only six interferograms, which shows the great potential of the proposed framework for bistatic SAR tomography with Tandem-L or other prospective bistatic or multistatic missions.

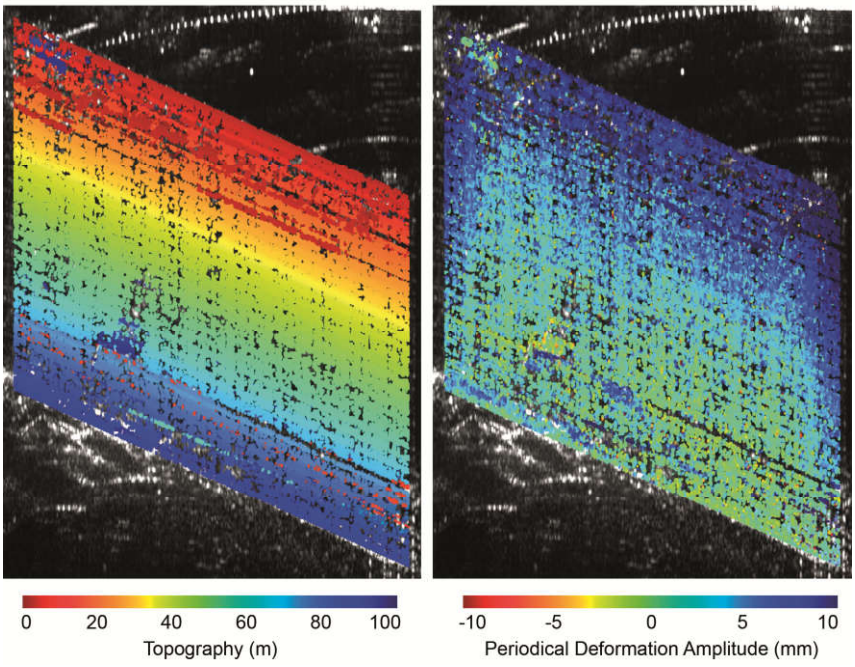

The DefoSAR framework: Topography (left) and amplitudes of seasonal motion (right) of a building façade estimated using only six TanDEM-X high resolution spotlight acquisitions.

Geodetic SAR Tomography

The abovementioned 3D building reconstruction using TomoSAR or large-scale deformation using PSI provide *relative* measures, with respect to some reference point chosen during processing. Although these relative measures are highly accurate, *absolute* positioning is often required in many geodetic applications. Therefore, with *geodetic SAR tomography* we combined the strengths of both TomoSAR and SAR Imaging Geodesy. For the first time, rather than retrieving only a sparse set of points, it has been possible to obtain detailed multi-dimensional maps with large coverage characterized by absolute geo-localization accuracy in the decimeter level and deformation estimation accuracy in the order of mm/a.

The ingredients of geodetic TomoSAR are Imaging Geodesy, stereo-radargrammetry and TomoSAR. In a first step, a set of common ground control points (GCPs) is extracted from geodetically corrected SAR images. Their absolute positions are then calculated by means of stereo triangulation.

Obviously, the best absolute positioning accuracy can be achieved with images acquired from cross-heading orbits (ascending and descending). However, common GCPs are difficult to identify in such configuration, because the SAR sensor sees opposite sides of an object.

To address this challenge, we developed a framework which first carries out the PSI/TomoSAR reconstruction of individual stacks from different viewing angles, and then identifies the reflection correspondences of certain objects in 3D space, finally projects these points back to the radar images. With this method and using meter resolution TerraSAR-X data, it is possible to identify thousands of such GCPs in a city. Once the GCPs are identified, the best candidates among them will be chosen to form the reference network for PSI/TomoSAR processing. After the TomoSAR inversion, the absolute height offset of the GCPs to the reference DEM is added to the heights of the relative 4D TomoSAR point cloud during the final geocoding phase, which results in absolute coordinates of the TomoSAR point cloud.

Due to the high accuracy of these geodetic TomoSAR measurements, they can be easily used to fuse TomoSAR point clouds acquired from different imaging geometries to an unprecedented accuracy or also to absolutely geocode imagery from different sensors. In particular, optical satellite images have notoriously high geolocation errors, and will benefit from the new methods. It also enhances the understanding and interpretation of the observed area/object and its motion due to ground subsidence or thermal dilation.

Selected publications: [258], [557], [60]

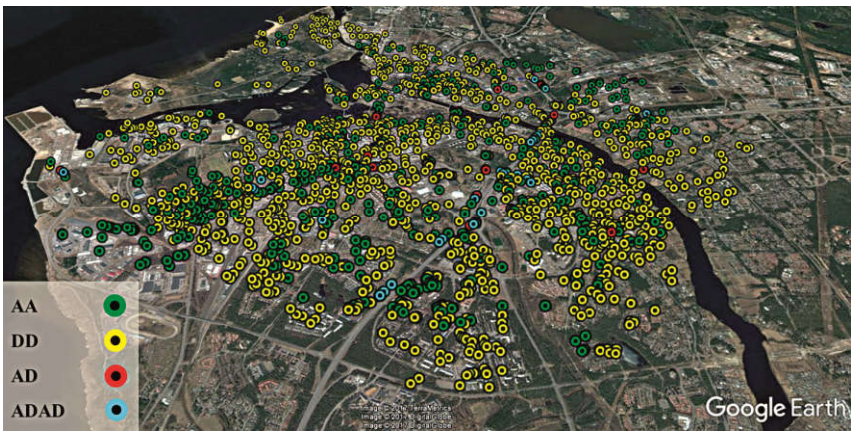

A total number of 2,049 ground control points found in Oulu, Finland, color-coded based on the geometry configuration used for their positioning. A: ascending, D: descending orbits.

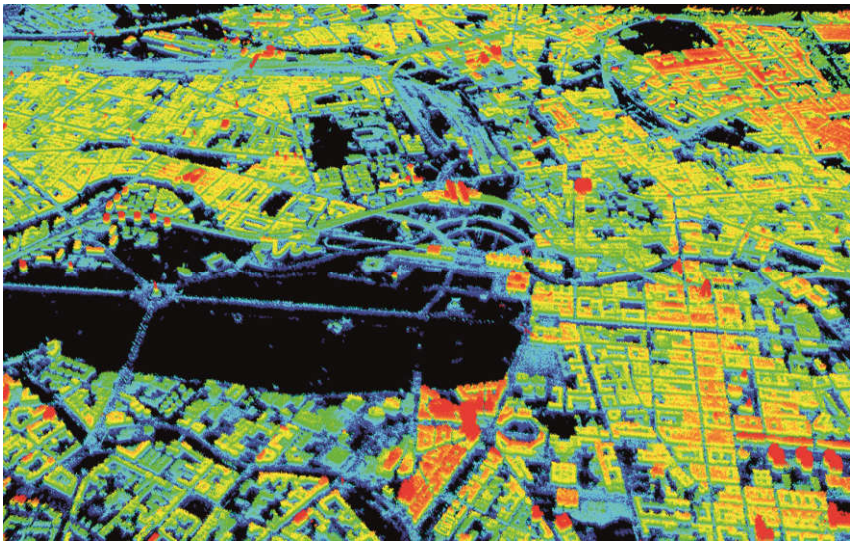

3D geodetic point cloud of Berlin reconstructed by geodetic SAR tomography. Although the absolute location cannot be directly seen in the figure, our experiments show an accuracy of about 20 cm in horizontal directions.

SAR Oceanography

Oceans cover more than 70 % of the Earth's surface and are of paramount importance for global processes in many domains. They are a source of nutrition, energy and other resources and a key element in global logistics and the transportation of goods. The character of the maritime domain is changing in response to societal, economic, ecological and technological development. Likewise, coastal population, ecosystems and technology have to adapt worldwide to changes in the oceans.

The dimensions and remoteness of the oceans, including sea ice regions at polar latitudes, are best observed by SAR satellite-based Earth observation. In this context, satellite data are favorable for both the generation of long-term time series to detect and monitor regional or global trends in the oceans, and the provision of near real-time (NRT) information to enhance maritime situational awareness for safety and security.

Responding to these challenges, DLR founded the Maritime Safety and Security Labs in Bremen and Neustrelitz in 2013. Our IMF team in Bremen develops methods to automatically derive information about the ocean from spaceborne SAR data, while the DFD team in Neustrelitz is responsible for the integration of our software into the operational data processing chain at DFD's ground station Neustrelitz and to adapt the user interfaces, if required. Due to our joint efforts we can provide the maritime community with up-to-date high-quality information almost instantaneously after the reception of the SAR data – often within 15 minutes.

A real challenge during development is achieving high accuracy and numerical robustness in a very short time to meet the NRT requirements of many safety and security related information services. That is why all of our methods are implemented in a single modular software suite called SAINT. This enables us to combine different product types during processing, increasing the quality of the results and reducing errors. SAINT is currently comprised of modules for wind and sea state parameter determination, surface film detection (e.g. oil), vessel detection and classification, coastline extraction, bathymetry estimation, sea ice classification, sea ice motion tracking, iceberg detection, and the discrimination of icebergs from ships.

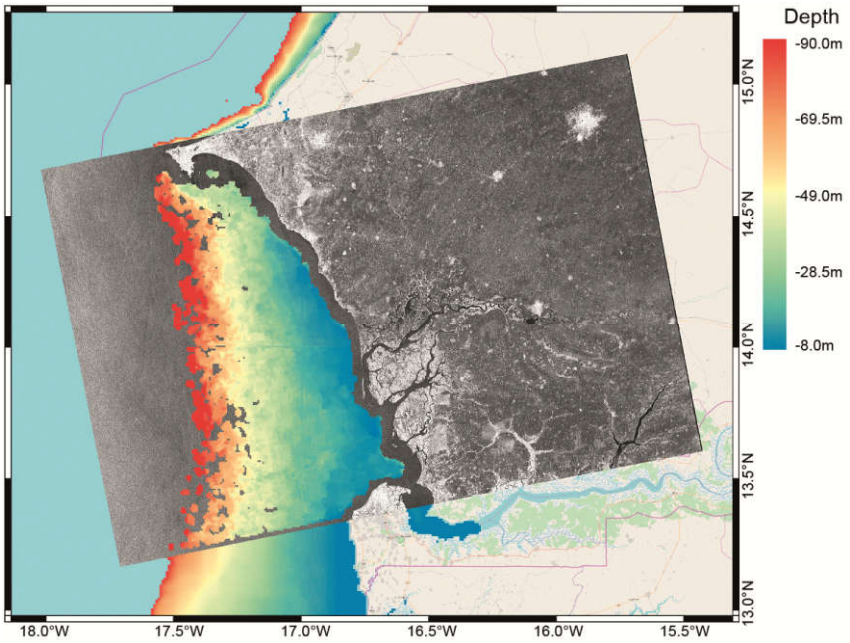

Retrieved bathymetry from a Sentinel-1 scene of West Africa. The depths shown outside the scene are from the GEBCO dataset.

Sea State and Bathymetry

Numerous ships are lost at sea each year in severe weather and heavy seas. Better forecasts and on-the-fly model validation with NRT satellite data could help to reduce the dangers to maritime traffic. Therefore sea state information derived from SAR data, particularly in combination with wind data, are most valuable tools for the validation and improvement of meteorology and physical oceanography models.

Established SAR-based sea state extraction methods fail for short waves or for high sea state due to limitations in the image resolution and nonlinear effects of wave motions such as velocity bunching and wave breaking effects that result in blurred signatures in the image. Therefore, we developed a new empirical algorithm that combines spectral with textural information to overcome this problem. The resulting high resolution sea state map is capable of resolving small-scale features like wave groups that were hitherto barely studied with regular observations over large areas.

With high resolution wave information, local variations of the lengths of visible long swell waves can also be interpreted to deduce the underwater topography between depths of 10 – 100 m, depending on the sea state conditions. Given that for large parts of the world's seas only coarse bathymetry information is available, a high resolution SAR-based information product can fill data gaps in many places. The method has been successfully validated and demonstrated in the EU supported H2020 project 'BASE-platform'.

Vessel Detection, Feature Determination and Target Classification

In order to detect illegal or harmful conduct (e.g. pollution, illegal fishing, piracy, smuggling and human trafficking) and to increase maritime safety in emergencies, monitoring of vessel activities is imperative. While a ship's automatic identification system (AIS) sends relevant information over up to 100 km, the device can be turned off, manipulated or may be beyond the range of coastal receivers. Hence, independent information derived from satellite SAR is needed to validate or complement AIS information. We have developed automatic algorithms to detect maritime

Ships and other infrastructure as they appear in TerraSAR-X imagery. Our neural network-based classification approach discriminates between these automatically, as shown in the confusion matrix.

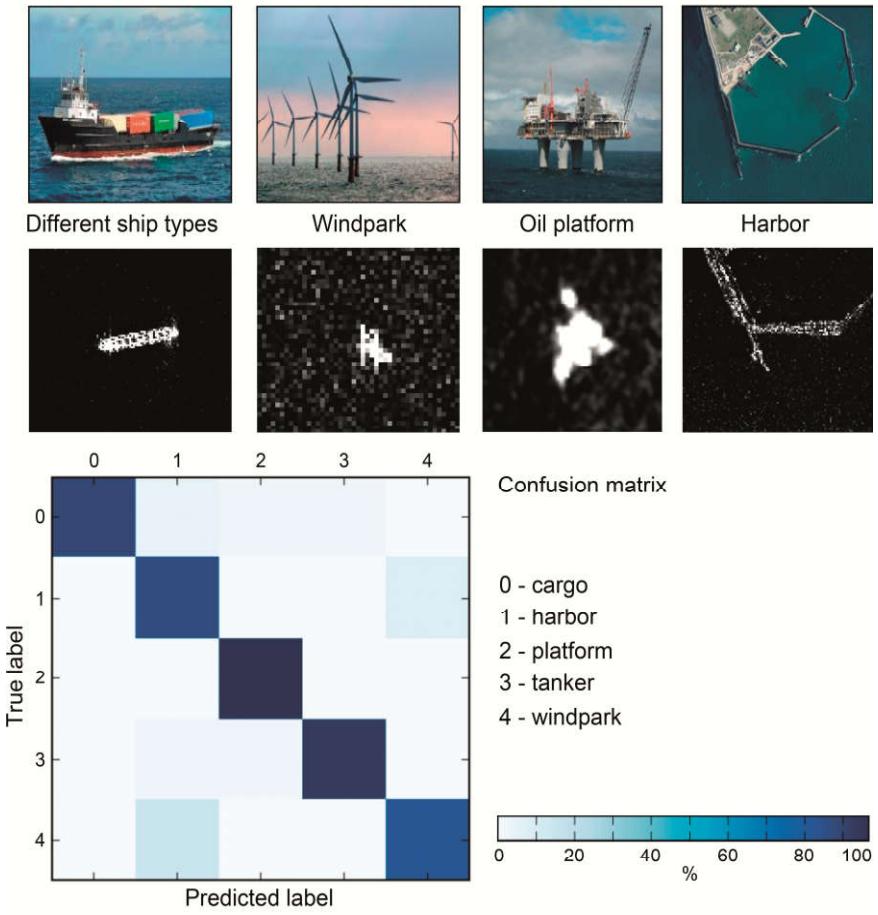

targets, apply artificial intelligence to distinguish between different vessel types such as cargo or tankers, and methods to estimate vessel parameters such as length, width, course and speed from the radar signature. Similar algorithms are applied for iceberg detection and to differentiate between ships and icebergs – a capability required by national ice services, because traditional airborne iceberg sighting regularly suffers from low visibility conditions. Satellite-based iceberg detection is a valuable, complementary and cost-efficient approach.

Surface Film and Oil Detection

Oil is present on the seas in large quantities. It propels ships, is transported by tankers and produced on offshore oil rigs. However, if released into the open seas intentionally or by accident, it creates a surface film and becomes a severe threat to the marine and coastal ecosystem.

Such surface films change the surface tension and smooth capillary waves. They are hence easily detectable as dark areas in SAR imagery. However, natural films like algae occur alongside oil and distinguishing between both types in an automated process is challenging and not entirely reliable. We developed new approaches exploiting the most significant polarimetric features with neural networks to improve automatic surface film classification from 82 % to 90 %. Furthermore, we combined information from different microwave bands where available to further increase classification accuracy.

Ocean Winds and Waves

Wind retrieval from SAR data exploits the influence of wind-induced sea surface roughness on the observed radar backscatter. It has been used for many years for the generation of global wind and wave fields.

Our new high resolution wind information product based on TerraSAR-X data reveals small features never before seen. For example, it shows the shadowing effects of offshore wind turbine arrays on adjacent wind parks, and can be used to quantify and predict the electric power reduction caused by these effects. Cross-validation with ground based lidar systems has shown that the wind information and particularly the lateral wind variations induced by obstacles such as wind turbines at greater heights can indeed be inferred from wind speeds at sea level.

Sea Ice Information

The Arctic is receiving increased attention as during the summer months the Northwest and Northeast passages become accessible for commercial shipping and oil and gas exploration. However, navigation in ice-infested waters is challenging. Especially at high latitudes, where the infrastructure for rescue operations and counter measures after environmental disasters is extremely sparse, the safety of ships and maritime infrastructure is of great importance. This has also been acknowledged by the International Maritime Organization in the latest International Code for Ships Operating in Polar Waters (Polar Code), where the need for up-to-date and precise sea ice and meteorological information is identified as the core element for safe navigation in ice-infested waters.

To provide the maritime community with detailed information on the current sea ice condition we developed methods exploiting textural and polarimetric features for X-, C- and L-band SAR to distinguish between different ice types. In addition, a new algorithm has been developed that calculates high resolution ice drift fields on the basis of consecutive SAR acquisitions by the same or different SAR sensors. The algorithm estimates drift vectors in sub-pixel space by applying pattern matching techniques.

Picture taken during the Antarctic Circumnavigation Expedition (Dec 2016 – Mar 2017) on board the Russian research vessel Akademik Treshnikov. DLR supported the campaign with SAR acquisitions, sea state parameters and sea ice classes in near real time.

A comparison with drift buoy data confirms that resulting drift vectors have an accuracy 2 – 4 times better than the resolution of the input image data. The information gained is extremely useful for ship routing at high latitudes. First, divergence and convergence zones can be identified based on the drift vector field, revealing the position of emerging open leads and compressed ice ridges and representing areas of lowest and highest ice resistivity, respectively. Second, the measured drift data forms the basis of short-term predictions on ice drift, which enables crews to anticipate dangerous situations in advance and take appropriate actions, or avoid unnecessary detours. Finally, the fusion of drift and ice type information can help to identify key factors which determine ice motion and to improve model-based forecasts of ice dynamics. The developed methods have been implemented in software prototypes in DFD's receiving stations NRT environment and are tested by supporting diverse polar expeditions such as the German research vessel *Polarstern* campaigns led by the Alfred Wegener Institute with EO-based ice information in exchange for valuable and rare in-situ data.

Selected publications: [198], [317], [240], [241], [333], [227], [329], [249], [535]

Optical Imaging

Optical Imaging

Within the reporting period optical imaging by spaceborne and airborne sensors has been a dynamic field of research and development. Three trends have boosted its application potential: the growing availability of data through more and higher-quality missions (including the Copernicus program and new satellite constellations), rapid developments in machine learning and increased computer power. This chapter presents highlights of our methodological and application-oriented developments for automatic geoinformation extraction from optical or fused data sets in the following topics:

- **stereo and 3D processing**
- **hyperspectral data analysis**
- **atmospheric correction**
- **real-time methods for imagery from airborne sensors**
- **thermal image processing.**

In contrast to SAR and atmospheric sounding, there was neither a German nor a European long-term optical remote sensing mission line for which we could have been commissioned to develop the operational processors. Therefore, our research focus had always been on data analysis algorithms applicable for a broad variety of sensors. This situation changed with DESIS and EnMAP, where we lead the ground processing system development, and with Sentinel-2 which is becoming the multi-spectral data source of the future.

3D stereo imaging from space: The generation of digital surface models from VHR spaceborne satellite data (here WorldView-3 with 30 cm pixel size) allows unseen highly detailed realistic representations of city models from space. In this case (suburb of Muscat, Oman) oblique views with approx. 45° viewing direction have been acquired and used for texturing the building façades (image was generated in collaboration with GAF AG, based on data from DigitalGlobe © 2014).

Stereo and 3D Processing

The generation of Digital Surface Models (DSMs) from optical stereo data has a long heritage at IMF. Starting from the first space mission using a digital stereo camera (MOMS) in the early 90s, continuous improvements in stereo image matching have been the focus of our research. Our strategy is to not only generate the best possible DSMs using the latest computer vision methods, but also to derive higher-level information such as 3D changes, DTMs, building footprints and full 3D models, e.g. for urban planning or disaster management.

DSM Generation

Several methods and improvements for the generation of DSMs from airborne and spaceborne optical stereo data have been developed at IMF. The DSM generation process starts with image orientation using bundle adjustment with or without reference data such as reference images, reference DSM or ground control points. The oriented imagery is then further processed by pairwise dense matching using regularization through energy minimization of a cost function. This includes a pixel similarity data term, such as Census, Mutual Information or CNN-based cost functions, as well as an edge preserving smoothness term, which allows robust and detailed reconstruction of the surface presented by flat areas, buildings, vegetation etc. For operational processing, we developed a novel variant of the well-known Semi-Global Matching (SGM) algorithm. Our modifications to standard SGM include a robust hierarchical search strategy that dynamically reduces the search range for flat areas and results in faster computation and denser DSMs, as well as a combined data term employing several cost functions.


web version - reduced graphics quality

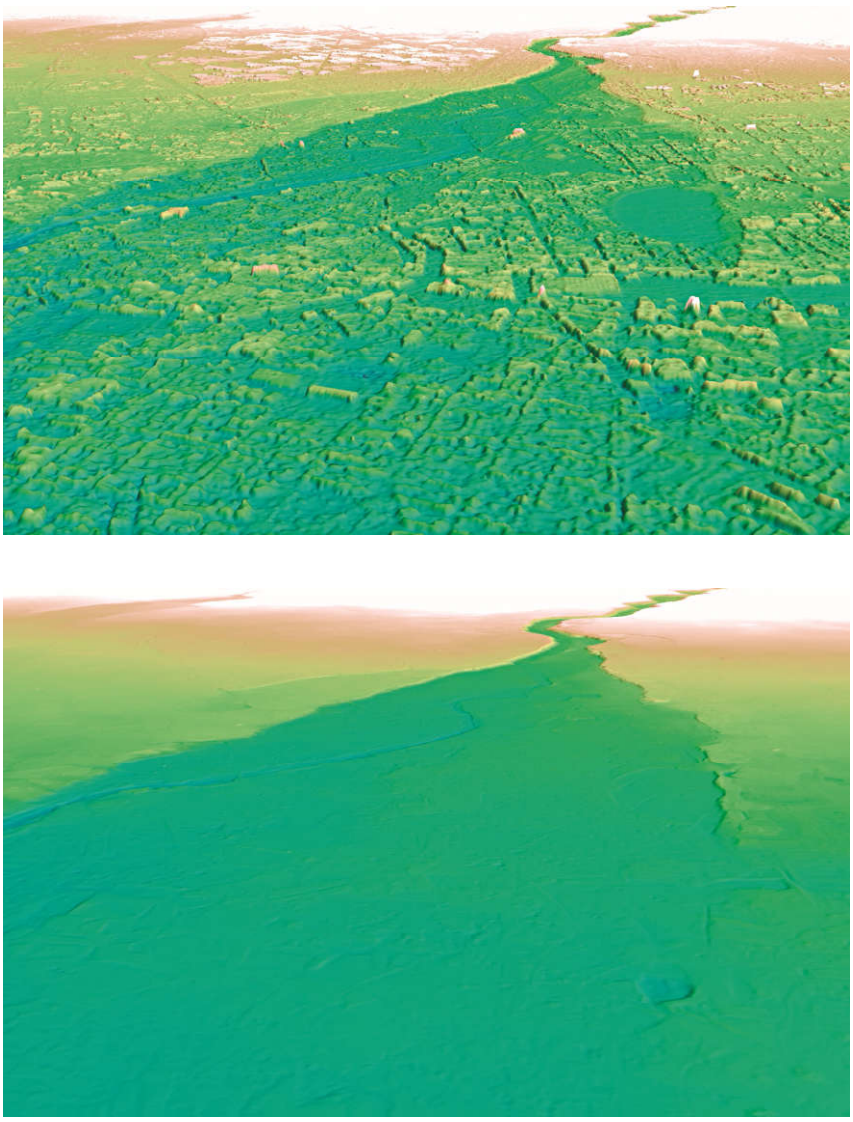

DSM (top) to DTM (bottom) generation using Deep Learning.

These algorithms can be applied to data from almost all satellites capable of capturing stereo data, as well as aerial and UAV-based data. Our processor supports single stereo pairs and triplets as well as modalities where thousands of images need to be processed. It is used in many projects at DLR, providing important 3D information on both coarser resolutions for topographic purposes or high resolution models of difficult areas from the Earth's highest mountains to very dense city centers. For example, the stunning virtual images in the Book 'm⁴ Mountains', authored by DFD together with Reinhold Messner, have been generated by our processor using VHR triple stereo DSMs.

Our software is licensed to GAF AG, Munich, who very successfully applies it to produce satellite-based stereo DSMs for commercial applications, including continent-wide 5 m resolution DSMs from Cartosat-1 stereo imagery. Elevation models from VHR satellites with a resolution of up to 30 cm are especially successful in the commercial market.

Selected publications: [129], [163], [281], [228], [397]

Digital Terrain Models

The generation of DSMs is just the first step in extracting geoinformation from stereo imagery. Further steps are deriving digital terrain models (DTMs) from DSMs, extracting building outlines and roof shapes, reconstructing forest and plant shapes and using 3D information for improved automatic change detection.

For many applications a DTM, representing the ground without objects like buildings or trees, is needed rather than a DSM. The derivation of a high-quality DTM from an existing DSM and optionally ortho-imagery is still a challenging task. In recent years many existing approaches such as hierarchical filtering or extended morphological filtering were improved and new methods such as height step detection have been implemented. However, these traditional model-based algorithms have been difficult to apply in a generic sense as they require scene specific parameter tuning, especially when using DSMs generated from satellite stereo data, which contain higher noise and no last-pulse information present in lidar point

clouds. Thus, they cannot be applied as part of an automatic processing chain when performing large scale processing. Recent approaches based on Deep Learning, especially Conditional Adversarial Networks (see *Data Science* chapter), together with the increasing availability of lidar reference data for training allow robust and high performance filtering of DSMs. We developed a new methodology based on extensively trained nets which leads to robust DTM generation and even outperforms DTMs from official authorities. A further advantage is the very high level of automation which requires only a low level of manual improvements in final editing.

Selected publications: [62], [550], [328], [445]

Building Footprint Generation and Refinement from VHR Stereo Data

Although the DSM matching algorithms are highly developed a full reconstruction of 3D building models from, e.g. WorldView-2, satellite imagery is still challenging. This is due to the limited resolution that leads to blurred building edges in the DSM. Using additional multi-spectral and panchromatic images is therefore recommended to remedy the deficiencies of DSMs and to achieve real 3D models of buildings. After masks are generated by simple thresholding of the DSM, an effective first step is to use machine learning for improving the footprints. Based on the advantages of fully convolutional networks (FCNs, see *Data Science*), we developed a hybrid FCN which effectively combines spectral and height information from the different data sources and automatically generates a full resolution binary building mask. Our architecture consists of three parallel networks merged at a late stage,

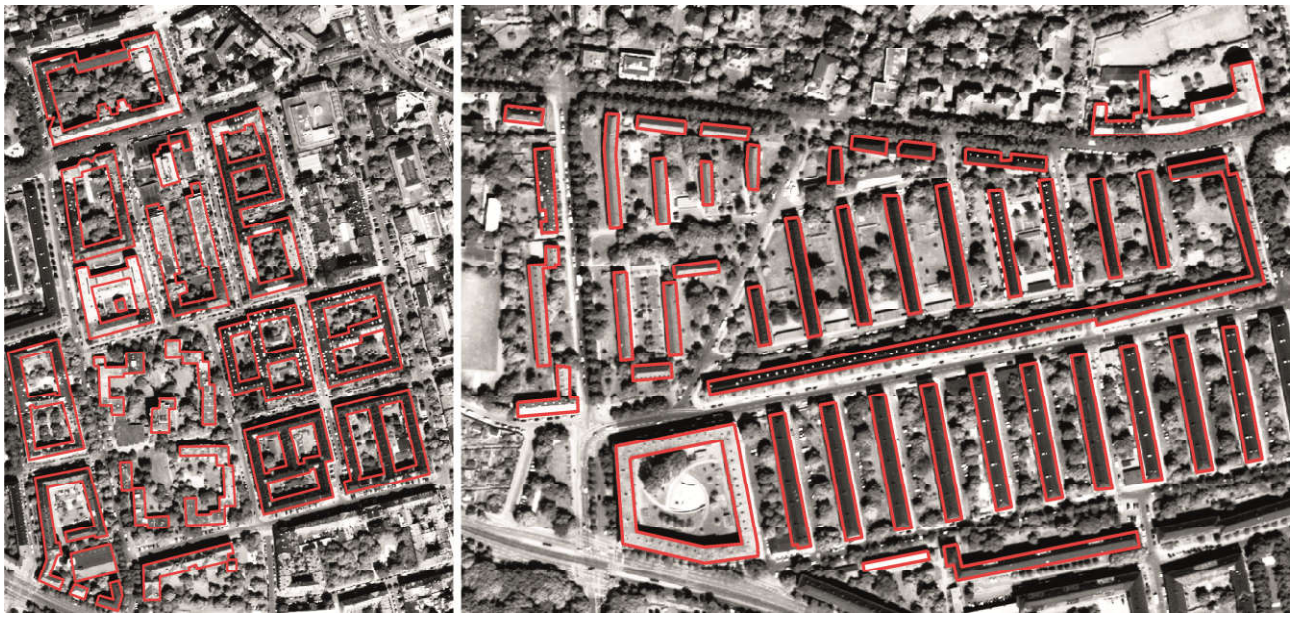

Two examples of different complexity for final results of building boundary extraction in Munich.

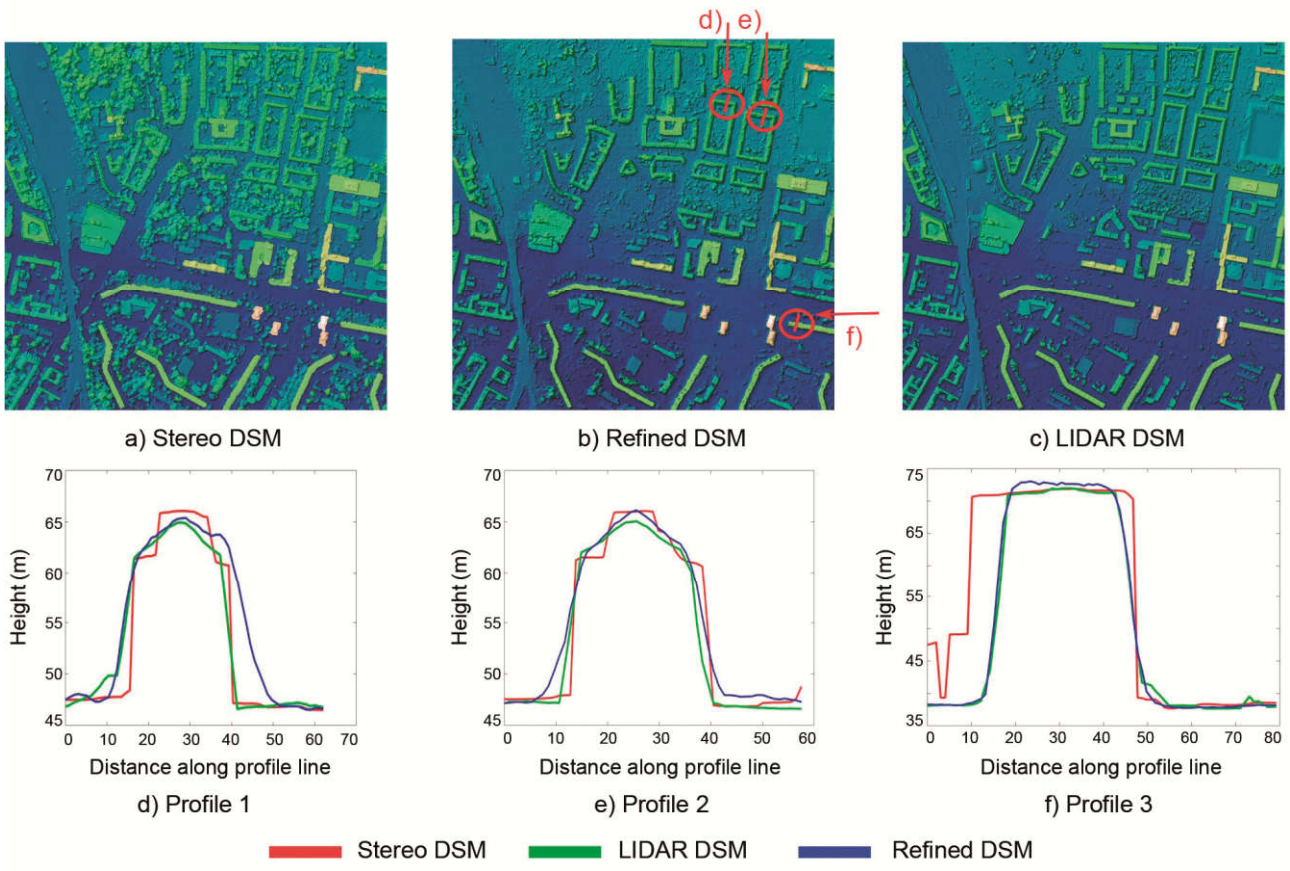

Improving DSM shapes of VHR images by a Generative Adversarial Networks (GAN) trained on very high resolution lidar DSMs.

which helps propagating fine detailed information from earlier layers to higher-levels, in order to produce an output with more accurate building outlines.

After a refinement step a rough building linear outline extraction is performed followed by line simplification. The results show that mask refinement with FCN can increase the precision of the extracted building outlines by up to 25 %, proved by comparing it with the *Polygons and Line Segments* metric to state-of-the-art methods. After line segment regularization and connection steps, the precision even increases up to 35 %. These results have been achieved for different city areas in Europe.

A method for improving all DSM properties (not only footprints) from satellite data is to use higher level DSMs, e.g. from airborne lidar data, to learn the shape of buildings by Generative Adversarial Networks (GANs, see *Data Science* chapter). As the lidar DSM was generated from last pulse data there is nearly no vegetation within the scene in comparison to the stereo DSM. The results demonstrate that the geometric structures of buildings from stereo DSMs are better preserved in the generated samples and their appearance is closer to that in the lidar DSM. Besides, the network has learned about the non-existing vegetation from these data, leading to its elimination in the improved stereo DSM. By investigating the profiles of selected buildings, we can confirm that the GAN successfully learned and refined the 3D building representation close to that of a lidar data representation.

Roof Type Classification

For classifying a roof as one of the main roof types (e.g. flat, gable, half-hip, hip, mansard, and pyramid), we developed an image-based classification using two pre-trained deep networks, VGGNet and ResNet. The junction points of the footprint mask are projected onto the pan-sharpened satellite images. The results are promising with an accuracy higher than 80 % for most roof types. To reconstruct even complex roof shapes, a decomposition of the building outline splits it into simpler rectangular shapes. The roofs are finally modeled by using an optimized selection of the overlaying rectangles.

Selected publications: [595], [144]

3D Change Detection

Automatic change detection using DSMs for urban and forest applications is a long-term focus of our research. Information on change can play an important role in different applications such as disaster assessment (e.g. after earthquakes) and urban construction or destruction monitoring. Change detection methods using only optical imagery rely on changes related to the reflectance values and/or local textural changes, which are often insufficient when dealing with changes in the vertical direction. On the other hand the limited quality of DSMs generated from spaceborne stereo imagery hinder reliable change detection using only DSMs from different acquisition times. Therefore, depending on the DSM quality, multispectral channel availability and change detection requirements we have developed several approaches for automatic change detection for urban and forest areas by fusing changes from DSMs and optical images.

As one of the highlights, the belief functions including Dempster-Shafer theory and Dezert-Smarandache theory have been adopted and further developed for 3D building change detection. In the proposed fusion model, change indicators are automatically extracted from the images and the DSMs, and projected to a sigmoid distribution to provide the initial basic belief assignments as indications of changes.

We have studied the possibility of using high temporal resolution stereo VHR images to enhance remote sensing image interpretation in the context of building change detection. A spatiotemporal inference filter has been developed by IMF considering the spectral, spatial and

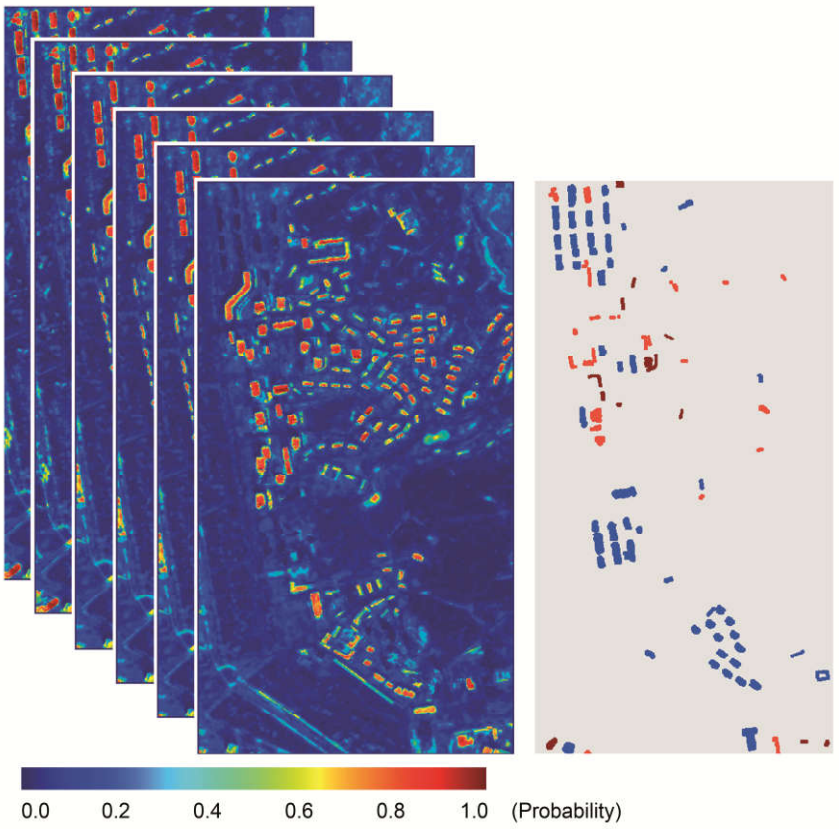

Building change detection in VHR satellite stereo image time series. Left: time series building probability maps, right: detected change class map, blue: built before 2009; yellow: built between 2009 and 05/2010; orange: built between 05/2010 and 01/2011; dark red: built between 01/2011 and 05/2011.

Classified roof types. Green: gable, blue: half-hip, red: flat, yellow: hip, light blue: mansard, pink: pyramid roofs.

temporal aspects to enhance the building probability maps. The aim is to homogenize the building probability values, while being robust to the silhouette of the objects and geometric discrepancies of the multitemporal data. Subsequently, the improved time-series building probability maps are analyzed to highlight changes in buildings and identify the type of changes. The method proposed has been successfully evaluated by performing an experiment on six stereo pairs of the same region over a time period of five years.

Another important DSM and 3D change application is to monitor forest vertical structures over large areas. For quantitative analysis of forest 3D properties we used various spaceborne and airborne sensors: WorldView-2, Cartosat-1, PRISM, RapidEye, aerial stereo and lidar data. In addition to a statistical comparison, their performance in monitoring forest changes has been assessed. In particular, DSMs from WorldView-2 and aerial data have been analyzed by adopting them for forest 3D structure monitoring to perform canopy gap detection, single tree segmentation and tree species classification. We found that large area 3D forest change can be assessed with nearly the same accuracy when using lower resolution data like Cartosat-1 in comparison to aerial or WorldView-2 data. The reason is the structure of crown surfaces which are displayed similarly in DSM with 5 m and with 1 m spacing for forest canopies.

Forest canopy gaps are an important parameter in forest management: automatic gap analysis is based on DSM, multispectral aerial camera and WorldView-2 data.

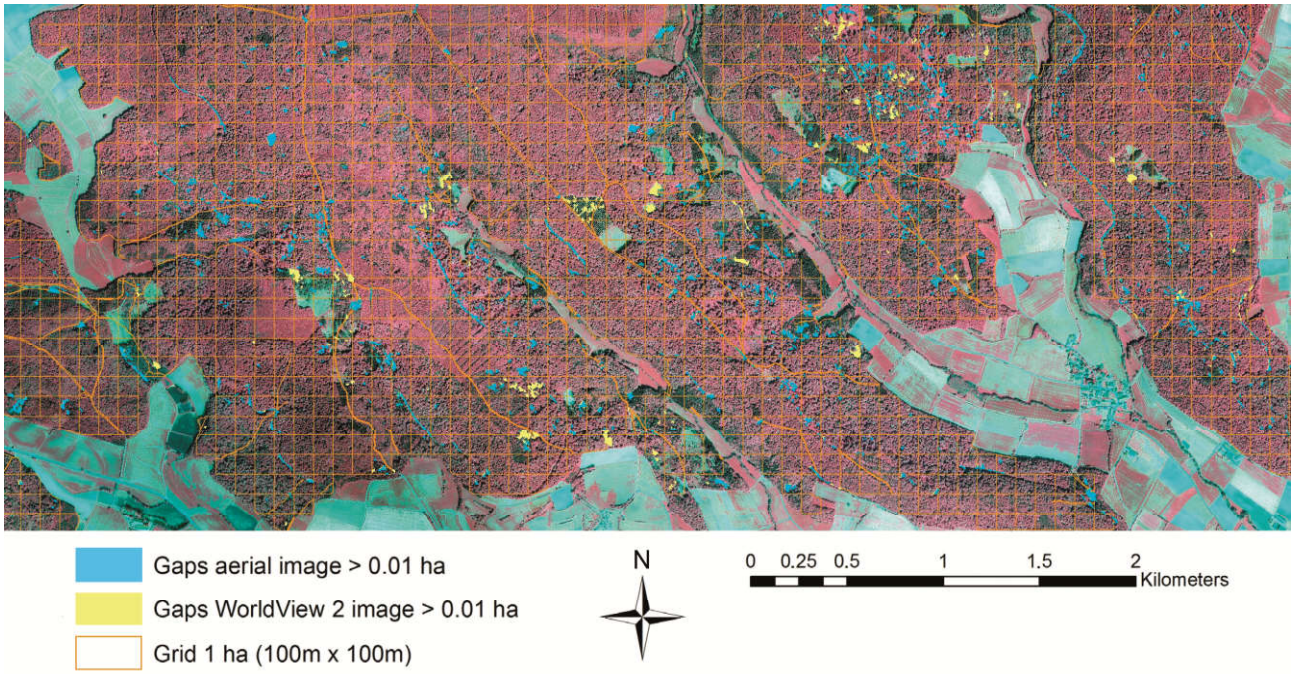

In a recent project we also study close-range 3D analysis of trees: If very high resolution aerial or close-range stereo/multi-view imagery is available, we can model or even reconstruct 3D plant architecture. This is useful for assessing tree health condition (e.g. drought stress) through characterizing the different orientation behavior of leaf or branch structures.

Selected publications: [163], [229], [393], [446], [445]

3D from UAV Data

Image data acquired by UAVs can provide richer details and additional views to complement DSMs from airborne or satellite data. However, the application of UAV images is limited by their low geo-referencing accuracy. Therefore we developed a robust methodology to co-register UAV images with high-accuracy to airborne images. In face of their large differences in view, scale and appearance, traditional matching methods fail to detect reliable matches. The novel matching approach includes a dense feature detection scheme, a one-to-many matching strategy and a global geometric verification scheme which is able to detect thousands of reliable matches.

These matches are used to geo-register UAV image blocks to the airborne images within 10 – 20 cm ground sampling distance.

After co-registration, the UAV images not only exhibit high local accuracy but also present rich information on the building façades. We developed algorithms and a framework to leverage the semantic information of UAV images to optimize the footprints in OpenStreetMap (OSM), as one application.

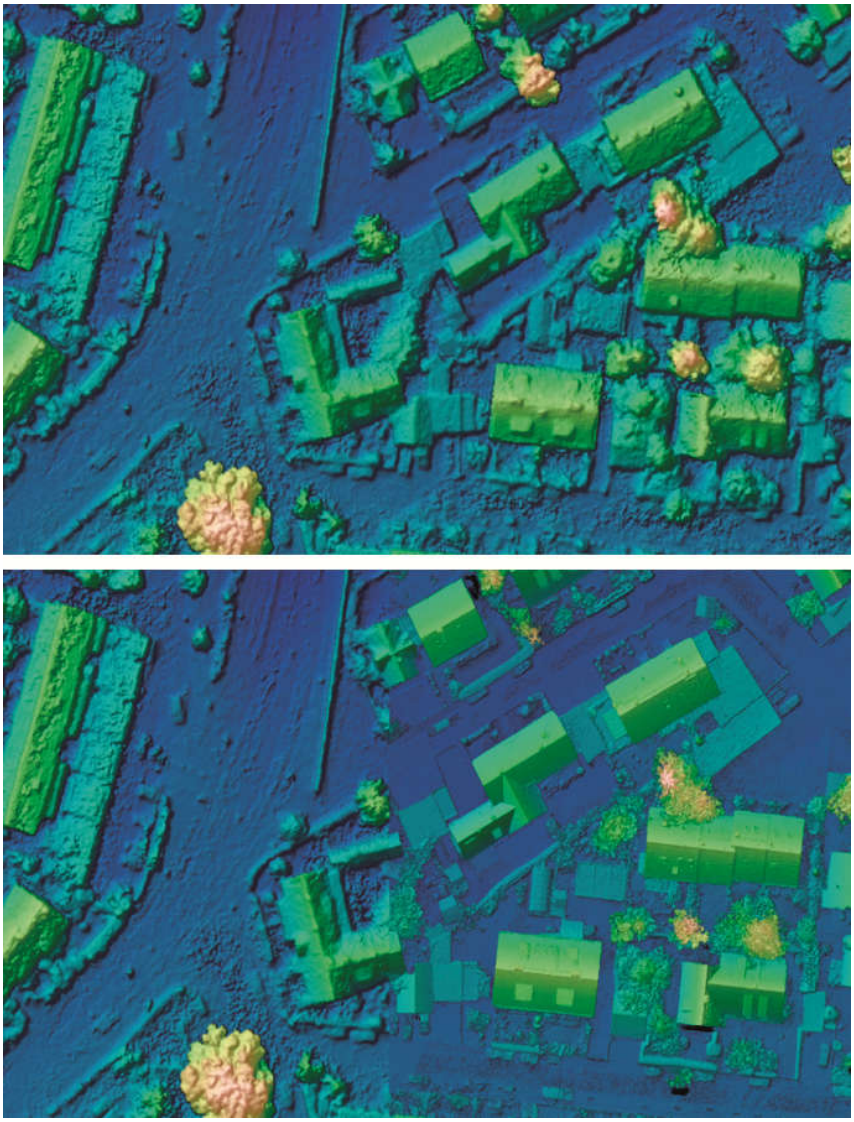

Comparison of automatically derived DSMs, result using only the aerial DSM (top) and fused DSM using Aerial and UAV data (bottom). On the right side of the latter the strong improvements in details of the roofs can be seen.

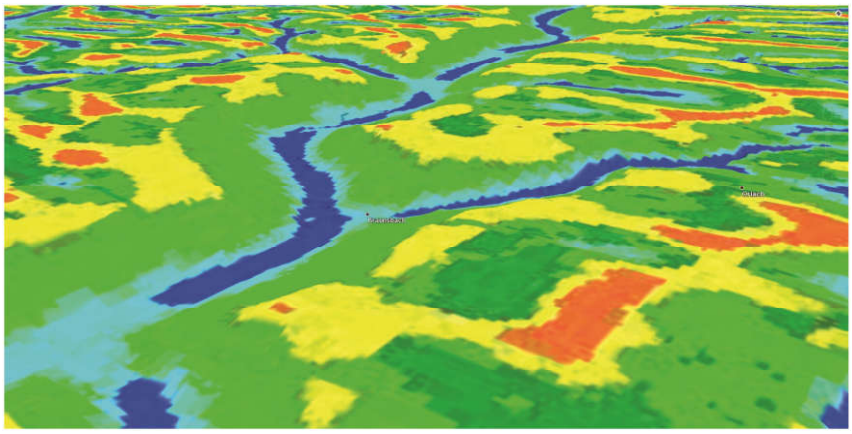

3D view Braunsbach, Germany: Strong rain endangerment classes. Red: ridge, orange/yellow/light blue: high/middle/low slope, blue: sink, green: flat

First, we obtain semantic information from UAV images via deep learning-based segmentation. Afterwards, we extract the boundaries of building segments as contour evidence. In parallel, a 3D building sketch is initialized from the OSM footprint and a DSM. Under the constraint that the image projection of the 3D building sketch fits the contour evidence, the OSM footprint and building height are optimized. Furthermore the building facades are generated from the oblique looking UAV iimages.

Selected publications: [83], [176], [620]

Application: Strong Rain Risk Estimation

In a project with a German insurance company funded by DLR Technology Marketing the influence of terrain on strong rain events has been investigated. The methodology developed was calibrated and verified using damage information from the insurance company. It reveals a very good correlation of both probability and damage cost caused by strong rain far from rivers. The method uses the so-called terrain positioning index on 25 m SRTM-DSMs. The resulting classes (ridge, high/middle/low slope, sink and flat) show an over three times higher probability in class ‘sink’ to be affected by damage due to strong rain than class ‘ridge’. Damage cost are more than seven times higher. Using our methodology and processing a strong rain vulnerability map of Germany, Austria and Switzerland was licensed to a company providing real estate information to finance companies for risk assessment.

Hyperspectral Data Evaluation

In preparation of the space missions DESIS and EnMAP we have considerably intensified our research in hyperspectral data analysis, in particular in spectral unmixing, data fusion for image sharpening and denoising. In the period under review we were awarded two hyperspectral experts as Humboldt fellowships, highlighting our attractivity as a center for methodological hyperspectral data research.

The richness of the fine structured spectral information of hyperspectral data comes at the cost of a moderate spatial resolution (typically 30 m from satellites) and requires new algorithmic approaches. On the one hand, a single resolution cell often contains several materials, making their identification and quantification a paramount pre-processing step for most hyperspectral application. This concept is known as spectral unmixing, and can be improved by embedding in the process sparse priors, derived from compressive sensing theory.

On the other hand, future years will witness the availability of spaceborne sensors acquiring simultaneously hyperspectral, multispectral and panchromatic images at different spectral and spatial resolution on the same focal plane. We are ready to meet the foreseen demand for products combining the detailed spectral information of hyperspectral sensors with the higher spatial details observable in multispectral sensors. This can be achieved by developing state-of-the-art data fusion algorithms, along with innovative image enhancement methods such as denoising, also based on sparse representation and regularization of such complex signals. Data fusion can also be carried out at feature or decision level: we yearly test the efficiency of our algorithms in the annual IEEE GRSS Data Fusion Contests where, since 2013, we won twice, came second twice and came third once, in spite of the steadily growing number of competitors.

Selected publications: [151], [84], [150], [11], [273]

Declouding within Image Time Series

The analysis of Satellite Image Time Series (SITS) is often hindered by the presence of clouds within a multitemporal stack, which makes it difficult to observe the evolution of a given ground cover in time. Exploiting the inherent high dimensionality of multispectral SITS, it becomes possible to use algorithms originally defined for hyperspectral data processing to solve this problem. We propose the use of sparse spectral unmixing, which

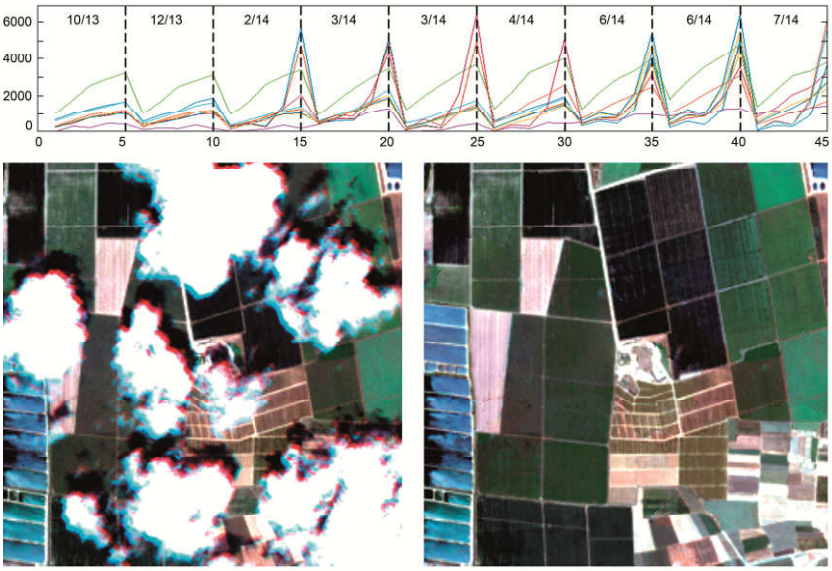

Cloud removal in satellite image time series: Sample result of cloud removal based on sparse reconstruction from random measurements using spectral/temporal object signatures. Top row: Sample basis vectors for the synthesis of pixels covered by clouds, represented in radiance as a function of five spectral bands (blue, green, red, red edge, and near infrared) and acquisition date (nine scenes with dates shown in the top graphic). Bottom row: true colorRGB composite of cloudy image (left) and result of the proposed cloud removal algorithm.

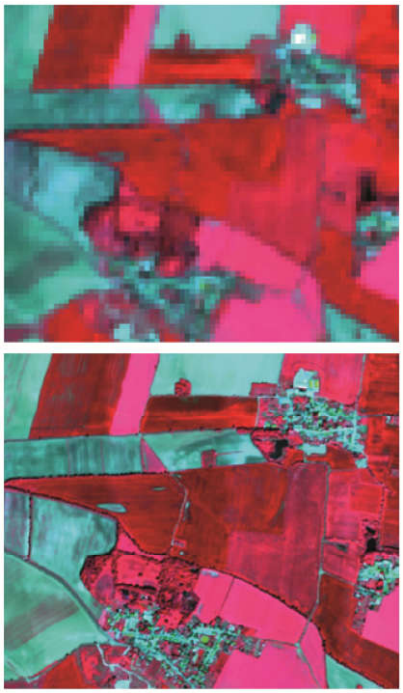

Hyperspectral image sharpening: Fusing low spatial resolution hyperspectral images (top) with high spatial resolution multispectral images increases the resolution of the hyperspectral images substantially (bottom). Since this fusion algorithm includes spectral unmixing, the spectral fidelity of the results is higher than those of conventional sharpening algorithms.

decomposes hyperspectral image elements into a fractional abundance of reference spectra related to the materials present in a given scene, to perform inpainting of cloud-obscured areas in SITS. In our case, a spectrum in hyperspectral analysis becomes a spectro-temporal pattern, conveying information on the spectral evolution of an image element on the ground. Areas obscured by clouds are represented as linear combinations of a large set of pixels randomly selected from the image in cloud-free areas. The method exploits the full spectral and temporal information of each image element along with their spatial correlation, leading to convincing reconstructions of areas affected by both real and simulated clouds. The transition between cloud-free pixels and reconstructed regions is seamless. Analysis shows the higher reconstruction compared to state-of-the-art methods.

Selected publications: [186], [277], [345]

Denoising of Hyperspectral Data

Spectral unmixing is also exploited by our development called *Unmixing-based Denoising* to recover noisy spectral bands in a hyperspectral dataset. The use of sparse reconstruction algorithms allows employing largest dictionaries in the process, yielding a more accurate reconstruction of the spectra. For denoising of low-SNR spectral bands (mostly in the UV regime), the spectrally unmixed abundance vectors are used to reconstruct the noisy band(s) in the hyperspectral dataset. These denoised bands can improve the data usability considerably for different applications, especially for water remote sensing.

Selected publications: [647], [345]

Fusion of Hyperspectral and Multispectral Data

Fusion and synergy of hyperspectral and multispectral data are important opportunities to enhance the capability of future optical satellites, like EnMAP, in a wide range of applications. To extract change information at subpixel scale from a set of multi-sensor time series data, we propose a new data fusion and unmixing framework, called *multi-sensor coupled spectral unmixing*. This technology allows the transfer of knowledge obtained from hyperspectral data to multispectral images, while increasing the temporal resolution of the analysis. We achieved promising results in the monitoring of the aftereffects of natural disasters using an image time series composed of EO-1/Hyperion and Landsat-8 data.

Sharpening of individual multi- or hyperspectral images by fusion with higher resolution imagery is performed by our algorithms J-SparseFI and J-SparseFI-HM, respectively (see *Data Science in Earth Observation* chapter). These sparsity-based methods proved to be superior to the state-of-the-art, in particular when it comes to spectral purity, e.g. in the vicinity of transitions of different materials, and for the sharpening of out-of-band spectral channels. Both properties are essential if the images need to be used for object classification.

Selected publications: [150], [123], [110], [172], [273]

Classification using Multi-modal Data Sources

Novel methods and method aggregations for supervised classification have been developed using traditional machine learning methods such as Support Vector Machines (SVM) and new deep learning concepts such as the CNN architectures.

The IEEE GRSS Data Fusion Contest 2018 provided as input hyperspectral data (48 bands in the spectral range between 380 – 1050 nm, 1 m ground resolution), RGB data (5 cm ground resolution), a lidar-derived digital elevation model, and a multispectral lidar intensity image with 50 cm ground resolution. The required task was the classification of 20 target species in a complex urban environment. In this frame, we developed novel methods and method aggregations for supervised classification combining traditional machine learning algorithms such as Support Vector Machines (SVM) with recent deep learning concepts such as the new CNN architectures. After preprocessing and feature extraction (e.g. band selection, denoising, bag-of-topics model feature extraction), a 100-dimensional feature stack was used as input for an ensemble of classifiers and ad hoc detectors (e.g. Deep Convolutional Neural Network, Random Forest, Spectral Angle Mapper). A final decision-based model merged the different levels of classification. Our result ranked second among 1,300 submissions from all over the world with an overall accuracy of 80.74 %, just 0.04 % below the first-ranked classification.

Selected publications: [139], [405]

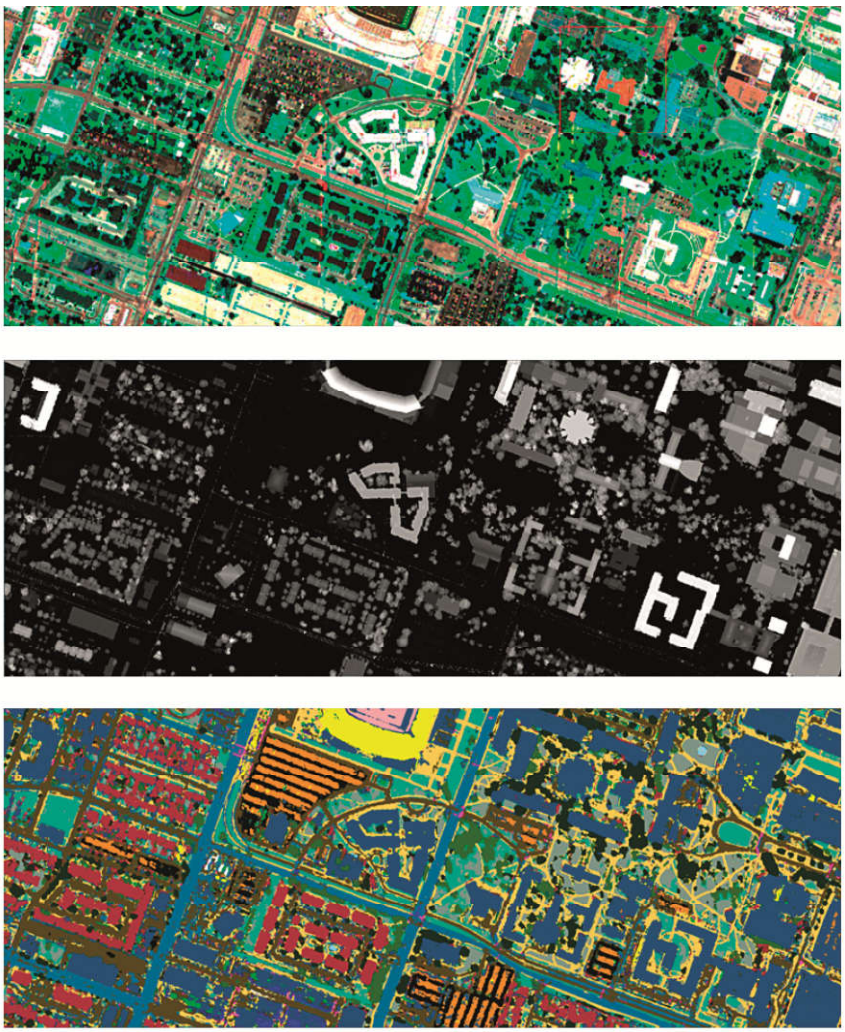

Detail for our submission to the IEEE GRSS Data Fusion Contest 2018: multispectral lidar intensity image (top), refined Digital Surface Model (middle), classification results (bottom).

Archaeological Applications

Remote sensing allows non-invasive large-scale analysis and monitoring of archaeological sites. Within the EU project ATHENA we cooperate with Cyprus University of Technology and the Greek Foundation for Research & Technology to find buried structures with remote sensing. Hyperspectral images can highlight crop marks in vegetated areas which may indicate the presence of such structures. For the first time we objectively estimated the suitability of maps derived from spectral features for the detection of archaeological structures in vegetated areas by computing the statistical dependence between the extracted features and a digital map indicating the presence of buried structures, using information theoretical notions. Based on the obtained scores on known targets, the features can be ranked and the most suitable ones chosen to aid in the discovery of previously undetected crop marks in the area under similar conditions. For a low score the buried relics are expected to be hardly visible in the image, while they stand out clearly as the score increases.

Selected publications: [34], [815], [132]

Optical Water Remote Sensing

Water remote sensing is one of the most challenging applications of hyperspectral remote sensing. IMF has a long legacy in retrieval algorithms for complex waters. Assessment and control of the aquatic environment are important for responding to the challenges created by climatic and ecological changes. The main challenge of optical water remote sensing is to determine the complex relationship between the water body, its constituents and the incident light spectrum. This has been achieved by developing a special inversion method that takes into account the complex make-up of coastal and inland waters. For validation and verification of the remote sensing results, reliable underwater spectrometers were also developed at IMF.

In 2017 IMF staff participated in a field campaign of the German research vessel *Polarstern* to collect spectral data from melting ice and to develop an optical model for parameterizing the spectral properties of ice and melt ponds. The impact of climate change on air temperature is most pronounced in Arctic regions. One of the effects that is not covered adequately by the models is the change of ice albedo during the melting season. Wet snow and – even more – melt ponds reduce albedo significantly, increasing the absorbed energy and intensifying the melting process (photo: G. Birnbaum, AWI).

Due to the high complexity of inland and shallow waters, processing of spectral measurements from such water types cannot be considered operational so far. Major challenges are atmospheric correction, reflections at the water surface, complex composition, variability of optical properties and spectral ambiguities of the measurements. Most satellite and airborne data are not processed with such optimized algorithms. The usually applied generic algorithms can introduce large and unknown errors. Better results could be obtained if users had the possibility to include regional expert knowledge in data processing, but user-friendly and publicly available software is lacking. Such software, the Water Color Simulator WASI, has been developed at IMF. Originally designed for processing of field measurements, it has been extended recently to atmospherically corrected multi- and hyperspectral image

data (WASI-2D). It includes algorithms for all the above-mentioned challenges and can be adapted easily by the user to different environments and sensors. The software is available for free and has been used by many researchers worldwide.

Selected publications: [122], [121], [809], [357]

Inland Waters

Inland water ecosystems play an essential role for all human life. Although it may appear obvious to use satellites to obtain a synoptic view, routine monitoring of inland waters is still based on traditional water sampling and seldom makes use of remote sensing. Major reasons are the lack of satellite sensors with suitable spectral, radiometric, geometric resolution and timely acquisitions. The complex optics of inland waters coupled with the problems is a significant challenge. We have been developing algorithms and software for quantitative data analysis of inland and coastal waters to prepare the recent and upcoming generation of multi- and hyperspectral satellite sensors (e.g. Sentinel-2, DESIS, EnMAP) with pixel sizes of 10 to 30 m. In order to enable validation of remote sensing products at different processing levels (e.g. radiance, reflectance, absorption coefficient, concentrations of water constituents, water depth), algorithms and software have been developed to process spectral in-situ measurements (under water and above surface). The focus of the last years was on the following topics:

- shallow waters (bathymetry, bottom classification)
- correction of surface reflections (sun glint, sky glint)
- all weather monitoring
- ecological indices for water bodies.

Methodological developments as well as field and airborne campaigns have been carried out for all of these topics. Additionally, we participated in a CEOS feasibility study for an aquatic ecosystem Earth observation system.

As an example the sun/sky glint corrections may be mentioned here. The light reflected at the water surface is frequently as intense as or even much brighter than the water leaving radiance. Accurate correction of these reflections is thus essential for the analysis of above-water measurements. Conventional methods cannot cope with the statistical reflections induced by individual waves. These statistical effects smooth out only for pixel sizes above 100 × 100 m², typical for ocean color sensors. We developed a new correction algorithm able to correct reflections even from individual waves. It has been applied to multi- and hyperspectral airborne and satellite sensors (HySpex, Sentinel-2) and to field measurements.

Selected publications: [565], [118], [122], [193]

Seagrass Monitoring

Seagrasses are vital due to the numerous ecosystem services they provide including carbon sequestration, coastal erosion and nutrient cycling. Optical systems and methodologies now allow high spatio-temporal, large-scale seagrass monitoring, and therefore better management and conservation practices. We have developed seagrass monitoring techniques, exploiting the new wealth of data derived from Sentinel-2, PlanetScope, RapidEye and similar optical satellite sensors. Our new

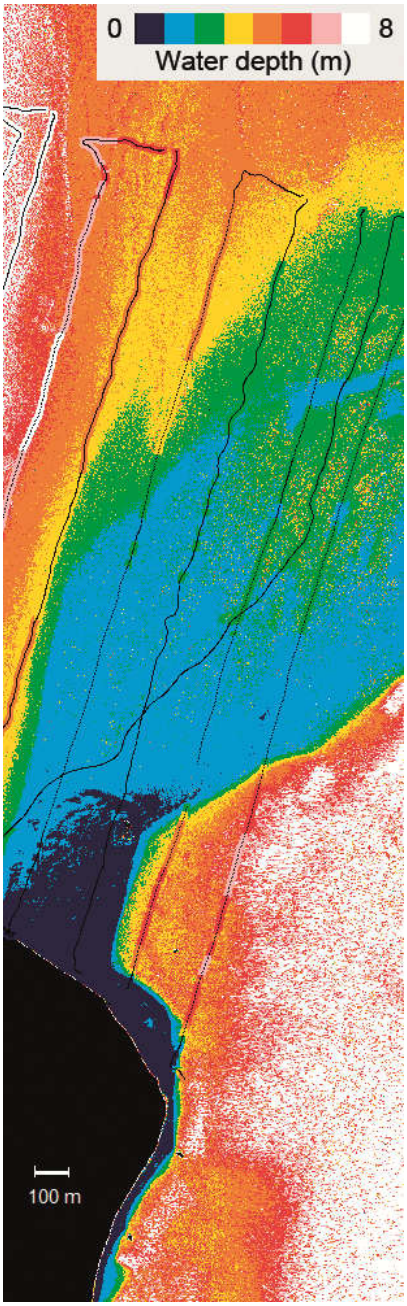

Bathymetry in shallow water near Boltenhagen (Baltic Sea). The water depth map was derived with the software WASI-2D from airborne data of the hyperspectral sensor HySpex, and validated using echo sounder measurements from ship. The same color coding was used for both data sets; black dots mark the corresponding pixels.

methodological workflow combines atmospheric, water-surface, sun glint, and water column corrections with satellite-derived bathymetry and machine learning classifiers. It has been employed to map Mediterranean seagrasses both in single-date (Sentinel-2) and multi-temporal (RapidEye, PlanetScope) approaches.

The results of these quantitative assessments in the Thermaikos Gulf (eastern Mediterranean) reveal that seagrass habitats are found up to a depth of 16.5 m and that their area has increased by 6.8 % between 2011 and 2016.

Selected publications: [75], [76], [27]

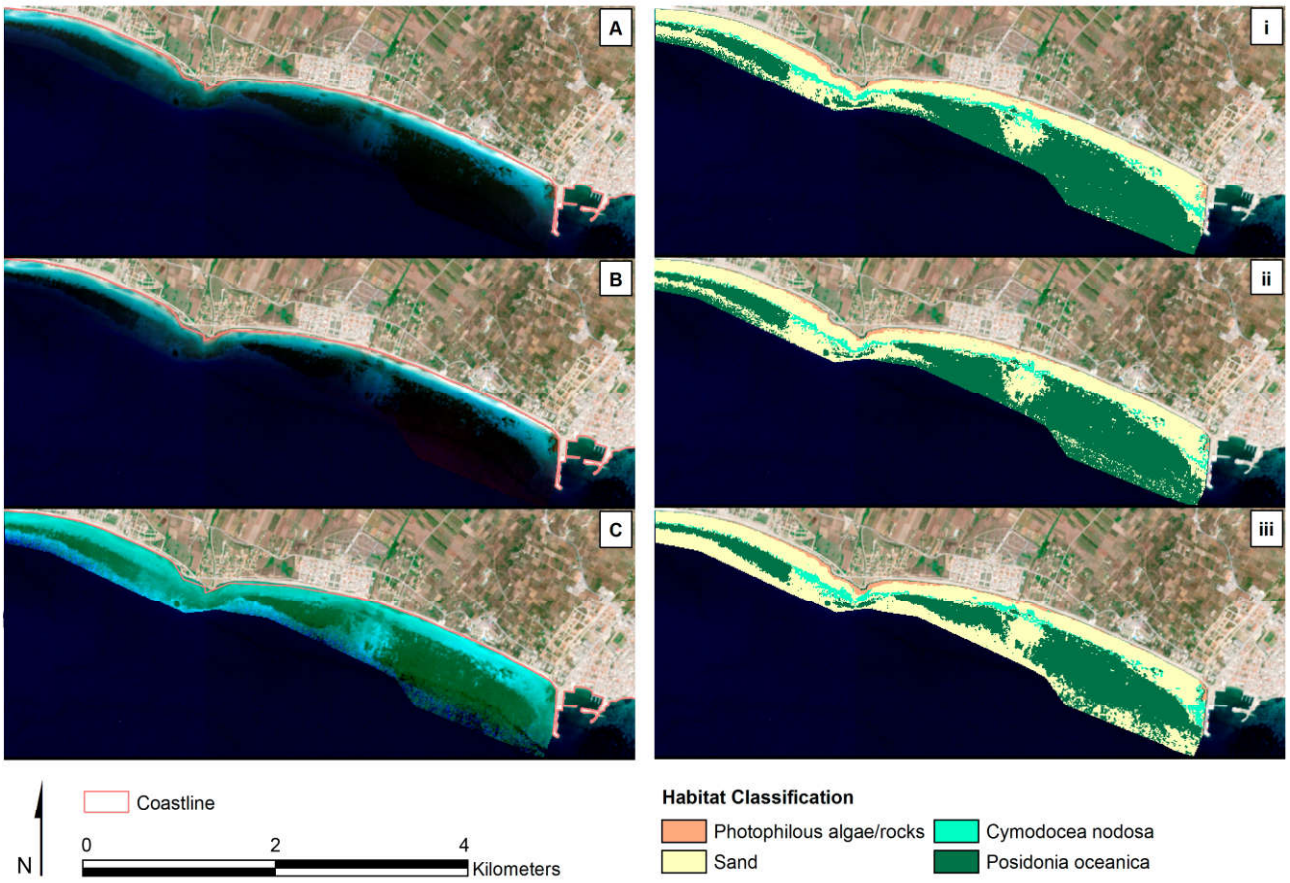

Sentinel-2A natural color composites of three methodological steps and corresponding best performing classifiers of Mediterranean seagrasses and neighboring habitats in the Thermaikos Gulf, NW Aegean Sea, Greece. A: L1C-composite (no correction applied), B: water surface reflectance composite (with atmospheric correction applied), C: seabed reflectance composite (with water column correction applied), i: Support Vector Machine (SVM) classification of A-composite, ii: Random Forest classification of B-composite, iii: SVM classification of C-composite.

Atmospheric Correction

Atmospheric correction of multispectral/ hyperspectral satellite imagery is inherently an under-determined inversion problem. The recorded top-of-atmosphere (TOA) radiance L depends not only on the surface reflectance ρ but on many atmospheric parameters, some of which are known while others must be estimated. The objective is to convert the TOA radiance image cube into surface reflectance.

In the spectral region of 400 – 2,500 nm the most important parameters to be retrieved are aerosol type, optical thickness and atmospheric water vapor column. If the necessary spectral channels are available, these parameters can be calculated from the scene based on radiative transfer calculations. This is the basis for the subsequent surface reflectance retrieval. Information from other sources are also needed, e.g. the ozone content and a DSM. However, this approach only works for clear atmospheric conditions, in other cases preprocessing steps are needed as described below.

New Generic Atmospheric Correction Processor PACO

The heritage of EOC's developments of atmospheric correction algorithms and software (ATCOR) for a large variety of optical spaceborne and airborne sensors dates back to the 1990s. Motivated by several new methodological developments and ATCOR's licenses requirements for IDL and MODTRAN, IMF decided in 2013 to build up a completely new generic atmospheric correction processor PACO (Python Atmospheric Correction) with strict modular design, based on Python, an in-house developed radiative transfer model and rigorous software engineering standards.

The processor is able to work with data from many satellite and airborne sensors that provide images in the VNIR to TIR spectral range. It uses our own radiation transport model code based on LibRadTran. Further processor evolutions are ongoing, such as extending the atmospheric correction to water surfaces, improved masking, providing independent quality layers for masks and bottom-of-atmosphere reflectance and correction of BRDF effects. PACO is designed to work as an operational processor without user interaction. Beta versions are already used for processing Sentinel-2 and Landsat-8 data. It is integrated in CATENA. Specific derivates of PACO are implemented in the ground prototype (level 2a) – and later operational – processor for the DESIS and EnMAP missions. PACO participated successfully in the Atmospheric Correction Exercise turning out to be one of the two best tools for Landsat-8 data.

Selected publications: [69], [133], [268], [322], [382]

Multi-temporal Atmospheric Correction of Multi-spectral Images (MAJA)

The MACCS-ATCOR Joint Algorithm processor, named MAJA, was devised in cooperation with CNES and IMF during an ESA project for developing a prototype atmospheric correction processor for Sentinel-2 data using image time series. MAJA detects clouds and cloud shadows and corrects for atmospheric effects providing a level 2a product for Sentinel-2. Pixels in this level 2a image data represent ground reflectance. MAJA merges the strengths of the two most renowned processors in Europe: MACCS (Multi sensor Atmospheric correction and Cloud Screening) from CNES, e.g., multi-temporal methods for cloud detection and aerosol estimation, and PACO from IMF, e.g., cirrus-correction and cloud detection for mono-temporal cases. As a key feature, MAJA exploits the fact that

surface reflectance changes slowly over time which eases the detection of temporally varying clouds in image stacks. MAJA runs at CNES and DLR as a basis for joint data processing. In this context, the focus is on sensors like Sentinel-2 and Landsat, where time series of level 1c data are available.

Selected publication: [624]

Haze-/Cirrus removal: Sentinel-2A scene near Wörgl, Austria, acquired May 2016. Top: original scene (true color), bottom: dehazed scene.

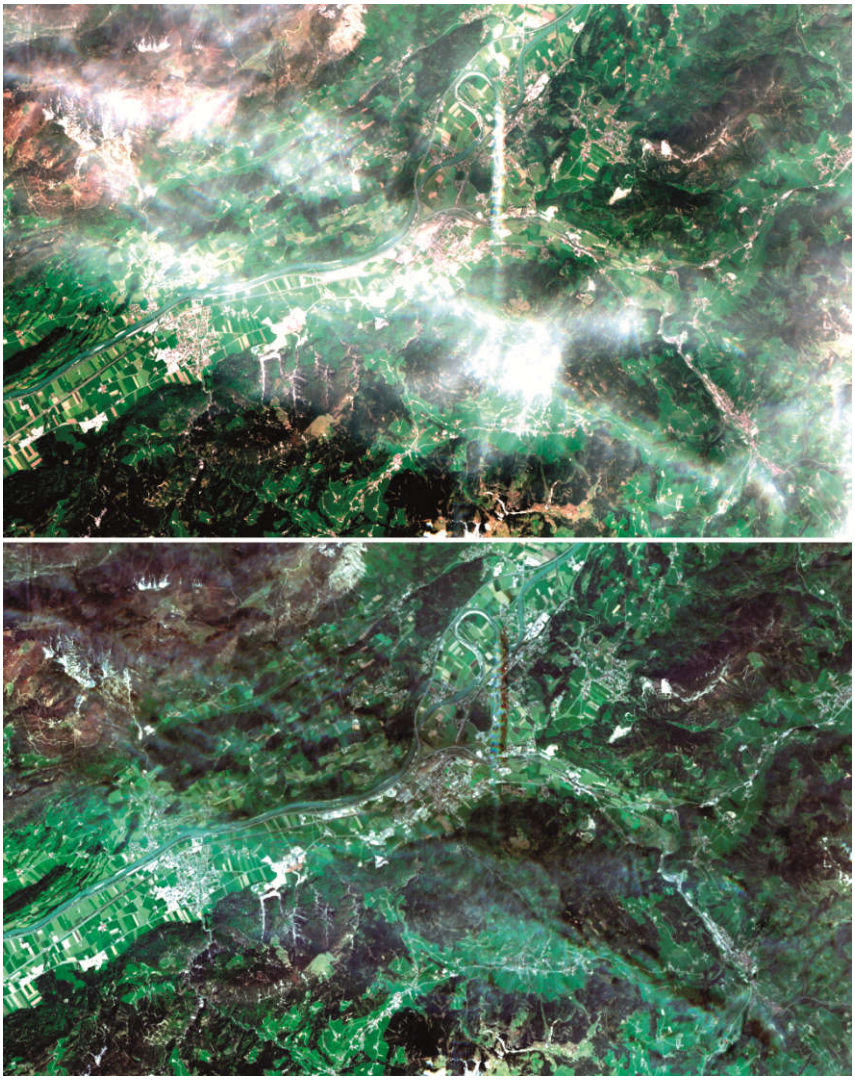

Haze-/Cirrus Removal

Optical satellite imagery is frequently contaminated by low-altitude haze and high-altitude cirrus clouds. We have developed a novel combined haze/cirrus removal algorithm as a very effective preprocessing step for atmospheric correction. It starts with calculating a haze thickness map (HTM) based on a local search of dark objects. The haze-free signal is restored by subtracting the HTM from the hazy image assuming an additive model of the haze influence. The HTM method is substantially improved by employing the 1.38 µm cirrus band. The top-of-atmosphere reflectance cirrus band is used as an additional source of information. The method masks haze and cirrus areas, calculates the spectrally variable haze thickness map for channels in the 400 – 2,500 nm range and removes theses effects seamlessly. Thereby it restores the information in highly inhomogeneous surfaces attenuated by a low-altitude haze and high-altitude cirrus, improving the semantic interpretation of the scene content while preserving the shape of the spectral signatures. The new enhanced HTM/cirrus method has been successfully applied to many Landsat-8 and Sentinel-2 real and simulated scenes and is now being integrated into PACO and MAJA.

Selected publications: [216], [374]

Real-Time Airborne Traffic and Situation Monitoring

In 2007 IMF acquired funding from DLR's program *Transport* for the project ARGOS to use airborne remote sensing for estimating traffic parameters. The project was carried out in close cooperation with the DLR Institute for Transportation Systems. It soon became evident that only a real-time system, which delivers relevant parameters directly to the ground, could fulfill the requirements of traffic and situation monitoring. In the subsequent projects VABENE and VABENE++ an innovative system has been built up at IMF. Since then real-time acquisition of traffic parameters, monitoring of mass events, disasters and large accidents with airborne optical sensors is an active topic of research and development at IMF. These data are highly welcomed by security-related organizations, like police and rescue forces, since they allow rapid mapping of affected regions, detailed monitoring of vehicle and pedestrian traffic flow, and the detection of hazardous situations.

In the frame of these projects we have developed our 3K (operated on fixed wing aircrafts) and 4k (operated on helicopters) airborne camera systems. Onboard orthorectification, radiometric homogenization and mosaicking allow rapid mapping. Since single images are acquired with high frequency (up to 5 Hz) or as video stream, a high overlap between subsequent frames is available. This is used for detecting and tracking moving objects as well as for the generation of high resolution DSMs from the multiple-stereo views. New developments in software/hardware efficiency at IMF have recently led to real-time onboard DSM generation and distribution.

Recently we switched from classical machine learning algorithms to deep learning and are improving the performance of onboard object extraction and tracking. The application focus is also changing from traffic monitoring to the generation of High Definition (HD) road maps for autonomous driving and for monitoring the static and dynamic environment of autonomously driving cars.

Automatic and fast multi-class vehicle segmentation (left) and 15 class semantic segmentation (right) in aerial images using deep learning.

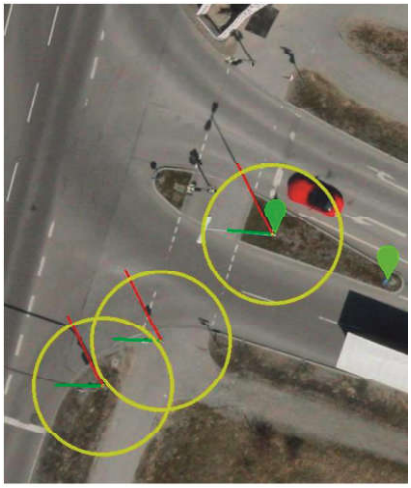

DriveMark® project: Fully automatic pole detection in airborne imagery (detected poles in green and correlated shadows in red are marked with circles) and correlation with geodetic SAR ground control points (position marks).

Vehicle Detection and Tracking

We have developed a fully automatic processing system for onboard real-time vehicle detection and tracking in aerial images. This is an important capability for a variety of applications such as traffic monitoring and parking lot utilization. Airborne imagery allows collection of traffic-relevant data over large areas in a short period of time. The microscopic acquisition of each vehicle in large areas by terrestrial imagery would require a large number of sensors. We recently developed new methods for the separation of parking vehicles and standing traffic (e.g. in front of a red traffic light). With this, it is possible to improve real-time traffic data quality in urban scenes and to identify parking spaces along the roads.

Recent developments in deep learning frameworks have been adapted to further improve vehicle detection and also differentiate between vehicle types. Vehicles can be categorized in five classes using Region-based Convolutional Neural Networks (RCNNs). Vehicles in remote sensing applications usually appear as small image patches and often with complex backgrounds which makes the detection challenging. Their classification into different types is even more difficult. By a specific modification of RCNNs, we have achieved a major improvement over the formerly applied methods. In airborne imagery, vehicles near to each others can in spite of their small size still be separated using non-maximum suppression (NMS). We have developed an NMS process which results in better performance compared with traditional NMS operation.

Selected publications: [368], [779], [447]

HD-Mapping for Autonomous Driving

A new field of research at IMF is using airborne high resolution data for the support of autonomous driving through detailed and accurate mapping using SAR data from space and by detecting traffic relevant objects in optical airborne data, e.g. lane markings or other objects at road level.

The available georeferenced maps for autonomous driving often suffer from low absolute geometric accuracies. In the Helmholtz Validation Fund Project DriveMark® (co-funded by DLR Technology Marketing) highly accurate geodetic SAR points from TerraSAR-X were used for absolute geometric correction of airborne images from the 3K camera system (see *SAR, Geodetic SAR Applications*). The SAR points are typically bright responses from the cylindrical poles of streetlights or traffic signs which form dihedral reflectors in combination with the road, each with a phase center at the base-point of the pole. The DriveMark® processor implemented in CATENA detects these pole base-points in airborne optical imagery and assigns them to the corresponding points detected in the SAR image. Using these SAR-optical point pairs the absolute geometric position of the airborne images is improved from about one or two meters to better than 10 cm.

One of the most important classes in the creation of HD maps for autonomous driving are lane markings including their absolute position on the road. Area-wide maps of lane markings can be used by autonomous vehicles for self-localization. While humans can locate themselves on a road by easily learned rules, an autonomous vehicle needs to be taught to localize itself absolutely in its environment. Therefore, an accurate and reliable lane marking segmentation in the imagery of roads and highways is needed. We have developed a Symmetric Fully Convolutional Neural Network

enhanced by Wavelet Transform in order to automatically carry out lane marking segmentation and classification in aerial imagery. Due to the heavily unbalanced problem in terms of low number of lane marking pixels compared with many background pixels, we use a customized loss function:

$$L(\boldsymbol{W}) = -\frac{1}{N}\left(\lambda_{lane}\sum_{n=1}^{N}\mathbb{1}_{lane}(x_n)\,y_n\log\hat{y}\,(x_n,\boldsymbol{W}) + \sum_{n=1}^{N}\mathbb{1}_{bg}(x_n)(1-y_n)\log\big(1-\hat{y}(x_n,\boldsymbol{W})\big)\right)$$

where x_n and y_n represent input and actual label data. $\hat{y}$ represents output data. $\boldsymbol{W}$ is the weight matrix and λ_{lane} is the parameter to compensate the unbalanced dataset. We achieve a very high accuracy of 86 % in pixel-wise localization of lane markings without using any existing GIS information.

HD maps for autonomous driving must also contain detailed semantic information on the relevant road classes and surfaces. The differentiation between road area, lane structure on the roads, pedestrian, bicycle and parking zones is of crucial importance in autonomous driving. We started developing methodologies to automatically detect these semantic classes and are currently comparing and optimizing these methodologies. To bring this methodology into use we closely cooperate with the DLR Institute for Transportation Systems and discuss with industry regarding the detailed properties of these maps. Furthermore we are building a benchmark data set called Skyscapes which will be publicly available for comparing methods of semantic segmentation and classification in this context.

Selected publication: [533]

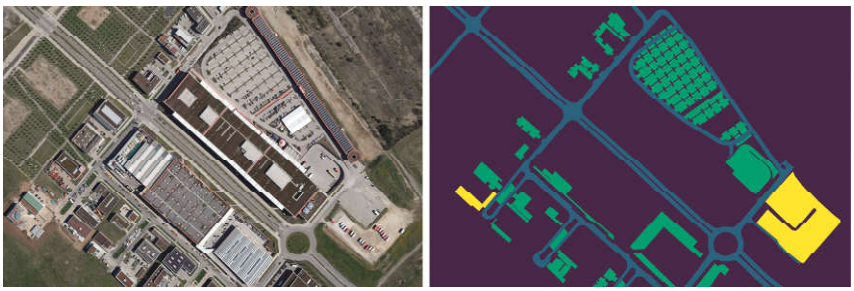

Mapping for autonomous driving: Automatic street and parking area mapping from aerial imagery. Light blue: streets, green: paved parking place, yellow: non-paved parking place.

Benchmark, Fusion of Street View and Bird's Eye View

Simultaneously acquired data from terrestrial and airborne platforms are an important prerequisite for autonomous driving evaluation and future traffic applications. The primary goals are the intelligent fusion of data from different platforms to reach an overarching and precise view of traffic situations and to validate the measurements acquired locally from autonomous driving cars. The simultaneous acquisition, though, is an organizational and aeronautical challenge.

In this context, a benchmark data set is under development where stationary, mobile and airborne sensors simultaneously monitor the environment around a reference vehicle.

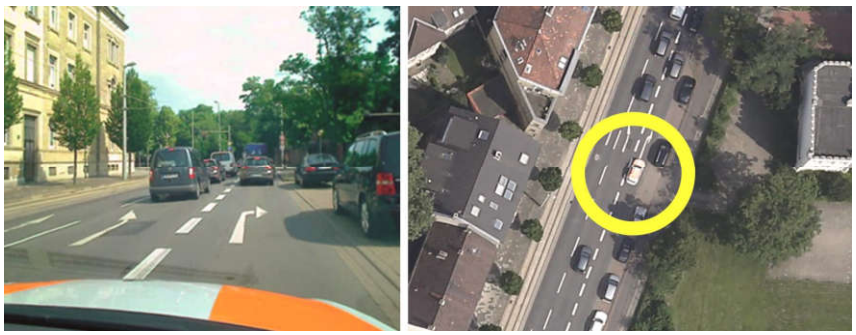

Example of simultaneous data acquisition from vehicle (left) and helicopter (right).

This vehicle was driving on urban, suburban and rural roads in and around the city of Braunschweig, Germany. Airborne images were acquired with IMF's 4k sensor system on board a helicopter. The DLR reference car FASCarE is equipped with the latest car sensor technology like front/rear radar, ultrasound and lidar sensors, GNSS/IMU, optical single and stereo cameras. Additionally, stationary terrestrial sensors like optical mono and stereo cameras, radar and laser scanners monitor defined sections of the path. The stationary sensors are installed on gantries at main crossings and on pylons.

Crowd and Pedestrian Monitoring

IMF's real-time sensor systems are also used to monitor pedestrian movements and large crowds. The automated real-time analysis of human crowds in aerial imagery can help authorities improve public safety at large public gatherings such as sporting events, open-air festivals and demonstrations, ward off catastrophes such as panic-driven stampedes, and for the planning of large-scale events.

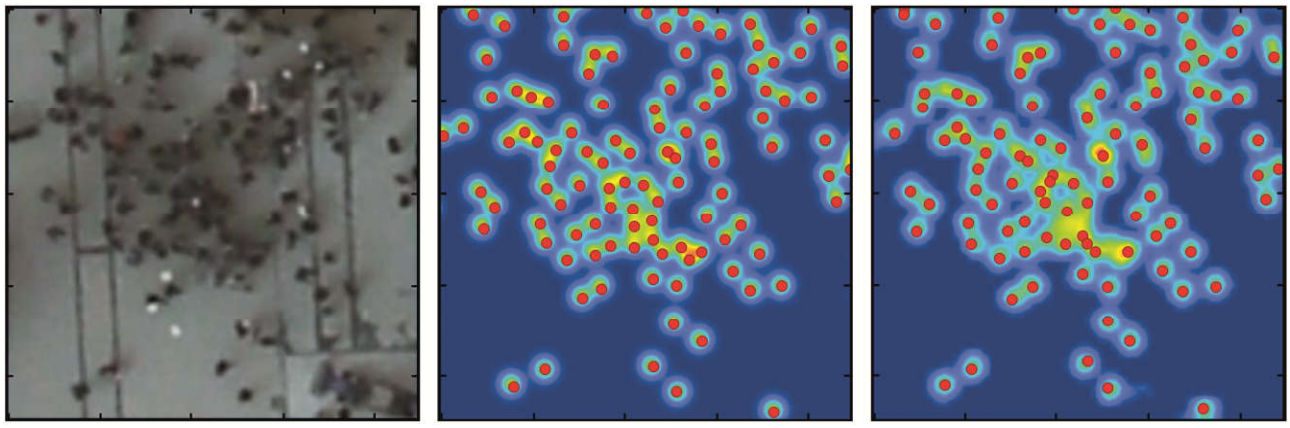

Top: Orthorectified aerial view of the *Bauma 2016* construction trade fair in Munich, Germany, with collected annotations (marked in red). Bottom: For a given image patch (yellow frame) of a crowd we show the ground truth density map with person locations (center) as well as the predicted density map (right) with estimated person detections (marked by red dots). The predictions were obtained with a novel convolutional deep regression network trained to jointly solve crowd counting and person localization. 105 people were annotated in the original image patch, and the predicted count of 110 persons comes close.

In order to address different needs, we tackled several tasks in crowd analysis, from density estimation and counting of high-density crowds, to the localization and tracking of individuals in medium-density crowd scenarios. For crowd density estimation, local texture features in a Bag of Words classification pipeline as well as Bayesian regression algorithms were initially developed at IMF. Results were then further improved with a novel deep regression network trained to jointly solve crowd counting and person localization. For person tracking, person locations, provided by a Haar filter-based Adaboost detector or – more recently – by the aforementioned deep person detector, are grouped to trajectories using multiple hypothesis tracking. Deep learning methods require large amounts of annotated data for training; therefore, significant effort was invested into collecting person annotations on a large scale by developing an easy to use annotation tool. The developed methods were successfully tested onboard a helicopter during several campaigns, including the 'Bauma' construction trade fair and the Wacken Open Air music festival in 2016.

Selected publications: [526], [222], [299]

User Campaigns

One of the most exciting moments in engineering research is when scientific developments can be applied in practice. In regular campaigns, IMF has cooperated with national, regional and local users from authorities and organizations with security roles. Especially in crisis situations, those responsible for disaster management depend on the most recent situational knowledge possible in order to make decisions on traffic control or the allocation of emergency services and aids. Through our system we provide up-to-date situation maps as well as additional information on traffic situation and passenger flows, which are made directly available to users on site. Several disaster management exercises and large-scale events have been accompanied by our real-time airborne monitoring systems in order to test new developments, to demonstrate existing procedures and to collect valuable data for validation. In this way, the results of image acquisition and data processing have made a valuable contribution to disaster management and, at the same time, user campaigns have offered us the opportunity to collect direct feedback from practitioners to drive future developments in this direction and meet their requirements.

Some examples of campaigns under real conditions are the flood event in Germany in 2013, the national exercise of the Medical Task Force in 2014, the G7 summit in 2015, the Wacken Open Air music festival in 2014 and 2016 and the German Protestant Church Assembly in 2017 (see *Laboratory Infrastructure and User Services* chapter).

Disaster management support during the flood in Germany in 2013: Images of the 3K camera system showing the flood extent around Deggendorf, Bavaria.

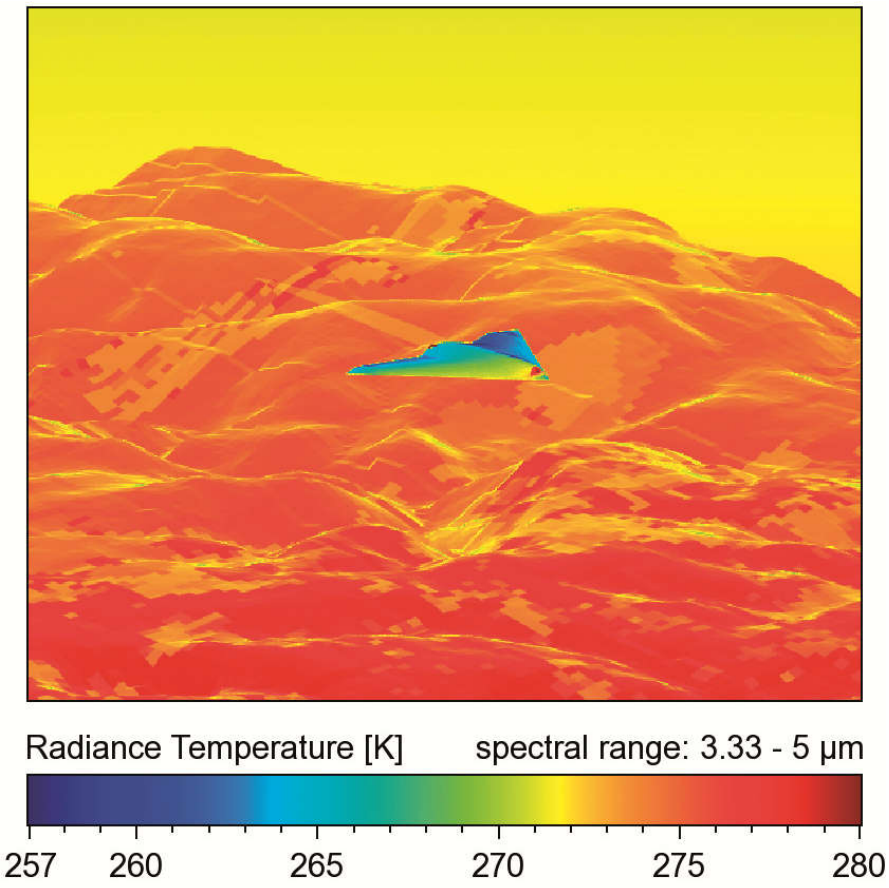

IR signature of an aircraft flying in front of Mount Brocken in the Harz area (Germany). The image is computed by IMF´s IR signature model MIRA using a digital elevation model of the Harz area together with a classification of the ground surfaces determined from satellite data.

Thermal Image Processing

Infrared Scene Simulation

IMF has improved and extended its infrared signature modeling capabilities by developing the new IR signature model MIRA (Model for infrared scene analysis). The current version is predominantly useful in predicting IR signatures of air vehicles (aircraft, missiles, rockets). MIRA is based on a ray tracer and Monte Carlo integration. This permits handling of multiple reflections in cavity-like components like an aircraft's inlet or exhaust duct. For the design of stealth aircraft correct modeling of these cavities is especially important as they contain hot parts of the propulsion system. These may cause important contributions to the total IR emission. In addition, MIRA is able to determine the IR radiation emitted by a vehicle's exhaust gas which may form an arbitrary volume. Constraints imposed by former models (axisymmetric shape and properties) have hence been overcome. The latest feature that was implemented is a first version of a terrain model. Based on a digital elevation model and corresponding ground classification, MIRA can generate a structured background which greatly enhances the realism of the simulation.

Flying Infrared Wildlife Finder

Every year many wild animals, especially roe deer fawns, are killed during pasture mowing. Under reasonable effort until now no measure succeeded to reduce the amount of mowing victims to a tolerable level. At IMF we developed a specialized system for fawn detection and rescue, the Flying Infrared Wildlife Finder. The UAV-based system detects roe deer fawns by means of a thermal camera: From the bird's eye a warm animal like a roe deer fawn is much easier to detect than with traditional methods.

The IR camera and the dedicated software tools for mission planning, flight control, image data evaluation, fawn detection and georeferencing (both latter in near real-time) are optimized for fast usability, high detection reliability even under challenging environmental conditions (high ambient temperature, direct solar radiation) and high area performance during the search. The key data of our system demonstrator are:

- area output per battery charge: approx. 7 ha in 12 minutes (flight altitude: 80 m)
- fully automatic detection and location of the fawns in the IR images at dusk or under cloudy conditions
- semi-automated detection and geolocation for sunlit meadows (temperature > 30 °C in the shade)
- overlooked fawns: 0 % at dawn or in cloudy weather, < 10 % during sunshine
- all process steps, i.e. system setup, flight planning, flight, image evaluation, georeferencing, briefing of search personnel) can be accommodated at intervals of approx. 30 minutes.

The Flying Infrared Wildlife Finder thus surpasses all other fawn search systems in both, area performance and detection rate by far. Amongst others, it was awarded the *Innovationspreis 2013 der Gesellschaft von Freunden des DLR*.

Selected publications: [546], [996], [1171]

Fawn positions (red dots) in the meadows (green) searched by the Flying Infrared Wildlife Finder during the 2015 campaign. An area of 170 ha was scanned within a total flight time of 8.5 h, 43 fawns were detected and rescued, two were overlooked. About 50 % of the area observed is shown (aerial photo: Bayerische Vermessungsverwaltung).

Spectrometric Sounding of the Atmosphere

Spectrometric Sounding of the Atmosphere

In its third technology line IMF carries out research on methods for deriving atmospheric state variables from spectrometric remote sensing data. Our expertise ranges from basic research on electromagnetic scattering, radiative transfer, inverse problems, spectroscopic laboratory measurements and sensor calibration to professional software implementation, mission support and geoscientific research (in selected topics). We strive for highest precision in determining atmospheric state variables and for retrieval of new parameters from remote sensing data.

Our mission-specific developments for GOME, SCIAMACHY, GOME-2, Sentinel-5P, -4 and -5, MERLIN and Aeolus – mostly under ESA, EUMETSAT or industry contracts – have already been described in the *Missions and Sensors* chapter. Here our scientific activities are presented following a workflow logic from raw data processing to geoscientific research:

- **sensor calibration**
- **radiative transfer**
- **inversion and regularization**
- **electromagnetic scattering**
- **spectroscopic references**
- **geoscientific research.**

Our geoscientific research concentrates on topics where we greatly benefit from our long-lasting involvement in spaceborne spectrometric sounding missions. It includes long-term observations of climate relevant quantities like total O_3 and H_2O, air quality indicators such as tropospheric NO_2 or O_3 and hazard monitoring with volcanic SO_2. Beyond Earth, sounding the atmospheres of exoplanets belongs to our portfolio.

SO_2 plume of the Ambae volcanic eruption on the archipelago of Vanuatu on November 11, 2017 as retrieved from Sentinel-5P data.

Sensor Calibration

Deriving atmospheric characteristics from electromagnetic spectra requires input data of the highest possible quality. Therefore, we develop calibration algorithms for the entire suite of atmospheric sensors exploited at IMF. The first step in the derivation of geophysical parameters from remote sensing data is the generation of level 1 data by applying the full arsenal of calibration steps to the instrument raw data. By the end of this procedure, the raw measurements have been converted to physical quantities. IMF is actively pursuing:

- development and continuous improvement of calibration algorithms
- conceptual design and development of operational level 1 processors.

As a subcontractor for industry, IMF has provided level 1b processing design and algorithm descriptions in the phase A/B studies for Sentinel-5 and CarbonSat (meanwhile abandoned in favor of another proposed CO_2 monitoring mission). Furthermore IMF has significantly contributed to the processor design and algorithm descriptions for the level 1b prototype processor for Sentinel-4. In the framework of these projects, extensive studies were carried out for several calibration algorithms. Since the accuracy requirements for the new generation of instruments are significantly higher than those for past or existing ones, we had to refine or devise new calibration concepts.

For spectral calibration, a non-linear model for fitting solar and/or atmospheric lines was developed. This included, for several instruments and wavelength ranges, the derivation of optimal micro-windows.

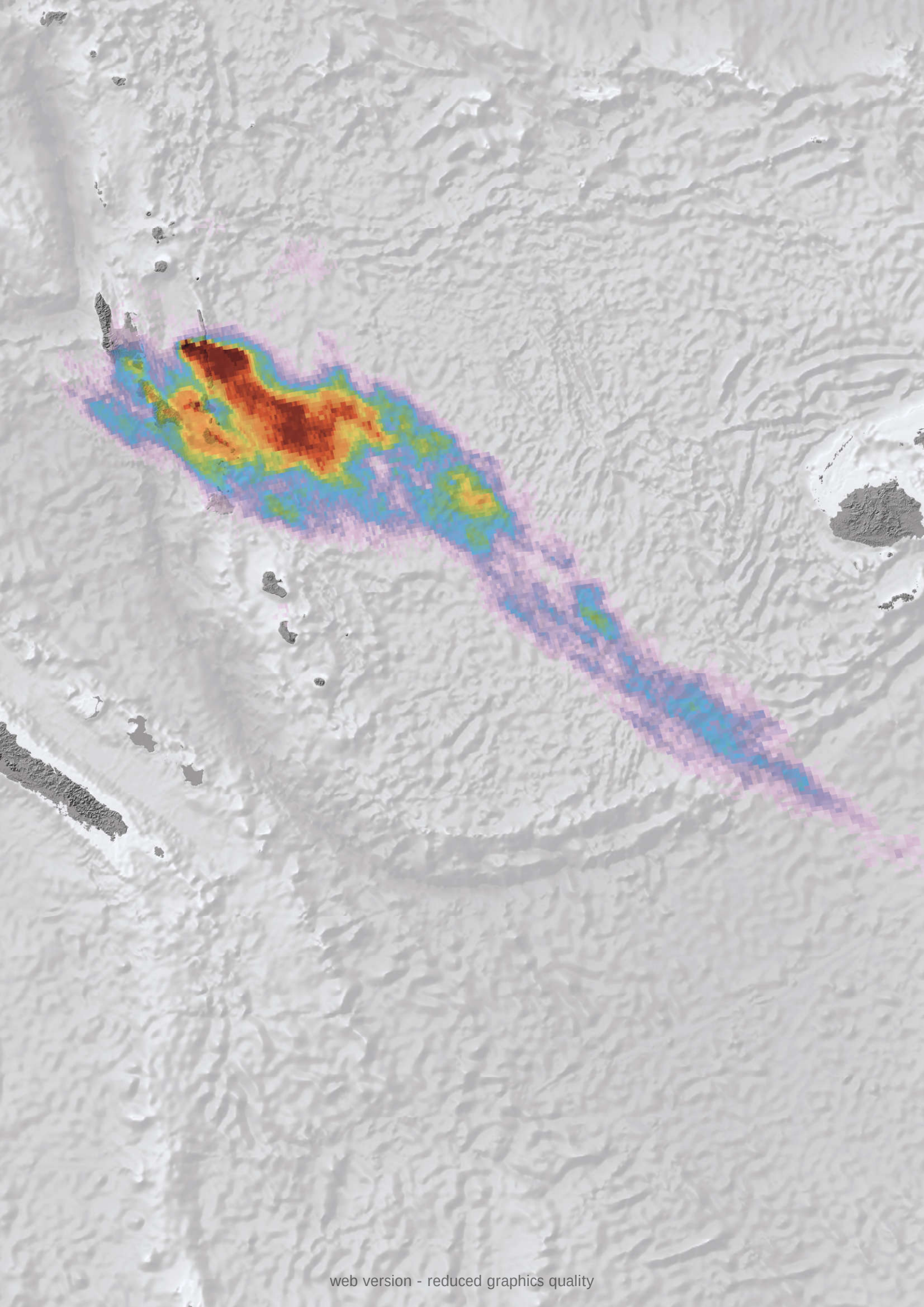

A fast computational procedure could be implemented. We also performed studies on how to retrieve the instrument's spectral response function (ISRF), which is one of the key components of reliable spectral calibration and level 1b and level 2 data generation. The ISRF is measured on-ground, using a homogeneous illumination of the instrument. However, depending on the blur of the telescope system in front of the spectrometer, this may not always be representative for the in-flight situation. As a result, the ISRF may be narrower due to incomplete illumination of the slit and may be spectrally shifted. This can have significant consequences for trace gas retrieval. Our studies, first performed for Sentinel-5 and then expanded to Sentinel-4, help to mitigate the effects of ISRF deformation. If uncorrected, the error of the trace gas retrieval could be as high as several 10 %, depending on the species.

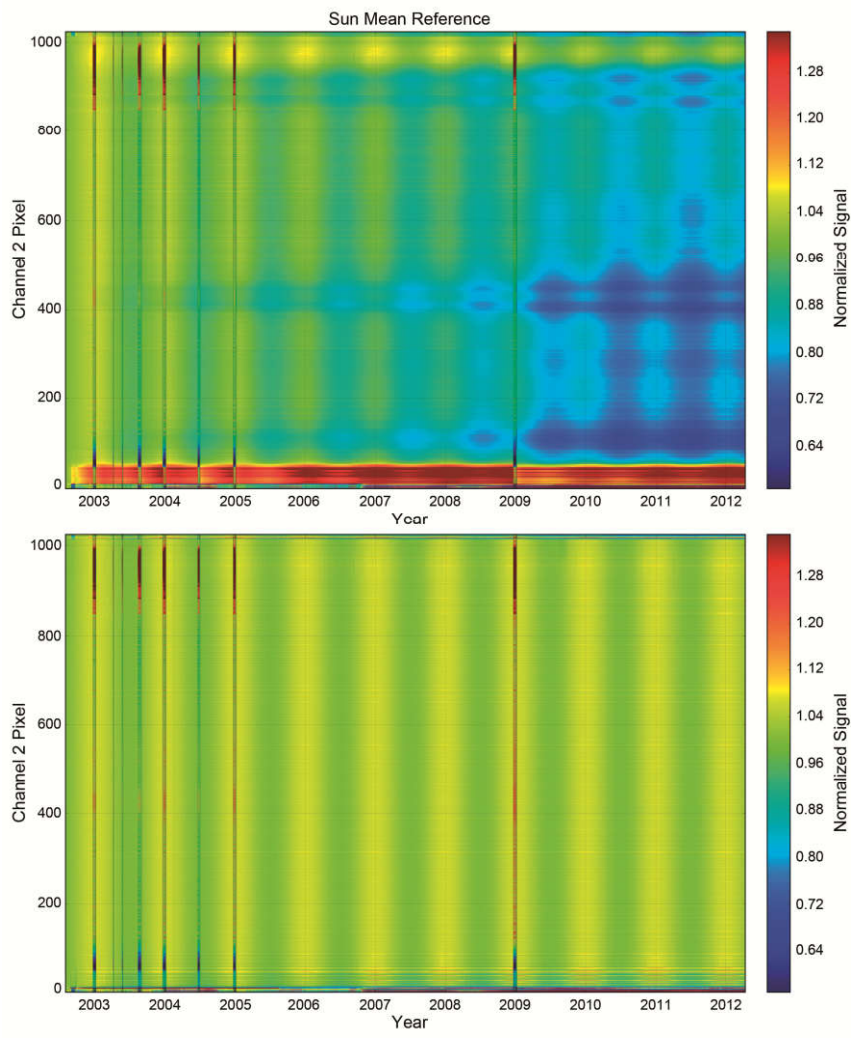

Signal in SCIAMACHY channel 2 normalized to the first measurement for each pixel over time without (top) and with full degradation correction as implemented in the new version of the level 0-1b processor (bottom). Shaded regions mark decontaminations. The regular change over a year is caused by the varying distance of the sun.

Stray light can considerably hamper accurate sensor calibration. In collaboration with industry, which provided simulations of the instrument, IMF has carried out a study to correct the expected stray light from Sentinel-4 to a level within tight requirements. Since on-ground stray light measurements are very time consuming, the calibration approach had to be optimized. To this end we simulated stray light measurement based on the industry-provided instrument model and calculated the resulting calibration data. They were in turn used in our correction algorithm. The findings were then compared to the instrument requirements. This was done for several scenarios under the boundary conditions of limited time for on-ground calibration and limited level 1b processing time. The final result was an optimized stray light correction algorithm and on-ground measurement scheme.

For the instruments where IMF has a long history of level 1b processing and maintenance (GOME and SCIAMACHY) further calibration studies have been performed. For SCIAMACHY this occurred in the framework of its phase F tasks. One important topic was to investigate how changes in level 1b algorithms affected the level 2 retrieval ('level 1b-2 feedback') of the CO column based on weak lines in the SWIR channel.

As a result, spectral calibration and dark signal calibration in the SWIR range could be improved. SCIAMACHY's ISRF could also be re-calculated.

As a result of our work in the post in-orbit phase, both for SCIAMACHY and GOME, level 1 algorithms and processor updates could be achieved. This allowed generating improved level 1b products for the full missions. Utmost level 1b quality is a prerequisite for achieving accuracies on the order of 1 % in the retrievals of certain climate-relevant trace gases, a value comparable to ground-based measurements.

Selected publications: [43], [46]

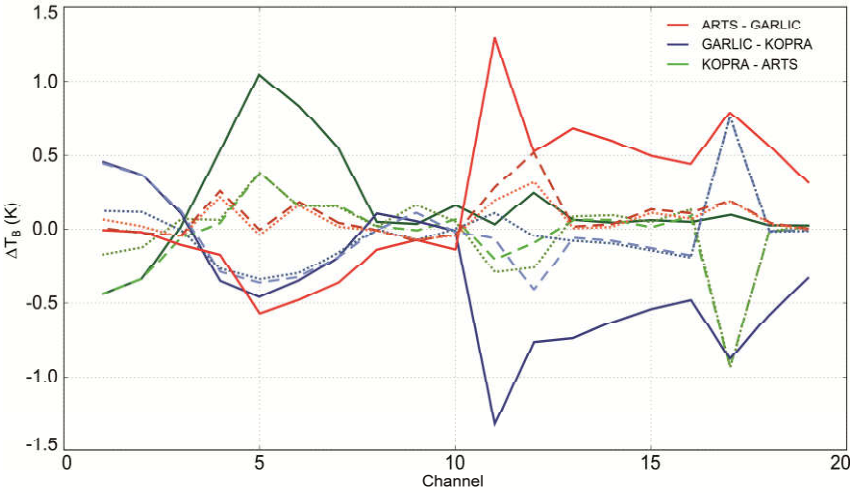

Brightness temperatures differences obtained from modeled IR spectra using three independent model inputs (GARLIC, ARTS and KOPRA). Line types denote different atmospheric configurations. Whereas models' accuracies are comparable IMF's GARLIC code provides superior speed and is therefore our model of choice for operational processors.

Radiative Transfer

Data analysis methods and mathematical modeling of the spectra are the main components of atmospheric processors. They reflect our understanding of atmospheric physics and serve to convert the measured spectral radiances (level 1 data) to the retrieved geophysical parameters (level 2 data). Mathematical modeling is based on solving the integral-differential radiative transfer (RT) equation. In the ultraviolet and visible ranges multiple scattering of solar radiation plays an important role in the radiative budget, while in the infrared spectral region thermal radiation from the surface and atmosphere dominates. In general, the radiative transfer equation cannot be solved analytically. Special numerical algorithms, referred to as radiative transfer solvers, are designed. To make a treatment more efficient, RT solvers are usually developed separately for UV-VIS and IR regions. Our asset is expertise covering the very wide range of wavelengths from UV-VIS to IR and microwave.

Infrared and Microwave

Infrared and microwave line-by-line (LbL) models are mandatory for the analysis of high resolution observations and for generation and verification of fast parameterized models. Furthermore they are essential for exoplanet spectroscopic studies where parameterizations usually developed for Earth are not applicable. LbL models are challenging because thousands to billions of lines have to be computed on thousands to millions of frequency grid points. Moreover, the number of spectra to be processed in operational Earth observation has increased dramatically in the past decades. At the core of every LbL code is the Voigt function, the convolution of a Lorentzian and Gaussian that is notoriously difficult to compute accurately and efficiently. The increasing quality of spectroscopic observations has indicated the limitations of the Voigt profile and physical processes beyond pressure and Doppler broadening have to be considered. The speed-dependent Voigt (SDV) profile can be readily computed as the difference of two Voigt functions.

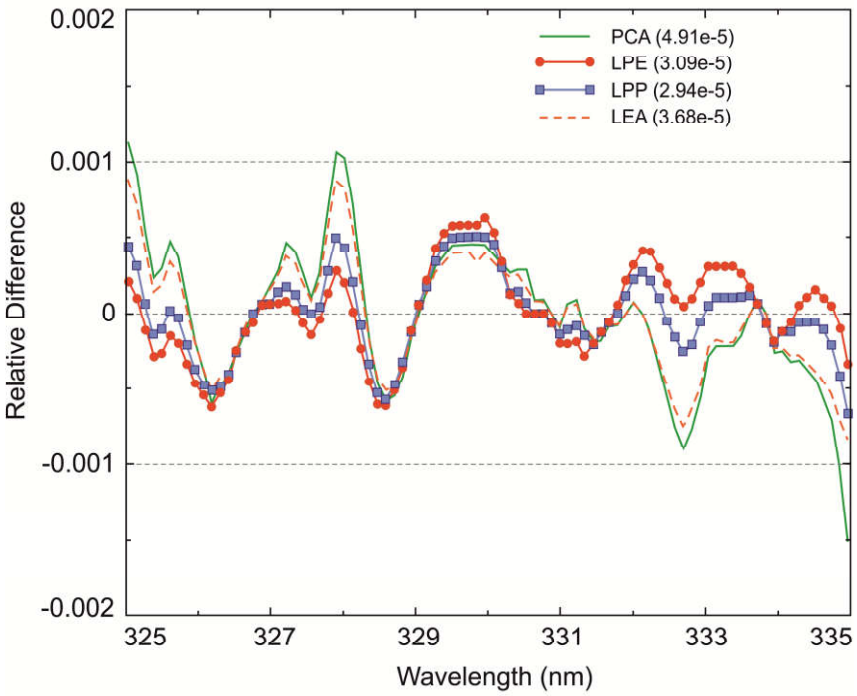

Relative differences in the radiance corresponding to the exact radiative transfer model using PCA and the radiative transfer models with linear embedding methods (LPE, LPP, LEA). The numbers in parentheses indicate the RMS of the relative difference. These values show that our new embedding methods provide a considerable improvement in accuracy.

We have examined various implementations of the SDV function and suggested a new algorithm based on a combination of two rational approximations.

The quality of remote sensing products critically depends on the accuracy of the radiative transfer used as the forward model in the inversion, with verification and validation being crucial. An intercomparison of IR spectra modeled by three independent LbL codes including our Generic Atmospheric Radiation LbL Infrared Code (GARLIC) was performed for a nadir viewing instrument.

It indicates brightness temperature differences mostly only in the sub-Kelvin range. This proved that GARLIC, the fastest code, is indeed a suitable choice for operational processor software where timeliness is pivotal.

Jacobians, i.e. matrices of partial derivatives of the spectrum with respect to the atmospheric state parameters, are important for the iterative solution of nonlinear inverse problems. Finite difference Jacobians are easy to implement but computationally expensive and of dubious quality. GARLIC utilizes algorithmic differentiation techniques to implement derivatives w.r.t. temperature and molecular concentrations. An in-depth assessment of finite differences clearly demonstrated the superior speed and accuracy of 'exact' algorithmic differentiation Jacobians.

LbL models are usually 'black boxes', given inputs such as line data and geometry they return radiance or transmission spectra. Py4CAtS (Python for Computational Atmospheric Spectroscopy), our partial re-implementation of GARLIC, allows radiative transfer modelling 'step-by-step'. The individual steps of an IR/microwave radiative transfer computation are implemented in separate functions. Until recently the tools provided in Py4CAtS could only be used as commands from the Unix/Linux shell. Now the functions can also be called within the Python interpreter, allowing easy visualization of intermediate quantities.[1]

[1] Py4CAtS is available at https://atmos.eoc.dlr.de/tools/Py4CAtS.

Ultraviolet and Visible

In the UV-VIS spectral range, multiple scattering has to be taken into account in RT modeling. Nowadays the Discrete Ordinate method for solving the RT equation is one of the most popular techniques in radiative transfer as it is stable for arbitrary optical thicknesses in a multi-layer stratified medium. An important parameter controlling the computational time and accuracy is the number of streams in the polar hemisphere N_{do}. RT models are called 'multi-stream' if $N_{do} \geq 2$, and 'two-stream', i.e. one stream per hemisphere, if $N_{do} = 1$. The accuracy is enhanced when N_{do} increases. However the computational time required for solving the RT equation also increases approximately as $(N_{do})^{2.5}$.

The atmospheric composition Sentinel missions generate two orders of magnitude more data than current missions and the operational processing of such big data is a challenge. Trace gas retrieval from remote sensing data usually requires high-performance RT model simulations. This is where usually the bottleneck for operational processing of the satellite data occurs. In this regard, acceleration techniques play an important role in the development chain.

Therefore, we developed techniques specifically designed for efficient computation of data with high spatial and spectral resolution. We pursued two ways. One was by developing suitable algorithm/code optimization methods based on dimensionality reduction techniques and correlation analysis of the hyperspectral data. The performance of this approach is remarkable: The Huggins band is reproduced with an accuracy of 0.1 %, while achieving an order of magnitude improvement in speed.

More hardware oriented, we have exploited multi-CPU and GPU parallelization techniques to achieve maximum performance. Our radiative transfer solvers have been parallelized by using an OpenMP interface, parallel libraries of matrix computing (Intel MKL) and the CUDA (Compute Unified Device Architecture) framework. For the latter, a crucial issue regarding performance is memory management. Our UV-VIS solver for simulating the level 1 spectra in the Huggins band has been implemented on a GPU platform. It takes into account memory limitations with additional GPU-specific implementation features including dynamic parallelism, CPU/GPU overlapping and asynchronous data CPU/GPU data transfer. With such acceleration techniques we finally achieved a total performance enhancement of an impressive factor 300.

Selected publications: [324], [70], [238], [157], [158], [72], [355], [354], [356], [351], [23], [352], [385], [784]

Inversion and Regularization

In atmospheric remote sensing we are confronted with discrete ill-posed problems which are unstable under data perturbations. These problems are solved by numerical regularization where the solution is stabilized by taking additional information into account. The regularization tool DRACULA (aDvanced Retrieval of the Atmosphere with Constrained and Unconstrained Least squares Algorithms), developed at IMF, is devoted to the retrieval of atmospheric state parameters from a variety of atmospheric sounding instruments. DRACULA includes direct and iterative regularization methods based on different principles. From the class of direct methods we mention the Tikhonov regularization with a priori, a posteriori and error-free regularization parameter choice methods, the regularized total least squares method, mollifier methods in which the generalized inverse is

constructed by means of a priori information, and the maximum entropy regularization which uses the relative or cross entropy as a non-quadratic penalty term. The iterative approaches included in DRACULA are the nonlinear Landweber iteration, the iteratively regularized Gauss-Newton method, the regularizing Levenberg-Marquardt method, the Newton-CG method and asymptotic regularization methods. They are insensitive to overestimation of the regularization parameter, do not depend on a priori information and can be applied to large scale problems.

DRACULA modules have been used in data processing for SCIAMACHY, MIPAS, GOME, and more recently, for GOME-2 and Sentinel-5P where they became part of UPAS2 (see *Generic Processing Systems* chapter). DRACULA also served for the analysis of observations from the balloon-borne FIR limb sounder TELIS and the airborne microwave radiometer MTP where a comparison between various regularization schemes was performed, to achieve an optimal retrieval setting. For trace gas retrievals where the spectral signal was strong, the direct methods turned out to be favorable while under noisy conditions, e.g. retrieval of aerosol and cloud parameters, iterative methods yielded reliable results. In addition, we applied DRACULA successfully in the SWIR spectral range for the retrieval of CO and CH_4 column densities from SWIR nadir observations allowing an intercomparison with NDACC (Network for the Detection of Atmospheric Composition Change) and TCCON (Total Carbon Column Observing Network) ground-based measurements.

Selected publications: [286], [351], [352], [415], [416], [418], [419], [253]

Cloud Retrieval

Clouds play a crucial role in the global radiation budget and are therefore of particular interest for climate studies and long-term monitoring. However, they are also an important factor in the retrieval of atmospheric constituents because their presence significantly affects the calculation of the trace gas vertical columns. Knowledge of main cloud properties including cloud fraction, cloud height and cloud optical thickness in the

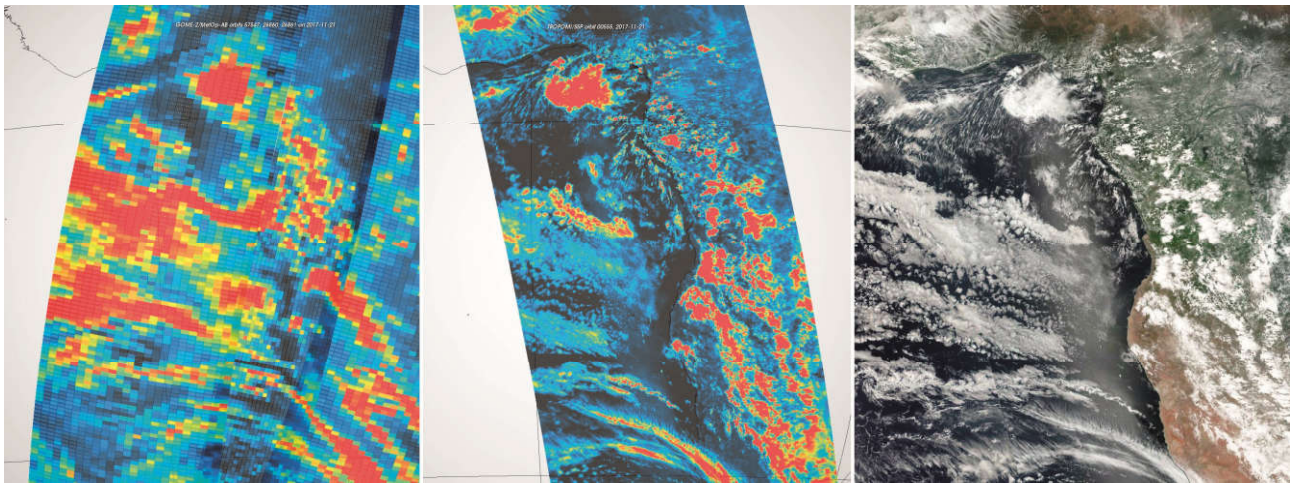

Cloud fraction for the same region around the west coast of Africa seen with GOME-2A/B (left), TROPOMI/Sentinel-5P (middle) and the corresponding visible scene from VIIRS (right) on November 21, 2017. TROPOMI results based on our cloud retrieval algorithm in the operational processor are comparable in resolution with visible imagery.

UV-VIS-NIR spectral region, where most of the trace gases such as O_3, NO_2, SO_2 and HCHO are retrieved, is therefore a necessity. Furthermore, cloud information from the UV-VIS spectral range is complementary to the information extracted from imagers operating in the VIS, NIR, SWIR and thermal IR region. We have developed two algorithms to retrieve cloud properties: OCRA, the Optical Cloud Recognition Algorithm for cloud fraction and ROCINN, the Retrieval of Cloud Information using Neural Networks for cloud height, cloud optical thickness and cloud albedo. The latter allows treating clouds either as Lambertian reflecting boundaries (CRB model) or, more realistically, as layers of scattering water droplets (CAL model). OCRA uses broad band reflectance information obtained in the UVN spectral range while ROCINN exploits information contained in the oxygen A-band in the near infrared. Both algorithms have been successfully applied in operational processing for GOME, SCIAMACHY, GOME-2 and recently TROPOMI on Sentinel-5P. They are constantly being improved and further developed to cope with the increasing demands and requirements posed by the next generation of atmospheric sounding instruments.

Selected publications: [215], [54]

Machine Learning

One of our prospective long-term studies is related to the development of machine learning techniques for atmospheric retrieval. We use machine learning to create a nonlinear mapping between the satellite measured radiances and the geophysical parameters of interest. We developed a special kind of algorithms specifically designed to construct an inverse operator. This type of algorithms is referred to as a 'full-physics inverse learning machine' (FP-ILM). The FP-ILM consists, as any machine learning algorithm, of a training and a subsequent operational phase.

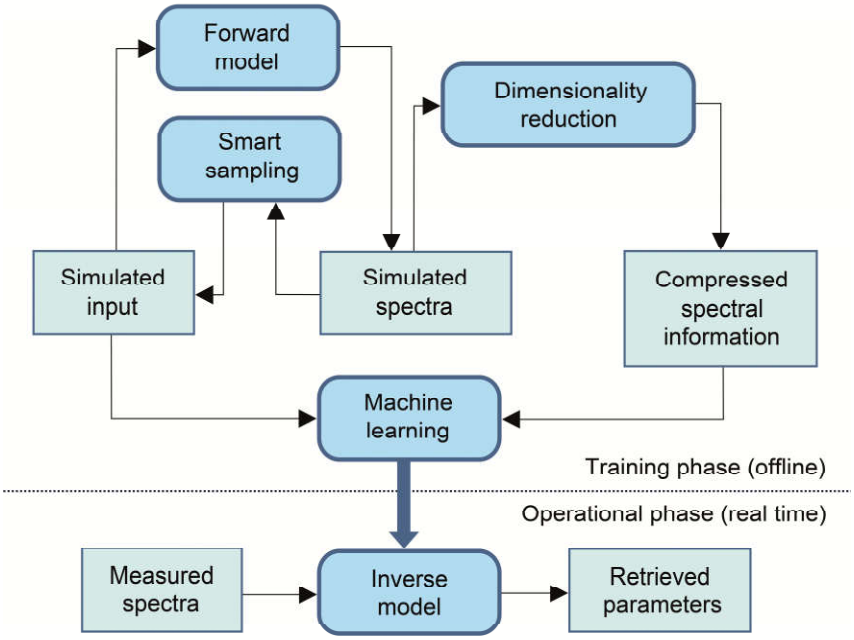

New scheme for the operational SO_2 plume height retrieval at the occurrence of volcanic eruptions. The algorithm relies on the combination of accelerated, smart spectral sampling-based radiative transfer modeling and neural network/machine learning inversion techniques.

The smart sampling technique as developed at IMF allows a reduction in the number of training samples required to fully cover the multi-dimensional function to be approximated by at least one order of magnitude. The main advantage of FP-ILM over conventional inversion algorithms is that the time-consuming training phase involving complex RT modeling is performed off-line; the inverse operator itself is computationally efficient. FP-ILM has been successfully applied to SO_2 plume height retrieval from GOME-2 and Sentinel-5P/TROPOMI, and ozone profile shape estimation from GOME-2. The retrieval results have shown that FP-ILM enables accurate prediction of atmospheric parameters and agrees very well with conventional methods. Furthermore, the FP-ILM produces a significant speed-up of two orders of magnitude compared to traditional

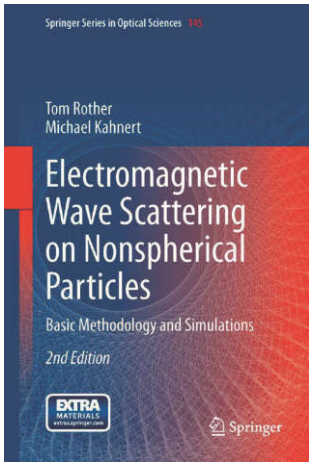

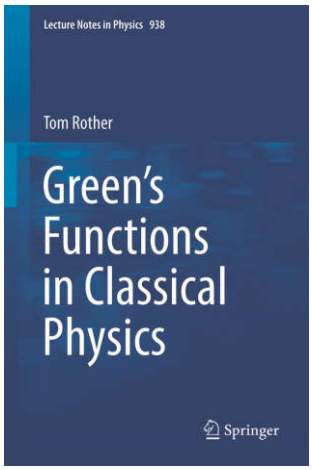

Monography and textbook (co-)authored by IMF scientist.

retrieval algorithms without degrading the retrieval quality. The FP-ILM algorithms are being integrated into UPAS and UPAS2 where they are paving the way for an efficient exploitation of the Big Data from the Copernicus satellite measurements.

Selected publications: [103], [170], [214]

Electromagnetic Scattering

Electromagnetic wave scattering is a basic physical process which has to be considered in a wide variety of different remote sensing techniques. Our expertise covers many of its aspects – from light scattering at non-spherical particles to sound scattering on bispheres. In particular, we have recently developed different scattering data bases for various applications. One of these data bases has been established in cooperation with TU Berlin and DLR's Institute of Planetary Research for studying the scattering greenhouse effect of CO_2 ice clouds in the atmospheres of exoplanets. Another scattering data base was implemented in cooperation with the Institute of Materials Research at DLR. It is designed and applied to estimate multiple scattering effects in THz extinction spectroscopy on dense particle clusters.

Beside the application of the scattering models and software developed so far, we refined our theoretical basis for modeling single scattering on nonspherical particles. This theoretical progress was published by Springer in the second edition of the textbook 'Electromagnetic Wave Scattering on Nonspherical Particles'. Moreover, a monograph 'Green's Functions in Classical Physics' was recently published in the Springer series 'Lecture Notes in Physics'. We demonstrated that the theoretical basis of light scattering used in our models can also be applied with benefit to other areas of physics.

In a theoretical study we dealt with the Einstein-Podolsky-Rosen paradox and Bell's inequality for a certain class of probability experiments. As proven in the past, this inequality must hold for any classical probability experiment but may be violated in quantum mechanics. Later the so-called CHSH-inequality – an inequality that better fits correlation measurements than Bell's inequality – was proposed by Clauser, Horne, Shimony and Holtas as alternative. The impossibility of violating it in any classical experiment remains a controversial aspect being discussed in physics. Based on our experience in light scattering we were able to propose an alternative classical optics experiment which results in a violation of the CHSH-inequality if formulated in terms of intensities. In our experiment the correlation measurements are highly sensitive and can be applied in a similar manner as known from scattering experiments. Furthermore we demonstrated that a T-matrix and a Green's function both relate to the mentioned experiment. The T-matrix is determined in a similar way known from light scattering. It represents the decisive element of the interaction part of the Green's function. Even though our approach to combine classical light scattering with correlation experiments may seem rather theoretical, it may open new doors for the development of diagnostic methods in modern optics.

Selected publications: [802], [234], [799]

Spectroscopic References

The retrieval of atmospheric parameters from remote sensing data requires quantitative knowledge of molecular absorption features for radiative transfer calculations. Therefore, a number of data bases, e.g. HITRAN, GEISA exist to provide the necessary information such as line parameters or absorption cross-sections. These data bases must be continually updated, either to improve their completeness and accuracy or because new missions have additional needs.

Our spectroscopic reference lab (see *Laboratory Infrastructure and User Services* chapter) belongs to the few world-wide capable of providing spectroscopic data with well-defined error bars. Of the many results obtained in recent years, those particularly worth mentioning are:

– New absorption cross sections for bromine nitrate, $BrONO_2$, a reservoir for bromine, previously only known to 20 % accuracy, were generated with 2 % accuracy. Improved spectroscopic data help to quantify the inorganic bromine budget in the atmosphere which is important for mid-latitude ozone chemistry.

– Within a DFG-funded project the mid infrared spectroscopic data base of water was updated, dedicated to ground-based high resolution solar occultation spectroscopy as employed by the TCCON and NDACC networks. For the first time, parameters of the enhanced partially correlated quadratic speed dependence hard collision line shape model, the so-called Hartmann-Tran profile, have been determined for water in an extended spectral range.

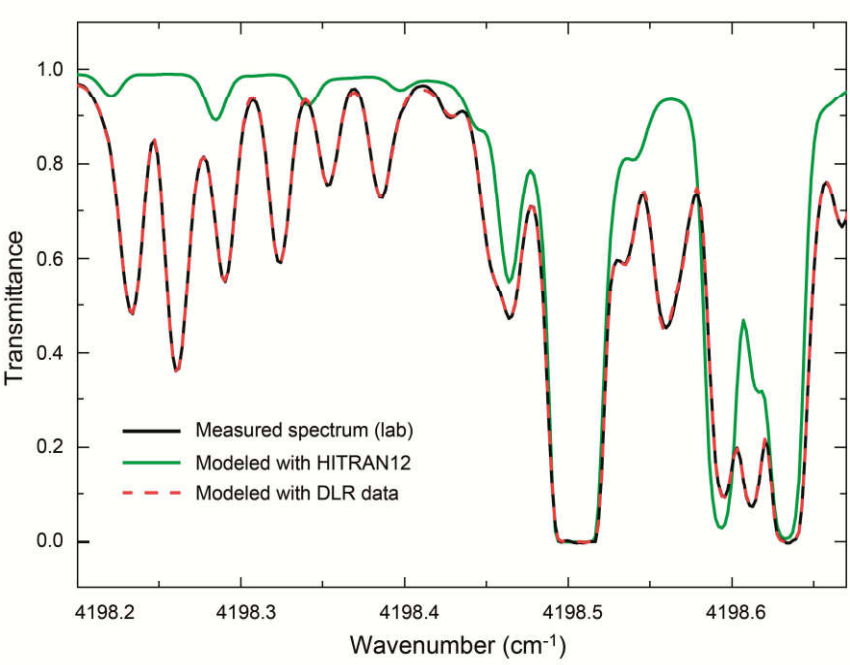

Improvement of CH_4 spectroscopic data using laboratory transmittance measurements. IMF's measurement and analysis activities improved the CH_4 spectroscopic database according to the needs of the TROPOMI instrument on Sentinel-5P.

– Within the ESA-funded spectroscopy project SEOM-IAS the spectroscopy of CH_4, H_2O, and CO in the 2.3 µm region has been updated for Sentinel-5P/TROPOMI measurements. The new spectroscopy was validated by ground-based high resolution solar occultation measurements where the spectra could be modelled down to the noise level, a feat never before achieved. Furthermore, the new spectroscopy allowed meaningful retrieval of methane profiles for the first time. Within the same project a new UV spectroscopic data base for ozone was generated. A new mid-infrared line intensity data base is now under way.

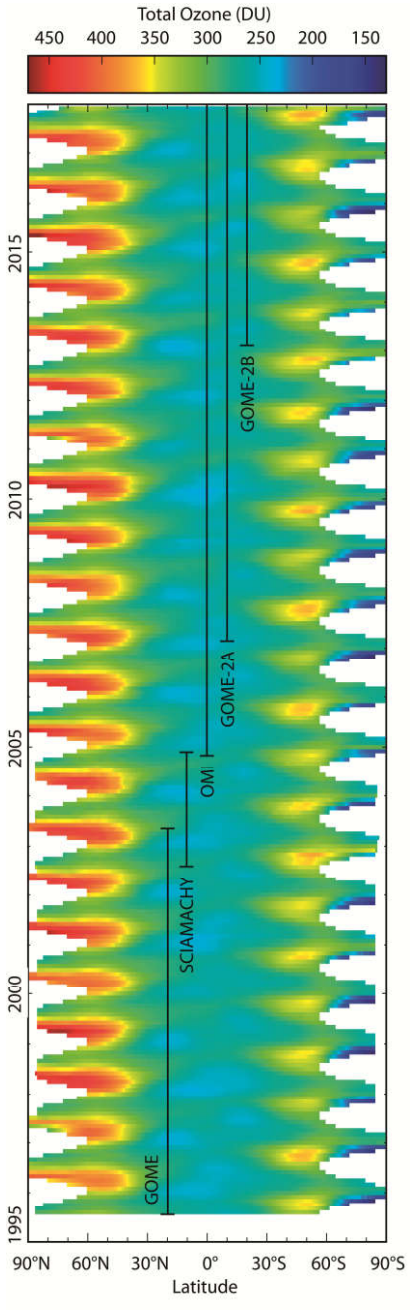

Homogenized global GOME-type total ozone from 1995 until 2017.

– Water line intensities from different projects at DLR were compared to purely ab initio calculations. For a large number of transitions the agreement was within 1 %, validating theory and experiment. However, large differences up to 13 % were also identified which could be traced back to problems in the ab initio calculation. Our experimental findings have meanwhile triggered efforts to improve those calculation.

Selected publications: [98], [117], [130], [131]

Geoscientific Research

Long-term Observation of Ozone

The Global Climate Observing System (GCOS) identified a number of Essential Climate Variables (ECVs) from the atmospheric, oceanic and terrestrial domains which are required to characterize the Earth's climate system and its changes, and to support the climate research community addressing climate-relevant concerns. In the framework of ESA's Climate Change Initiative and the EU Copernicus Climate Change Service ozone projects IMF was assigned the task of development and quasi-operational production of the satellite-based total ozone ECV.

We used data from GOME, SCIAMACHY, GOME-2 and OMI to create homogenized global GOME-type total ozone (GTO) ECV which currently covers the 22-year period 1995 – 2017. New multi-satellite merging algorithms were developed using traditional and machine learning techniques. Geophysical validation by independent ground-based observations has shown that the accuracy and long-term stability of this data record are at the percent level, thereby convincingly meeting the official user requirements defined by GCOS.

Hence the GTO-ECV data record is valuable for a variety of climate-relevant applications such as long-term monitoring of the past evolution of the ozone layer, decadal trend analysis on global and regional scales, and the evaluation of chemistry-climate model simulations. The data record enables us to disentangle different aspects of ozone variability and its drivers using multivariate linear regression. The main contributors are the quasi-biennial oscillation, the 11-year solar cycle, the El Niño – Southern Oscillation and the Brewer-Dobson circulation. Of particular interest is the search for signs of recovery of the stratospheric ozone layer as a consequence of the 1987 Montreal Protocol and its subsequent amendments. Various total ozone observational data records indicate that for most regions the trends since the mid-1990s are mostly not significantly different from zero because they are still considerably masked by large dynamically induced inter-annual variability. However, for some latitudes and seasons there are signs that stratospheric ozone is starting to emerge into the expected recovery phase. The results clearly indicate a need for continuous monitoring of ozone and an extension of the current data records using future missions. Since 2010 our GTO-ECV data record contributes to the quadrennial WMO/UNEP Scientific Assessment of Ozone Depletion as well as the yearly State of the Climate bulletin from the American Meteorological Society.

Selected publications: [347], [348], [279], [40], [212], [369], [79], [813]

Sulphur Dioxide

Sulphur dioxide (SO_2) is a natural trace gas in the Earth's atmosphere. The largest source is the burning of fossil fuels by power plants and other facilities while industrial processes such as extracting metal from ore produce less SO_2 pollution. These anthropogenic emissions are mostly confined to the lower troposphere where SO_2 is subject to wet and dry deposition within a few days. Natural SO_2 sources are volcanic degassing events and eruptions. They inject SO_2 into the atmosphere, ranging from the lower troposphere in the case of passive degassing up to the stratosphere for explosive eruptions. Especially in the latter case, the lifetime of SO_2 in the atmosphere may reach up to a month. Chemical reactions then form sulfate-aerosols and acid rain.

The timely retrieval of SO_2 is important for monitoring volcanic eruptions which are a major natural hazard, not only to the local environment and local population but also to aviation. When entering the aircraft SO_2 can cause breath disease for passengers or sulphidation of the engines. An even more severe danger are volcanic ash emissions which, in the worst case, can lead to the loss of the aircraft. Since detection of volcanic ash is not straightforward, our SO_2 retrievals derived within two hours after sensing, serve as a fast means to locate remote volcano eruptions that may pose a potential hazard to aviation.

Current and near-future spaceborne atmospheric sensors are capable of detecting global anthropogenic emissions and volcanic eruptions on a daily basis, even in remote regions, where ground-based monitoring is impossible. Our retrieval of the total column density of SO_2 uses solar backscatter measurements in the UV wavelength region, around 320 nm. In the framework of EUMETSATs Atmospheric Composition Satellite Application Facility (AC-SAF), we retrieve total SO_2 columns in near-real time, i.e. within 2.5 h after measurements, from GOME-2 continuously since 2007. Once MetOp-C is launched in 2018, data will be available up to at least 2025. This is important for studying atmospheric variations or long-term trends in

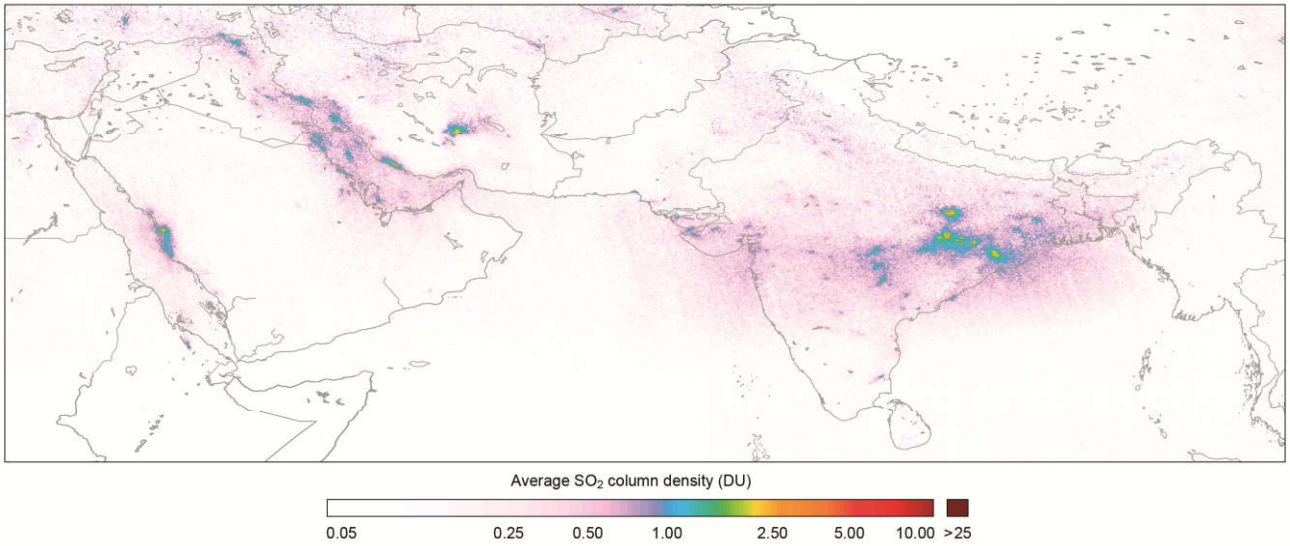

Weak anthropogenic SO_2 emissions in the Middle East (offshore flaring and refineries) and India (coal-fired power plants) detected by Sentinel-5P. The image was created by averaging daily measurements from November 8, 2017 to April 15, 2018.

anthropogenic emissions. With Sentinel-5P in orbit, our SO_2 work has reached a new quality. UV spectral measurements can now be made with an unprecedented spatial resolution of 3.5 × 7 km². Together with the high spectral resolution and low noise level, Sentinel-5P allows for the detection of weak emission sources within a single day where GOME-2 required an appreciably larger timespan. This opens up new prospects for future spaceborne SO_2 monitoring.

Furthermore, we have developed a volcanic activity detection algorithm which provides crucial information for activity monitoring and SO_2 plume forecast calculations. The derived volcanic SO_2 flag is used, e.g. by ECMWF which assimilates the data to forecast the movement of the SO_2 cloud. Precise knowledge of the location and height of the volcanic SO_2 plume, parameters which are mostly unknown at the time of measurement, is essential for accurate determination of SO_2 emitted by volcanic eruptions. We avoided the very time-consuming, and thus for near real-time applications unsuitable approaches of current UV-based SO_2 plume height retrieval algorithms by applying our novel method for extremely fast and accurate retrieval based on machine learning techniques. Very promising results have been obtained for the GOME-2 data from the Eyjafjallajökull/Iceland eruption in May 2010 and Kasatochi/Aleutian in August 2008, as well as for the TROPOMI data from Mt. Agung/Indonesia in November 2017 and Sabancaya/Peru in March 2018.

The SO_2 products provided by IMF are used by:

- Aviation Control Service (ESA-SACS), which assists the Volcanic Ash Advisory Centers in providing expertise to civil aviation authorities in case of significant volcanic eruptions
- Copernicus Atmosphere Monitoring Service (ECMWF-CAMS) which assimilates the data to forecast the movement of volcanic SO2 clouds
- European Natural Airborne Disaster Information and Coordination System for Aviation (EUNADICS-AV) whose main objective is closing the gap in European-wide data and information availability during airborne hazards by developing and deploying a data platform that provides all necessary information to decision makers in real-time in case of an airborne hazard.

Selected publications: [103], [389], [344], [826], [422], [162]

Global distribution of SO_2 hot spots derived from Sentinel-5P measurements discriminating volcanic (yellow) and anthropogenic (red) origin. Green dots denote unknown origins but most likely plumes drifted off from volcanic or anthropogenic sources.

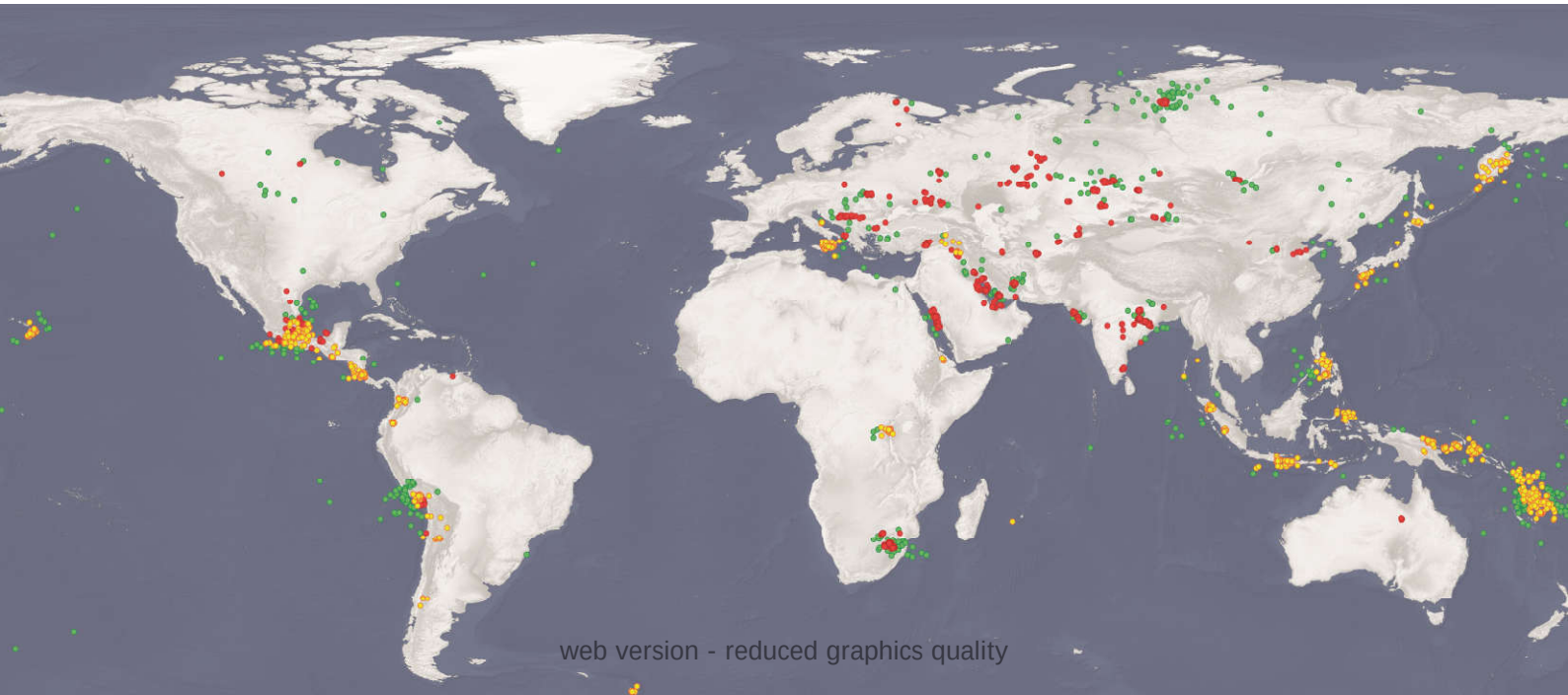

Tropospheric Nitrogen Dioxide and Air Quality

Satellite remote sensing of air quality on urban, regional and global scales is of great importance since air pollutants are responsible for strong environmental and health impacts, and also play an important role in global climate change.

Measurements from GOME-2, OMI and recently TROPOMI on Sentinel-5P, make it possible to study the large-scale temporal and spatial variability of tropospheric NO_2, permit the detection of anthropogenic SO_2 emissions over polluted regions and provide access to the tropospheric O_3 columns. We have developed a tropospheric ozone retrieval for the (sub)-tropical region based on the convective cloud differential method. Using total ozone and cloud property data from GOME, SCIAMACHY, OMI and GOME-2, a 20-year time series (1995 – 2015) of tropospheric column ozone was generated. In the tropics, a positive trend in tropospheric ozone of 0.7 DU per decade was found.

In the last three decades, air pollution has become a major environmental issue in metropolitan areas of China as a consequence of fast industrialization and urbanization. The world's largest area with high NO_2 pollution is found over east China. Apart from the economic recession period 2008/2009, a clear increase of tropospheric NO_2 over northeast China is found from 2007 – 2013, followed by a strong decrease continuing through to 2018. Our GOME-2 NO_2 measurements indicate that recent control strategies and economic transformations in China were effective in reducing emissions. To estimate ground-level NO_2 concentrations over Eastern China, tropospheric NO_2 columns from the Ozone Monitoring Instrument (OMI) together with ambient monitoring station measurements and meteorological data have been used in a geographically and temporally weighted regression model.

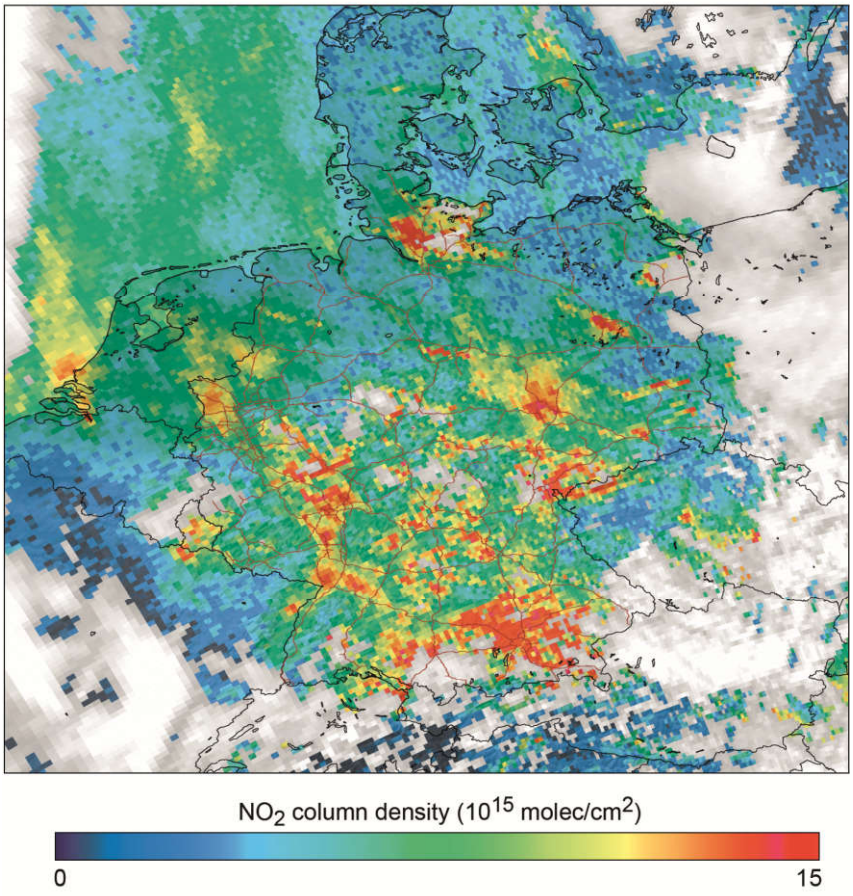

Tropospheric NO_2 over Germany as measured by TROPOMI aboard Sentinel-5P on February 14, 2018. This map has been produced in the commissioning phase from only a single overpass with moderate cloud coverage. Even though the processor still needed optimizing, the map already demonstrates the tremendous improvement in atmospheric composition retrievals achievable in the coming years.

IMF's expertise in satellite observations of important trace gases has also been used to monitor air quality changes over China caused by the East Asian monsoon circulation within the framework of the ESA-MOST Dragon project. The East Asian monsoon plays a significant role in characterizing the temporal variation and spatial patterns of air pollution over China. The Infrared Atmospheric Sounding Interferometer (IASI) detected a decrease in tropospheric ozone during

the monsoon period over the East Asian cities. Seasonal cycling of tropospheric NO_2 as measured by GOME-2 shows consistent higher values during winter due to the higher anthropogenic sources and longer lifetime.

One of the key topics in today's discussion about air pollution is the impact of traffic and transport, particularly from motor vehicles. The spatial resolution of past spectrometric sensors was too low to unambiguously permit detection of the effects of their emissions. With Sentinel-5P, the situation has changed. Due to its high resolution, these data, in conjunction with chemistry transport models, will allow transport-induced emission patterns to be inferred. Together with partners we have started initial work to prepare our algorithms and processors for NO_2 measurements from Sentinel-5P and to combine these with vehicle inventories and suitable transport models.

Selected publications: [394], [210], [271], [146], [439], [456], [235]

Monthly average tropospheric NO_2 over Eastern China from 2006 until 2017. Since 2014 a general decrease can be observed. The difference between GOME-2A and -2B at peak values falls within the error range of the NO_2 densities and can partially be attributed to different instrument properties affecting the retrieval.

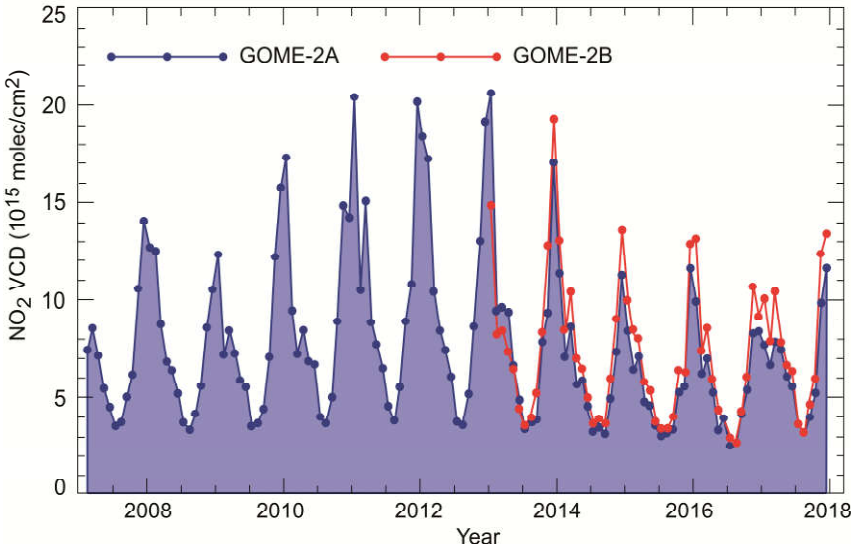

Atmospheres of Exoplanets

Today, 23 years after the discovery of the first extra-solar planet orbiting a main-sequence star, more than 3,700 exoplanets have been detected, including a few dozen super-Earths and Earth-like planets. In the last decade the characterization of these remote worlds has increasingly gained attention. The question of the spectral appearance of terrestrial exoplanets and the possibility to identify signatures of life have been the focus of a series of modeling studies, whereas the quantitative characterization by atmospheric retrieval techniques is so far mainly confined to larger objects such as hot Jupiters and Neptune-sized planets. Clearly the analysis of smaller objects such as super-Earths and Earth-like exoplanets is more challenging. Together with TU Berlin we addressed this particular exoplanet regime in the DFG project *Characterization and retrieval of atmospheric parameters of terrestrial extrasolar planets around cool host stars*.

For an assessment of exoplanet atmospheric remote sensing, Earth seen from space is an ideal test case; in fact it is the only planet that can be used for validation of retrieval codes. However, data from spaceborne EO missions have rarely been used to demonstrate the capabilities of exoplanet atmospheric studies. The Canadian Atmospheric Chemistry Experiment – Fourier Transform Spectrometer (ACE-FTS) observes the Earth's limb in solar occultation. Hundreds of spectra recorded in the 2004 – 2008 timeframe have been averaged to compile five infrared spectral atlases for various seasons and latitude bands. We used these atlases to generate effective height spectra of the Earth and to compare these with spectra modeled with GARLIC to assess the visibility and detectability of atmospheric gases in transit spectra. Our analysis has demonstrated that 10 gases substantially contribute to Earth's transit spectrum: CO_2, O_3, H_2O, CH_4, N_2O, N_2,

HNO_3, O_2 and the CFCs CCl_3F and CCl_2F_2. Some remaining discrepancies can be attributed to small contributions of CO, NO, NO_2, OCS, CF_4, $ClONO_2$ and N_2O_5. However, the importance of these 17 gases for modeling does not necessarily imply their detectability in noisy low resolution spectra.

For the quantitative estimation of atmospheric state parameters by spectroscopy, inversion by numerical optimization techniques is well established for planets of the solar system and has also been applied successfully to large extrasolar objects such as hot Jupiters. In general, the lack of any a priori knowledge presents a considerable challenge with remote sensing of the atmospheres of Earth-like or terrestrial exoplanets being even more demanding because of the few known objects and the even fainter signals. We have coupled a nonlinear least squares solver to GARLIC to investigate the feasibility of column density retrievals from Earth transit spectra using a set of Earth climatological profiles. The results obtained so far show that it is indeed possible to retrieve the molecular abundances of an atmosphere with the right pressure-temperature profile. GARLIC continues to be an important tool for us and our partners in spectroscopic studies concerning the atmospheres of exoplanets.

Selected publications: [71, [451], [22], [452], [455], [424]

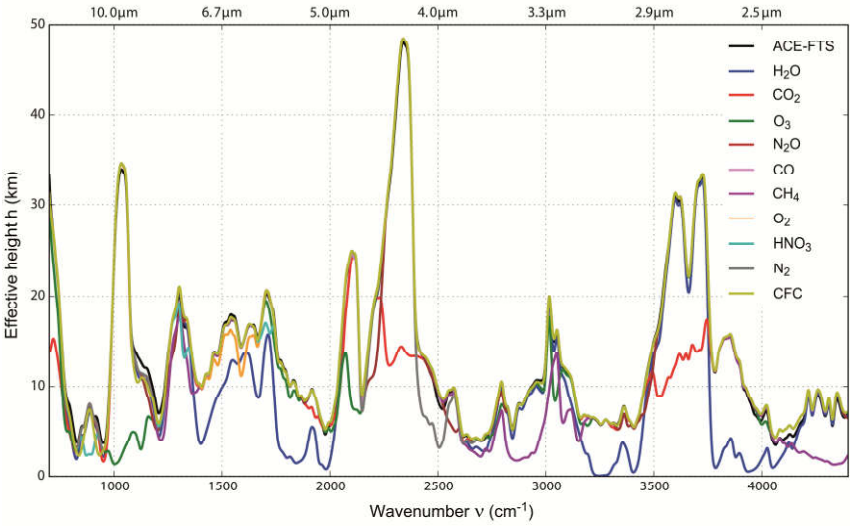

Modeled Earth's atmospheric effective height spectrum for the ten 'main' gases in comparison to the measured spectrum during solar occultation by the Canadian ACE-FTS sensor aboard the SCISAT-1 mission. It illustrates the height where an atmosphere becomes opaque.

Data Science in Earth Observation

Data Science in Earth Observation

Besides the IMF's pool of expertise in sensor technologies for SAR, optical imaging and atmospheric spectrometry, algorithms fusing these technologies have been gaining importance for years. Furthermore, EO has irreversibly arrived in the Big Data era with the Sentinel satellites (and in the future with Tandem-L). This requires not only new technological approaches to manage large amounts of data (as pursued by DFD), but also new analytical methods. Here, the methods of data science and artificial intelligence (AI), such as machine learning, become indispensable. Deep learning in particular has led to a revolution in AI in recent years, but its potential for EO has only recently been discovered. Motivated by these facts, IMF has placed one of its research foci on EO Data Science. These are our research goals:

- **explorative model-based signal processing algorithms to improve information retrieval from remote sensing data of current and next generation EO missions**
- **exploration of AI for EO**
- **sophisticated algorithms for discovering novel applications fusing sensor technologies**
- **Big Earth Data analytics – from knowledge discovery, HPC to geoscientific applications**
- **harvesting unconventional geodata sources, such as social media and NewSpace satellites.**

This section summarizes our research highlights in this reporting period, with respect to the aforementioned goals.

Modern Model-based Signal Processing Algorithms

Sparse Reconstruction

Sparse signals are common in remote sensing. By exploiting signal sparsity, e.g. by using the Compressive Sensing theory, we can either achieve higher resolution compared to the Nyquist sampling theory or reduce the required number of measurements for achieving a given resolution request. IMF explores this idea for tomographic SAR inversion, SAR imaging, hyperspectral unmixing and data fusion for multi- and hyperspectral resolution enhancement.

One highlight is tomographic SAR (TomoSAR, see also *Synthetic Aperture Radar* chapter). It uses stacks of acquisitions to reconstruct the reflectivity of scattering objects along the elevation coordinate for every azimuth-range pixel, and hence allows SAR imaging in 3D or 4D considering the time dimension (long-term motion). For many imaging geometries, e.g. in urban environment, the signal is sparse in elevation. We were the first to use Compressive Sensing and sparse reconstruction for tomographic SAR inversion. In the previous reporting period we showed that in the range direction for SAR, we could achieve a super-resolution factor between 1.5 and 25. Since then we have worked on finding the lower limit for the required number of images for TomoSAR. By introducing geometric priors by means of group sparsity or structured sparsity, we are now able to reduce the minimum required number of images from typically 20 to only six.

Sentinel-2

Sentinel-1

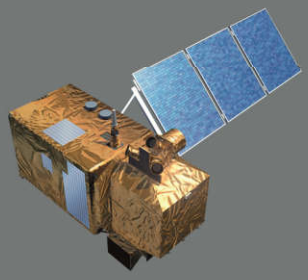

EnMap

TerraSAR-X

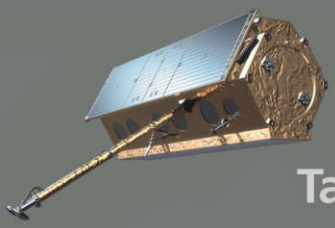

TanDEM-X

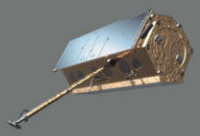

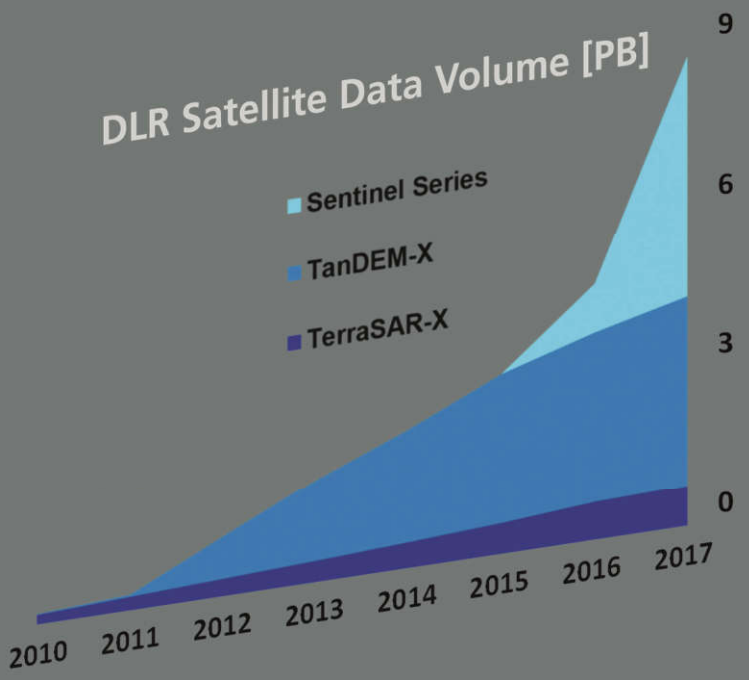

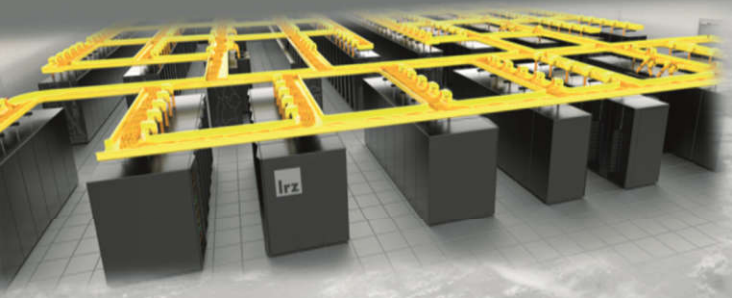

flickr

Google

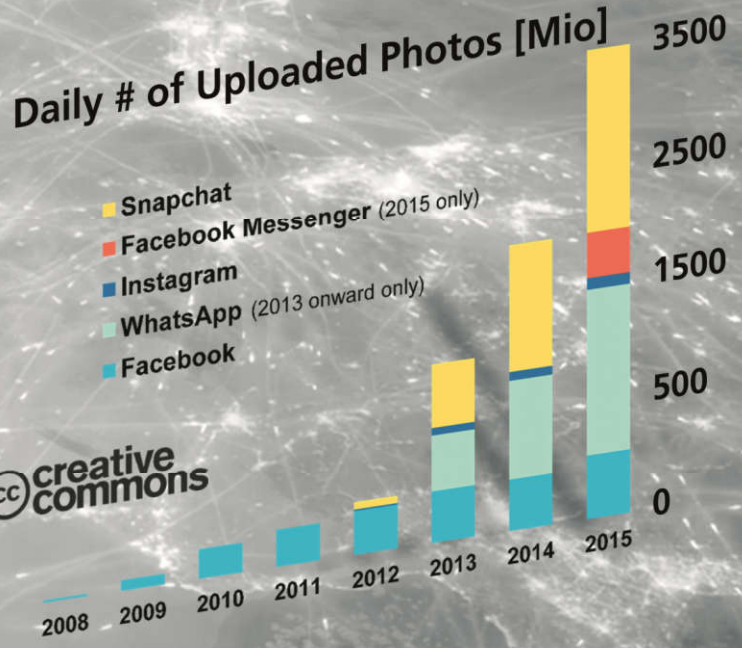

creative commons

web version - reduced graphics quality

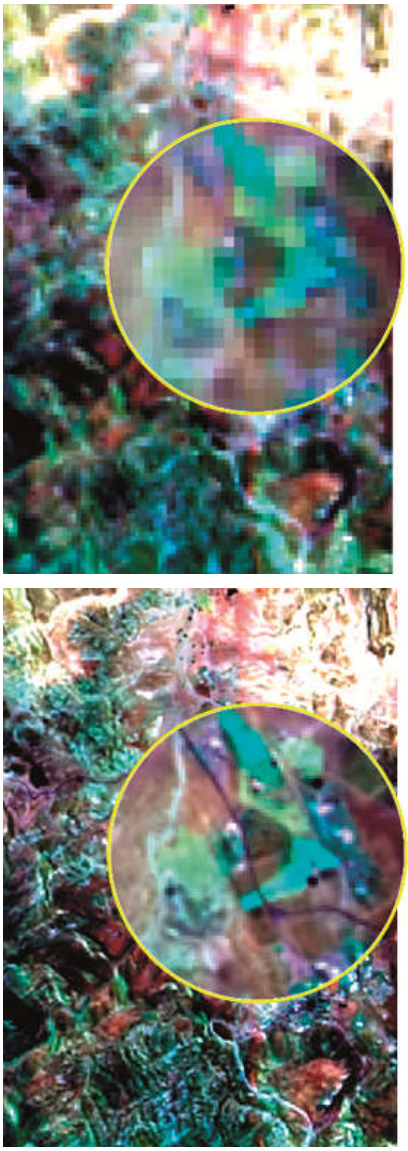

Top: EnMAP-like hyperspectral input data of 30 m resolution, synthesized from HyMAP data. Bottom: J-SparseFI-HM-super-resolved hyperspectral data cube with a spatial resolution of 10 m. Site: Cabo de Gata National Park, Spain.

Another highlight is the fusion of multi-resolution imagery. Optical remote sensing technology has rapidly advanced in terms of spatial, spectral and temporal resolutions over the last decade; however, there remain trade-offs between spatial and spectral resolution, signal-to-noise ratio and swath width. These limitations call for sophisticated data fusion techniques which are capable of merging images from complementary sensors to generate data that features both high spatial and high spectral resolution at a high signal-to-noise ratio. We have developed a series of sparse image fusion methods, including SparseFI, J-SparseFI and J-SparseFI-HM that are capable of super-resolving multi-, super- and hyperspectral remote sensing imagery at quantitatively better image quality than what is obtainable with other state-of-the-art methods.

Selected publications: [257], [656], [657], [721], [797], [277], [647], [273], [651], [701], [761], [796], [457], [754], [755], [396], [798]

Robust Estimation

TomoSAR research conducted by SAR experts is mostly limited to reconstructing point clouds. We went a step further and developed the first approaches for reconstructing building models and even individual trees from these tomographic point clouds. This is a challenge, since due to multiple scattering and limited resolution the quality of TomoSAR clouds is by no means comparable to lidar measurements. Outlier points strongly influence the reconstruction results when using classical estimation methods. Robust estimators such as RANSAC, robust PCA, L_1-norm minimization and M-estimators are employed in the proposed approaches. In this regard, we were the first to present façade and building roof reconstruction based on spaceborne TomoSAR point clouds, which even further extended the framework to robustly work on city scales. We also presented a full processing pipeline for single-tree reconstruction from airborne SAR observations. We were able to successfully reconstruct about 74 % of all trees in a study subset, for which core tree parameters such as height, crown radius and spatial location could be reconstructed with sub-meter accuracy.

Robust covariance matrix estimation is a key for multi-baseline InSAR – one of the most popular techniques to access long-term deformation over large areas. Algorithms like SqueeSAR involve the estimate of the covariance matrix and its inversion. Typically, the optimal estimators are derived on the assumption of ergodic complex Gaussian-distributed

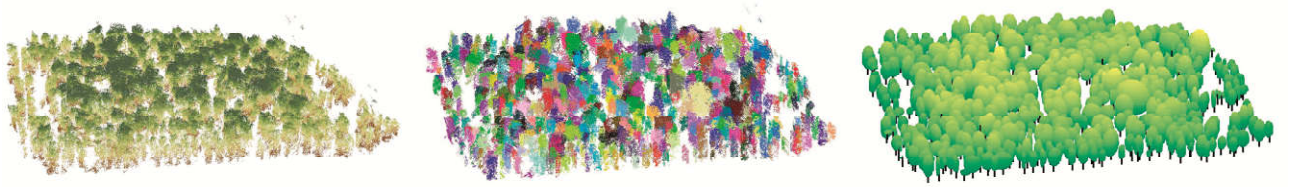

Analyzing forests on the single-tree level with SAR imagery: raw airborne TomoSAR point cloud (left), point clusters corresponding to individual trees (center) and the final tree reconstruction result via a robust fitting of tree crown ellipsoids (right). SAR data: MEMPHIS Data provided by Fraunhofer Institute for High Frequency Physics and Radar Techniques.

observations which does not always hold for SAR data. As the spatial resolution improves in modern SAR systems, the statistics and deformation history of SAR image pixels become more heterogeneous. We developed a solution named *robust InSAR optimization* (RIO) for robustly estimating InSAR covariance matrices, as well as the phase history parameters, e.g. deformation rate, under the existence of nonergodic non-Gaussian samples and unmodeled interferometric phase. Simulations show that in the typical setting of TerraSAR-X data stacks RIO can improve the accuracy of the deformation rate estimates by 2 – 6 times when the data is contaminated by an outlier rate of up to 40 %, while preserving 90 % of the relative estimation efficiency under the ideal ergodic complex Gaussian distribution.

Selected publications: [239], [326], [323], [674], [676], [675], [399], [755], [787], [788], [252], [580], [945], [640], [684], [750]

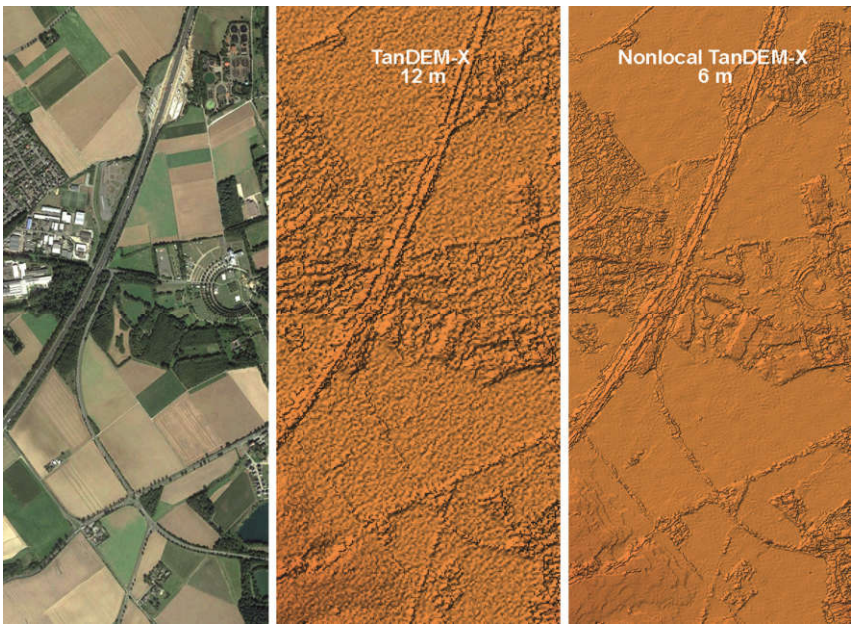

A comparison of standard TanDEM-X raw DEM (middle) and improved nonlocal filtered TanDEM-X DEM (right). Site: Jülich area, Germany.

Nonlocal Filtering

Noise reduction is a standard step in EO data processing. Often classical local filters are used, e.g. multilook-processing for SAR and InSAR data, which always reduce the spatial resolution. This calls for nonlocal approaches that take advantage of the high degree of redundancy in natural images. We explored nonlocal concepts for filtering TanDEM-X interferometric data, as mentioned in the *SAR* chapter. By introducing tailored nonlocal InSAR filtering, we demonstrated the possibility of achieving a resolution of 6 m and a relative height error below 0.8 m, i.e. an increase in quality by a factor of 2 × 2 in resolution and a factor of 2 m/0.8 m = 2.5 in height accuracy – all in all one order of magnitude.

Selected publications: [524], [587], [753]

Tensor Analysis

Thanks to the increasing availability of EO data, time series analysis is becoming standard and opens up opportunities for new applications. Time series data can be considered as tensors allowing all the advances in tensor analysis to be exploited. We developed tensor-based algorithms for the retrieval of geo-parameters, such as topography, deformation and cloud coverage from SAR and optical time series data.

Previous research on multi-baseline InSAR, i.e. InSAR time series analysis, was mostly focused on the retrieval of geophysical parameters on the basis of a single pixel or a pixel cluster. They require a fairly large stack of images (usually more than 20) for reliable estimation. For areas with a limited number of images, these methods are not directly applicable. To tackle such a challenge, we proposed a framework of object-based (instead of pixel-based) algorithms,

named Robust Multi-pass InSAR technique via Object-based low-rank tensor decomposition (RoMIO) that fuses geometric information with traditional multi-baseline InSAR via tensor analysis techniques. RoMIO reaches comparable filtering performance to state-of-the-art filtering algorithms, i.e. nonlocal means filtering. However, it outperforms nonlocal means filtering by a factor of two in the interferometric phase variance when the interferogram is corrupted by 50 % outliers. This extreme robustness in turn improves the parameter estimation in multi-baseline InSAR algorithms.

One of the major nuisances of working with Sentinel-2, Landsat, WorldView and other optical EO data is the presence of clouds, which, on average, cover 35 % of the Earth's surface. Many methods have been developed to reconstruct ground information that is missing due to the presence of clouds. Established techniques primarily use spatial information from non-occluded pixels, spectral information from other channels or temporal information from cloud-free images acquired at different times. We have developed a hybrid data reconstruction algorithm to make full use of spatial, spectral and temporal information. The Non-Local Low-Rank Tensor Completion (NL-LRTC) method concatenates multi-temporal remote sensing imagery, reshapes it to 4D tensors and reconstructs cloudy parts and other irregularities in the data by minimizing the tensors' ranks. The quality of the N--LRTC products was assessed to be consistently comparable or better than those obtained with state-of-the-art methods. In tests with real cloudy images, for which no ground truth is available, NL-LRTC gives reconstructions visually most natural and similar to cloud-free acquisitions taken at similar times.

Selected publications: [50], [126], [548], [499], [471], [49]

Artificial Intelligence for Earth Observation (AI4EO)

Artificial intelligence is currently penetrating many technological areas. Even though the term is in inflationary use today, it often refers to machine learning, usually with deep neural networks (Deep Learning). Internet giants such as Google, Facebook and Microsoft with their almost unlimited computing capacities achieved spectacular results in image classification, text translation and in the *Go* game. We consider ourselves one of the pioneers in using Deep Learning in remote sensing and are enthusiastic about its possibilities. Going beyond quick-wins by fine-tuning existing architectures for the usual classification and detection tasks, we take particular care of the fact that EO data and problems are in many aspects different from standard imagery found on the internet.

Multi-modality

Remote sensing data are often multi-modal, e.g. from optical (multi- and hyperspectral) and SAR sensors, where both the imaging geometries and the scattering properties are completely different. Data and information fusion uses these complementary data sources in a synergistic way. To this end, we have developed different multiple-stream convolutional neural networks (CNNs) for the fusion of hyperspectral data with PolSAR, lidar and multispectral data.

Prior to joint information extraction, a crucial step is to develop novel architectures for the matching of images taken from different perspectives and even different imaging modalities, preferably without requiring an existing

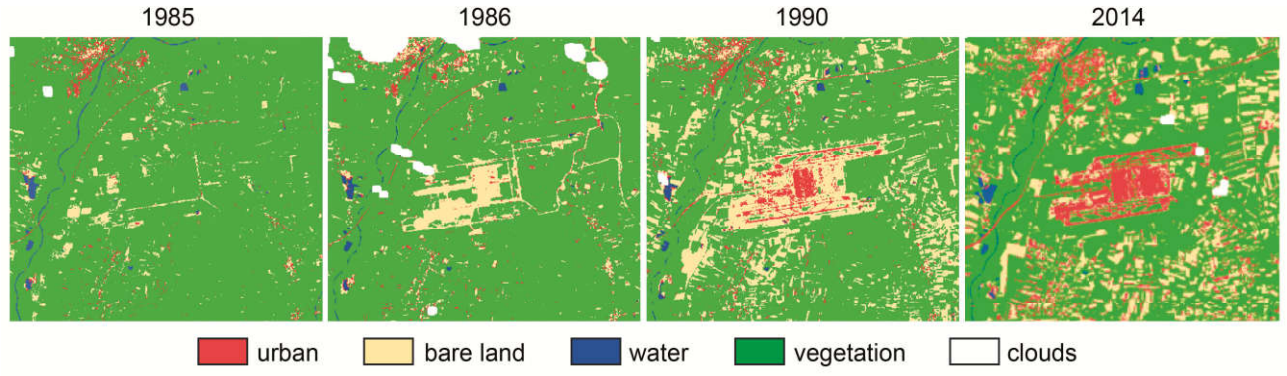

Transfer learning for land cover classification: Deep learning requires large amounts of labelled training data which are not readily available in remote sensing. To classify land cover over 30 years (1984 – 2014) for four different cities (Munich, Beijing, New York and Melbourne) from Landsat data we used transfer learning based on labeled data from only one city and one year (Beijing, 1990) and achieved an overall accuracy of better than 95 %. This example illustrates how Munich airport has been built.

3D model. Here, we developed tailored CNN-based architectures for SAR/optical image coregistration. Also, besides conventional decision fusion, an alternative is to investigate the transferability of trained networks to other imaging modalities. To address this, we designed generative adversarial network (GAN)-based deep architectures for SAR-optical and optical-SAR translation with the applications of change detection and colorizing SAR images with optical textures.

Selected publications: [57], [137], [497], [110], [150]

Geolocation

Remote sensing data are geolocated, which facilitates the fusion of information with other sources of data, such as GIS, geo-tagged images from social media, or simply other sensors (as above). This fact allows data fusion to be tackled with non-traditional data modalities. For example, we have combined GIS data with the globally available TanDEM-X SAR amplitude images to estimate building height on a large scale. In addition, street-view images are fused with optical satellite imagery to detect building changes, and to classify building functions.

Selected publication: [516]

Time Series Data

As mentioned before we observe a shift from individual image analysis to time-series processing. Novel network architectures must be developed for optimally exploiting temporal information jointly with spatial and spectral information. We proposed an end-to-end trainable network that combines a convolutional subnetwork which is very suitable for high level spatial and spectral feature extraction with a recurrent subnetwork, be it a standard recurrent neural network or a Long Short-Term Memory version, which can model the sequential property of the data. This framework is generic – it can be applied to bi-temporal remote sensing images or to long time series data for binary or multi-class change detection.

Combining CNN and RNN in an end-to-end trainable fashion can provide better change detection results than state-of-the-art methods. Site: Taizhou, China.

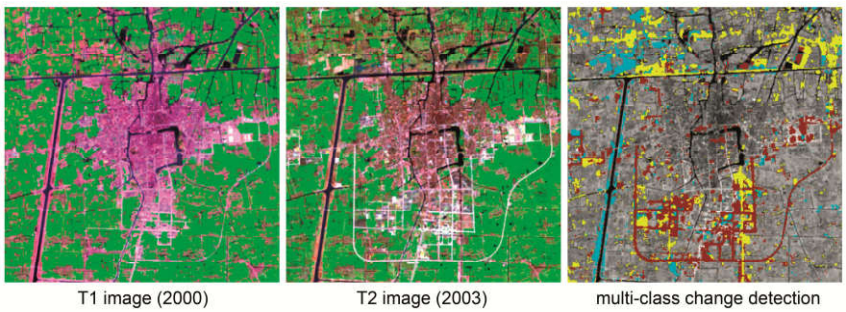

Concepts for Large-scale Applications

In the Copernicus era, we are dealing with very large and ever-growing data rates and volumes. Since 2014, Sentinel satellites have already acquired about 25 Petabytes of data. The Copernicus concept allows for global applications, i.e., algorithms must be fast enough and sufficiently transferrable to be applied to the whole Earth's surface. We have developed transfer learning-based architectures for urban applications, including building footprint generation, semantic mapping, as well as for crop type classification that can work with available, usually small or geographically restricted, training data sets. In some cases, however, large training data sets might be generated (semi-)automatically. We have used massive quality-controlled historical DSMs and DTMs to train a deep neural network that converts DSMs to DTMs with the highest possible quality to date (see the *Optical Imaging* chapter). Similar developments are the translations of image to height, image to building footprint, traffic lane extraction and ship detection from SAR and optical images.

Open Research Questions

The field of AI4EO is still young and we see a great need for research in the future: aside from current developments, important questions, including theoretical ones, will have to be dealt with. For example, in many cases remote sensing aims at retrieving geophysical or bio-chemical quantities rather than detecting or classifying objects. Often process models and expert knowledge exists that is traditionally used as priors for the estimates. This particularity suggests that the dogma of expert-free fully automated end-to-end learning should be questioned for remote sensing and physical models should be re-introduced into the concept. Other problems we will address in the future are e.g. small and erroneous training data sets and networks for complex SAR data.

Unconventional Geodata Sources Harvesting

Street Level Imagery

Street level images from open platforms, such as geotagged social media images (e.g. from Flickr, Facebook and Instagram) and street-view images (e.g. Google Street View and Mapillary), can serve as complementary data sources to EO satellite data for geoinformation harvesting at a ground level. For example, land-use classes can be extracted from social media images via computer vision techniques. Also, millions of high-resolution panoramic street view photos freely available on the internet can better furnish the view of cities around the world, compared to top view satellite imagery. Based on street view images, we developed a novel deep learning-based framework for fine-grained land-use classification at building instance level, reaching a prediction accuracy of around 80 %. We also introduced change detection techniques based on panoramic street view images, which can be exploited for city-scale dynamic monitoring. Beyond this, we conducted the first research of fusing social media and SAR images for urban mapping. We demonstrated that one can obtain a new kind of 3D city model that includes the optical texture from close-range social media imagery for better scene understanding and the precise deformation retrieved from SAR interferometry.

Social Media Texts

A valuable source of information for analyzing urban areas encoded in social media is text. In contrast to other social media information, text messages are widely available. For example, Twitter provides access to geo-located tweets through the free streaming API as well as

through the commercial Firehose API. Second, as Twitter is a mainly text-based social medium, the text information actually transports the meaning or purpose of the posting in many cases. This is different for multi-media social networks such as Instagram in which the available text information cannot be analyzed outside the context of the image. For tweets, we analyzed both the spatio-temporal distribution and the textual content. Using the spatio-temporal distribution, macroscopic as well as microscopic structures of cities can be observed: the density reveals the shape of cities on a macroscopic scale, but even structures like streets on a finer scale. We are working towards extracting useful spatial data sets from text messages including spatial sentiment, block-level functions, and the functions of individual buildings such as residential, commercial, or industrial. It is worth noting that the density of social media is highly imbalanced with respect to building function and that these building functions are, in turn, highly imbalanced in a spatial sense. Therefore, the fusion of social media with additional data sources, especially from remote sensing and volunteered geographic information is a prerequisite for scalable and reliable urban mapping. For the city of Los Angeles OpenStreetMap contains roughly 340,000 building instances with assigned classes *commercial* or *residential*. In half a year, we observed roughly 600,000 geo-located tweets in this area from about 25,000 buildings.

Applying the well-known skipgram model with vector space embeddings learned from Wikipedia, we are able to detect indicators for residential and commercial buildings with a high accuracy of about 85 % and a respectable recall of at least 70 %. Aggregating these tweets to buildings assigns a class to more than 21,000 buildings.

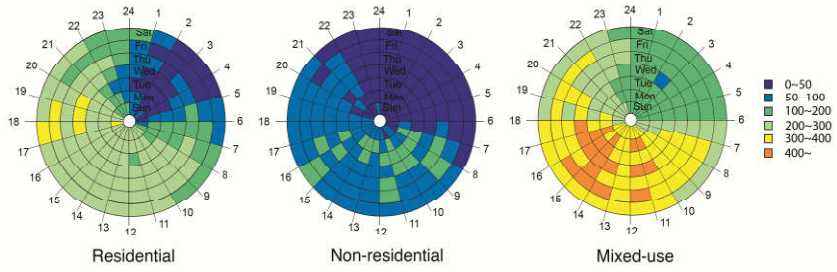

Social media data for urban settlement type classification: Histograms of twitter messages in Munich as a function of day-of-the-week (radial) and hour-of-the-day (azimuthal) exhibit distinct patterns for different settlement types. Social media data are an important source of geo-information and can complement EO data for urban mapping

Building type classification by fusion of opportunistic street level images and satellite data: Convolutional neural networks have been trained to classify settlement types based on top-view satellite images and the façade structures available from street view images. For training this network we built up a labelled benchmark dataset (top) with eight classes consisting of 19,658 street view images of buildings. Sites: Vancouver (bottom, left), Munich (bottom, right).

Residential (cyan) and commercial (magenta) buildings in the south of Los Angeles as modeled in OSM (top) and as predicted from tweet texts (bottom). It demonstrates the classified buildings instances using opportunistic tweets are sufficient to correctly resemble the functional areas inside this city.

Data Fusion

Fusion of multi-modal data has been a classic and crucial task, yet boosted by big Earth data, it has gained growing attention in the community during this reporting period. Intelligent use of the complementary peculiarities of the ever-increasing number of diverse remote sensing sensors and other geodata sources has become the natural choice for many applications. For example, to derive building information models that characterize both physical and functional properties, leads inevitably to fuse multimodal data fusion.

Fusion of SAR and Optical Imagery

One of our particular strengths in data fusion lies in the fusion of SAR and optical imagery which is one of the most important examples for the exploitation of complementary information. In the last reporting period, SAR-optical data fusion has gained new drive, mainly caused by two major developments: The first was the growing availability of imagery with very high spatial resolution that was meant to enable a precise mapping of the Earth's surface, especially in urban areas.

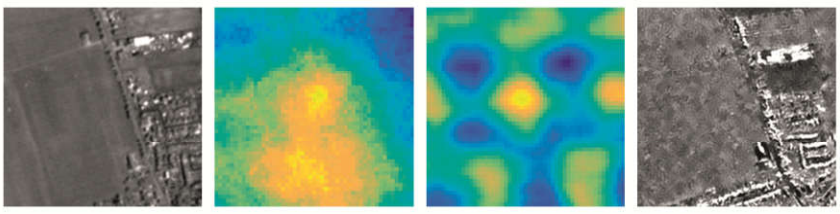

Comparison between the score maps of mutual information-based matching (2nd left) between optical (left) and SAR (right) image patches and our deep learning-based matching approach (DeepMatch, 2nd right). The more distinct peak in the DeepMatch result is clearly visible.

The second development was the implementation of international space programs, such as Copernicus, which incorporate various sensor technologies by design. In the Copernicus context, there is much potential for a joint exploitation of SAR data provided by the Sentinel-1 satellites and multi-spectral data provided by the Sentinel-2 mission.

One example is SAR/optical image co-registration. Any data fusion undertaking requires the individual input data sources to be aligned to each other and to the object of interest. For multi-sensor remote sensing imagery, this is usually achieved by either object matching or image co-registration. Both approaches are still non-trivial tasks due to the aforementioned peculiarities of SAR and optical images, which lead to severe differences both in radiometry and geometry, especially when very-high-resolution data of urban areas are concerned. In order to solve the problem of SAR-optical image matching, we have developed different CNN approaches. While one class aims at learning to predict patch correspondences directly using (pseudo-)siamese deep matching architectures, another class exploits conditional GANs to generate artificial images of one data source based on an input image of the other data source. Afterwards, a real image of one data source can easily be matched to its artificial counterpart using standard similarity measures.

Another application of the prediction of artificial optical images from SAR images is cloud-removal in multi-spectral Sentinel-2 data. Again, a conditional GAN can be used to predict cloud-free Sentinel-2 bands from cloud-affected Sentinel-2 input bands and an auxiliary Sentinel-1 image. A similar task is the colorization of SAR images using information provided by corresponding optical imagery acquired at more or less the same time. While this has been used operationally for decades using engineering approaches, we are currently

working on deep generative models that are able to predict optical-like colorizations for input SAR images without the availability of corresponding optical information. Our approach is based on learning conditional color distributions from large numbers of existing examples. At production time, these learned distributions can then be used to create plausible colorizations for previously unseen images.

Selected publications: [236], [48], [93], [562], [564], [561], [522], [572]

Fusion of SAR and Optical 3D Point Clouds

Fusing very high resolution SAR and optical images in dense urban areas is impossible in 2D because of the non-injective imaging geometry of SAR. A novel approach has been devised for fusion of 3D SAR tomographic point clouds and 3D stereo-optical DSM. The proposed approach provides the first 'SARptical' point cloud of an urban area, which is the TomoSAR point cloud textured with attributes from aerial stereo-optical images. This opens up a new perspective for understanding InSAR-derived deformation estimates. Furthermore, thanks to this effort, by re-projecting the SAR-optical correspondence in 3D back to the original image space, we are able to provide the first benchmark data set to the community which consists of over 10,000 matched pairs of very high resolution SAR and optical image patches over dense urban areas.

Selected publications: [579], [251], [683], [484]

Fusion of PolSAR, Hyperspectral, Lidar and More

Besides our focus on SAR-optical data fusion, we are also investigating the potential of fusion for other remote sensing and geodata sources. Still relying on SAR data, whose analysis is our core expertise, examples of our multi-sensor data fusion endeavors include the estimation of building height from single SAR images by fusing building footprints extracted from OpenStreetMap data, and the fusion of polarimetric SAR measurements and hyperspectral imagery for land use classification. Beyond SAR, we also work on multi-sensor spectral unmixing, which aims at understanding dynamic changes of observed surfaces at a subpixel scale by jointly exploiting multi-spectral and hyperspectral image time series. In addition, we developed a framework based on so-called extinction profiles and deep convolutional neural networks in order to fuse hyperspectral and lidar data for classification purposes.

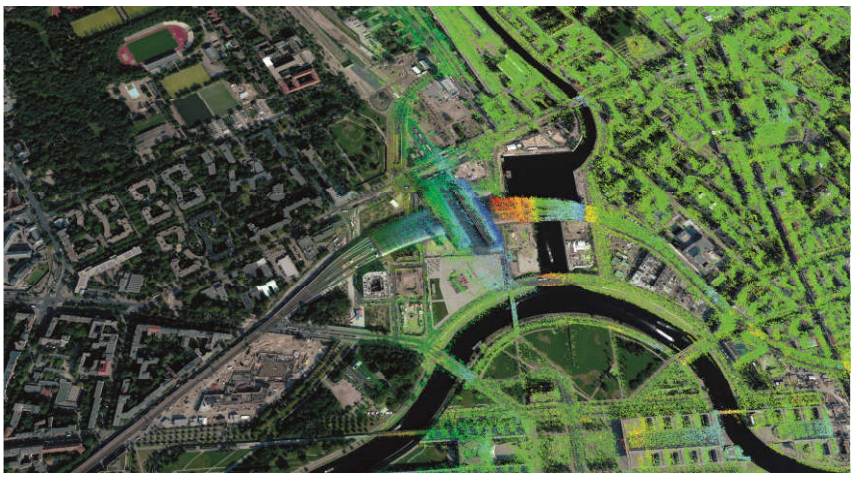

The first SARptical, i.e. better interpretable, view of a dynamic city: a 4D tomographic SAR point cloud (right, color stands for the thermal dilation induced season motion in mm range) textured and fused with a 3D optical stereo point cloud (left).

Our data fusion research has received high international recognition which is illustrated, e.g. by two first prizes in the renowned IEEE GRSS Data Fusion Contests in 2016 and 2017 and a second prize in 2018.

Selected publications: [544], [614], [575], [150], [101], [537], [110], [149]

Big Earth Data Analytics

Geoscientific Application – Urban Mapping

Many of the above mentioned methods from data science are used across disciplines and have found their way into geoscientific applications at IMF. Within an ERC-funded project, a strong focus of IMF has been on global urban mapping. Our methodological research line is complemented by a cooperating group specialized in urban geography at DFD.

By 2050, around three quarters of the world's population will live in cities. The ongoing new dimension of global migration into the cities poses fundamental challenges to our societies across the globe. Despite increasing efforts, global urban mapping approaches still drag behind the geometric, thematic and temporal resolutions of geoinformation needed to address these challenges with resilient spatial data. For example, DFD's Global Urban Footprint (GUF) and GUF+, binary masks of urban vs. non-urban and its temporal updates are still among the most prominent examples capturing the complex settlement patterns at unprecedented resolutions at global scale. Going far beyond GUF, we aim at 3D/4D urban modelling, infrastructure occupancy classification, and very high resolution population density mapping on a global scale for revolutionizing urban geographic research.

Global 3D Tomographic Urban Modeling

Global 3D/4D urban models play a fundamental role for stakeholders in understanding rapid urbanization. Yet our knowledge of global urban morphology so far is restricted to a 2D binary classification map. The TanDEM-X

First impression of the global 3D urban LOD1 models: Munich city reconstructed using only five TanDEM-X acquisitions. The building footprints have been reconstructed from PlanetScope data, the building heights (color) from the TomoSAR point cloud.

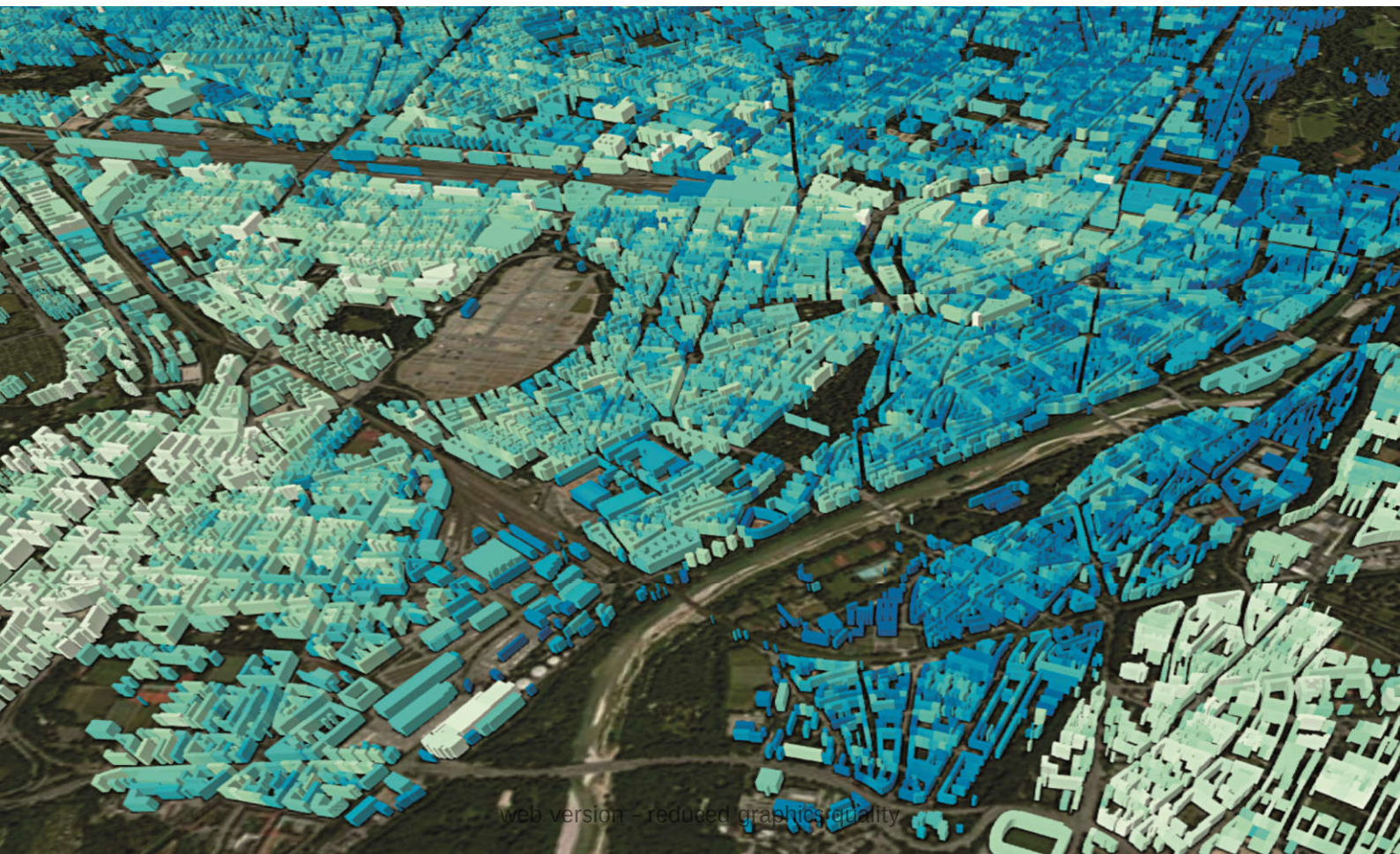

mission delivers a global digital elevation model of high quality (12 m posting), which is optimized for nonurban areas. When it comes to urban areas, however, a full tomographic inversion on the TanDEM-X data stack is required for reliable 3D reconstruction. This calls for novel tomographic inversion algorithms for TanDEM-X stacks with very few interferograms, because global TanDEM-X data coverage over urban areas is usually only 4 – 7 images. We are taking the lead in developing such an algorithm aiming at generating and providing the world's first global 3D urban model using primarily TanDEM-X data. A prototype version is already available. Using just five TanDEM-X interferograms, the height accuracy is better than 2 m compared to lidar point clouds. Furthermore, by fusing this with building footprints extracted from globally available PlanetScope data, followed by robust building height estimation, it is even possible to generate LOD1-type building models. Currently, we are processing the first 1,700 cities with a population greater than 300,000, and expect to make the global 3D urban model available to the community in 2020.

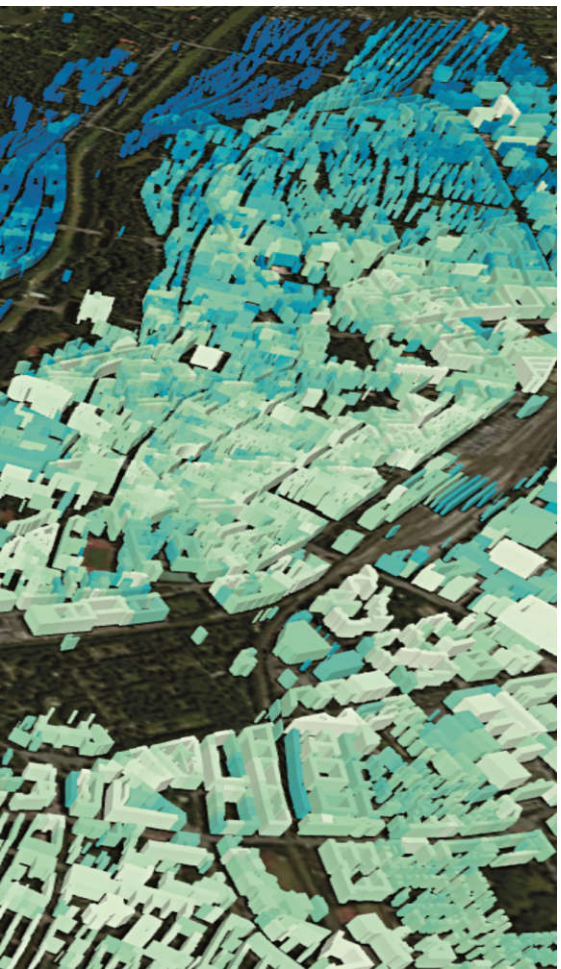

Global Local Climate Zone Classification

Local Climate Zones (LCZs) comprise a classification scheme for urban areas that has gained great importance across various disciplines in the last years. Originally developed by urban climatologists to describe and characterize the physical nature of cities in a way that is transferable across cultural and geographical regions, the LCZ classification scheme has found its way into EO as well. The 17 LCZ classes are based on climate-relevant surface properties mainly related to 3D surface structure (height and density of buildings and trees) as well as surface cover (pervious or impervious). Due to the scheme's interdisciplinary and transferable nature, researchers have started to use the LCZ classes as standard to describe the internal structure of urban areas. We are currently working on generalizing and scalable classifiers that allow us to carry out LCZ mapping on a global scale, with a particular focus on urban areas. Besides the development and application of machine learning methods, this comprises the manual generation of ground truth labels by human remote sensing experts for which we created ground truth labels for 42 representative cities selected across the globe. The result of our concerted labeling efforts is called the *LCZ42* data set, which is used to train and evaluate our algorithms. We aim at generating the first ever global LCZ map in the near future.

Selected publications: [549], [516], [24], [582], [475], [469]

Data Mining and Knowledge Discovery

Throughout the years various EO satellites have gathered huge quantities of data. This in turn made the data archives grow in size, variety and complexity. In order to extract the latent information residing in these repositories, new methodologies and tools are required. The users require support in the process in order to find and retrieve specific collections from these huge volumes of data. They also require fast methods and algorithms in order to extract knowledge from this data.We have a long history of development in Image Information Mining (I²M), i.e. the retrieval of relevant information from large remote sensing data archives. Within I²M a framework of methods has been developed for the creation of large semantically annotated reference data bases, semantic catalogues and image epitomes. The goal is automatic knowledge discovery about image content which is very effectively usable for Big EO Data applications. One highlight example is the ESA project EOLib (Earth Observation Image Librarian) which resulted in a prototype implementation of the EOlib query system within the DLR ground segment. It is a modular system which offers Data Mining and Knowledge and Data Discovery capabilities for TerraSAR-X data and EO data in general. EOLib is a paradigm shift from data to information and knowledge distribution. Its main goal is to fill the gap between the PDGS and the end-user which desires specific information. EOLib's modules offer functionalities such as ingestion and feature extraction from SAR data, metadata extraction, semantic definition of the image content through machine learning and data mining methods, advanced querying of the image archives based on content, meta-data and semantic categories, as well as 3D visualization of the processed image archives. EOLib is a Big Data solution bringing the algorithms close to the data. It is integrated in the Multi-Mission Payload Ground Segment of DLR. Among its achievements, EOLib enabled the generation of a semantic catalogue with 1,300 categories for TerraSAR-X spotlight images of 300 cities. It was also applied to quantitatively assess from TerraSAR-X time series the effects of the 2010 Tsunami in Japan and their recovery.

Immersive data mining: Semantic navigation by machine learning in Virtual Reality.

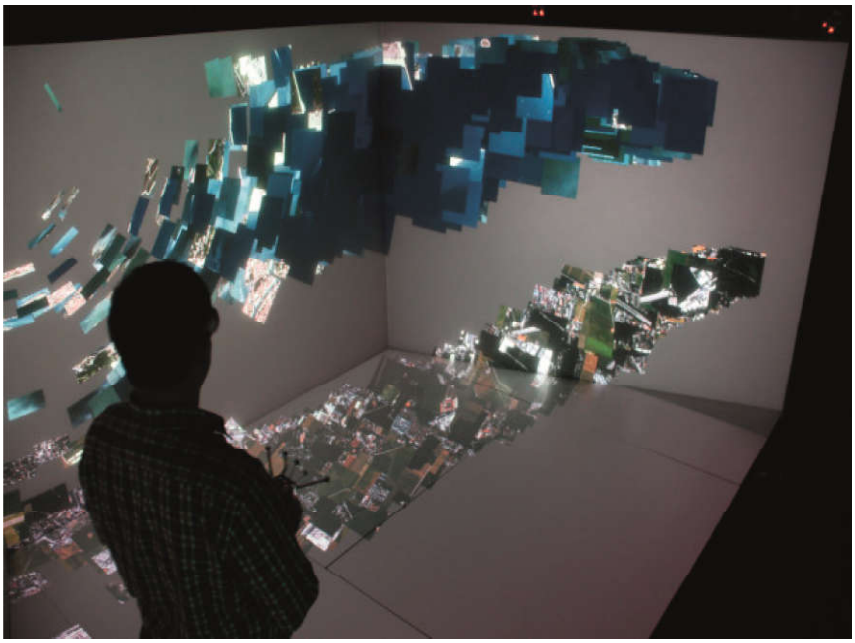

The AI components of EOLib have been integrated in a light open-source tool EOMiner which is dedicated to Copernicus and third party data users. It can be applied to any multispectral or SAR data with resolutions from tens of cm to 100 m. EOMiner was used to solve environmental and costal problems in the frame of Horizon 2020 and ESA projects. It was also used to generate large EO image benchmark data sets from TerraSAR-X, Sentinel-1 and Sentinel-2 images.

Selected publications: [343], [421], [194]

High Performance Computing

Analysis of Big Earth Data involves a significant amount of resources, both in terms of computational power provided by CPU and GPU clusters, as well as in terms of storage capacities and data transfer capabilities. We have been working closely with the Leibniz Supercomputing Centre (LRZ) and the Jülich Supercomputing Centre since 2012 and 2017, respectively. A project led by IMF scientists has been selected as a pilot project for shaping LRZ's Next Generation system. Social impact of our EO projects has been acknowledged by the European HPC society, e.g. by awarding an IMF scientist the PRACE Ada Lovelace Award for HPC 2018.

Selected publications: [257], [656], [8], [516], [251], [753], [677], [579], [484]

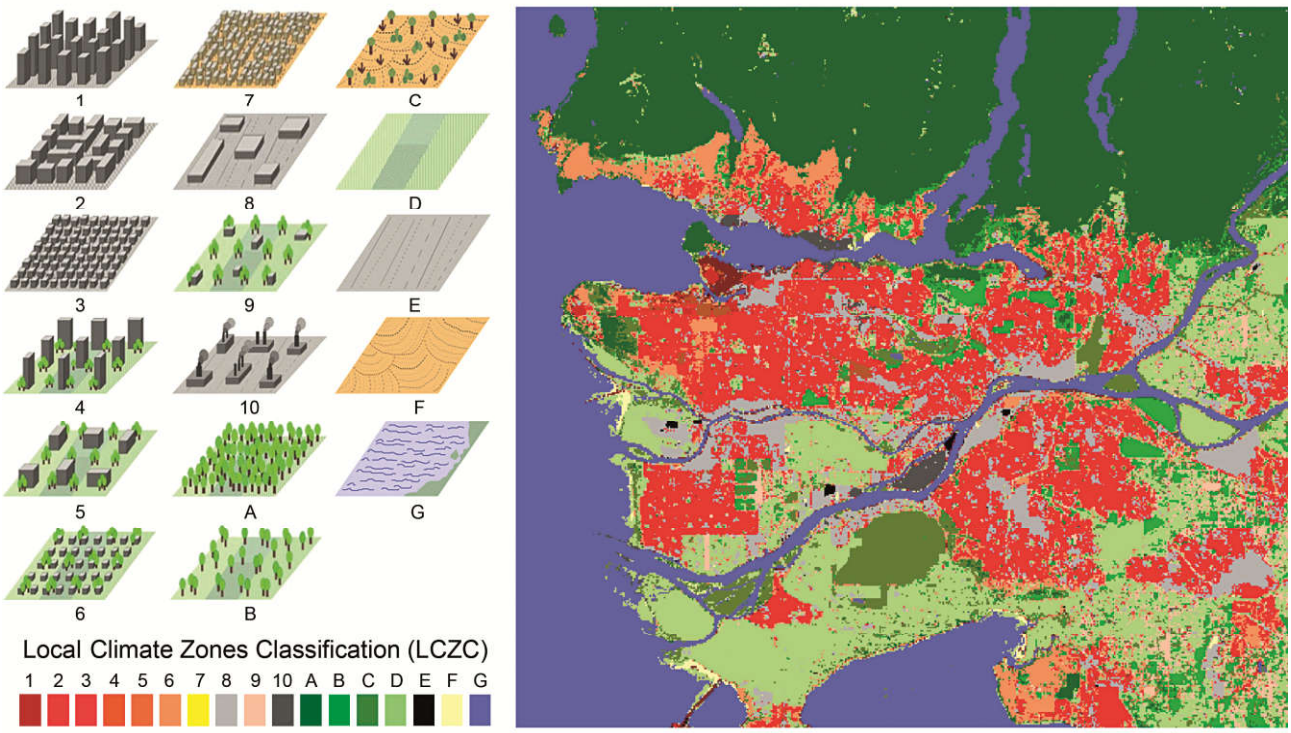

Local climate zones (LCZ) classification using Sentinel-1, Sentinel-2 and TanDEM-X data. Site: Vancouver, Canada (left graphic modified after Stewart et al. 2011).

Documentation

Documentation

This Documentation chapter covers scientific activities of IMF and TUM-LMF/-SiPEO staff in the time period between January 2013 and mid 2018.

Teaching and Education

Lectures at Technical University of Munich (TUM)

University courses conducted by IMF/LMF/SiPEO staff from 2013 until 2018 (lecturers of TUM-LMF/SiPEO in *italic typeface*). Winter semester courses are listed in the year of beginning.

University	Title	Lecturers	2013	2014	2015	2016	2017	2018
TUM	Photogrammetrie und Fernerkundung IV (Vorlesung + Übung)	*Körner, M.* *Auer, S.* *Schmitt, M.* *Frey, D.* Avbelj, J. Eineder, M.	■	■	■	■	■	■
TUM	Satellitenfernerkundung (Vorlesung + Übung)	*Körner, M.* *Auer, S.* *Schmitt, M.* *Frey, D.* Eineder, M. Avbelj, J.	■	■	■	■	■	■
TUM	Systems Theory and Signal Processing (Lecture + Tutorial)	Bamler, R. Zhu, X.	■	■	■	■	■	■
TUM	Systemtheorie u. Signalverarbeitung (Vorlesung + Übung)	Bamler, R. Zhu, X.	■	■	■	■	■	■
TUM	Introduction into Microwave and SAR Remote Sensing	Eineder, M.	■	■	■	■	■	■
TUM	Estimation Theory (Lecture + Tutorial)	Bamler, R. Avbelj, J. Kurz, F. *Shahzad, M.* *Szottka, I.* Zhu, X.	■	■	■	■	■	■
TUM	Schätztheorie (Vorlesung + Übung)	Bamler, R. Avbelj, J. Kurz, F. *Shahzad, M.* Zhu, X.	■	■	■	■	■	■

University	Title	Lecturers	2013	2014	2015	2016	2017	2018
TUM	Remote Sensing – Advanced Methods	Eineder, M. Trautmann, T. Adam, N. Lehner, S. Zhu, X. *Burkert, F.* *Fraundorfer, F.* *Gernhardt, S.* *Schmitt, M.* Gamisi, P. Yokoya, N.	■	■	■	■	■	■
TUM	Seminar Remote Sensing	Zhu, X.	■	■	■	■	■	■
TUM	Fernerkundung und Signalverarbeitung	Eineder, M. Trautmann, T. Adam, N. Lehner, S. Zhu, X. *Burkert, F.* *Fraundorfer, F.* *Gernhardt, S.* *Schmitt, M.* Gamisi, P. Yokoya, N.	■	■	■	■	■	■
TUM	Bildverstehen Grundlagen – Übung	*Koch, T.* *Burkert, F.*	■	■	■	■	■	■
TUM	Bildverstehen – Vertiefte Methoden	*Körner, M.* *Fraundorfer, F.* *Frey, D.* *Szottka, I.* Cui, S. *Zhu, K.*	■	■	■	■	■	■
TUM	Bildverstehen – Aktuelle Ansätze des Maschinellen Lernens	*Körner, M.*				■	■	■
TUM	Electrodynamics	Doicu, A. Trautmann, T. Efremenko, D.	■	■	■	■	■	■
TUM	Nonlinear Optimisation	Doicu, A.	■	■	■	■	■	■
TUM	Multisensor-Datenfusion	*Schmitt, M.*				■	■	■

Lectures at other Universities

University courses conducted by IMF staff from 2013 until 2018.
Winter semester courses are listed in the year of beginning.

University	Title	Lecturers	2013	2014	2015	2016	2017	2018
Jena	SAR-Signalverarbeitung (SAR-EDU)	Auer, S. Brcic, R. Eineder, M. Lehner, S. Parizzi, A. Pleskachevsky, A.	■	■	■	■	■	■
Beijing, CN (Institute of Electronics)	SAR Signal Processing	Bamler, R. Zhu, X.		■				
Alcala, SP	Hyperspectral Remote Sensing	Cerra, D.	■	■	■	■	■	■
Limassol, CY (Cyprus Univ. of Technology)	Hyperspectral Image Processing	Cerra, D.					■	
Osnabrück	Methoden der Bildverarbeitung II	Cerra, D.	■	■				■
Calabria, IT	Introduction to Digital Image Processing in Remote Sensing	Cerra, D.				■		
Tehran, IR	Hyperspectral Remote Sensing	Cerra, D.		■		■		
Beijing, CN (Institute of Technology)	Perspectives of SAR Imaging	Datcu, M.	■					1
Bukarest, RO (Politehnica)	Theory of Information Transmission	Datcu, M.	■					2
Bukarest, RO (Politehnica)	Decision and Estimation/Data Mining	Datcu, M.	■	■	■		■	3
Bukarest, RO (Politehnica)	Remote sensing and Space Communication	Datcu, M.				■	■	4
Campinas, BR	Principles, Analysis and Applications of SAR Images	Datcu, M.				■		5
Maryland, USA	Big Data from Earth Observation: Analytics, Mining, Semantics	Datcu, M.				■		6
Bern, CH	SAR–Concepts & Geodetic Measurements	Eineder, M.		■				
Augsburg	Applied Remote Sensing	Fischer, P. Langheinrich, M.						■

University	Title	Lecturers	2013	2014	2015	2016	2017	2018
München (HS)	PC-gestütztes Messen	Haschberger, P.	■	■	■			
München (HS)	Messtechnik II	Haschberger, P.				■	■	■
Hannover	Radar Ozeanographie	Lehner, S.	■					
Miami, USA (Nova Southeastern University)	Maritime Remote Sensing	Lehner, S.	■					
Port Everglades, USA (Nova Southeastern University)	SAR-Tutorial	Lehner, S.			■			
Bremen (Sino-German Summer School)	Radar Oceanography	Lehner, S.			■			
University of Victoria, CA	Radar Oceanography	Lehner, S.			■			
Thessaloniki, GR	Satellite Remote Sensing	Loyola, D.						■
Osnabrück	Fernerkundungliche Umweltanalyse	Reinartz, P.	■	■	■	■	■	■
Hannover	Operationelle Fernerkundung	Reinartz, P. Storch, T.	■	■	■	■	■	■
Leipzig	Strahlungstransferlabor	Trautmann, T.	■	■	■			
Hannover	Big Geospatial Data	Werner, M.						■

CA: Canada
GR: Greece
HS: Hochschule
LMU: Ludwig-Maximilians-Universität

Non University Courses and Tutorials

Non university courses and tutorials conducted by IMF staff between 2013 and 2018 (Courses of the LMF/SiPOE in *italic* typeface)

Lecturer	Location	Subject	2013	2014	2015	2016	2017	2018
Bamler, R.	EUSAR	SAR Interferometry and Tomography		■				■
Bamler, R.	CAST	Introduction to SAR Interferometry					■	
Bamler, R.	Hongkong, CN	SAR Interferometry					■	
Bamler, R.	CCG	SAR Interferometry			■	■	■	■
Cerra, D.	CCG	Processing of Remotely Sensed Data	■					
Cerra, D.	Tehran, IR	Imaging Spaceborne Systems, Processing of Remotely Sensed Data		■				
Cerra, D.	CCG/ESA	Hyperspectral Remote Sensing		■	■	■	■	■
Datcu, M.	Beijing, CN	Lecture on SAR		■				
Datcu, M.	Beijing, CN	Big Data Mining			■			
Datcu, M.	Beijing, CN	SAR Image Understanding			■			
Datcu, M.	IET Intern. Radar Conference	Methods and Algorithms for Understanding of High Resolution SAR Images	■					
Datcu, M.	Hangzhou, CN	SAR Information Extraction in the Era of Big Data			■			
Datcu, M.	Campinas, BR	SAR Principles and Applications			■			
Datcu, M.	Joao Pessoa, BR	Information Mining for Satellite Image Time Series: Methods and Perspectives			■			
Datcu, M.	IGARSS	Earth Observation Data Mining	■	■				
Datcu, M.	IGARSS	Big Data from Earth Observation: Analytics, Mining, Semantics			■			
Datcu, M.	Wuhan, CN	Big Data Mining and Analytics: Methods and Algorithms				■		
Datcu, M.	Beijing, CN	Advancing EO Data Science					■	
Eineder, M.	CCG	Active Microwave Sensing	■					
Eineder, M.	CCG	SAR Interferometry	■	■				
Eineder, M.	TUM Int.	SAR Introduction			■	■	■	■

Lecturer	Location	Subject	2013	2014	2015	2016	2017	2018
Eineder, M.	CCG	SAR Remote Sensing			■	■	■	■
Eineder, M.	CCG/ESA	Microwave Remote Sensing		■	■	■	■	■
Hamidouche, M.	CCG	Infrared Astronomy: Unveiling the Hidden Universe	■	■	■	■	■	■
Haschberger, P.	CCG	Spektrometer und Kalibrierung	■	■	■	■	■	■
Körner, M.	ISPRS	ISPRS 3S Student Summer School				■		
Krauß, T.	CCG	Fernerkundung aus dem Weltraum mit multispektralen, hyperspektralen und Stereoaufnahmen			■	■	■	■
Kuschk, G.	SMPR	3D Reconstruction Chain – from Images to 3D City Model	■					
Lehner, S.	EUSAR	Ship and Oil Detection		■				
Lehner, S.	EUSAR	Maritime Security				■		
Lehner, S.	EUSAR	Operational Remote Sensing by Exploiting Space-Based SAR Data						■
Lehner, S.	CCG	SAR Oceanography	■	■	■	■	■	■
Lichtenberg, G.	CCG/ESA	Atmospheric Remote Sensing, Radiative Transfer, Neutral Atmosphere		■	■			■
Loyola, D.	NASA GSFC, USA	Computational Intelligence Techniques in Remote Sensing					■	
Pleskachevsky, A.	Oldenburg	SAR Ozeanographie			■			
Reinartz, P.	CCG	Fernerkundung aus dem Weltraum mit multispektralen, hyperspektralen und Stereoaufnahmen	■					
Schreier, F.	CCG	Atmosphärische Fernerkundung – Strahlungstransportmodelle und Inversionsverfahren	■	■	■	■	■	■
Schmitt, M.	CAST	Remote Sensing Data Fusion					■	
Trautmann, T.	CCG	Physical Principles of Spaceborne Remote Sensing	■					
Trautmann, T.	CAST	Atmospheric Remote Sensing					■	
Trautmann, T.	CCG/ESA	Atmospheric Remote Sensing, Radiative Transfer, Neutral Atmosphere				■	■	

Lecturer	Location	Subject	2013	2014	2015	2016	2017	2018
Zhu, X.	TUM	Summer School: Signal Processing in Earth Observation		■		■		
Zhu, X.	CCG	Intelligente Sensorik II		■	■	■	■	■
Zhu, X.	CAST	Signal Processing and Data Science in Earth Observation					■	
Zhu, X.	CAST	Very High Resolution Multi-Dimensional SAR Imaging					■	
Zhu, X.	EUSAR	Deep Learning in Remote Sensing						■
Zhu, X.	WHISPERS	Deep Learning in Remote Sensing						■

CAST: China Academy of Space Technology
CCG: Carl-Cranz-Gesellschaft
ESA: European Space Agency
EUSAR: European Conference on Synthetic Aperture Radar
IGARSS: International Geoscience and Remote Sensing Symposium
ISPRS: International Society for Photogrammetry and Remote Sensing
NASA GSFC: National Aeronautics and Space Administration, Goddard Space Flight Center
SMPR: Sensors and Models in Photogrammetry and Remote Sensing
WHISPERS: Workshop on Hyperspectral Image and Signal Processing

Internal Seminar Series

Title	Comments
IMF Seminar	10 – 15 presentations per year, IMF and guest scientists
Seminars of IMF sections	seminars of IMF-ATP: 15 – 20 and IMF-SAR: 5 – 10 presentations per year, IMF and guest scientists
IMF Doktorandentage	annual event, 15 – 20 PhD status presentations
Doktorandenseminar TUM (LMF, SiPEO)	approx. 15 presentations per year, PhD presentations and reading sessions
TUM/DLR Summer School	annual 3 days event, 50 PhD and scientists, guest lecturers
Various Summer Schools	HGF Alliances, Munich Aerospace, SAR Education Initiative

Academic Degrees

Professorship Appointments

Professorship appointments of IMF or TUM-LMF/SiPEO (in *italic* typeface) staff between 2013 and mid 2018.

Name	Professorship	University	Year
Cerra, D.	Deputy Professor	Osnabrück	2018
Loyola, D.	Visiting Professor	Thessaloniki/Greece (Aristotle University)	2018
Datcu, M.	Chaire Blaise Pascal	Paris/France (l'Ecole Normale Supérieure)	2017
Shahzad, M.	Assistant Professorship	Islamabad/Pakistan (National University of Sciences and Technology)	2016
Fraundorfer, F.	Assistant Professorship	Graz/Austria	2015
Zhu, X.	Professorship for Signal Processing in Earth Observation	München (TU)	2015
Eineder, M.	Honorary Professorship	München (TU)	2013
Lehner, S.	Affiliate Faculty Member	Miami/USA (Nova Southeastern University)	2013

Habilitations and Veniae Legendi

Habilitations awarded, supervised or completed by IMF or TUM-LMF/SiPEO (in *italic* typeface) staff between 2013 and mid 2018.

Name	Subject	University	Year	Reviewers
Körner, M.	Machine Learning and Computer Vision (working title)	München (TU)	ongoing	Prof. Bamler Prof. Fraundorfer Prof. Lepetit
Schmitt, M.	Data Fusion in Remote Sensing (working title)	München (TU)	ongoing	Prof. Zhu Prof. Bamler Prof. Hinz
Efremenko, D.	Technology of Fast Interpretation of Optoelectronic Systems' Signals for Determining the Atmospheric Parameters and Solid-State Samples Parameters	Moscow Power Engineering Institute	2017	Prof. Belov Prof. Kataev Prof. Smirnov
Zhu, X.	Modern Signal Processing Concepts for Remote Sensing	München (TU)	2013	Prof. Meng Prof. Bamler Prof. Hinz

Doctoral Theses

Doctoral Theses completed or supervised by IMF or TUM-LMF/SiPEO (in *italic* typeface) staff between 2013 and mid 2018.

Name	Title	University	Year	Reviewers
Adam, F.	Urban Classification Using Machine Learning and Deep Learning	Osnabrück	ongoing	Reinartz, P. Esch, T. Datcu, M.
Aigner, S.	Video Generation for Traffic Prediction using Deep Learning Methods	München (TU)	ongoing	Bamler, R.
Ansari, H.	Development of Differential Shift Based Stacking Techniques and Fusion with the InSAR Approaches	München (TU)	submitted	Bamler, R. Eineder, M. Hanssen, R.
Ao, D.	Adavanced Methods for SAR Image Understanding	Beijing (Institute of Technology)	ongoing	Cheng, Hu Zeng, Tao Datcu, M.
Azimi, M.	Development of Deep Learning methods for airborne traffic and infrastructure monitoring	München (TU)	ongoing	Bamler, R.
Bagheri, H.	Fusion of TanDEM-X data and optical imagery for 3D reconstruction of urban areas	München (TU)	ongoing	Zhu, X.
Baier, G.	Interferometric Algorithms for Medium Resolution Sensors with Massive Coverage	München (TU)	submitted	Zhu, X. Bamler, R. Reigber, A.
Baumgartner, A.	Modelling and Calibration of Imaging Spectrometer Data	Osnabrück	ongoing	Reinartz, P.
Bentes da Silva, C.	Automatische Schiffsdetektion in Radarbildern	München (TU)	ongoing	Eineder, M. Zhu, X. …
Bittner, K.	Building Extraction from Digital Surface Models by Deep Learning Techniques	Osnabrück	ongoing	Reinartz, P. Ehlers, M.
Cagatay, N.	Feature Extraction for Bistatic SAR Images	Siegen	ongoing	Loffeld, O. Datcu, M.
Cosmin, D.	4 D measurments of urban structures based on SAR	Bucharest	ongoing	Fornaro, Gianfranco Datcu, M.
Ge, N.	Advanced Tomographic Techniques for EHR Systems	München (TU)	ongoing	Zhu, X. Bamler, R.
Gisinger, Ch.	Joint processing of SAR, GNSS and gravimetry for geophysical signals	München (TU)	ongoing	Pail, R. Eineder, M.
Göritz, A.	From laboratory spectroscopy to remote sensing: Methods for the retrieval of water constituents in optically complex waters	München (TU)	submitted	Bamler, R. Bracher, A. Damm, A.

Name	Title	University	Year	Reviewers
Grivei, A.	Machine Learning for Satellite Image Time Series	Bucharest	ongoing	Datcu, M.
Häberle, M.	Fusion of social media and remote sensing data using deep learning and natural language processing	München (TU)	ongoing	Zhu, X.
Henry, C.	Airborne Traffic Data for validation of vehicle data	München (TU)	ongoing	Vig, E.
Heublein, M.	Atmospheric Tomography using GNSS and InSAR Measurements	Karlsruhe	ongoing	Hinz, S. Zhu, X.
Hochstaffl, P.	Trace gas concentration retrieval from near infrared nadir sounding spaceborne spectrometers	München (LMU)	ongoing	Wenig, M.
Hong, D.	Hyperspectral Data Analysis: data compression and unmixing	München (TU)	ongoing	Zhu, X.
Hu, J.	Settlement Type Classification of urban area using PolSAR and hyperspectral image	München (TU)	ongoing	Zhu, X.
Hughes, L.	Machine-learning-based matching of optical and SAR data	München (TU)	ongoing	Zhu, X.
Johnson, E.	Mass balance and dynamics of calving glaciers from high resolution SAR data.	München (TU)	ongoing	Eineder, M.
Kang, J.	Intelligent Synthetic Aperture Radar Interferometry Techniques for Deformation Monitoring	München (TU)	ongoing	Zhu, X.
Koch, T.	Automatic visual reconstruction system for building interior and exterior using Mavs	München (TU)	ongoing	Bamler, R. Fraundorfer, F.
Krieger, L.	Retrieval of glaciolocical parameters from SAR data and mass balance modelling of glaciers in Northeast Greenland	München (TU)	ongoing	Eineder, M.
Kuschk, G.	Fast and Accurate Large-scale Stereo Reconstruction using Variational Methods	München (TU)	ongoing	Cremers, D.
Liebel, L.	Prädiktion von Bildfolgen aus FAS-Videosequenzen durch implizite Modellierung von Aktivitätsmustern	München (TU)	ongoing	Bamler, R.
Liu, S.	Satellite measurements of total and tropospheric NO2	München (TU)	ongoing	Doicu, A.
Marmanis, D.	Deep Learning for VHR EO image understanding	München (TU)	ongoing	Stilla, U. Datcu, M. Zhu, X.
Meynberg, O.	Real-Time Crowd Density Estimation in Aerial Images	Karlsruhe	ongoing	Hinz, S. Reinartz, P.
Molina, V.	Satellite measurements of cloud properties	München (TU)	ongoing	Doicu, A.

Name	Title	University	Year	Reviewers
Montazeri, S.	Absolute three-dimensional positioning of InSAR point clouds by automatic point correspondence detection in multiple viewing angles data stacks	München (TU)	ongoing	Zhu, X. Eineder, M. Hanssen, R.
Mou, L.	Deep learning in remote sensing video analysis	München (TU)	ongoing	Zhu, X.
Murillo, A.	Acceptance of technology based conceptual artifacts in knowledge communities: applications to EO Image Information Mining	München (LMU)	ongoing	Nistor, N. Datcu, M.
Partovi, T.	Levels of Generalization on Automatic Building Reconstruction from Digital Surface Models	Osnabrück	ongoing	Reinartz, P. Fraundorfer, F.
Qui, C.	Local climate zone classification from Sentinel-2 data	München (TU)	ongoing	Zhu, X.
Riedel, S.	Entwicklung einer Atmosphärenkorrektur für Flugzeug- und Satellitendaten	Kiel	ongoing	Oppelt, N. Gege, P.
Rodríguez González, F.	Absolute 3D Rekonstruktionsverfahren aus Satelliten-SAR-Daten	München (TU)	ongoing	Eineder, M. Bamler, R.
Röske, C.	Verbesserung der spektroskopischen Datenbank und des theoretischen Verständnisses von Infrarot-Kontinua	Karlsruhe	ongoing	Orphal, J.
Shi, Y.	3D urban mapping with SAR interferometry	München (TU)	ongoing	Bamler, R.
Städt, S.	Retrieval of atmospheric parameters of terrestrial extrasolar planets around cool host stars	Berlin (TU)	ongoing	Breitschwerdt, D.
Stark, T.	Machine-learning-based detection of informal settlements	München (TU)	ongoing	Zhu, X.
Sun, Y.	3D / 4D global urban footprint reconstruction using multi-sensory data	München (TU)	ongoing	Zhu, X.
Tings, B.	Erkennung von Bug- und Heckwellen von Schiffen auf Satelliten-SAR	Hamburg (HSU)	ongoing	Rothe, H. Soloviev, A.
Traganos, D.	Multispectral remote sensing for mapping and monitoring of Mediterranean seagrass habitats	Osnabrück	ongoing	Reinartz, P. Ehlers, M.
Tudose, M.	Advanced GB SAR for precise infrastructure monitoring	Bucharest	ongoing	Datcu, M. Anghel, A.
Wang, Z.	MAX-DOAS measurements of trace gases and aerosol in the atmosphere	München (TU)	ongoing	Doicu, A.
Wiercioch, M.	Entwicklung von Algorithmen zur Analyse der Meereisentwicklung aus echtzeitnahen SAR Satellitendaten unterschiedlicher Missionen	München (TU)	ongoing	Eineder, M.
Xia, Y.	3D tree architecture modelling from close range photogrammetry	Osnabrück	ongoing	Reinartz, P.

Name	Title	University	Year	Reviewers
Yuan, X.	Building change detection in very high resolution image time series	Osnabrück	ongoing	Reinartz, P.
Zhuo, X.	Fusion of UAV and Airborne Optical Imagery	München (TU)	ongoing	Bamler, R. Reinartz, P.
Alonso-Gonzalez, K.	Heterogeneous Data Mining for EO Applications: an Information Theoretical Approach	München (TU)	2017	Rigoll, G. Datcu, M.
Grohnfeldt, C.	Multi-Sensor Data Fusion for Multi- and Hyperspectral Resolution Enhancement Based on Sparse Representation	München (TU)	2017	Zhu, X. Bamler, R. Yokoya, N.
Loos, J.	Verbesserung der spektroskopischen Datenbasis von H_2O für die Anwendung in bodengebundener Fernerkundung der Atmosphäre	Karlsruhe	2017	Orphal, J. Höpfner, M.
Yao, W.	Semi-Supervised Classification and Segmentation of Multi-Modal Satellite Images	Siegen	2017	Loffeld, O. Datcu, M.
Abdel Jaber, W.	Derivation of Mass Balance and Surface Velocity of Glaciers by Means of High Resolution Synthetic Aperture Radar: Application to the Patagonian Icefields and Antarctica	München (TU)	2016	Bamler, R. Eineder, M. Rott, H.
Bahmanyar, G.	Conception and Assessment of Semantic Feature Descriptors for Earth Observation Images	München (TU)	2016	Rigoll, G. Cremers, D. Datcu, M.
Gomba, G.	Estimation and Compensation of Ionospheric Propagation Delay in Synthetic Aperture Radar (SAR) Signals	München (TU)	2016	Bamler, R. Eineder, M. Meyer, F.
Mattyus, G.	Joint Information Augmentation of Road Maps, Aerial Images and Ground Images	München (TU)	2016	Bamler, R. Fraundorfer, F. Urtasun, R.
Rossi, C.	Uncertainty Assessment of Single-Pass TanDEM-X DEMs in Selected Applications	München (TU)	2016	Bamler, R. Eineder, M. Tebaldini, S.
Shahzad, M.	From TomoSAR Point Clouds to Objects	München (TU)	2016	Bamler, R. Zhu, X.
Velotto, D.	Oil Spill and Ship Detection Using High Resolution X-Band SAR Data	München (TU)	2016	Bamler, R. Eineder, M. Migliaccio, M.
Avbelj, J.	Fusion of Hyperspectral Imags and Digital Surface Models for Urban Object Extraction	München (TU)	2015	Bamler, R. Reinartz, P.
Bieniarz, J.	Sparse Methods for Hyperspectral Unmixing and Image Fusion	Osnabrück	2015	Reinartz, P. Ehlers, M.

Name	Title	University	Year	Reviewers
Bruck, M.	Sea State Measurements Using TerraSAR-X/TanDEM-X Data	Kiel	2015	Mayerle, R. Latif, M. Lehner, S.
Eckel, I.	Particle Filters for Airborne Tracking and Lane-Level Map-Matching of Vehicles	München (TU)	2015	Bamler, R. Burgard, W. Wunderlich, T.
Israel, M.	Entwicklung eines UAV-basierten Systems zur Rehkitzsuche und Methoden zur Detektion und Georeferenzierung von Rehkitzen in Thermalbildern	Osnabrück	2015	Reinartz, P. Tank, V.
Lachaise, M.	Phase Unwrapping of Multi-Channel Synthetic Aperture Radar: Application to the TanDEM-X Mission	München (TU)	2015	Bamler, R. Eineder, M. Ferraioli, G.
Lenhard, K.	Improving the Calibration of Airborne Hyperspectral Sensors for Earth Observation	Zürich (Uni)	2015	Schaepman, M. Hüni, A. Purves, R.
Rieger, S.	Vertical Motion Above a Subduction Zone over Different Time Scales	München (LMU)	2015	Friedrich, A. Bamler, R.
Tao, J.	Combination of LiDAR and SAR Data with Simulation Techniques for Image Interpretation and Change Detection in Complex Urban Scenarios	München (TU)	2015	Bamler, R. Sörgel, U. Reinartz, P.
Wang, Y.	Advances in Meter-resolution Multipass Synthetic Aperture Radar Interferometry	München (TU)	2015	Zhu, X. Bamler, R.
Xu, J.	Inversion for Limb Infrared Atmospheric Sounding	München (TU)	2015	Doicu, A. Bamler, R. Bühler, S.
Cong, X.	SAR Interferometry for Volcano Monitoring: 3D-PSI Analysis and Mitigation of Atmospheric Refractivity	München (TU)	2014	Eineder, M. Bamler, R. Hinz, S.
Cui, S.	Spatial and Temporal SAR Image Information Mining	Siegen	2014	Loffeld, O. Datcu, M.
Goel, K.	Advanced Stacking Techniques and Applications in High Resolution SAR Interferometry	München (TU)	2014	Bamler, R. Sörgel, U. Hanssen, R.
Singh, J.	Spatial Content Understanding of Very-High-Resolution Synthetic Aperture Radar Images	Siegen	2014	Loffeld, O. Datcu, M. Reinartz, P.
Singha, S.	Offshore Oil Spill Detection Using Synthetic Aperture Radar	Hull	2014	Bellerby, T.
Türmer, S.	Car Detection in Low Frame-Rate Aerial Imagery of Dense Urban Areas	München (TU)	2014	Stilla, U. Reinartz, P. Reulke, R.
Zhu, K.	Dense Stereo Matching with Robust Cost Functions and Confidence-Based Surface Prior	München (TU)	2014	Bamler, R. Reinartz, P.

Name	Title	University	Year	Reviewers
Köhler, C.	Radiative Effect of Mixed Mineral Dust and Biomass Burning Aerosol in the Thermal Infrared	Leipzig	2013	Trautmann, T. Wendisch, M.
Loyola, D.	Methodologies for Solving Satellite Remote Sensing Problems Using Neuro Computing Techniques	München (TU)	2013	Bamler, R. Wirsing, M. Mayer, B.
Riha, S.	Detektion und Quantifizierung von Cyanobakterien in der Ostsee mittels Satellitenfernerkundung	Rostock	2013	Miegel, K. Bill, R. Reinartz, P.
Tian, J.	3D Change Detection from High and very High Resolution Satellite Stereo Imagery	Osnabrück	2013	Reinartz, P. Ehlers, M.
Vasquez, M.	Radiative Transfer in Planetary Atmospheres with Clouds	Berlin (TU)	2013	Rauer, H. Trautmann, T.

HSU: Helmut-Schmidt-Universität
LMU: Ludwig-Maximilians-Universität München
TU: Technical University

Master/Diploma/Bachelor Theses

Master (M) / Diploma (D) / Bachelor (B) theses being supervised or completed at IMF orTUM-LMF/SiPEO (in *italic typeface*) between 2013 and mid 2018.

Name	Subject	University	Year	M/D/B
Bürgmann, T.	Matching of TerraSAR-X derived ground control points to optical image elements using deep learning	München (TU)	ongoing	M
Fuentes Reyes, M.	Translating SAR to optical images using conditional Generative Adversarial Networks (cGANs)	München (TU)	ongoing	M
Villamil Fajardo, S.	Synthetic retrievals of cloud parameters from DSCOVR/EPIC measurements	München (TU)	ongoing	M
Wenzl, M.	Hyperspektrale Klassifizierung des Untergrunds im Flachwasser	München (TU)	ongoing	M
Geißendörfer, O.	Evaluierung von Methoden zur monokularen Tiefenschätzung aus Bildern	München (TU)	2018	B
Kolsch, K.-H.	Google Earth Engine: Globale Analysen basierend auf Fernerkundungsdaten	München (TU)	2018	B
Han, S.	Building modeling and monitoring using social media images	München (TU)	2018	M
Knöttner, J.	Trennung von parkenden und am Verkehr teilnehmenden Fahrzeugen basierend auf einer automatischen Verkehrserfassung aus Luftbildern	Würzburg-Schweinfurt (HS)	2018	B
Kretz, M.	Design and construction of a light source setup for stray light measurements in array spectrometers	Karlsruhe (KIT)	2018	M
Li, Q.	Building Footprint Generation Using Deep Learning Methods	München (TU)	2018	M
Okuneva E.	Global Non-urban Local Climate Zones Classification with Sentinel-2 Images	München (TU)	2018	M
Rußwurm, M.	Multi-temporal land cover classification with convolutional recurrent networks	München (TU)	2018	M
Sheu, C.-Y.	Automatic 3D lane marking reconstruction using multi-view aerial imagery	Stuttgart	2018	M
Wang, Y.	Unsupervised Domain Adaptation for Image Classification	München (TU)	2018	M
Albrecht, L.	Rekonstruktion von 3D-Oberflächen mittels Polarisationsinformationen	München (TU)	2017	B
Beuchel, H.	Analyse von Verhalten und Differenzierbarkeit von Radarreflektoren auf See	Bremen (HS)	2017	D

Name	Subject	University	Year	M/D/B
Fitzthum, T.	Merkmalsdeskriptoren zur Messung der Ähnlichkeit zwischen optischen und SAR-Bildern	München (TU)	2017	B
Hua, Y.	Opening the Black Box: Deep Convolutional Neural Networks with Attention Mechanism for Aerial Scene Classification	München (TU)	2017	M
Huang, R.	Geo-information Extraction from Tweets	München (TU)	2017	M
Janas, J.	Extracting Atmospheric Parameters from Spectrometer Measurements and Comparison with Established Methods	Nürnberg	2017	M
Karam, S.	3D-Building Reconstruction with Different Height Levels from Airborne LiDAR Data	Stuttgart	2017	M
Liebel, L.	Deep Convolutional Neural Networks zur Semantischen Segmentierung von Multispektralen Sentinel-2-Bildern	München (TU)	2017	M
Plaß, B.	Ableiten von Straßenmarkierungen für das Autonome Fahren aus Digitalen Orthophotos mittels Deep Learning	Mainz (HS)	2017	B
Scharpf, J.	Development of an Independent UAV Payload Electronics for Real-Time Capable Direct Georeferencing of Camera Images Involving Gimbal Orientation Data	München (TU)	2017	M
Schnalzger, K.	Spektrale Datenbank für den Untergrund der Ostsee sowie Einfluss auf die Bestimmung der Wassertiefe	Augsburg	2017	M
Stolz, O.	Abschätzung der Möglichkeiten des Einsatzes optischer Fernerkundungsdaten bei der Bestimmung von Wassertiefen und deren Genauigkeit	Potsdam	2017	M
Wilzewski, J.	Experimental Study of Temperature-Dependence Laws of Absorption Line Shape Parameters Based on an Analysis of CO_2 v3 Transmittance Spectra	München (LMU)	2017	M
Xu, H.	Impact of Molecular Absorption Spectroscopy Data on Methane Retrieval from SCIAMACHY and GOSAT Shortwave Infrared Spectra	München (TU)	2017	M
Yokoya, N.	Analysis of Phase Inconsistencies in SAR Interferometry	München (TU)	2017	M
Zhang, G.	Fusion of Sentinel-2 and OpenStreetMap Data for the Classification of Local Climate Zones	München (TU)	2017	M
Zhang, J.	Estimation of Atmospheric Temperature Using Airborne Microwave Remote Sensing	München (TU)	2017	M
Alcaya, R.	Vom Bild zum Objekt – Ableitung von 3D-Gebäudemodellen aus Fernerkundungsdaten	München (HS)	2016	B

Name	Subject	University	Year	M/D/B
Dirscherl, M. C.	Topographic Change Quantification and DEM Uncertainty Assessment Using TanDEM-X and F-SAR DEM Time Series and Quality Maps: Application to the 2014-2015 Bardarbunga Volcanic Eruption, Iceland	London (University College)	2016	M
Ehrensperger, S.	Ableitung windgefährdeter Regionen unter Verwendung nichtparametrischer Regressionsanalyse	München (HS)	2016	B
Fast, S.	Mosaikierung von Orthobildern mit Saumlinien aus Geoinformation	Ostwestfalen-Lippe (HS)	2016	B
Han, L.	An Algorithm for the Detection of Calving Glaciers Frontal Position from TerraSAR-X and Sentinel-1 Imagery	München (TU)	2016	M
Hornig, I.	Automatisierte Interpretation von optischen Satellitenaufnahmen urbaner Gebiete anhand von Simulationsverfahren	München (TU)	2016	M
Hu, W.	Object-Based Multi-View Façade Matching in SAR Images of Dense Urban Areas	München (TU)	2016	M
Ilehag, R.	Exploitation of Digital Surface Models from Optical Satellites for the Identification of Buildings in High Resolution SAR Imagery	Stockholm (KTH Royal Institute of Technology)	2016	M
Kerkhoff, S.	Anwendung und Untersuchung einer Methode zur Analyse von IT-Sicherheitsrisiken anhand eines hochwertigen Erdfernerkundungssystems	Hagen	2016	M
Langheinrich, M.	Sufficiency of Features Extracted from Satellite Remote Sensing Data for the Estimation of Local Wind Damage Loss in Urban Areas	München (TU)	2016	M
Liu, Y.	InSAR Surface Elevation Derived from Bistatic TanDEM-X Data over the Schirmacher Oasis Area, East Antarctica	München (TU)	2016	M
Qian, W.	Application of Remote Sensing Technology on the Drought Monitoring of the Yangtze River Basin	München (TU)	2016	M
Richter, D.	Partikelfilter-basierte Landmarken-Navigation mit Hilfe geodätischer Radar-Fernerkundung	München (HS)	2016	M
Risse, E.-A.	Modelling Air-Pollution in Beijing: Emission Reduction vs. Meteorological Influence	Berlin (TU)	2016	M
Städt, S.	Mini MAX-DOAS Measurements of Air Pollutants over China	Berlin (FU)	2016	M
Sun, Y.	3D Building Reconstruction from Spaceborne TomoSAR Point Cloud	München (TU)	2016	M

Name	Subject	University	Year	M/D/B
Suttner, M.	Analyse des Geokodierungsfehlers für die gemeinsame Bearbeitung von SAR und optischen Daten	München (TU)	2016	B
Szajkowski, M.	Development of Pre- and Post-Processing Tools for the Analysis of Microwave Temperature Profiling Observations	Wrocław	2016	M
Xia, Y.	Homogeneous Pixel Selection for Distributed Scatterers Using Multitemporal SAR Data Stacks	München (TU)	2016	M
Xu, X.	Using SBAS-InSAR for Beijing-Tianjin Intercity Railway Subsidence Monitoring	München (TU)	2016	M
Zeitlhöfer, J.	Robuste Schätzung durch Approximation von Matrizen niedrigen Ranges	München (TU)	2016	B
Zeng, L.	Analysis on Recent Changes of Water Area in China's Poyang Lake Region Using Sentinel-1 Data	München (TU)	2016	M
Zhao, J.	Assessment of SAR Signal Penetration Effect on TanDEM-X Elevations in Antarctica with Laser Altimetry and GNSS Measurements	München (TU)	2016	M
Bellos, D.	A Case Study at Lake Constance for Water Depth Determination from Hyperspectral Data	München (TU)	2015	M
Hieronimus, J.	Wind Speed Measurements in an Offshore Wind Farm by Remote Sensing. A Comparison of Radar Satellite TerraSAR-X and Ground-Based LiDAR Systems	Oldenburg	2015	M
Hochstaffl, P.	Validation of Carbon Monoxide Total Columns from SCIAMACHY Near Infrared Nadir Spectra with NDACC/TCCON Ground-Based Measurements	Innsbruck	2015	M
von Hößlin, S.	Development and Validation of an Automated Photobioreactor System for Measuring Absorption and Fluorescence of Phytoplankton	München (TU)	2015	M
Hundhausen, F.	Aufbau, Charakterisierung und Ansteuerung eines Beleuchtungs-Moduls zur Simulation variabler Unterwasser-Lichtspektren unter Verwendung von Hochleistungs-Leuchtdioden	Esslingen (HS)	2015	B
Ionescu, A.	Evaluierung bestehender Algorithmen zur 3D-Rekonstruktion statischer Objekte aus monokularen Bildserien	München (TU)	2015	B
Kölling, T.	Characterization, Calibration and Operation of a Hyperspectral Sky Imager	München (LMU)	2015	M
Metzlaff, L.	Region Based Building Footprint Extraction and Change Detection for Urban Areas	Augsburg	2015	M

Name	Subject	University	Year	M/D/B
Niebisch, M.	Simulation des Satelliten EnMAP und Scheduling mithilfe von evolutionären Algorithmen	München (HS)	2015	B
Petri, C.	Determination of Storm Endangered Regions Based on Digital Elevation Models	Augsburg	2015	M
Piñuela Garcia, F.	Activando búsquedas por longitud de onda en una base de datos de índices hiperespectrales	Alcalá	2015	M
Riegler, M.	A Study and Comparison of Feature Matching	München (HS)	2015	M
Sakar, N.	Development of Advanced Co-Registration Methods for Sentinel-1 TOPS Mode	München (TU)	2015	M
Sasi, S.	Cloud Internal Mixing Model for Ozone Retrieval	München (TU)	2015	M
Schreiner, P.	Analyse der Penetrationsfähigkeit von Millimeterwellen-SAR am Beispiel von Baumkronen	München (TU)	2015	B
Thumm, B.	Entwicklung und Anwendung einer robusten Atmosphärenkorrektur auf der Basis des Angstroem-schätzers (MOS) für räumlich höherauflösende Fernerkundungssensoren, sowie Anwendung auf Binnengewässer zur Abschätzung der Gewässergüte	Berlin (FU)	2015	B
Wei, L.	Quantification of Low-Rank Information in Multi-Temporal SAR Datasets	München (TU)	2015	M
Willberg, M.	Geodätisches SAR zur Höhenmessung von Gezeitenpegelstationen	München (TU)	2015	M
Adam, F.	Non-Local Filtering of TanDEM-X Interferograms for Improving DEM Quality	München (TU)	2014	M
Beverborg, H.	Entwicklung einheitlicher Regelsätze in eCognition für die objektorientierte Klassifikation von verschiedenen multispektralen Datensätzen in Kombination mit Höhendaten	Osnabrück	2014	M
Borchardt, S.	Der Mehrwert des Cyanobakterienalgorithmus bei der räumlich-zeitlichen Verfolgung von Algenblüten in der Ostsee anhand einer Jahresanalyse von MERIS-Daten	Berlin (FU)	2014	B
Bräuninger, S.	Erfassung von Verkehrsdaten aus monotemporalen Satellitenbildaufnahmen	München (HS)	2014	B
Brunnengräber, M.	Kalibration des UAV Kamerasystems Asctec Firefly	München (TU)	2014	B
Burns, T.	Dictionary Learning for Sparse Representation Based Image Fusion	Queensland	2014	B

Name	Subject	University	Year	M/D/B
Davydova, K.	Consistent Multi-View Texturing of Detailed 3D Surface Models	München (TU)	2014	M
Hornig, I.	Charakterisierung von Corner-Reflektoren mit Teilverglasung	München (TU)	2014	B
Hu, J.	Non-local Means for Polarimetric SAR Speckle Reduction - Experiments Using TerraSAR-X Data	München (TU)	2014	M
Koch, T.	Robustes Tracking mithilfe des Partikel Filters	München (TU)	2014	M
Lang, F.	Analyse digitaler Oberflächenmodelle aus multitemporalen hochauflösenden optischen Satellitendaten	München (HS)	2014	M
Langheinrich, M.	On the Influence of Coregistration Errors on Satellite Image Pansharpening Methods	München (HS)	2014	B
Liu, K.	Fast Multiclass Vehicle Detection in Very High Resolution Aerial Images	München (TU)	2014	M
Liu, S.	Retrieval and Validation of Aerosol and NO_2 Profiles over Nanjing Using Mini-MAX-DOAS Instrument	München (TU)	2014	M
Magin, J.	Erprobung kostengünstiger Ultraschallsensoren mit dem Raspberry Pi	München (TU)	2014	B
*Matay*eva, A.	Deriving the Distribution of Population from Nighttime Lights Data	München (TU)	2014	M
Mende, M.	Flugassistenzsoftware für unbemannte Kleinfluggeräte	Mannheim (DHBW)	2014	B
Moie, R.	A Detailed Survey and Efficient Implementation of the SGM Algorithm	München (TU)	2014	M
Montazeri, S.	The Fusion of SAR Tomography and Stereo-SAR for 3D Absolute Scatterer Positioning	Delft	2014	M
Naumann, A.	Detektion Regelmäßiger Gitter in Persistent Scatterer Punktwolken	München (TU)	2014	B
Orthuber, E.	3D Building Reconstruction from Airborne LiDAR Pointclouds	München (TU)	2014	M
Pültz, M.	Integration von 3D-Geoinformation in die Veränderungsanalyse aus hochaufgelösten SAR-Daten	München (TU)	2014	B
Schmidt, D.	Carbon Monoxide from SCIAMACHY Near Infrared Nadir Spectra: Impact of Retrieval Settings	München (TU)	2014	M
Schütz, A.	Photogrammetrische Auswertung von Bildern der Spacelab-Metric Camera	München (TU)	2014	B

Name	Subject	University	Year	M/D/B
Ansari, H.	Bayesian Estimation and Applications in PSI	München (TU)	2013	M
Alexy, M.	Synergetische Nutzung von solaren und thermischen Kanälen zur Fernerkundung von Zirruswolken	München (TU)	2013	M
Fischer, P.	Solving Optimization and Inverse Problems in Remote Sensing by Using Evolutionary Algorithms	München (TU)	2013	M
Hanrieder, B.	Hochwasser in Thailand- Erstellung und Validierung von Flutmasken aus HR- und VHR- Daten zur Abschätzung monetär bewertbarer ökonomischer Verluste	München (TU)	2013	M
Leister, W.	Hypothesenvalidierung von Fahrzeugdetektionen mit Hilfe von Color-Cooccurance-Histogrammen im HSV-Farbraum	Chemnitz (TU)	2013	M
Meßner, M.	Robust and Efficient Monocular SLAM	München (TU)	2013	M
Reinhardt, V.	Methodenentwicklung für Spektrophotometer	München (LMU)	2013	B
Robatsch, E.	Adjustment and Mosaicking of Satellite Images	Kärnten (FH)	2013	B
Schneider, N.	Transfer der Kalibrierung von einem Strahldichtenormal auf Hyperspektralsensoren	München (LMU)	2013	B
Serr, P.	Vollautomatisches Mosaikieren von Satellitenbildern	München (LMU)	2013	M
Shah, M.	Accurate Estimation of Travel Times on the Traffic Data, Extracted from Aerial Image Time Series	München (TU)	2013	M
Soria Villalba, S.	Advanced Algorithms for Denoising of Hyperspectral Data for Bands with Low Signal-To-Noise Ratio	Alcala	2013	M
Vérité, M.	Evaluation of Satellite Based Traffic Data Using Compartments Flow Model and Particles Filtering	Compiègne	2013	M

DHBW: Duale Hochschule Baden-Württemberg
FH: Fachhochschule
FU: Freie Universität
HS: Hochschule
KIT: Karlsruher Institut für Technologie
LMU: Ludwig-Maximilians-Universität
TU: Technical University

Scientific Exchange

Guest Scientists

Visiting scientists (≥ 4 weeks) hosted by IMF between 2013 and mid 2018.

Name	Period	Home Institution	Funding
Alam, K.	Jun – Jul 2013	University of Peshawar, Pakistan	HEC, Pakistan
Andreou, C.	Apr – Jun 2013	National Technical University of Athens, Greece	DAAD
Ao, D.	Oct – Dec 2016	Beijing Institute of Technology, China	Chinese Academy of Science
Arefi, H.	Jun – Aug 2015	University of Tehran, Iran	DAAD
Burns, T.	Apr – Sep 2014	University of Queensland, Australia	HGF
Che, M.	Nov – Dec 2017	University of Pavia	University of Pavia
Damian, C.	Aug – Oct 2015	Politehnica Bucharest, Romania	Politehnica Bucharest
Deo, R.	Oct 2013 – Sep 2014	Indian Institute of Technology	DAAD
Dirscherl, M.	Feb – Jun 2018	University of Island	University of Island
Eppler, J.	Jun – Sep 2018	Simon Frazer University, Canada	Simon Frazer University
Eremin, Y.	Sep 2013	Moscow Lomonosov State University, Russia	DAAD
Focsa, A.	Aug – Oct 2015	Military Academy, Romania	Military Academy
Fraser, C.	Jun – Aug 2014	University of Melbourne, Australia	DAAD Senior Scientist
Georgescu, F.	Aug – Dec 2015	Military Academy, Romania	Military Academy
Ghamisi, P.	Oct 2015 – Sep 2017	University of Iceland, Reykjavik, Iceland	Alexander von Humboldt Research Fellowship for Postdoctoral Researchers
Giardino, G.	Apr – Oct 2014	University of Rome Tor Vergata, Italy	University of Rome Tor Vergata
Guo, R.	Nov 2012 – Nov 2014	Xidian University, China	DAAD, Postdoc
Kai, Q.	Feb 2016 – Feb 2017	China University of Mining and Technology, China	China Overseas Training Program for Young Teachers
Kar, A.	Nov 2013 – Mar 2015		DAAD
Kiselev, O.	Mar 2013 – Mar 2015	Moscow State University, Russia	DAAD Postdoc
Maier, S.	Jul – Sep 2014	University of Darwin, Australia	DAAD Senior Scientist

Name	Period	Home Institution	Funding
Main-Knorn, M.	Jan 2013 – Jan 2015		DAAD Postdoc
Nielsen, A.	May 2013	Technical University of Denmark	DAAD
Patrascu, C.	Oct 2012 – Feb 2013	Politehnica Bucharest, Romania	Politehnica Bucharest
Qin, R.	Sep – Nov 2014	ETH Zürich, Switzerland	Singapore ETH Center
Radoi, A.	Feb – Apr 2015	Politehnica Bucharest, Romania	Politehnica Bucharest
Rikka, S.	Nov 2016 – Aug 2017	Tallinn University of Technology, Estonia	Archimedes Foundation, Tallinn
Roman Gonzalez, A.	May – Oct 2013	ParisTech, France	DLR
Sarris, A.	Jan – Mar 2018	Foundation for Research and Technology Hellas, Greece	DAAD
Tanase, R.	Oct – Dec 2014, Apr – Jun 2016	Politehnica Bucharest, Romania	Politehnica Bucharest
Vaduva, C.	Sep – Oct 2014	Politehnica Bucharest, Romania	Politehnica Bucharest
Xie, C.	Apr 2014 – Mar 2015	Chinese Academy of Science, Beijing, China	Chinese Academy of Science
Yao, W.	Aug 2014 – Jun 2017	Universität Siegen	Universität Siegen
Yokoya, N.	Dec 2015 – Nov 2017	University of Tokyo, Japan	Alexander von Humboldt Research Fellowship for Postdoctoral Researchers
Zhang, C.	Aug – Nov 2016	University of Science and Technology of China, Hefei, China	USTC, China
Zhu, B.	Sep – Nov 2015	Fudan University, China	DAAD

Professional Leaves

Periods of stay (≥ 4 weeks) by IMF and TUM-LMF/SiPEO (*italic*) staff at external institutions between 2013 and mid 2018.

Staff Member	Institution	Period	Funding
Avbelj, J.	Tel-Aviv University, Israel	Aug – Oct 2013	DLR, TUM
Bieniarz, J.	University of Massachusetts, USA	Sep – Oct 2013	DLR
Cui, S.	University of Toronto, Canada	May – Jun 2015	DLR
Floricioiu, D.	University Canterbury, New Zealand (Antarctica expedition)	Oct – Dec 2016	Antarctica New Zealand, Gateway Antarctica, DLR
Gege, P.	German research vessel "Polarstern"	May – Jul 2017	DLR
Göritz, A.	Plymouth Marine Lab, England	Mar – Jun 2016	TUM
Hong, D.	Grenoble Institute of Technology, France	Mar – Jun 2018	DLR
Koch, T.	IPN - Computing Research Center, Mexico City, Mexico	Mar – Apr 2018	TUM
Kuschk, G.	TU Graz, Austria	May – Jun 2013	DLR
Lehner, S.	Nova Southeastern University, Miami, USA UVIC University, Victoria, Canada Simon Fraser University, Vancouver, Canada	Feb – Apr 2017 Sep – Oct 2017 May – Jun 2017 Feb – Apr 2018	DLR DLR DLR
Loyola, D.	NASA, Goddard, Greenbelt, USA	Aug 2016 – Jul 2017	DLR
Mattyus, G.	University of Toronto, Canada	May – Jun 2014 Feb – Mar 2015	DLR
Merkle, N.	University of Toronto, Canada	Apr – May 2016 Oct – Nov 2016	DLR
Meynberg, O.	University of Otago, New Zealand	Nov – Dec 2016	DLR
Murillo, A.	Google, Zurich, CH	Oct – Dec 2016	Google
Partovi, T.	University Twente, Netherlands	Oct – Nov 2015	DLR
Rußwurm, M.	ESRIN PhiLab, Frascati, Italy	Jun 2018	TUM
Schmitt, M.	University of Massachusetts Amherst, USA	Jul – Sep 2016	TUM
Shahzad, M.	TU Graz, Austria	Nov 2015 – Jan 2016	TUM
Singha, S.	University of Tromsø, Norway	Feb – Mar 2017 Apr – May 2018	DLR
Traganos, D.	University of Queensland, Brisane, Australia	Apr 2018 – Jun 2018	DLR

Staff Member	Institution	Period	Funding
Trautmann, T.	University of New South Wales, Sydney, Australia	Nov 2014 – Feb 2015	DLR
Wang, Y.	ETH Zürich, Switzerland	Jun – Jul 2014	TUM
Zhu, X.	Fudan University, China University of California, Los Angeles, USA University of Tokyo, Japan	Jan – Feb 2014 Mar – May 2016 May – Jun 2016	DLR DLR DLR
Zhuo, X.	TU Graz, Austria	Oct – Nov 2017	DLR

Conferences

Major conferences, colloquia and workshops (co-)organized by IMF and TUM-LMF/SiPEO between 2013 and 2018.

Date	Event	Location	Participants
23 – 26 Sep 2018	WHISPERS 2018 (General Chair)	Amsterdam, NL	400
1 Jul 2016	Third Workshop on Geo-Spatial Computer Vision: Visual Analysis of Satellite to Street Imagery (in conjunction with IEEE Conference on Computer Vision and Pattern Recognition, CVPR)	Las Vegas, USA	20
21 – 26 Jun 2015	15th Electromagnetic and Light Scattering Conference	Leipzig	180
25 – 27 Mar 2015	ISPRS Conference: High resolution earth imaging for geospatial information (HRIGI)	München	200
5 – 7 Mar 2014	Image Information Mining: Geospatial Intelligence from Earth Observation Conference (ESA-EUSC-JRC 2014)	Bucharest, Romania	90
5 – 8 Oct 2013	ISPRS Conference: Sensors and Models in Photogrammetry and Remote Sensing	Tehran, Iran	250
23 – 26 Sep 2013	SAR-EDU Summer School	Jena	20
21 – 24 May 2013	ISPRS Workshop High-Resolution Earth Imaging for Geospatial Information	Hannover	120

Patents

Filed Patent Applications

Name	Patent	Patent No	Year	Countries
Klarner, R. Runge, H.	Fahrerassistenzsystem bzw. autonomes Fahrsystem zum Schutz von anderen Verkehrsteilnehmern durch das eigene Fahrzeug	DE 10 2017 106032.4	2017	DE, EP
Dreher, A. Runge, H. Klarner, R.	RF-QR-Code	DE 10 2016 101156.8	2016	DE
Klarner, R. Runge, H.	Fahrerassistenzsystem zur optimierten Fahrzeugsteuerung und Hindernis-Prävention mittels Umfeld-Informationen	DE 10 2016 101901.1	2016	DE
Klarner, R. Runge, H.	Automatische Darstellung von Umgebungs-Bildern in der gewünschten Ansicht	DE 10 2016 120366.1	2016	DE
Runge, H. Krauß, T.	Bestimmung von Passpunkten in Radar-Bildern und optischen Aufnahmen	DE 10 2016 123286.6	2016	DE
Caron, S. Pernpeintner, S. Meyen, S. Cerra, D.	Zerstörungsfreies Messverfahren zur lokalen Ermittlung des spektralaufgelösten hemisphärischen Emissionsgrads und absoluten Oberflächentemperatur eines Körpers	DE 10 2015 219727.1	2015	DE
Duque Biarge, S. Parizzi, A. De Zan, F.	Automatic three-dimensional geolocation of SAR targets and simultaneous estimation of tropospheric propagation delays using two long-aperture SAR images	DE 10 2015 220218.6	2015	DE
Klarner, R. Runge, H.	Spurhalteassistent	DE 10 2015 111925.0	2015	DE
Krauß, T. Fischer P.	Frühwarnsystem vor Abflussrückstau verursacht durch Starkregen	DE 10 2015 109208.5	2015	DE
Avbelj, J.	Qualitätssicherung für Geoinformationen	DE 10 2014 211088.2	2014	DE
Fraundorfer, F. Mattyus, G. S.	Georeferenzierung von Bilddaten	DE 10 2014 108255.9	2014	DE
Israel, M.	Verfahren zum Auffinden von Lebewesen aus der Luft sowie Flugobjekte zum Auffinden von Lebewesen aus der Luft	DE 10 2012 221580.8	2013	DE, CH, AT

DE = Germany, AT = Austria, AU = Australia, BR = Brasilien, CA = Canada, CH = Switzerland,
ES = Spain, EP = European Patent Organization, FR = France, GB = United Kingdom,
IT = Italy, NL = The Netherlands, RU = Russia, SE = Sweden, US = USA

Granted Patents

Name	Patent	Patent No.	Year	Countries
Klarner, R. Runge, H.	System zur Fahrerunterstützung	DE 10 2014 106890.4	2018	DE
Adam, N.	Verfahren und System zur Ermittlung von Bewegungen langzeitstabiler Radarstreuer auf einer Oberfläche eines Planeten mittels SAR-Interferometrie	DE 10 2016 107065.3	2017	DE
Rosenbaum, D. Leitloff, J.	Verfahren und Vorrichtung zur Erfassung von Verkehrsdaten aus digitalen Luftbildsequenzen	EP 2387017	2016	AT, FR, GB, EP
Israel, M. Tank, V. Haschberger, P.	Verfahren zur Erkennung von Tieren einschließlich Brutgelegen in landwirtschaftlich genutzten Feldern und Wiesen sowie Vorrichtung zur Durchführung	CH 701643	2015	CH
Runge, H. Klarner, R.	Positionsbestimmung eines Fahrzeugs auf oder über einer Planetenoberfläche	DE 10 2013 015892.3	2015	DE
Baumgartner, A.	Relative radiometrische Homogenitätsmessung von Flächen und einhergehende relative radiometrische Kalibrierung von abbildenden Detektoren	DE 10 2013 106571.6	2014	DE
Dequet, W. Tank, V.	Hochelastischer Verbundwerkstoff sowie Sportbogen aus einem hochelastischen Verbundwerkstoff	DE 10 2009 032663	2014	DE
Eineder, M.	Verfahren zur Messung des Wasserstands eines Gewässers	DE 10 2010 001440	2014	DE, CA
Israel, M. Tank, V. Fackelmeier, A. Nitsche, R. Ruprecht, V. Schwarzmaier, T.	Verfahren und Vorrichtung zur Suche und Erkennung von in landwirtschaftlichen Feldern und Wiesen versteckten Tieren	CH 701808	2014	CH
Reinartz, P. Bamler, R. Suri, S.	Verfahren zur Georeferenzierung optischer Fernerkundungsbilder	EP 2225533	2014	DE, FR, IT, US
Schwarzmaier, T. Gege, P.	Vorrichtung zur Kalibrierung eines optischen Sensors	DE 10 2012 014263	2014	DE
Suchandt, S. Runge, H.	Schiffsdetektion in Interferometrie-Radardaten	DE 10 2013 107402.2	2014	DE, EP
Tank, V. Israel, M.	Einrichtung zum Detektieren von Objekten, wie Tieren und Vogelgelegen, im Acker und Pflanzenbau	DE 10 2008 035888	2014	DE
Schreier, F. Kohlert, D. Pöppel, G.	Vorrichtung zur Ermittlung von Gaskonzentrationen	DE 10 2012 006047	2013	DE, USA

For country abbreviations see footnote to previous table of Filed Patent Applications

Awards

Awards granted to IMF and TUM-LMF/SiPEO (in *italic* typeface) staff between 2013 and mid 2018.

Year	Award	Laureates (only IMF, LMF/SiPEO)	Subject
2018	2nd Prize IEEE GRSS Data Fusion Contest 2018	Cerra, D. Figueiredo Vaz Pato, M. Carmona, E. Tian J. Azimi, S. Müller, R. Bittner, K. Henry, C. Vig, E. Kurz, F. Bahmanyar, R. d'Angelo, P. Alonso, K. Fischer, P. Reinartz, P.	Deep convolutional and shallow neural networks on a simplified set of classes, completed by a series of specific detectors and ad hoc classifiers
2018	Best Paper Award, ALLDATA 2018 (Athens/Greece)	Dumitru, C. Schwarz, G. Datcu, M.	Monitoring of Coastal Environments Using Data Mining
2018	2018 Richard M. Goody Award	Efremenko, D.	Atmospheric Radiation and Remote Sensing
2018	Best Reviewer Award 2017 (IEEE Geoscience and Remote Sensing Letters)	Ghamisi, P.	
2018	1st Place Student Paper Award, EUSAR 2018 (Aachen)	Kang, J. Wang, Y. Zhu, X.	Low Rank Modeling based Multipass InSAR technique
2018	Ada Lovelace Award for HPC 2018 (Partnership for Advanced Computing in Europe)	Zhu, X.	Global Urban Modeling
2018	Leopoldina Early Career Award 2018	Zhu, X.	
2017	Helmut-Rott-Preis 2017	Abdel Jaber, W.	Derivation of mass balance and surface velocity of glaciers by means of high resolution synthetic aperture radar: application to the Patagonian Icefields and Antarctica (Dissertation)
2017	DLR Senior Scientist 2017	Adam, N.	
2017	IEEE GRSS Mikio Takagi Student Prize	Ansari, H.	Sequential Estimator: Toward Efficient InSAR Time Series Analysis

Year	Award	Laureates (only IMF, LMF/SiPEO)	Subject
2017	ASTO-Preis 2017	Bittner, K.	Building extraction using a deep learning framework
2017	Chaire Blaise Pascal 2017 (Fondation de l'Ecole Normale Supérieure, France)	Datcu, M.	New challenges for machine learning posed by very heterogeneous data
2017	DLR-Nachwuchsgruppenleitung	Efremenko, D.	Mathematical and Physical Models for Analyzing Big Data from Atmospheric Composition Sensors
2017	Laura Bassi-Preis (TU München)	*Göritz, A.*	Improving Remote Sensing of Cyanobacteria by Exploiting Fluorescence Signals
2017	Best Presentation Award, LRZ Deep Learning Meeting (Garching)	*Rußwurm, M.* *Körner, M.*	Temporal Vegetation Modelling using Long Short-Term Memory Networks for Crop Identification from Medium-Resolution Multi-Spectral Satellite Images
2017	Best Paper Prize, CVPR 2017 EarthVision Workshop (Honolulu)	*Rußwurm, M.* *Körner, M.*	Temporal Vegetation Modelling using Long Short-Term Memory Networks for Crop Identification from Medium-Resolution Multi-Spectral Satellite Images
2017	Travel Grant, ISPRS Hannover Workshop (The ISPRS Foundation)	*Rußwurm, M.* *Körner, M.*	Multitemporal Crop Identification from Medium-Resolution Multi-Spectral Satellite Images based on Long Short-Term Memory Neural Networks
2017	Helmholtz Young Investigators Group	Vig, E.	ARIADNE: AeRial Imagery Analytics by Deep Neural Networks
2017	Best Reviewer Award 2016 (IEEE Transactions on Geoscience and Remote Sensing)	*Wang, Y.*	
2017	1st Prize, IEEE GRSS Data Fusion Contest 2017	Yokoya, N. Ghamisi, P.	Ensemble Classifier (including Canonical Correlation Forests and Rotation Forests) over Landsat8 Images and OpenStreetMap Data
2017	Transactions Prize Paper Award 2016 (IEEE Geoscience and Remote Sensing Society)	Zhu, X. Montazeri, S. Bamler, R.	Geodetic SAR Tomography
2017	Helmholtz-Exzellenzprofessur	Zhu, X.	Data Science in Earth Observation

Year	Award	Laureates (only IMF, LMF/SiPEO)	Subject
2016	Ausgezeichneter Ort 2016 im Land der Ideen (Deutschland – Land der Ideen)	Adam, N. Bamler, R. Eineder, M. Goel, K. König, T. Rodriguez Gonzalez, F. Shau, R.	Satellitengestützte Bodenbewegungskarte für Deutschland
2016	VDV Hochschulpreis (beste Bachelorarbeit) (Verband deutscher Vermessungsingenieure)	Ehrensperger, S.	Ableitung windgefährdeter Regionen unter Verwendung nichtparametrischer Regressionsanalyse
2016	Best Paper Award, VISAPP 2016 (Rom)	Fraundorfer, F.	Direct Stereo Visual Odometry based on Lines
2016	Letters Prize Paper Award 2016 (IEEE Geoscience and Remote Sensing Society)	Liu, K. Mattyus, G.	Fast Multiclass Vehicle Detection on Aerial Images
2016	1st Prize, IEEE GRSS Data Fusion Contest 2016	Mou, L. Zhu, X.	Spatiotemporal Scene Interpretation of Space Videos via Deep Neural Networks and Tracklet Analysis
2016	DLR Senior Scientist 2016	Müller, R.	
2016	Regional Winner Bayern Copernicus Masters Competition 2016	Runge, H.	RETRIEVE - Sentinels for Safe Transportation and Retrieval of High-value Goods
2016	Special Prize: BMVI Earth Observation Challenge for Digital Transport Applications Copernicus Masters Competition 2016	Runge, H.	Herausragende und innovative Nutzungsideen zur Erdbeobachtung
2016	Best Reviewer Award 2015 (IEEE Geoscience and Remote Sensing Letters)	*Schmitt, M.*	
2016	IEEE Senior Member	*Schmitt, M.*	
2016	Dimitris N. Chorafas Foundation Prize 2016	*Wang, Y.*	Advances in Meter-Resolution Multipass SAR Interferometry
2016	Mitglied "Junges Kolleg" (Bayerische Akademie der Wissenschaften)	Zhu, X.	Modern Signal Processing Methods for the Next Generation of Earth Observation Satellite Missions
2016	Mitglied "Junge Akademie" (Berlin-Brandenburgischen Akademie der Wissenschaften und der Deutschen Akademie der Naturforscher Leopoldina)	Zhu, X.	

Year	Award	Laureates (only IMF, LMF/SiPEO)	Subject
2016	Early Career Award 2016 (IEEE Geoscience and Remote Sensing Society)	Zhu, X.	Outstanding contributions in innovative signal processing algorithms for remote sensing
2016	ERC Starting Grant	Zhu, X.	So2Sat: Big Data for 4D Global Urban Mapping – 10^{16} Bytes from Social Media to EO Satellites
2016	DLR-Wissenschaftspreis 2016	Zhu, X. *Montazeri, S.*	Geodetic SAR tomography
2015	IEEE Fellow	Eineder, M.	Contributions to SAR image processing for geodesy
2015	Symposium Paper Award, IGARSS 2015 (Milan)	Grohnfeldt, C. Zhu, X.	Towards a Combined Sparse Representation and Unmixing Based Hybrid Hyperspectral Resolution Enhancement Method
2015	DLR Senior Scientist 2015	Loyola, D.	
2015	Outstanding PhD Thesis Award (Munich GeoCenter)	*Schmitt, M.*	Reconstruction of urban surface models from multi-aspect and multi-baseline interferometric SAR
2015	Georg-Burg-Preis der Ingenieurfakultät Bau Geo Umwelt (TU München)	*Schmitt, M.*	Reconstruction of urban surface models from multi-aspect and multi-baseline interferometric SAR
2015	3. Platz, IGSSE Forum 2015 Vodafone Poster Preis	*Wang, Y.,* *Shahzad, M.*	4D City
2015	Heinz Maier-Leibnitz Preis 2015 (Deutsche Forschungsgemeinschaft)	Zhu, X.	Remote Sensing
2015	Helene-Lange-Preis 2015 (EWE-Stiftung, Universität Oldenburg)	Zhu, X.	Jahresnachwuchswissenschaftlerin in den MINT Disziplinen
2015	ASTO Förderpreis (Gesellschaft von Freunden des DLR)	Zhuo, X.	Fusion of multi-view and multi-scale aerial imagery
2014	Franz-Xaver-Erlacher Förderpreis (Gesellschaft von Freunden des DLR)	Baier, G.	Interferometrische Algorithmen für mittelauflösende SAR-Systeme mit hoher Abbildungsleistung
2014	Best Paper Award, EUSAR 2014 (Berlin)	Lachaise, M. Fritz, T. Eineder, M.	Dual-Baseline phase unwrapping challenges in the TanDEM-X Mission
2014	IEEE Senior Member	Zhu, X.	Significant contributions to the profession

Year	Award	Laureates (only IMF, LMF/SiPEO)	Subject
2014	Innovatoren unter 35 (MIT Technology Review, German Section)	Zhu, X.	4D City
2013	3nd Prize, IEEE GRSS Data Fusion Contest 2013	*Avbelj, J.* Bieniarz, J. Cerra, D. Makarau, A. Müller, R.	Hyperspectral and lidar fusion
2013	DLR Science Slam	Cerra, D. Makarau, A. *Grohnfeldt, C.,* Alonso Gonzalez, K. et al.	Remote Sensing: a Melodic Introduction
2013	IEEE Fellow	Datcu, M.	Contributions to information mining of high resolution SAR and optical earth observation images
2013	3rd Prize, Student Paper Contest, JURSE 2013 (Sao Paulo)	Goel, K. Adam, N.	Advanced Stacking of TerraSAR-X and TanDEM-X Data in Complex Urban Areas
2013	Innovationspreis 2013 (Gesellschaft von Freunden des DLR)	Israel, M. Haschberger, P. Schwarzmaier, T. Wimmer, T. Wörishofer, J. Wenisch, A. et al.	Fliegender Wildretter
2013	BMW Connected Drive Challenge Winner, Copernicus Masters Competition 2013	Runge, H.	Radarlösungen für hochautonomes Fahren
2013	Overall Winner, Copernicus Masters Competition 2013	Runge, H.	Landmark navigation using high precision fix points from radar-satellite imagery
2013	Helmholtz Young Investigators Group	Zhu, X.	SiPEO – Modern Signal Processing Methods for the Next Generation of Earth Observation Satellite Missions

Memberships

Memberships in Space Mission related Boards

Member	Agency	Board	2013	2014	2015	2016	2017	2018
Birk, M.	ESA	MIPAS Quality Working Group	■	■	■	■	■	■
Eineder, M.	HGF	Remote Sensing and Earth System Dynamics Alliance Steering Committee (Tandem-L)	■	■	■	■	■	
Eineder, M.	DLR/JAXA	Tandem-L/ALOS-Next Science Team	■	■	■			
Floricioiu, D.	WMO	Polar Space Task Group	■	■	■			
Gottwald, M.	DLR	SCIAMACHY Science Advisory Group	■	■	■	■	■	■
Gottwald, M.	WMO	Polar Space Task Group	■	■	■	■	■	■
Lichtenberg, G.	DLR	SCIAMACHY Science Advisory Group	■	■	■	■	■	■
Lichtenberg, G.	ESA	CarbonSat Mission Advisory Group	■	■	■			
Loyola, D.	CEOS	Atmospheric Composition Constellation	■	■	■	■	■	■
Loyola, D.	ESA	Sentinel 4 Mission Advisory Group	■	■	■	■	■	■
Loyola, D.	ESA	Sentinel 5 Mission Advisory Group	■	■	■	■	■	■
Loyola, D.	ESA	Sentinel 5 Precursor Quality Working Group						■
Loyola, D.	EUMETSAT	Data Record Generation Working Group	■	■	■	■		
Schättler, B.	CEOS	WGCV SAR Subgroup	■					
Slijkhuis, S.	ESA/ EUMETSAT	GOME/GOME-2 Science Advisory Group	■	■	■	■	■	■
Trautmann, T.	ESA	Sentinel 5 Precursor Mission Advisory Group	■	■	■	■	■	■
Trautmann, T.	DLR	METimage Science Advisory Group	■	■	■	■	■	■
Wagner, G.	ESA	MIPAS Quality Working Group	■	■	■	■	■	■

CEOS: Committee on Earth ObservationSatellites
ESA: European Space Agency
EUMETSAT: European Organisation for the Exploitation of Meteorological Satellites
HGF: Helmholtz-Gemeinschaft Deutscher Forschungszentren
JAXA: Japan Aerospace Exploration Agency
WMO: World Meteorological Organization

Editorial Memberships

Member	Journal / Book / Series	Publisher	2013	2014	2015	2016	2017	2018
Bamler, R.	Remote Sensing Special Issue, Guest Editor	MDPI					■	■
Datcu, M.	International Journal of Image and Data Fusion	Taylor & Francis	■	■	■	■	■	■
Datcu, M.	Transactions on Big Data	IEEE					■	■
Eineder, M.	Remote Sensing Special Issue, Guest Editor	MDPI					■	■
Lehner, S.	Remote Sensing Special Issue, Guest Editor	MDPI						■
Loyola, D.	Journal of Selected Topics in Applied Earth Observations and Remote Sensing	IEEE	■	■	■			
Loyola, D.	Atmospheric Measurement Techniques	EGU	■	■	■	■	■	■
Reinartz, P.	International Journal of Image and Data Fusion	Taylor & Francis		■	■	■	■	■
Reinartz, P.	Remote Sensing	MDPI					■	■
Schmitt, M.	Geoscience and Remote Sensing Letters	IEEE				■	■	■
Schmitt, M.	Journal of Photogrammetry, Remote Sensing and Geoinformation Science	DGPF						■
Slijkhuis, S.	Atmospheric Measurement Techniques	EGU	■	■	■	■	■	■
Zhu, X.	Transactions on Geoscience and Remote Sensing	IEEE			■	■	■	■
Zhu, X.	Remote Sensing Special Issue, Guest Editor	MDPI					■	■
Zhu, X.	Journal of Selected Topics in Applied Earth Observations and Remote Sensing	IEEE						■
Zhu, X.	Journal of Applied Remote Sensing	SPIE					■	■
Zhu, X.	International Journal of Geoinformatics	AgIT						■
Zhu, X.	Computer Vision and Image Understanding	Elsevier						■

AgIT: Association for Geoinformation Technology
DGPF: Deutsche Gesellschaft für Photogrammetrie, Fernerkundung und Geoinformation
EGU: European Geosciences Union
IEEE: Institute of Electrical and Electronics Engineers
MDPI: Multidisciplinary Digital Publishing Institute
SPIE: International Society for Optics and Photonic

Publications

This chapter lists in reverse chronological order for the time period between January 2013 and June 2018

- publications in ISI and SCOPUS journals
- other publications with full paper review
- books and book contributions
- other publications.

Internal reports as well as doctoral, diploma, Master and Bachelor theses are not listed.

IMF authors appear in **bold** typeface, employees of the TUM-LMF/SiPEO are ***in bold and italic*** typeface.

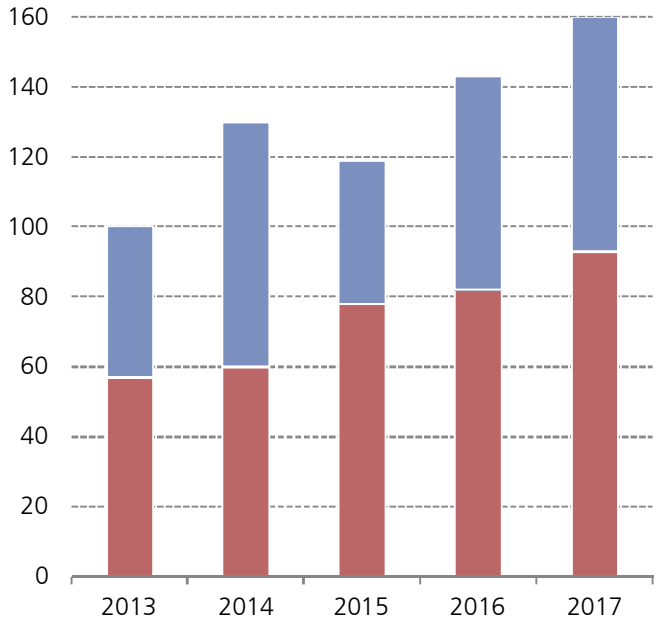

IMF's publication activities 2013 – 2017; red: publications in ISI and SCOPUS journals; blue: other publications with full paper review.

Publications in ISI or Scopus Journals

2018 under review

[1] **Adolph, W.**, Farke, H., **Lehner, S.**, Ehlers, M.: *Remote Sensing Intertidal Flats with Terra-SAR-X. A SAR Perspective of the structural elements of the tidal basin for Monitoring the Wadden Sea*, Remote Sensing, accepted, 2018.

[2] **Ansari, H.**, **De Zan, F.**, **Bamler, R.**: *Efficient Phase Estimation for Interferogram Stacks*, IEEE Transactions on Geoscience and Remote Sensing, accepted, 2018.

[3] Ao, D., **Schwarz, G.**, **Datcu, M.**: *Moving Ship Velocity Estimation Using TanDEM-X Data Based on Sub-Aperture Decomposition*, IEEE Geoscience and Remote Sensing Letters, accepted, 2018.

[4] **Baier, G.**, **Rossi, C.**, **Lachaise, M.**, **Zhu, X. X.**, **Bamler, R.**: *A Nonlocal InSAR Filter for High-Resolution DEM Generation from TanDEM-X Interferograms*, IEEE Transactions on Geoscience and Remote Sensing, in press, 2018.

[5] Boynard, A., Hurtmans, D., Garane, K., Goutail, F., Hadji-Lazaro, J., Koukouli, M., Wespes, C., Keppens, A., Pommereau, J. P., Pazmino, A., Balis, D., **Loyola, D.**, **Valks, P.**, Coheur, P.-F., Clerbaux, C.: *Validation of the IASI FORLI/Eumetsat ozone products using satellite (GOME-2), ground-based (Brewer-Dobson, SAOZ) and ozonesonde measurements*, Atmospheric Measurement Techniques, accepted, 2018.

[6] Coldewey-Egbers, M., **Slijkhuis, S.**, **Aberle, B.**, **Loyola, D.**, Dehn, A.: *The Global Ozone Monitoring Experiment: Review of in-flight performance and new reprocessed 1995-2011 level 1 product*, Atmospheric Measurement Techniques, under review, 2018.

[7] Fang, L., He, N., Li, S., **Ghamisi, P.**, Benediktsson, J. A.: *Extinction Profiles Fusion for Hyperspectral Images Classification*, IEEE Transactions on Geoscience and Remote Sensing, PP (99), in press, 2018.

[8] **Ge, N.**, **Rodriguez Gonzalez, F.**, ***Wang, Y.***, ***Shi, Y.***, **Zhu, X. X.**: *Spaceborne Staring Spotlight SAR Tomography-A First Demonstration with TerraSAR-X*, IEEE JSTARS, accepted, 2018.

[9] **Gemmrich, J.**, Rogers, W. E., Thomson, J., **Lehner, S.**: *Wave Evolution in Off-Ice Wind Conditions*, Journal of Geophysical Research - Oceans, accepted, 2018.

[10] **Ghamisi, P.**, **Yokoya, N.**: *IMG2DSM: Height Simulation from Single Imagery Using Conditional Generative Adversarial Nets*, IEEE Geoscience and Remote Sensing Letters, PP (99), in press, 2018.

[11] **Hong, D.**, **Yokoya, N.**, Chanussot, J., **Zhu, X. X.**: *An Extended Bilinear Mixing Model to Address Spectral Variability for Hyperspectral Unmixing*, IEEE Transactions on Image Processing, submitted, 2018.

[12] Howe, K., Dean, C., Kluge, J., Soloviev, A., Tartar, A., Shivji, M., **Lehner, S.**, Shen, H., Perrie, W.: *DNA analysis of surfactant-associated bacteria in a natural sea slick observed by TerraSAR-X and RADARSAT-2 over the Gulf of Mexico*, International Journal of Remote Sensing, accepted, 2018.

[13] ***Kang, J.***, ***Körner, M.***, ***Wang, Y.***, Taubenböck, H., **Zhu, X. X.**: *Building instance classification using street view images*, ISPRS Journal of Photogrammetry and Remote Sensing, in press, 2018.

[14] Kleinert, A., **Birk, M.**, Perron, G., **Wagner, G.**: *Level 1b error budget for MIPAS on ENVISAT*, Atmospheric Measurement Techniques, under review, 2018.

[15] Lin, Z., Chen, Y., **Ghamisi, P.**, Benediktsson, J. A.: *Generative Adversarial Networks for Hyperspectral Image Classification*, IEEE Transactions on Geoscience and Remote Sensing, PP (99), in press, 2018.

[16] Mayer, C., Schaffer, J., Hattermann, T., **Floricioiu, D.**, **Krieger, L.**, Dodd, P., Kanzow, T., Schannwell, C., Licciullo, C.: *Large ice loss variability at Nioghalvfjerdsfjorden Glacier, NE-Greenland*, Nature Communications, in press, 2018.

[17] Mostegel, C., **Fraundorfer, F.**, Bischof, H.: *Prioritized multi-view stereo depth map generation using confidence prediction*, ISPRS Journal of Photogrammetry and Remote Sensing, in press, 2018.

[18] ***Mou, L.***, Bruzzone, L., **Zhu, X. X.**: *Learning Spectral-Spatial-Temporal Features via a Recurrent Convolutional Neural Network for Change Detection in Multispectral Imagery*, IEEE Transactions on Geoscience and Remote Sensing, submitted, 2018.

[19] ***Mou, L.***, **Zhu, X. X.**: *Vehicle Instance Segmentation from Aerial Image and Video Using a Multi-Task Learning Residual Fully Convolutional Network*, IEEE Transactions on Geoscience and Remote Sensing, accepted, 2018.

[20] **Parizzi, A.**, **Abdel Jaber, W.**: *Estimating Strain and Rotation tensors of glacier flow from wrapped SAR interferograms*, IEEE Geoscience and Remote Sensing Letters, accepted, 2018.

[21] Prats-Iraola, P., Lopez-Dekker, P., De Zan, M., ***Yague-Martinez, N.***, Zonno, M., Rodriguez-Cassola, M.: *Performance of 3-D Surface Deformation Estimation for Simultaneous Squinted SAR Acquisitions*, IEEE Transactions on Geoscience and Remote Sensing, accepted, 2018.

[22] Scheucher, M., Grenfell, L., Wunderlich, F., Godolt, M., **Schreier, F.**, Rauer, H.: *New Insights into Cosmic Ray induced Biosignature Chemistry in Earth-like Atmospheres*, Astrophysical Journal, accepted, 2018.

[23] **Schreier, F.**: *The Voigt and complex error function: Humlicek's rational approximation generalized*, Monthly Notices of the Royal Astronomical Society, 213, in press, 2018.

[24] ***Shi, Y.***, **Zhu, X. X.**, Yin, W., **Bamler, R.**: *A fast and accurate basis pursuit denoising algorithm with application to super-resolving tomographic SAR*, IEEE Transactions on Geoscience and Remote Sensing, accepted, 2018.

[25] Thomson, J., Ackley, S., Girard-Ardhuin, F., Ardhuin, F., Babanin, A. V., Boutin, G., Brozena, J., Cheng, S., Collins, C., Doble, M., Fairall, C., Guest, P., **Gebhardt, C. P.**, **Gemmrich, J.**, Graber, H. C., Holt, B., **Lehner, S.**, Lund, B., Meylan, M. H., Maksym, T., Montiel, F., Perrie, W., Persson, O., Rainville, L., Rogers, W. E., Shen, H., Shen, H., Squire, V., Stammerjohn, S., Stopa, J., Smith, M. M., Sutherland, P., Wadhams, P.: *Overview of the Arctic Sea State and Boundary Layer Physics Program*, Journal of Geophysical Research - Oceans, in press, 2018.

[26] **Tings, B.**, **Velotto, D.**: *Comparison of ship wake detectability on C-band and X-band SAR*, International Journal of Remote Sensing, in press, 2018.

[27] **Traganos, D.**, **Reinartz, P.**: *Mapping Mediterranean seagrasses with Sentinel-2 imagery*, Marine Pollution Bulletin, in press, 2018.

2018

[28] Abdi, G., **Samadzadegan, F.**, **Reinartz, P.**: *Deep learning decision fusion for the classification of urban remote sensing data*, Journal of Applied Remote Sensing, 12 (1), pp. 1-19, 2018.

[29] **Bahmanyar, R.**, **Espinoza-Molina, D.**, **Datcu, M.**: *Multisensor Earth Observation Image Classification Based on a Multimodal Latent Dirichlet Allocation Model*, IEEE Geoscience and Remote Sensing Letters, 15 (3), pp. 459-463, 2018.

[30] **Balss, U.**, **Gisinger, C.**, **Eineder, M.**: *Measurements on the Absolute 2-D and 3-D Localization Accuracy of TerraSAR-X*, Remote Sensing, 10, pp. 1-21, 2018.

[31] Beirle, S., Lampel, J., Wang, Y., Mies, K., **Grossi, M.**, **Loyola, D.**, Dehn, A., Danielczok, A., Schroeder, M., Wagner, T.: *The ESA GOME-Evolution "Climate" water vapor product: a homogenized time-series of H2O columns from GOME, SCIAMACHY, and GOME-2*, Earth System Science Data, 10, pp. 449-468, 2018.

[32] Broccardo, S., **Heue, K.-P.**, Walter, D., Meyer, C., Kokhanovsky, A., van der A, R., Langermann, K., Piketh, S., Platt, U.: *Intra-pixel variability in satellite NO2 measurements*, Atmospheric Measurement Techniques (AMT), 11, pp. 2797-2819, 2018.

[33] Buckreuss, S., **Schättler, B.**, **Fritz, T.**, Mittermayer, J., Kahle, R., Maurer, E., Böer, J., Bachmann, M., Mrowka, F., Schwarz, E., **Breit, H.**, Steinbrecher, U.: *Ten Years of TerraSAR-X Operations*, Remote Sensing, 10 (6), pp. 1-28, 2018.

[34] **Cerra, D.**, Agapiou, A., Cavalli, R. M., **Sarris, A.**: *An Objective Assessment of Hyperspectral Indicators for the Detection of Buried Archaeological Relics*, Remote Sensing, 10 (4), pp. 1-25, 2018.

[35] Chipperfield, M. P., Dhomse, S., Hossaini, R., Feng, W., Santee, M., Weber, M., Burrows, J. P., Wild, J., **Loyola, D.**, Coldewey-Egbers, M.: *On the Cause of Recent Variations in Lower Stratospheric Ozone*, Geophysical Research Letters, 45, pp. 1-9, 2018.

[36] De Smedt, I., Theys, N., Yu, H., Danckaert, T., Lerot, C., Compernolle, S., Van Roozendael, M., Richter, A., Hilboll, A., Peters, E., ***Pedergnana, M.***, **Loyola, D.**, Beirle, S., Wagner, T., Eskes, H., van Geffen, J., Folkert Boersma, K., Veefkind, P.: *Algorithm theoretical baseline for formaldehyde retrievals from S5P TROPOMI and from the QA4ECV project*, Atmospheric Measurement Techniques, 11 (4), pp. 2395-2426, 2018.

[37] **Dirscherl, M. C.**, **Rossi, C.**: *Geomorphometric analysis of the 2014-2015 Bárðarbunga volcanic eruption, Iceland*, Remote Sensing of Environment, 204, pp. 244-259, 2018.

[38] Doxani, G., Vermote, E., Roger, J.-C., Gascon, F., Adriaensen, S., Frantz, D., Hagolle, O., Hollstein, A., Kirches, G., Li, F., Louis, J., Mangin, A., Pahlevan, N., **Pflug, B.**, Vanhellemont, Q.: *Atmospheric Correction Inter-Comparison Exercise*, Remote Sensing, 10 (352), pp. 1-18, 2018.

[39] **Dumitru, C. O.**, **Schwarz, G.**, **Datcu, M.**: *SAR Image Land Cover Datasets for Classification Benchmarking of Temporal Changes*, IEEE JSTARS, 11 (5), pp. 1571-1592, 2018.

[40] Garane, K., Lerot, C., Coldewey-Egbers, M., Verhoelst, T., Zyrichidou, I., Balis, D., Danckaert, T., Goutail, F., Granville, J., Hubert, D., Koukouli, M., Keppens, A., Lambert, J.-C., **Loyola, D.**, Pommereau, J. P., Van Roozendael, M., Zehner, C.: *Quality assessment of the Ozone_cci Climate Research Data Package (release 2017): 1. Ground-based validation of total ozone column data products*, Atmospheric Measurement Techniques (AMT), 11, pp. 1385-1402, 2018.

[41] Giardino, C., Brando, V., **Gege, P.**, Pinnel, N., Hochberg, E., Knaeps, E., Reusen, I., Doerffer, R., Bresciani, M., Braga, F., Foerster, S., Champollion, N., Dekker, A.: *Imaging Spectrometry of Inland and Coastal Waters: State of the Art, Achievements and Perspectives*, Surveys in Geophysics, pp. 1-29, 2018.

[42] Guan, B., Yu, Q., **Fraundorfer, F.**: *Minimal solutions for the rotational alignment of IMU-camera systems using homography constraints*, Computer Vision and Image Understanding, 170, pp. 79-91, 2018.

[43] **Hamidouche, M.**, **Lichtenberg, G.**: *In-flight Retrieval of SCIAMACHY Instrument Spectral Response Function*, Remote Sensing, 10 (3), pp. 1-18, 2018.

[44] Häne, C., Heng, L., Lee, G. H., **Fraundorfer, F.**, Furgale, P., Sattler, T., Pollefeys, M.: *3d visual perception for self-driving cars using a multi-camera system: Calibration, mapping, localization, and obstacle detection*, Image and Vision Computing, 68, pp. 14-27, 2018.

[45] ***Heublein, M.***, Alshawaf, F., Erdnüß, B., **Zhu, X. X.**, Hinz, S.: *Compressive sensing reconstruction of 3D wet refractivity based on GNSS and InSAR observations*, Journal of Geodesy, pp. 1-21, 2018.

[46] **Hochstaffl, P.**, **Schreier, F.**, **Lichtenberg, G.**, ***Gimeno Garcia, S.***: *Validation of Carbon Monoxide Total Column Retrievals from SCIAMACHY Observations with NDACC/TCCON Ground-Based Measurements*, Remote Sensing, 10 (2), pp. 223-252, 2018.

[47] Howe, K. L., Dean, C. W., Kluge, J., Soloviev, A., Tartar, A., Shivji, M., **Lehner, S.**, Perrie, W.: *Relative abundance of Bacillus spp., surfactant-associated bacterium present in a natural sea slick observed by satellite SAR imagery over the Gulf of Mexico*, Elementa : Science of the Anthropocene, 6, pp. 1-8, 2018.

[48] ***Hughes, L.***, ***Schmitt, M.***, ***Mou, L.***, ***Wang, Y.***, **Zhu, X.**: *Identifying Corresponding Patches in SAR and Optical Images with a Pseudo-Siamese CNN*, IEEE Geoscience and Remote Sensing Letters, 15 (5), pp. 784-788, 2018.

[49] Ji, T.-y., **Yokoya, N.**, **Zhu, X. X.**, Huang, T.-z.: *Non-local tensor completion for multitemporal remotely sensed images inpainting*, IEEE Transactions on Geoscience and Remote Sensing, 56 (6), pp. 3047-3061, 2018.

[50] ***Kang, J.***, ***Wang, Y.***, ***Schmitt, M.***, **Zhu, X. X.**: *Object-based multipass InSAR via robust low-rank tensor decomposition*, IEEE Transactions on Geoscience and Remote Sensing, 56 (6), pp. 3062-3077, 2018.

[51] **Lachaise, M.**, **Fritz, T.**, **Bamler, R.**: *The Dual-Baseline Phase Unwrapping Correction framework for the TanDEM-X Mission Part 1: Theoretical description and algorithms*, IEEE Transactions on Geoscience and Remote Sensing, 56 (2), pp. 780-798, 2018.

[52] Lambrecht, A., Mayer, C., **Wendt, A.**, **Floricioiu, D.**, Völksen, C.: *Elevation change of Fedchenko Glacier, Pamir Mountains, from GNSS field measurements and TanDEM-X elevation models, with a focus on the upper glacier*, Journal of Glaciology, pp. 1-12, 2018.

[53] Levetiduo, E., Weber, M., Eichmann, K.-U., Burrows, J. P., **Heue, K.-P.**, Thompson, A. M., Johnson, B.: *Harmonisation and trends of 20-years tropical tropospheric ozone data*, Atmospheric Chemistry and Physics (ACP), 18, pp. 9189-9205, 2018.

[54] **Loyola, D.**, ***Gimeno-Garcia, S.***, **Lutz, R.**, **Argyrouli, A.**, **Romahn, F.**, Spurr, R., ***Pedergnana, M.***, **Doicu, A.**, Molina García, V., ***Schüssler, O.***: *The operational cloud retrieval algorithms from TROPOMI on board Sentinel-5 Precursor*, Atmospheric Measurement Techniques (AMT), 11 (1), pp. 409-427, 2018.

[55] Lyu, H., Lu, H., ***Mou, L.***, Li, W., Wright, J., Li, X., Li, X., **Zhu, X.**, Wang, J., Yu, L., Gong, P.: *Long-Term Annual Mapping of Four Cities on Different Continents by Applying a Deep Information Learning Method to Landsat Data*, Remote Sensing, 10 (3), pp. 471-493, 2018.

[56] **Marmanis, D.**, Schindler, K., Wegner, J. D., Galliani, S., **Datcu, M.**, Stilla, U.: *Classification with an edge: Improving semantic image segmentation with boundary detection*, ISPRS Journal of Photogrammetry and Remote Sensing, 135, pp. 158-172, 2018.

[57] **Merkle, N. M.**, **Auer, S.**, **Müller, R.**, **Reinartz, P.**: *Exploring the Potential of Conditional Adversarial Networks for Optical and SAR Image Matching*, IEEE JSTARS, 11 (6), pp. 1811-1820, 2018.

[58] Molina García, V., **Sasi, S.**, **Efremenko, D.**, **Doicu, A.**, **Loyola, D.**: *Linearized radiative transfer models for retrieval of cloud parameters from EPIC/DSCOVR measurements*, Journal of Quantitative Spectroscopy & Radiative Transfer, 213, pp. 241-251, 2018.

[59] Molina García, V., **Sasi, S.**, **Efremenko, D.**, **Doicu, A.**, **Loyola, D.**: *Radiative transfer models for retrieval of cloud parameters from EPIC/DSCOVR measurements*, Journal of Quantitative Spectroscopy & Radiative Transfer, 213, pp. 228-240, 2018.

[60] **Montazeri, S.**, **Gisinger, C.**, **Eineder, M.**, **Zhu, X. X.**: *Automatic Detection and Positioning of Ground Control Points Using TerraSAR-X Multi-Aspect Acquisitions*, IEEE Transactions on Geoscience and Remote Sensing, 56 (5), pp. 2613-2632, 2018.

[61] ***Mou, L.***, **Ghamisi, P.**, **Zhu, X.**: *Unsupervised Spectral-Spatial Feature Learning via Deep Residual Conv-Deconv Network for Hyperspectral Image Classification*, IEEE Transactions on Geoscience and Remote Sensing, 56 (1), pp. 391-406, 2018.

[62] Özcan, A. H., Unsalan, C., **Reinartz, P.**: *Ground filtering and DTM generation from DSM data using probabilistic voting and segmentation*, International Journal of Remote Sensing, 39 (9), pp. 2860-2883, 2018.

[63] **Qin, K.**, Wang, L., **Xu, J.**, Letu, H., Zhang, K., Li, D., Zou, J., Fan, W.: *Haze optical properties from long-term ground-based remote sensing over Beijing and Xuzhou, China*, Remote Sensing, 10 (4), pp. 1-17, 2018.

[64] ***Qiu, C.***, ***Schmitt, M.***, **Zhu, X. X.**: *Towards automatic SAR-optical stereogrammetry over urban areas using very high resolution imagery*, ISPRS Journal of Photogrammetry and Remote Sensing, 138, pp. 218-231, 2018.

[65] Rasti, B., Scheunders, P., **Ghamisi, P.**, Licciardi, G., Chanussot, J.: *Noise Reduction in Hyperspectral Imagery: Overview and Application*, Remote Sensing, 3 (482), pp. 1-28, 2018.

[66] **Rikka, S.**, **Pleskachevsky, A.**, **Jacobsen, S.**, Alari, V., Uiboupin, R.: *Meteo-Marine Parameters from Sentinel-1 SAR Imagery: Towards Near Real-Time Services for the Baltic Sea*, Remote Sensing, 10 (5), pp. 1-17, 2018.

[67] Rott, H., **Abdel Jaber, W.**, Wuite, J., Scheiblauer, S., **Floricioiu, D.**, van Wessem, J. M., Nagler, T., Miranda, N., van den Broeke, M. R.: *Changing pattern of ice flow and mass balance for glaciers discharging into the Larsen A and B embayments, Antarctic Peninsula, 2011 to 2016*, The Cryosphere, 12, pp. 1273-1291, 2018.

[68] ***Rußwurm, M.***, ***Körner, M.***: *Multi-Temporal Land Cover Classification with Sequential Recurrent Encoders*. ISPRS International Journal of Geo-Information, 7 (4), 129-146, 2018.

[69] Schläpfer, D., Hueni, A., **Richter, R.**: *Cast Shadow Detection to Quantify the Aerosol Optical Thickness for Atmospheric Correction of High Spatial Resolution Optical Imagery*, Remote Sensing, 10 (2), pp. 1-25, 2018.

[70] **Schreier, F.**, Milz, M., Buehler, S. A., Clarmann von, T.: *Intercomparison of Three Microwave/Infrared High Resolution Line-by-Line Radiative Transfer Codes*, Journal of Quantitative Spectroscopy and Radiative Transfer, 211, pp. 64-77, 2018.

[71] **Schreier, F.**, **Städt, S.**, **Hedelt, P.**, Godolt, M.: *Transmission Spectroscopy with the ACE-FTS Infrared Spectral Atlas of Earth: A Model Validation and Feasibility Study*, Molecular Astrophysics, 11, pp. 1-22, 2018.

[72] **Schreier, F.**: *Comments on the Voigt function implementation in the Astropy and SpectraPlot.com packages*, Journal of Quantitative Spectroscopy and Radiative Transfer, 213, pp. 13-16, 2018.

[73] Schröder, M., Lockhoff, M., Fellmoser, F., Forsythe, J., Trent, T., Bennartz, T.-., Borbas, E., Bosilovich, M., Castelli, E., Hersbach, H., Kachi, M., Kobayashi, H., Kursinski, R., **Loyola, D.**, Mears, C., Preusker, R., Rossow, W., Saha, S.: *The GEWEX Water Vapor Assessment archive of water vapour products from satellite observations and reanalyses*, Earth System Science Data, 10, pp. 1093-1117, 2018.

[74] **Singha, S.**, Johansson, A. M., Hughes, N., Hvidegaard, S. M., Skourup, H.: *Arctic Sea Ice Characterization using Spaceborne Fully Polarimetric L-, C- and X-Band SAR with Validation by Airborne Measurements*, IEEE Transactions on Geoscience and Remote Sensing, 56 (7), pp. 3715-3734, 2018.

[75] **Traganos, D.**, Dimitris, P., **Aggarwal, B.**, Chrysoulakis, N., **Reinartz, P.**: *Estimating Satellite-Derived Bathymetry (SDB) with the Google Earth Engine and Sentinel-2*, Remote Sensing, 10 (859), pp. 1-18, 2018.

[76] **Traganos, D.**, **Reinartz, P.**: *Interannual change detection of Mediterranean seagrasses using RapidEye image time series*, Frontiers in Plant Science (FPLS), pp. 1-15, 2018.

[77] **Vaduva, C.**, Georgescu, F. A., **Datcu, M.**: *Understanding Heterogeneous EO Datasets: A Framework for Semantic Representations*, IEEE Access, 6, pp. 11184-11202, 2018.

[78] Vaquero-Martinez, J., Anton, M., de Galisteo, J. P., Cachorro, V. E., Roman, R., **Loyola, D.**, Costa, M. J., Wang, H., Abad, G. G.: *Inter-comparison of integrated water vapor from satellite instruments using reference GPS data at the Iberian Peninsula*, Remote Sensing of Environment, 204, pp. 729-740, 2018.

[79] Weber, M., Coldewey-Egbers, M., Fioletov, V. E., Frith, S., Wild, J., Burrows, J. P., Long, C., **Loyola, D.**: *Total ozone trends from 1979 to 2016 derived from five merged observational datasets - the emergence into ozone recovery*, Atmospheric Chemistry and Physics, 18, pp. 2097-2117, 2018.

[80] **Wilzewski, J.**, **Birk, M.**, **Loos, J.**, **Wagner, G.**: *Temperature-Dependence Laws of Absorption Line Shape Parameters of the CO2 v3 Band*, Journal of Quantitative Spectroscopy and Radiative Transfer, 206, pp. 296-305, 2018.

[81] Xia, J., **Ghamisi, P.**, **Yokoya, N.**, Iwasaki, A.: *Random Forest Ensembles and Extended Multi-Extinction Profiles for Hyperspectral Image Classification*, IEEE Transactions on Geoscience and Remote Sensing, 56 (1), pp. 202-216, 2018.

[82] **Xu, J.**, **Schreier, F.**, Wetzel, G., de Lange, A., **Birk, M.**, **Trautmann, T.**, **Doicu, A.**, **Wagner, G.**: *Performance assessment of balloon-borne trace gas sounding with the terahertz channel of TELIS*, Remote Sensing, 10 (2), pp. 1-31, 2018.

[83] **Zhuo, X.**, **Fraundorfer, F.**, **Kurz, F.**, **Reinartz, P.**: *Optimization of OpenStreetMap Building Footprints Based on Semantic Information of Oblique UAV Images*, Remote Sensing, 10 (624), pp. 1-18, 2018.

2017

[84] Abdi, G., Farhad, S., **Reinartz, P.**: *Spectral-spatial feature learning for hyperspectral imagery classification using deep stacked sparse autoencoder*, Journal of Applied Remote Sensing, 11 (4), pp. 042604-1-042604-15, 2017.

[85] Abdi, G., **Samadzadegan, F.**, **Reinartz, P.**: *A decision-based multi-sensor classification system using thermal hyperspectral and visible data in urban area*, European Journal of Remote Sensing, 50 (1), pp. 414-427, 2017.

[86] **Adolph, W.**, Jung, R., Schmidt, A., Ehlers, M., Heipke, C., Bartholomä, A., Farke, H.: *Integration of TerraSAR-X, RapidEye and airborne lidar for remote sensing of intertidal bedforms on the upper flats of Norderney (German Wadden Sea)*, Geo-Marine Letters, 37 (2), pp. 193-205, 2017.

[87] **Adolph, W.**, Schückel, U., Son, C. S., Jung, R., Bartholomä, A., Ehlers, M., Kröncke, I., **Lehner, S.**, Farke, H.: *Monitoring spatiotemporal trends in intertidal bedforms of the German Wadden Sea in 2009–2015 with TerraSAR-X, including links with sediments and benthic macrofauna*, Geo-Marine Letters, 37 (2), pp. 79-91, 2017.

[88] Afanas'ev, V. P., Gryazev, A. S., **Efremenko, D.**, Kaplya, P. S., Kuznetcova, A. V.: *Extracting the differential inverse inelastic mean free path and differential surface excitation probability of Tungsten from X-ray photoelectron spectra and electron energy loss spectra*, Journal of Physics: Conference Series, 941 (1), pp. 1-6, 2017.

[89] Afanas'ev, V. P., Gryazev, A. S., **Efremenko, D.**, Kaplya, P. S.: *Differential inverse inelastic mean free path and differential surface excitation probability retrieval from electron energy loss spectra*, Vacuum, 136, pp. 146-155, 2017.

[90] **Alonso, K.**, **Espinoza Molina, D.**, **Datcu, M.**: *Mining Multitemporal In Situ Heterogeneous Monitoring Information for the Assurance of Recorded Land Cover Changes*, IEEE JSTARS, 10 (3), pp. 877-887, 2017.

[91] **Alonso, K.**, **Espinoza-Molina, D.**, **Datcu, M.**: *Multilayer Architecture for Heterogeneous Geospatial Data Analytics: Querying and Understanding EO Archives*, IEEE JSTARS, 10 (3), pp. 791-801, 2017.

[92] **Ansari, H.**, **De Zan, F.**, **Bamler, R.**: *Sequential Estimator: Toward Efficient InSAR Time Series Analysis*, IEEE Transactions on Geoscience and Remote Sensing, 55 (10), pp. 5637-5652, 2017.

[93] **Auer, S.**, **Hornig, I.**, ***Schmitt, M.***, **Reinartz, P.**: *Simulation-based Interpretation and Alignment of High-Resolution Optical and SAR Images*, IEEE JSTARS, 10 (11), pp. 4779-4793, 2017.

[94] **Bentes da Silva, C. A.**, **Velotto, D.**, **Tings, B.**: *Ship Classification in TerraSAR-X Images with Convolutional Neural Networks*, IEEE Journal of Oceanic Engineering, 43 (1), pp. 258-266, 2017.

[95] Bi, H., Zhang, B. C., **Zhu, X. X.**, Hong, W.: *Azimuth-range decouple-based L1 regularization method for wide ScanSAR imaging via extended chirp scaling*, Journal of Applied Remote Sensing, 11 (1), pp. 1-13, 2017.

[96] Bi, H., Zhang, B. C., **Zhu, X. X.**, Hong, W., Wu, Y.: *L1 Regularization Based SAR Imaging and CFAR Detection via Complex Approximated Message Passing*, IEEE Transactions on Geoscience and Remote Sensing, 55 (6), pp. 3426-3440, 2017.

[97] Bi, H., Zhang, B. C., **Zhu, X. X.**, Jiang, C., Hong, W.: *Extended Chirp Scaling-Baseband Azimuth Scaling-Based Azimuth-Range Decouple L1 Regularization for TOPS SAR Imaging via CAMP*, IEEE Transactions on Geoscience and Remote Sensing, 55 (7), pp. 3748-3763, 2017.

[98] **Birk, M.**, **Wagner, G.**, **Loos, J.**, Lodi, L., Polyanski, O., Kyuberis, A., Zobov, N., Tennyson, J.: *Accurate line intensities for water transitions in the infrared: comparison of theory and experiment*, Journal of Quantitative Spectroscopy & Radiative Transfer, 203, pp. 88-102, 2017.

[99] Bramstedt, K., Stone, T. C., **Gottwald, M.**, Noel, S., Bovensmann, H., Burrows, J. P.: *Improved pointing information for SCIAMACHY from in-flight measurements of the viewing directions towards sun and moon*, Atmospheric Measurement Techniques (AMT), 10, pp. 2413-2423, 2017.

[100] Buchwitz, M., Reuter, M., Schneising, O., Hewson, W., Detmers, R. G., Boesch, H., Hasekamp, O., Aben, I., Bovensmann, H., Burrows, J. P., Butz, A., Chevallier, F., Dils, B., Frankenberg, C., Heymann, J., **Lichtenberg, G.**, De Maiziere, M., Notholt, J., Parker, R., Warneke, T., Zehner, C., Griffith, D. W., Deutscher, N. M., Kuze, A., Suto, H., Wunch, D.: *Global satellite observations of column-averaged carbon dioxide and methane: The GHG-CCI XCO2 and XCH4 CRDP3 data set*, Remote Sensing of Environment, 203, pp. 276-295, 2017.

[101] Chen, Y., Li, C., **Ghamisi, P.**, Jia, X., Gu, Y.: *Deep Fusion of Remote Sensing Data for Accurate Classification*, IEEE Geoscience and Remote Sensing Letters, 14 (8), pp. 1253-1257, 2017.

[102] Chen, Y., Zhu, L., **Ghamisi, P.**, Jia, X., Li, G., Tang, L.: *Hyperspectral Images Classification With Gabor Filtering and Convolutional Neural Network*, IEEE Geoscience and Remote Sensing Letters, 14 (12), pp. 2355-2359, 2017.

[103] **Efremenko, D.**, **Loyola, D.**, **Hedelt, P.**, Spurr, R.: *Volcanic SO2 plume height retrieval from UV sensors using a full-physics inverse learning machine algorithm*, International Journal of Remote Sensing, 38 (50), pp. 1-27, 2017.

[104] **Efremenko, D.**, Molina García, V., ***Gimeno García, S.***, **Doicu, A.**: *A review of the matrix-exponential formalism in radiative transfer*, Journal of Quantitative Spectroscopy and Radiative Transfer, 196, pp. 17-45, 2017.

[105] Florea, B.-F., Grigore, O., **Datcu, M.**: *Multi-Agent Exploration Based on Constraints Imposed with Graph Search Algorithms*, Revue roumaine des sciences techniques. Série Électrotechnique et Énergétique, 62 (1), pp. 87-92, 2017.

[106] Florea, B.-F., Grigore, O., **Datcu, M.**: *Compact Node Counting Exploration Algorithm*, UPB Scientific Bulletin, Series C: Electrical Engineering and Computer Science, 79 (1), pp. 113-124, 2017.

[107] Gascon, F., Thépaut, O., Jung, M., Francesconi, B., Louis, J., Lonjou, V., Lafrance, B., Massera, S., Gaudel-Vacaresse, A., Languille, F., Alhammoud, B., Viallefont, F., **Pflug, B.**, Clerc, S., Pessiot, L., Trémas, T., Cadau, E., De Bonis, R., **Bieniarz, J.**: *Copernicus Sentinel-2 Calibration and Products Validation Status*, Remote Sensing, 9 (6), pp. 1-81, 2017.

[108] **Gebhardt, C.**, Bidlot, J.-R., **Jacobsen, S.**, **Lehner, S.**, Persson, P. O., **Pleskachevsky, A.**: *The potential of TerraSAR-X to observe wind wave interaction at the ice edge*, IEEE JSTARS, 10 (3), pp. 2799-2809, 2017.

[109] Georgescu, F.-A., Raducanu, D., **Datcu, M.**: *New MPEG-7 Scalable Color Descriptor Based on Polar Coordinates for Multispectral Earth Observation Image Analysis*, IEEE Geoscience and Remote Sensing Letters, 14 (7), pp. 987-991, 2017.

[110] **Ghamisi, P.**, Höfle, B., **Zhu, X. X.**: *Hyperspectral and LiDAR Data Fusion Using Extinction Profiles and Deep Convolutional Neural Network*, IEEE JSTARS, 10 (6), pp. 3011-3024, 2017.

[111] **Ghamisi, P.**, Höfle, B.: *LiDAR Data Classification Using Extinction Profiles and a Composite Kernel Support Vector Machine*, IEEE Geoscience and Remote Sensing Letters, 14 (5), pp. 659-663, 2017.

[112] **Ghamisi, P.**, Plaza, J., Chen, Y., Li, J., Plaza, A.: *Advanced Spectral Classifiers for Hyperspectral Images: A Review*, IEEE Geoscience and Remote Sensing Magazine (GRSM), 5 (1), pp. 8-32, 2017.

[113] **Ghamisi, P.**, **Yokoya, N.**, Li, J., Liao, W., Liu, S., Plaza, J., Rasti, B., Plaza, A.: *Advances in Hyperspectral Image and Signal Processing: A Comprehensive Overview of the State of the Art*, IEEE Geoscience and Remote Sensing Magazine (GRSM), 5 (4), pp. 37-78, 2017.

[114] **Gisinger, C.**, **Willberg, M.**, **Balss, U.**, Klügel, T., Mähler, S., Pail, R., **Eineder, M.**: *Differential Geodetic Stereo SAR with TerraSAR-X by Exploiting Small Multi-Directional Radar Reflectors*, Journal of Geodesy, 91 (1), pp. 53-67, 2017.

[115] **Gomba, G.**, **De Zan, F.**: *Bayesian Data Combination for the Estimation of Ionospheric Effects in SAR Interferograms*, IEEE Transactions on Geoscience and Remote Sensing, 55 (11), pp. 6582-6593, 2017.

[116] **Gomba, G.**, **Rodriguez Gonzalez, F.**, **De Zan, F.**: *Ionospheric Phase Screen Compensation for the Sentinel-1 TOPS and ALOS-2 ScanSAR Modes*, IEEE Transactions on Geoscience and Remote Sensing, 55 (1), pp. 223-235, 2017.

[117] Gordon, I. E., Rothman, L. S., Hill, C., Kochanov, R., Yan, T., Bernath, P. F., **Birk, M.**, Boudon, V., Campargue, A., Chance, K., Drouin, B. J., Flaud, J.-M., Gamache, R. R., Hodges, J. T., Jacquemart, D., Perevalov, V. I., Perrin, A., Shine, K. P., Smith, M. A.H., Tennyson, J., Toon, G. C., Tran, H., Tyuterev, V., Barbe, A., Csaszar, A., Devi, V. M., Furtenbacher, T., Harrison, J., Jolly, A., Johnson, T., Karman, T., Kleiner, I., Kyuberis, A., **Loos, J.**, Lyulin, O., Massie, S. T., Mikhailenko, S., Moazzen-Ahmadi, N., Müller, H., Naumenko, O. V., Nikitin, A., Polyansky, O., Rey, M., Rotger, M., Sharpe, S., Sung, K., Starikova, E., Tashkun, S. A., Vander Auwera, J., **Wagner, G.**, **Wilzewski, J.**, Wcislo, P., Yu, S., Zak, E.: *The HITRAN2016 Molecular Spectroscopic Database*, Journal of Quantitative Spectroscopy & Radiative Transfer, 203, pp. 3-69, 2017.

[118] ***Göritz, A.***, **von Hoesslin, S.**, **Hundhausen, F.**, **Gege, P.**: *ENVILAB: Measuring phytoplankton in-vivo absorption and scattering properties under tunable environmental conditions*, Optics Express, 25 (21), pp. 25267-25277, 2017.

[119] **Gottwald, M.**, **Fritz, T.**, **Breit, H.**, **Schättler, B.**, Harris, A. W.: *Remote sensing of terrestrial impact craters: The TanDEM-X digital elevation model*, Meteoritics & Planetary Science, 52 (7), pp. 1412-1427, 2017.

[120] Griparis, A., Faur, D., **Datcu, M.**: *Quantitative Evaluation of the Feature Space Transformation Methods Used for Applications of Visual Semantic Clustering of EO Images*, IEEE JSTARS, 10 (6), pp. 2902-2909, 2017.

[121] Groetsch, P. M., **Gege, P.**, Simis, S. G., Eleveld, M. A., Peters, S. W.: *Variability of adjacency effects in sky reflectance measurements*, Optics Letters, 42 (17), pp. 3359-3362, 2017.

[122] Groetsch, P. M., **Gege, P.**, Simis, S. G., Eleveld, M. A., Peters, S.: *Validation of a spectral correction procedure for sun and sky reflections in above-water reflectance measurements*, Optics Express, 25 (16), pp. A742-A761, 2017.

[123] Hasani, H., **Samadzadegan, F.**, **Reinartz, P.**: *A metaheuristic feature-level fusion strategy in classification of urban area using hyperspectral imagery and LiDAR data*, European Journal of Remote Sensing, 50 (1), pp. 222-236, 2017.

[124] ***Hong, D.***, **Yokoya, N.**, **Zhu, X. X.**: *Learning a Robust Local Manifold Representation for Hyperspectral Dimensionality Reduction*, IEEE JSTARS, 10 (6), pp. 2960-2975, 2017.

[125] Johansson, M., King, J., Doulgeris, A. P., Gerland, S., **Singha, S.**, Spreen, G., Busche, T. E.: *Combined observations of Arctic sea ice with near-coincident co-located X, C and L-band SAR satellite remote sensing and helicopter-borne measurements*, Journal of Geophysical Research - Oceans, 122 (1), pp. 669-691, 2017.

[126] ***Kang, J.***, **Wang, Y.**, ***Körner, M.***, **Zhu, X. X.**: *Robust object-based multipass InSAR deformation reconstruction*, IEEE Transactions on Geoscience and Remote Sensing, 55 (8), pp. 4239-4251, 2017.

[127] Kehrl, L., Joughin, I., Shean, D., **Floricioiu, D.**, **Krieger, L.**: *Seasonal and interannual variabilities in terminus position, glacier velocity, and surface elevation at Helheim and Kangerlussuaq Glaciers from 2008 to 2016*, Journal of Geophysical Research – Earth Surface, 122 (9), pp. 1635-1652, 2017.

[128] **Kiemer, M.**, **Breit, H.**: *Efficient Evaluation of Multichannel SAR Data Recombination Filters*, IEEE Transactions on Geoscience and Remote Sensing, 55 (11), pp. 6277-6286, 2017.

[129] **Kuschk, G.**, **d'Angelo, P.**, Gaudrie, D., **Reinartz, P.**, Cremers, D.: *Spatially Regularized Fusion of Multiresolution Digital Surface Models*, IEEE Transactions on Geoscience and Remote Sensing, 55 (3), pp. 1477-1488, 2017.

[130] **Loos, J.**, **Birk, M.**, **Wagner, G.**: *Measurement of air-broadening line shape parameters and temperature dependence parameters of H2O lines in the spectral ranges 1850-2280 cm-1 and 2390-4000 cm-1*, Journal of Quantitative Spectroscopy & Radiative Transfer, 203, pp. 103-118, 2017.

[131] **Loos, J.**, **Birk, M.**, **Wagner, G.**: *Measurement of positions, intensities and self-broadening line shape parameters of H2O lines in the spectral ranges 1850-2280 cm-1 and 2390-4000 cm-1*, Journal of Quantitative Spectroscopy & Radiative Transfer, 203, pp. 119-132, 2017.

[132] Lysandrou, V., **Cerra, D.**, Agapiou, A., Charalambous, E., Hadjimitsis, D. G.: *Towards a spectral library of Roman to Early Christian Cypriot floor mosaics*, Journal of Archaeological Science: Reports, 14, pp. 782-791, 2017.

[133] **Makarau, A.**, **Richter, R.**, Schläpfer, D., **Reinartz, P.**: *APDA Water Vapor Retrieval Validation for Sentinel-2 Imagery*, IEEE Geoscience and Remote Sensing Letters, 14 (2), pp. 227-231, 2017.

[134] Marino, A., **Velotto, D.**, Nunziata, F.: *Offshore metallic platforms observation using dual-polarimetric TS-X/TD-X satellite imagery: a case study in the Gulf of Mexico*, IEEE JSTARS, 10 (10), pp. 4376-4386, 2017.

[135] **Meringer, M.**, Cleaves, H. J.: *Computational exploration of the chemical structure space of possible reverse tricarboxylic acid cycle constituents*, Scientific Reports, 7, pp. 1-11, 2017.

[136] **Meringer, M.**, Cleaves, H. J.: *Exploring astrobiology using in silico molecular structure generation*, Philosophical Transactions of the Royal Society A, 375 (2109), pp. 1-12, 2017.

[137] **Merkle, N.**, Wenjie, L., **Auer, S.**, **Müller, R.**, Urtasun, R.: *Exploiting Deep Matching and SAR Data for the Geo-Localization Accuracy Improvement of Optical Satellite Images*, Remote Sensing, 9 (9), pp. 586-603, 2017.

[138] **Mou, L.**, **Ghamisi, P.**, **Zhu, X.**: *Deep Recurrent Neural Networks for Hyperspectral Image Classification*, IEEE Transactions on Geoscience and Remote Sensing, 55 (7), pp. 3639-3655, 2017.

[139] **Mou, L.**, **Zhu, X.**, Vakalopoulou, M., Karantzalos, K., Paragios, N., Le Saux, B., Moser, G., Tuia, D.: *Multitemporal Very High Resolution From Space: Outcome of the 2016 IEEE GRSS Data Fusion Contest*, IEEE JSTARS, 10 (8), pp. 3435-3447, 2017.

[140] **Murillo Montes de Oca, A.**, **Bahmanyar, R.**, Nistor, N., **Datcu, M.**: *Earth Observation Image Semantic Bias: A Collaborative User Annotation Approach*, IEEE JSTARS, 10 (6), pp. 2462-2477, 2017.

[141] Orphal, J., **Birk, M.**, **Wagner, G.**, Flaud, J.-M.: *Analysis of the nu8 and nu8 + nu9 band spectral regions of BrONO2 and first determination of the nu9 band center at 111.9(7) cm-1*, Chemical Physics Letters, 690, pp. 82-85, 2017.

[142] Oumer, N. W., Kriegel, S., Ali, H., **Reinartz, P.**: *Appearance learning for 3D pose detection of a satellite at close-range*, ISPRS Journal of Photogrammetry and Remote Sensing, 125, pp. 1-15, 2017.

[143] **Palubinskas, G.**: *Image similarity/distance measures: what is really behind MSE and SSIM?*, International Journal of Image and Data Fusion, 8 (1), pp. 32-53, 2017.

[144] **Partovi, T.**, **Bahmanyar, R.**, **Krauß, T.**, **Reinartz, P.**: *Building Outline Extraction Using a Heuristic Approach Based on Generalization of Line Segments*, IEEE JSTARS, 10 (3), pp. 933-947, 2017.

[145] Pullanagari, R., Kereszturi, G., Yule, I., **Ghamisi, P.**: *Assessing the performance of multiple spectral–spatial features of a hyperspectral image for classification of urban land cover classes using support vector machines and artificial neural network*, Journal of Applied Remote Sensing, 11 (2), pp. 1-22, 2017.

[146] **Qin, K.**, **Rao, L.**, **Xu, J.**, Bai, Y., Zou, J., Hao, N., Li, S., Yu, C.: *Estimating ground level NO2 concentrations over central-eastern China using a satellite-based geographically and temporally weighted regression model*, Remote Sensing, 9 (9), pp. 1-20, 2017.

[147] **Qin, K.**, Wang, L., Wu, L., **Xu, J.**, **Rao, L.**, Letu, H., Shi, T., Wang, R.: *A campaign for investigating aerosol optical properties during winter hazes over Shijiazhuang, China*, Atmospheric Research, 198, pp. 113-122, 2017.

[148] Rack, W., King, M., Marsh, O. J., Wild, C. T., **Floricioiu, D.**: *Analysis of ice shelf flexure and its InSAR representation in the grounding zone of the southern McMurdo Ice Shelf*, The Cryosphere, 11 (6), pp. 2481-2490, 2017.

[149] Rasti, B., **Ghamisi, P.**, Gloaguen, R.: *Hyperspectral and LiDAR Fusion Using Extinction Profiles and Total Variation Component Analysis*, IEEE Transactions on Geoscience and Remote Sensing, 55 (7), pp. 3997-4007, 2017.

[150] Rasti, B., **Ghamisi, P.**, Plaza, J., Plaza, A.: *Fusion of Hyperspectral and LiDAR Data Using Sparse and Low-Rank Component Analysis*, IEEE Transactions on Geoscience and Remote Sensing, 55 (11), pp. 6354-6365, 2017.

[151] Rasti, B., Ulfarsson, M. O., **Ghamisi, P.**: *Automatic Hyperspectral Image Restoration Using Sparse and Low-Rank Modeling*, IEEE Geoscience and Remote Sensing Letters, 14 (12), pp. 2335-2339, 2017.

[152] Rikka, S., **Pleskachevsky, A.**, Uiboupin, R., **Jacobsen, S.**: *Sea State in the Baltic Sea from Space-borne High Resolution Synthetic Aperture Radar Imagery*, International Journal of Remote Sensing, 39 (4), pp. 1256-1284, 2017.

[153] Rizzoli, P., Martone, M., Gonzalez, C., Wecklich, C., Borla Tridon, D., Bräutigam, B., Bachmann, M., Schulze, D., **Fritz, T.**, Huber, M., Wessel, B., Krieger, G., Zink, M., Moreira, A.: *Generation and performance assessment of the global TanDEM-X digital elevation model*, ISPRS Journal of Photogrammetry and Remote Sensing, pp. 119-139, 2017.

[154] Rumpler, M., Tscharf, A., Mostegel, C., Daftry, S., Hoppe, C., Prettenthaler, R., **Fraundorfer, F.**, Mayer, G., Bischof, H.: *Evaluations on multi-scale camera networks for precise and geo-accurate reconstructions from aerial and terrestrial images with user guidance*, Computer Vision and Image Understanding, 157 (4), pp. 255-273, 2017.

[155] **Samadzadegan, F.**, Hasani, H., **Reinartz, P.**: *Toward Optimum Fusion of Thermal Hyperspectral and Visible Images in Classification of Urban Area*, Photogrammetric Engineering and Remote Sensing, 83 (4), pp. 269-280, 2017.

[156] Saurer, O., Vasseur, P., Boutteau, R., Demonceaux, C., Pollefeys, M., **Fraundorfer, F.**: *Homography based egomotion estimation with a common direction*, IEEE Transactions on Pattern Analysis and Machine Intelligence, 39 (2), pp. 327-341, 2017.

[157] **Schreier, F.**: *An assessment of some closed-form expressions for the Voigt function: II. Utilizing rational approximations for the Gauss function*, Journal of Quantitative Spectroscopy and Radiative Transfer, 202, pp. 81-89, 2017.

[158] **Schreier, F.**: *Computational Aspects of Speed-Dependent Voigt Profiles*, Journal of Quantitative Spectroscopy and Radiative Transfer, 187, pp. 44-53, 2017.

[159] **Singha, S.**, **Ressel, R.**: *Arctic Sea Ice Characterization using RISAT-1 Compact-Pol SAR Imagery and Feature Evaluation: A Case Study Over North-East Greenland*, IEEE JSTARS, 10 (8), pp. 3504-3514, 2017.

[160] **Suchandt, S.**, Romeiser, R.: *X-Band Sea Surface Coherence Time Inferred from Bi-static SAR Interferometry*, IEEE Transactions on Geoscience and Remote Sensing, 55 (7), pp. 3941-3948, 2017.

[161] Tănase, R., **Bahmanyar, R.**, **Schwarz, G.**, **Datcu, M.**: *Discovery of Semantic Relationships in PolSAR Images Using Latent Dirichlet Allocation*, IEEE Geoscience and Remote Sensing Letters, 14 (2), pp. 237-241, 2017.

[162] Theys, N., De Smedt, I., Yu, H., Danckaert, T., van Gent, J., Hörmann, C., Wagner, T., **Hedelt, P.**, **Bauer, H.**, **Romahn, F.**, ***Pedergnana, M.***, **Loyola, D.**, Van Roozendael, M.: *Sulfur dioxide retrievals from TROPOMI onboard Sentinel-5 Precursor: algorithm theoretical basis*, Atmospheric Measurement Techniques (AMT), pp. 119-153, 2017.

[163] **Tian, J.**, Schneider, T., Straub, C., Kugler, F., **Reinartz, P.**: *Exploring Digital Surface Models from Nine Different Sensors for Forest Monitoring and Change Detection*, Remote Sensing, 9 (3), pp. 1-26, 2017.

[164] Tudose, M., Anghel, A., Cacoveanu, R., **Datcu, M.**: *On the beat signal synchronisation of interferometric FMCW radars*, IET Radar Sonar & Navigation, 11 (8), pp. 1181-1187, 2017.

[165] Udelhoven, T., Schlerf, M., Segl, K., Mallick, K., Bossung, C., Retzlaff, R., Rock, G., **Fischer, P.**, Müller, A., **Storch, T.**, Eisele, A., Weise, D., Hupfer, W., Knigge, T.: *A Satellite-Based Imaging Instrumentation Concept for Hyperspectral Thermal Remote Sensing*, Sensors, 17 (7), pp. 1-16, 2017.

[166] **Ulmer, F.-G.**, **Adam, N.**: *Characterisation and improvement of the structure function estimation for application in PSI*, ISPRS Journal of Photogrammetry and Remote Sensing, 128, pp. 40-46, 2017.

[167] Vanselow, K. H., **Jacobsen, S.**, Garthe, S., Hall, C.: *Solar storms may trigger sperm whale strandings: explanation approaches for multiple strandings in the North Sea in 2016*, International Journal of Astrobiology, pp. 1-9, 2017.

[168] **Wendt, A.**, Mayer, C., Lambrecht, A., **Floricioiu, D.**: *A Glacier Surge of Bivachny Glacier, Pamir Mountains, Observed by a Time Series of High-Resolution Digital Elevation Models and Glacier Velocities*, Remote Sensing, 9 (388), pp. 1-17, 2017.

[169] Wollstadt, S., Lopez-Dekker, P., **De Zan, F.**, Younis, M.: *Design Principles and Considerations for Spaceborne ATI SAR-Based Observations of Ocean Surface Velocity Vectors*, IEEE Transactions on Geoscience and Remote Sensing, 55 (8), pp. 4500-4519, 2017.

[170] **Xu, J.**, ***Schüssler, O.***, **Loyola, D.**, **Romahn, F.**, **Doicu, A.**: *A novel ozone profile shape retrieval using full-physics inverse learning machine (FP-ILM)*, IEEE JSTARS, 10 (12), pp. 5442-5457, 2017.

[171] ***Yague-Martinez, N.***, **De Zan, F.**, Prats, P.: *Coregistration of Interferometric Stacks of Sentinel-1 TOPS Data*, IEEE Geoscience and Remote Sensing Letters, 14 (7), pp. 1002-1006, 2017.

[172] **Yokoya, N.**, **Grohnfeldt, C.**, Chanussot, J.: *Hyperspectral and multispectral data fusion: A comparative Review of the recent Literature*, IEEE Geoscience and Remote Sensing Magazine (GRSM), pp. 29-56, 2017.

[173] **Yokoya, N.**, **Zhu, X. X.**, Plaza, A.: *Multisensor coupled spectral unmixing for time-series analysis*, IEEE Transactions on Geoscience and Remote Sensing, 55 (5), pp. 2842-2857, 2017.

[174] Zeng, L., ***Schmitt, M.***, Li, L., **Zhu, X.**: *Analysing changes of the Poyang Lake water area using Sentinel-1 synthetic aperture radar imagery*, International Journal of Remote Sensing, 38 (23), pp. 7041-7069, 2017.

[175] **Zhu, X.**, Tuia, D., **Mou, L.**, Xia, G.-S., Zhang, L., Xu, F., **Fraundorfer, F.**: *Deep Learning in Remote Sensing: A Comprehensive Review and List of Resources*, IEEE Geoscience and Remote Sensing Magazine (GRSM), 5 (4), pp. 8-36, 2017.

[176] **Zhuo, X.**, ***Koch, T.***, **Kurz, F.**, **Fraundorfer, F.**, **Reinartz, P.**: *Automatic UAV Image Geo-Registration by Matching UAV Images to Georeferenced Image Data*, Remote Sensing, 9 (4), pp. 376-400, 2017.

2016

[177] Afanas'ev, V. P., **Efremenko, D. S.**, Kaplya, P. S.: *Analytical and numerical methods for computing electron partial intensities in the case of multilayer systems*, Journal of Electron Spectroscopy and Related Phenomena, 210, pp. 16-29, 2016.

[178] Afanas'ev, V. P., Gryazev, A. S., **Efremenko, D.**, Kaplya, P. S., Lyapunov, N. V.: *Differential inverse inelastic mean free path determination on the base of X-ray photoelectron emission spectra*, Surface Investigation X-Ray, Synchrotron and Neutron Techniques, 10 (5), pp. 906-911, 2016.

[179] Afanas'ev, V. P., Gryazev, A. S., **Efremenko, D.**, Kaplya, P. S., Ridzel, O. Y.: *Determination of atomic hydrogen in hydrocarbons by means of the reflected electron energy loss spectroscopy and the X-ray photoelectron spectroscopy*, Journal of Physics: Conference Series, 748 (1), pp. 1-8, 2016.

[180] **Andreou, C.**, Rogge, D., **Müller, R.**: *A new approach for endmember extraction and clustering addressing inter- and intra-class variability via multi-scaled-band partitioning*, IEEE JSTARS, 9 (9), pp. 4215-4231, 2016.

[181] **Ansari, H.**, **De Zan, F.**, **Parizzi, A.**, **Eineder, M.**, **Goel, K.**, **Adam, N.**: *Measuring 3D Surface Motion with Future SAR Systems based on Reflector Antennae*, IEEE Geoscience and Remote Sensing Letters, 13 (2), pp. 272-276, 2016.

[182] Babaee, M., Yu, X., Rigoll, G., **Datcu, M.**: *Immersive Interactive SAR Image Representation Using Non-negative Matrix Factorization*, IEEE JSTARS, 9 (7), pp. 2844-2853, 2016.

[183] Beirle, S., Hörmann, C., Jöckel, P., **Liu, S.**,Penning de Vries, M., Pozzer, A., Sihler, H., **Valks, P.**, Wagner, T.: *The STRatospheric Estimation Algorithm from Mainz (STREAM): estimating stratospheric NO2 from nadir-viewing satellites by weighted convolution*, Atmospheric Measurement Techniques (AMT), 9, pp. 2753-2779, 2016.

[184] **Birk, M.**, **Wagner, G.**: *Voigt profile introduces optical depth dependent systematic errors – detected in high resolution laboratory spectra of water*, Journal of Quantitative Spectroscopy and Radiative Transfer, 170, pp. 159-168, 2016.

[185] Boynard, A., Hurtmans, D., Koukouli, M., Goutail, F., Bureau, J., Safieddine, S., Lerot, C., Hadji-Lazaro, J., Wespes, C., Pommereau, J. P., Pazmino, A., Zyrichidou, I., Balis, D., Barbe, A., Mikhailenko, S., **Loyola, D.**, **Valks, P.**, Van Roozendael, M., Coheur, P.-F., Clerbaux, C.: *Seven years of IASI ozone retrievals from FORLI: validation with independent total column and vertical profile measurements*, Atmospheric Measurement Techniques (AMT), 9 (9), pp. 4327-4353, 2016.

[186] **Cerra, D.**, **Bieniarz, J.**, Beyer, F., **Tian, J.**, **Müller, R.**, Jarmer, T., **Reinartz, P.**: *Cloud Removal in Image Time Series through Sparse Reconstruction from Random Measurements*, IEEE JSTARS, 9 (8), pp. 3615-3628, 2016.

[187] **Cerra, D.**, Plank, S., Lysandrou, V., **Tian, J.**: *Cultural Heritage Sites in Danger—Towards Automatic Damage Detection from Space*, Remote Sensing, 8 (9), pp. 1-15, 2016.

[188] Chen, Y., Jiang, H., Li, C., Jia, X., **Ghamisi, P.**: *Deep Feature Extraction and Classification of Hyperspectral Images Based on Convolutional Neural Networks*, IEEE Transactions on Geoscience and Remote Sensing, 54 (10), pp. 6232-6251, 2016.

[189] **Cui, S.**, Luo, C.: *Feature based non parametric estimation of Kullback Leibler divergence for SAR image change detection*, Remote Sensing Letters, 7 (11), pp. 1102-1111, 2016.

[190] **Cui, S.**, **Schwarz, G.**, **Datcu, M.**: *A Benchmark Evaluation of Similarity Measures for Multi-temporal SAR Image Change Detection*, IEEE JSTARS, 9 (3), pp. 1101-1118, 2016.

[191] **Cui, S.**: *Comparison of Approximation Methods to Kullback-Leibler Divergence between Gaussian Mixture Models for Satellite Image Retrieval*, IEEE Geoscience and Remote Sensing Letters, 7 (7), pp. 651-660, 2016.

[192] Danisor, C., Fornaro, G., **Datcu, M.**: *Inversion Algorithms and PS Detection in SAR Tomography. Case Study of Bucharest City*, Telfor Journal, 8, pp. 20-25, 2016.

[193] Dörnhöfer, K., ***Göritz, A.***, **Gege, P.**, **Pflug, B.**, Oppelt, N.: *Water constituents and water depth retrieval from Sentinel-2A – a first evaluation in an oligotrophic lake*, Remote Sensing, 8 (11), pp. 1-25, 2016.

[194] **Dumitru, C. O.**, **Schwarz, G.**, **Datcu, M.**: *Land Cover Semantic Annotation Derived from High Resolution SAR Images*, IEEE JSTARS, 9 (6), pp. 2215-2232, 2016.

[195] **Efremenko, D. S.**, ***Schüssler, O.***, **Doicu, A.**, **Loyola, D.**: *A stochastic cloud model for cloud and ozone retrievals from UV measurements*, Journal of Quantitative Spectroscopy & Radiative Transfer, 184, pp. 167-179, 2016.

[196] **Espinoza Molina, D.**, **Datcu, M.**: *The Earth-Observation Epitome: A New Interactive Value-Added Product.*, IEEE Geoscience and Remote Sensing Letters, 13 (10), pp. 1438-1442, 2016.

[197] Ewald, F., **Kölling, T.**, **Baumgartner, A.**, Zinner, T., Mayer, B.: *Design and characterization of specMACS, a multipurpose hyperspectral cloud and sky imager*, Atmospheric Measurement Techniques (AMT), 9 (5), pp. 2015-2042, 2016.

[198] **Frost, A.**, **Ressel, R.**, **Lehner, S.**: *Automated Iceberg Detection over Northern Latitudes Using X-Band SAR Images*, Canadian Journal of Remote Sensing, 42 (4), pp. 354-366, 2016.

[199] **Gebhardt, C. P.**, Bidlot, J.-R., **Gemmrich, J.**, **Lehner, S.**, Rosenthal, W., **Pleskachevsky, A.**: *Wave observation in the marginal ice zone with the TerraSAR-X satellite*, Ocean Dynamics, 66 (6), pp. 839-852, 2016.

[200] **Gebhardt, C. P.**, **Pleskachevsky, A.**, Rosenthal, W., **Lehner, S.**, Hoffmann, P., Kieser, J., Bruns, T.: *Comparing wavelengths simulated by the coastal wave model CWAM and TerraSAR-X satellite data*, Ocean Modelling, 103 (July), pp. 133-144, 2016.

[201] **Gemmrich, J.**, Thomson, J., Rogers, E., **Pleskachevsky, A.**, **Lehner, S.**: *Spatial characteristics of ocean surface waves*, Ocean Dynamics, 66 (8), pp. 1025-1035, 2016.

[202] Geng, X., **Li, X.-M.**, **Velotto, D.**, Chen, K.-S.: *Study of the polarimetric characteristics of mud flats in an intertidal zone using C- and X-band spaceborne SAR data*, Remote Sensing of Environment, 176 (April), pp. 56-58, 2016.

[203] Georgescu, F.-A., **Vaduva, C.**, Raducanu, D., **Datcu, M.**: *Feature Extraction for Patch-Based Classification of Multispectral Earth Observation Images*, IEEE Geoscience and Remote Sensing Letters, 13 (6), pp. 865-869, 2016.

[204] **Ghamisi, P.**, Chen, Y., **Zhu, X. X.**: *A Self-Improving Convolution Neural Network for the Classification of Hyperspectral Data*, IEEE Geoscience and Remote Sensing Letters, 13 (10), pp. 1537-1541, 2016.

[205] **Ghamisi, P.**, Souza, R., Benediktsson, J. A., Rittner, L., Lotufo, R., **Zhu, X. X.**: *Hyperspectral Data Classification Using Extended Extinction Profiles*, IEEE Geoscience and Remote Sensing Letters, 13 (11), pp. 1641-1645, 2016.

[206] **Ghamisi, P.**, Souza, R., Benediktsson, J. A., **Zhu, X. X.**, Rittner, L., Lotufo, R.: *Extinction Profiles for the Classification of Remote Sensing Data*, IEEE Transactions on Geoscience and Remote Sensing, 54 (10), pp. 5631-5645, 2016.

[207] **Gomba, G.**, **Parizzi, A.**, **De Zan, F.**, **Eineder, M.**, **Bamler, R.**: *Toward Operational Compensation of Ionospheric Effects in SAR Interferograms: The Split-Spectrum Method*, IEEE Transactions on Geoscience and Remote Sensing, 54 (3), pp. 1446-1461, 2016.

[208] Griparis, A., Faur, D., **Datcu, M.**: *Dimensionality Reduction for Visual Data Mining of Earth Observation Archives*, IEEE Geoscience and Remote Sensing Letters, 13 (11), pp. 1701-1705, 2016.

[209] Hassinen, S., Balis, D., **Bauer, H.**, **Begoin, M.**, Delcloo, A., Eleftheratos, K., ***Gimeno Garcia, S.***, Granville, J., **Grossi, M.**, **Hao, N.**, **Hedelt, P.**, Hendrick, F., Hess, M., **Heue, K.-P.**, Hovila, J., Jønch-Sørensen, H., Kalakoski, N., Kauppi, A., Kiemle, S., Kins, L., Koukouli, M., Kujanpää, J., Lambert, J.-C., Lang, R., Lerot, C., **Loyola, D.**, ***Pedergnana, M.***, Pinardi, G., **Romahn, F.**, Van Roozendael, M., **Lutz, R.**, De Smedt, I., Stammes, P., Steinbrecht, W., Tamminen, J., Theys, N., Tilstra, L. G., Tuinder, O., **Valks, P.**, Zerefos, C. S., **Zimmer, W.**, Zyrichidou, I.: *Overview of the O3M SAF GOME-2 operational atmospheric composition and UV radiation data products and data availability*, Atmospheric Measurement Techniques (AMT), 9 (2), pp. 383-407, 2016.

[210] **Heue, K.-P.**, Coldewey-Egbers, M., Delcloo, A., Lerot, C., **Loyola, D.**, **Valks, P.**, Van Roozendael, M.: *Trends of tropical tropospheric ozone from 20 years of European satellite measurements and perspectives for the Sentinel-5 Precursor*, Atmospheric Measurement Techniques (AMT), 9, pp. 5037-5051, 2016.

[211] Kalakoski, N., Kujanpää, J., Sofieva, V., Tamminen, J., **Grossi, M.**, **Valks, P.**: *Validation of GOME-2/Metop total column water vapour with ground-based and in situ measurements*, Atmospheric Measurement Techniques (AMT), pp. 1533-1544, 2016.

[212] Koukouli, M., Lerot, C., Granville, J., Goutail, F., Lambert, J.-C., Pommereau, J. P., Balis, D., Zyrichidou, I., Van Roozendael, M., Coldewey-Egbers, M., **Loyola, D.**, Labow, G., Frith, S., Spurr, R., Zehner, C.: *Evaluating a new homogeneous total ozone climate data record from GOME/ERS-2, SCIAMACHY/Envisat, and GOME-2/MetOp-A*, Journal of Geophysical Research: Atmospheres, 120 (23), pp. 12296-12312, 2016.

[213] **Li, X.-M.**, Jia, T., **Velotto, D.**: *Spatial and temporal variations of oil spills in the North Sea observed by the satellite constellation of TerraSAR-X and TanDEM-X*, IEEE JSTARS, 9 (11), pp. 4941-4947, 2016.

[214] **Loyola, D.**, ***Pedergnana, M.***, ***Gimeno García, S.***: *Smart sampling and incremental function learning for very large high dimensional data*, Neural Networks, 78, pp. 75-87, 2016.

[215] **Lutz, R.**, **Loyola, D.**, ***Gimeno Garcia, S.***, **Romahn, F.**: *OCRA radiometric cloud fractions for GOME-2 on MetOp-A/B*, Atmospheric Measurement Techniques (AMT), 9, pp. 2357-2379, 2016.

[216] **Makarau, A.**, **Richter, R.**, Schläpfer, D., **Reinartz, P.**: *Combined haze and cirrus removal for multispectral imagery*, IEEE Geoscience and Remote Sensing Letters, 13 (3), pp. 379-389, 2016.

[217] **Marmanis, D.**, **Datcu, M.**, Esch, T., Stilla, U.: *Deep Learning Earth Observation Classification Using ImageNet Pre-trained Networks*, IEEE Geoscience and Remote Sensing Letters, 13 (1), pp. 105-109, 2016.

[218] Marsman, J.-B., Cornelissen, F., Dorr, M., **Vig, E.**, Barth, E., Renken, R.: *A novel measure to determine viewing priority and its neural correlates in the human brain*, Journal of Vision, 16 (6), pp. 1-18, 2016.

[219] Martone, M., Bräutigam, B., Rizzoli, P., ***Yague-Martinez, N.***, Krieger, G.: *Enhancing Interferometric SAR Performance over Sandy Areas: Experience from the TanDEM-X Mission*, IEEE JSTARS, 9 (3), pp. 1036-1046, 2016.

[220] **Mattyus, G.**, **Fraundorfer, F.**: *Aerial image sequence geolocalization with road traffic as invariant feature*, Image and Vision Computing, 52 (8), pp. 218-229, 2016.

[221] Mayer, C., Jaenicke, J., Lambrecht, A., Braun, L., Völksen, C., **Minet, C.**, Münzer, U.: *Local surface mass-balance reconstruction from a tephra layer – a case study on the northern slope of Mýrdalsjökull, Iceland*, Journal of Glaciology, 235, pp. 1-9, 2016.

[222] **Meynberg, O.**, **Cui, S.**, **Reinartz, P.**: *Detection of High-Density Crowds in Aerial Images Using Texture Classification*, Remote Sensing, 8 (6), pp. 1-17, 2016.

[223] ***Montazeri, S.***, **Zhu, X. X.**, **Eineder, M.**, **Bamler, R.**: *Three-Dimensonal Deformation Monitoring of Urban Infrastructure by Tomographic SAR Using Multitrack TerraSAR-X Data Stacks*, IEEE Transactions on Geoscience and Remote Sensing, 54 (12), pp. 6868-6878, 2016.

[224] Orphal, J., Staehelin, J., Tamminen, J., Braathen, G., De Backer, M.-R., Bais, A., Balis, D., Barbe, A., Bhartia, P. K., **Birk, M.**, Burkholder, J. B., Chance, K., von Clarmann, T., Cox, A., Degenstein, D., Evans, R., Flaud, J.-M., Flittner, D., Godin-Beekmann, S., Gorshelev, V., Gratien, A., Hare, E., Janssen, C., Kyrölä, E., McElroy, T., McPeters, R., Pastel, M., Petersen, M., Petropavlovskikh, I., Picquet-Varrault, B., Pitts, M., Labow, G., Rotger-Languereau, M., Leblanc, T., Lerot, C., Liu, X., Moussay, P., Redondas, A., Van Roozendael, M., Sander, S. P., Schneider, M., Serdyuchenko, A., Veefkind, P., Viallon, J., Viatte, C., **Wagner, G.**, Weber, M., Wielgosz, R. I., Zehner, C.: *Absorption cross-sections of ozone in the ultraviolet and visible spectral regions: Status report 2015*, Journal of Molecular Spectroscopy, 327, pp. 105-121, 2016.

[225] **Palubinskas, G.**: *Model based view at multi-resolution image fusion methods and quality assessment measures*, International Journal of Image and Data Fusion, 7 (3), pp. 203-218, 2016.

[226] Patrascu, C., Popescu, A. A., **Datcu, M.**: *Comparative Assessment of multi-temporal InSAR Techniques for Generation of Displacement Maps: A Case Study for Bucharest Area*, UPB Scientific Bulletin, Series C: Electrical Engineering and Computer Science, 78 (2), pp. 135-146, 2016.

[227] **Pleskachevsky, A.**, Rosenthal, W., **Lehner, S.**: *Meteo-Marine Parameters for Highly Variable Environment in Coastal Regions from Satellite Radar Images*, ISPRS Journal of Photogrammetry and Remote Sensing, 119, pp. 464-484, 2016.

[228] Qin, R., **Tian, J.**, **Reinartz, P.**: *Spatiotemporal inferences for use in building detection using series of very-high-resolution space-borne stereo images*, International Journal of Remote Sensing, 37 (15), pp. 3455-3476, 2016.

[229] Qina, R., **Tian, J.**, **Reinartz, P.**: *3D change detection – approaches and applications*, ISPRS Journal of Photogrammetry and Remote Sensing, 122, pp. 44-51, 2016.

[230] Quan, X., Zhang, B. C., **Zhu, X. X.**, Wu, Y.: *Unambiguous SAR Imaging for Nonuniform DPC Sampling: Lq Regularization Method Using Filter Bank*, IEEE Geoscience and Remote Sensing Letters, 13 (11), pp. 1596-1600, 2016.

[231] **Ressel, R.**, **Singha, S.**, **Lehner, S.**, Rösel, A., Spreen, G.: *Investigation into different polarimetric features for sea ice classification using X-band Synthetic Aperture Radar*, IEEE JSTARS, 9 (7), pp. 3131-3143, 2016.

[232] **Ressel, R.**, **Singha, S.**: *Comparing Near Coincident Space Borne C and X Band Fully*
Polarimetric SAR Data for Arctic Sea Ice Classification, Remote Sensing, 8 (3), pp. 1-27, 2016.

[233] **Rossi, C.**, **Minet, C.**, **Fritz, T.**, **Eineder, M.**, **Bamler, R.**: *Temporal monitoring of subglacial volcanoes with TanDEM-X — Application to the 2014–2015 eruption within the Bárðarbunga volcanic system, Iceland*, Remote Sensing of Environment, 181, pp. 186-197, 2016.

[234] **Rother, T.**: *Violation of a Bell-like inequality by a combination of Rayleigh scattering with a Mach-Zehnder setup*, Journal of Quantitative Spectroscopy & Radiative Transfer, 178, pp. 66-76, 2016.

[235] Safieddine, S., Boynard, A., **Hao, N.**, Huang, F., Wang, L., Ji, D., Barret, B., Ghude, D., Coheur, P.-F., Hurtmans, D., Clerbaux, C.: *Tropospheric Ozone Variability during the East Asian Summer Monsoon as Observed by Satellite (IASI), Aircraft (MOZAIC) and Ground Stations*, Atmospheric Chemistry and Physics, pp. 10489-10500, 2016.

[236] ***Schmitt, M.***, **Zhu, X. X.**: *Data Fusion and Remote Sensing – An Ever-Growing Relationship*, IEEE Geoscience and Remote Sensing Magazine (GRSM), 4 (4), pp. 6-23, 2016.

[237] ***Schmitt, M.***, **Zhu, X. X.**: *Demonstration of Single-Pass Millimeterwave SAR Tomography for Forest Volumes*, IEEE Geoscience and Remote Sensing Letters, 13 (2), pp. 202-206, 2016.

[238] **Schreier, F.**: *An assessment of some closed-form expressions for the Voigt function*, Journal of Quantitative Spectroscopy and Radiative Transfer, 176, pp. 1-5, 2016.

[239] ***Shahzad, M.***, **Zhu, X. X.**: *Automatic detection and reconstruction of 2D/3D building shapes from spaceborne TomoSAR point clouds*, IEEE Transactions on Geoscience and Remote Sensing, 54 (3), pp. 1292-1310, 2016.

[240] **Singha, S.**, **Ressel, R.**, **Velotto, D.**, **Lehner, S.**: *A Combination of Traditional and Polarimetric Features for Oil Spill Detection using TerraSAR-X*, IEEE JSTARS, 9 (11), pp. 4979-4990, 2016.

[241] **Singha, S.**, **Ressel, R.**: *Offshore platform sourced pollution monitoring using space-borne fully polarimetric C and X band synthetic aperture radar*, Marine Pollution Bulletin, 112, pp. 327 -340, 2016.

[242] **Storch, T.**: *Black-box complexity: Advantages of memory usage*, Information Processing Letters, 116 (6), pp. 428-432, 2016.

[243] Tănase, R., **Bahmanyar, R.**, **Schwarz, G.**, **Datcu, M.**: *Discovery of Semantic Relationships in PolSAR Images Using Latent Dirichlet Allocation*, IEEE Geoscience and Remote Sensing Letters, 14 (2), pp. 237-241, 2016.

[244] **Tao, J.**, **Auer, S.**: *Simulation-based Building Change Detection from Multi-Angle SAR Images and Digital Surface Models*, IEEE JSTARS, 9 (8), pp. 3777-3791, 2016.

[245] Thomson, J., Fan, Y., Stammerjohn, S., Stopa, J., Rogers, E., Girard-Ardhuin, F., Ardhuin, F., Shen, H., Perrie, W., Shen, H., Ackley, S., Babanin, A. V., Liu, Q., Guest, P., Maksym, T., Wadhams, P., Fairall, C., Persson, O., Doble, M., Graber, H. C., Lund, B., Squire, V., **Gemmrich, J.**, **Lehner, S.**, Holt, B., Meylan, M., Brozena, J., Bidlot, J.-R.: *Emerging trends in the sea state of the Beaufort and Chukchi seas*, Ocean Modelling, 105 (Sept), pp. 1-12, 2016.

[246] Topouzelis, K., **Singha, S.**, Kitsiou, D.: *Incidence angle Normalization of Wide Swath SAR Data for Oceanographic Applications*, Open Geosciences, 8 (1), pp. 450-464, 2016.

[247] **Ulmer, F.-G.**, **Balss, U.**: *Spin-up Time Research on the Weather Research and Forecasting Model for Atmospheric Delay Mitigations of Electromagnetic Waves*, Journal of Applied Remote Sensing, 10 (1), pp. 016027-1-016027-12, 2016.

[248] **Ulmer, F.-G.**: *On the accuracy gain of electromagnetic wave delay predictions derived by the digital filter initialization technique*, Journal of Applied Remote Sensing, 10 (1), pp. 016007-1-016007-7, 2016.

[249] **Velotto, D.**, **Bentes da Silva, C. A.**, **Tings, B.**, **Lehner, S.**: *First Comparison of Sentinel-1 and TerraSAR-X data in the framework of maritime targets detection: South Italy case*, IEEE Journal of Oceanic Engineering, 41 (4), pp. 993-1006, 2016.

[250] **Wagner, G.**, **Birk, M.**: *New infrared spectroscopic database for bromine nitrate*, Journal of Molecular Spectroscopy, 326, pp. 95-105, 2016.

[251] **Wang, Y.**, **Zhu, X. X.**, Zeisl, B., Pollefeys, M.: *Fusing meter-resolution 4-D InSAR point clouds and optical images for semantic urban infrastructure monitoring*, IEEE Transactions on Geoscience and Remote Sensing, 55 (1), pp. 14-26, 2016.

[252] **Wang, Y.**, **Zhu, X. X.**: *Robust estimators for multipass SAR interferometry*, IEEE Transactions on Geoscience and Remote Sensing, 54 (2), pp. 968-980, 2016.

[253] **Xu, J.**, **Schreier, F.**, **Doicu, A.**, **Trautmann, T.**: *Assessment of Tikhonov-type regularization methods for solving atmospheric inverse problems*, Journal of Quantitative Spectroscopy and Radiative Transfer, 184, pp. 274-286, 2016.

[254] ***Yague-Martinez, N.***, Prats-Iraola, P., **Rodriguez Gonzalez, F.**, **Brcic, R.**, **Shau, R.**, Geudtner, D., **Eineder, M.**, **Bamler, R.**: *Interferometric Processing of Sentinel-1 TOPS Data*, IEEE Transactions on Geoscience and Remote Sensing, 54 (04), pp. 2220-2234, 2016.

[255] **Yao, W.**, **Dumitru, C. O.**, Loffeld, O., **Datcu, M.**: *Semi-supervised Hierarchical Clustering for Semantic SAR Image Annotation*, IEEE JSTARS, 9 (5), pp. 1993-2008, 2016.

[256] **Yao, W.**, Loffeld, O., **Datcu, M.**: *Application and Evaluation of a Hierarchical Patch Clustering Method for Remote Sensing Images*, IEEE JSTARS, 9 (6), pp. 2279-2289, 2016.

[257] **Zhu, X. X.**, ***Grohnfeldt, C.***, **Bamler, R.**: *Exploiting Joint Sparsity for Pan-sharpening – The J-SparseFI Algorithm*, IEEE Transactions on Geoscience and Remote Sensing, 54 (5), pp. 2664-2681, 2016.

[258] **Zhu, X. X.**, ***Montazeri, S.***, Gisinger, C., Hanssen, R., **Bamler, R.**: *Geodetic SAR tomography*, IEEE Transactions on Geoscience and Remote Sensing, 54 (1), pp. 18-35, 2016.

2015

[259] Afanas'ev, V., Golovina, O., Gryazev, A., **Efremenko, D.**, Kaplya, P.: *Photoelectron spectra of finite-thickness layers*, Journal of Vacuum Science and Technology B: Nanotechnology and Microelectronics, 33, pp.03D101-1-03D101-6, 2015.

[260] **Alonso, K.**, **Datcu, M.**: *Accelerated Probabilistic Learning Concept for Mining Heterogeneous Earth Observation Images*, IEEE JSTARS, 8 (7), pp. 3356-3371, 2015.

[261] Antón, M., **Loyola, D.**, Roman, R., Vömel, H.: *Validation of GOME-2/MetOp-A total water vapour column using reference radiosonde data from the GRUAN network*, Atmospheric Measurement Techniques, 8 (3), pp. 1135-1145, 2015.

[262] **Auer, S.**, Gisinger, C., **Tao, J.**: *Characterization of Facade Regularities in High-Resolution SAR Images*, IEEE Transactions on Geoscience and Remote Sensing, 53 (5), pp. 2727-2737, 2015.

[263] **Avbelj, J.**, Iwaszczuk, D., **Müller, R.**, **Reinartz, P.**, Stilla, U.: *Coregistration refinement of hyperspectral images and DSM: An object-based approach using spectral information*, ISPRS Journal of Photogrammetry and Remote Sensing, 100, pp. 23-34, 2015.

[264] **Avbelj, J.**, **Müller, R.**, **Bamler, R.**: *A Metric for Polygon Comparison and Building Extraction Evaluation*, IEEE Geoscience and Remote Sensing Letters, 12 (1), pp. 170-174, 2015.

[265] Babaee, M., Tsoukalas, S., Babaee, M., Rigoll, G., **Datcu, M.**: *Discriminative Nonnegative Matrix Factorization for Dimensionality Reduction*, Neurocomputing, 173 (Part 2), pp. 212-223, 2015.

[266] Babaee, M., Tsoukalas, S., Rigoll, G., **Datcu, M.**: *Visualization-based Active Learning for the Annotation of SAR images*, IEEE JSTARS, 8 (10), pp. 4687-4698, 2015.

[267] Babaee, M., Tsoukalas, S., Rigoll, G., **Datcu, M.**: *Immersive Visualization of Visual Data Using Nonnegative Matrix Factorization*, Neurocomputing, 173 (2), pp. 245-255, 2015.

[268] Bachmann, M., **Makarau, A.**, Segl, K., **Richter, R.**: *Estimating the Influence of Spectral and Radiometric Calibration Uncertainties on EnMAP Data Products—Examples for Ground Reflectance Retrieval and Vegetation Indices*, Remote Sensing, 7 (8), pp. 10689-10714, 2015.

[269] **Bahmanyar, R.**, **Cui, S.**, **Datcu, M.**: *A Comparative Study of Bag-of-Words and Bag-of-Topics Models of EO Image Patches*, IEEE Geoscience and Remote Sensing Letters, 12 (6), pp. 1357-1361, 2015.

[270] **Bahmanyar, R.**, **Murillo Montes de Oca, A.**, **Datcu, M.**: *The Semantic Gap: An Exploration of User and Computer Perspectives in Earth Observation Images*, IEEE Geoscience and Remote Sensing Letters, 12 (10), pp. 2046-2050, 2015.

[271] Bai, J., Duhl, T., **Hao, N.**: *Biogenic volatile compound emissions from a temperate forest, China: model simulation*, Journal of Atmospheric Chemistry, pp. 1-31, 2015.

[272] Balz, T., Hammer, H., **Auer, S.**: *Potentials and Limitations of SAR Image Simulators - A Comparative Study of Three Simulation Approaches*, ISPRS Journal of Photogrammetry and Remote Sensing, 101, pp. 102-109, 2015.

[273] **Bieniarz, J.**, Aguilera, E., **Zhu, X. X.**, **Müller, R.**, **Reinartz, P.**: *Joint Sparsity Model for Multilook Hyperspectral Image Unmixing*, IEEE Geoscience and Remote Sensing Letters, 12 (4), pp. 696-700, 2015.

[274] Bigdeli, B., **Samadzadegan, F.**, **Reinartz, P.**: *Fusion of hyperspectral and LIDAR data using decisiontemplate-based fuzzy multiple classifier system*, International Journal of Applied Earth Observation and Geoinformation, 38, pp. 309-320, 2015.

[275] **Bruck, M.**, **Lehner, S.**: *TerraSAR-X/TanDEM-X sea state measurements using the XWAVE algorithm*, International Journal of Remote Sensing, 36 (15), pp. 3890-3912, 2015.

[276] **Cagatay, N. D.**, **Datcu, M.**: *FrFT-Based Scene Classification of Phase-Gradient InSAR Images and Effective Baseline Dependence*, IEEE Geoscience and Remote Sensing Letters, 12 (5), pp. 1131-1135, 2015.

[277] **Cerra, D.**, **Bieniarz, J.**, **Müller, R.**, **Storch, T.**, **Reinartz, P.**: *Restoration of Simulated EnMAP Data through Sparse Spectral Unmixing*, Remote Sensing, 7 (10), pp. 13190-13207, 2015.

[278] Cleaves, H. J., **Meringer, M.**, Goodwin, J. T.: *227 Views of RNA: Is RNA Unique in Its Chemical Isomer Space?*, Astrobiology, 15 (7), pp. 538-558, 2015.

[279] Coldewey-Egbers, M., **Loyola, D.**, Koukouli, M., Balis, D., Lambert, J.-C., Verhoelst, T., Granville, J., Van Roozendael, M., Lerot, C., Spurr, R., Frith, S., Zehner, C.: *The GOME-type Total Ozone Essential Climate Variable (GTO-ECV) data record from the ESA Climate Change Initiative*, Atmospheric Measurement Techniques, 8 (9), pp. 3923-3940, 2015.

[280] **Cui, S.**, **Schwarz, G.**, **Datcu, M.**: *Remote Sensing Image Classification: No Features, No Clustering*, IEEE JSTARS, 8 (11), pp.5158-5170, 2015

[281] **d'Angelo, P.**, **Máttyus, G.**, **Reinartz, P.**: *Skybox image and video product evaluation*, International Journal of Image and Data Fusion, 6, pp. 1-16, 2015.

[282] **De Zan, F.**, Prats-Iraoloa, P., Rodriguez-Cassola, M.: *On the Dependence of Delta-k Efficiency on Multilooking*, IEEE Geoscience and Remote Sensing Letters, 12 (8), pp. 1745-1749, 2015.

[283] **De Zan, F.**, Zonno, M., López-Dekker, P.: *Phase inconsistencies and multiple scattering in SAR interferometry*, IEEE Transactions on Geoscience and Remote Sensing, 53 (12), pp. 6608-6616, 2015.

[284] Deo, R., **Rossi, C.**, **Eineder, M.**, **Fritz, T.**, Rao, Y. S.: *Framework for Fusion of Ascending and Descending Pass TanDEM-X Raw DEMs*, IEEE JSTARS, 8 (7), pp. 3347-3355, 2015.

[285] Ding, J., van der A, R., Mijling, B., Levelt, P. F., **Hao, N.**: *NOx emission estimates during the 2014 Youth Olympic Games in Nanjing*, Atmospheric Chemistry and Physics, 15 (16), pp. 9399-9412, 2015.

[286] **Doicu, A.**, Eremin, Y., **Efremenko, D. Trautmann, T.**: *Methods with discrete sources for electromagnetic scattering by large axisymmetric particles with extreme geometries*, Journal of Quantitative Spectroscopy and Radiative Transfer, 164, pp. 137-146, 2015.

[287] **Dumitru, C.**, **Cui, S.**, Faur, D., **Datcu, M.**: *Data Analytics for Rapid Mapping: Case Study of a Flooding Event in Germany and the Tsunami in Japan Using Very High Resolution SAR Images*, IEEE JSTARS, 8 (1), pp. 114-129, 2015.

[288] **Dumitru, C.**, **Datcu, M.**, **Cui, S.**, **Schwarz, G.**: *Information Content of Very High Resolution SAR Images: Semantics, Geospatial Context, and Ontologies*, IEEE JSTARS, 8 (4), pp. 1635-1650, 2015.

[289] **Duque Biarge, S.**, **Rossi, C.**, **Fritz, T.**: *Single-Pass Tomography With Alternating Bistatic TanDEM-X Data*, IEEE Geoscience and Remote Sensing Letters, 12 (2), pp. 409-413, 2015.

[290] **Duque, S.**, **Breit, H.**, **Balss, U.**, **Parizzi, A.**: *Absolute Height Estimation Using a Single TerraSAR-X Staring Spotlight Acquisition*, IEEE Geoscience and Remote Sensing Letters, 12 (8), pp. 1735-1739, 2015.

[291] Erten, E., **Rossi, C.**, Yuzugullu, O.: *Polarization Impact in TanDEM-X Data Over Vertical-Oriented Vegetation: The Paddy-Rice Case Study*, IEEE Geoscience and Remote Sensing Letters, 12 (7), pp. 1501-1505, 2015.

[292] **Espinoza-Molina, D.**, Nikolaou, C., **Dumitru, C.**, Bereta, K., Koubarakis, M., **Schwarz, G.**, **Datcu, M.**: *Very-High-Resolution SAR Images and Linked Open Data Analytics Based on Ontologies*, IEEE JSTARS, 8 (4), pp. 1696-1708, 2015.

[293] ***Gernhardt, S.***, ***Auer, S.***, Eder, K.: *Persistent Scatterers at Building Facades - Evaluation of Appearance and Localization Accuracy*. ISPRS Journal of Photogrammetry and Remote Sensing, 100, pp. 92-105, 2015.

[294] Gisinger, C., **Balss, U.**, Pail, R., **Zhu, X. X.**, ***Montazeri, S.***, ***Gernhardt, S.***, **Eineder, M.**: *Precise Three-Dimensional Stereo Localization of Corner Reflectors and Persistent Scatterers With TerraSAR-X*, IEEE Transactions on Geoscience and Remote Sensing, 53 (4), pp. 1782-1802, 2015.

[295] Gleich, D., **Singh, J.**, Planinsic, P.: *Parametric and Nonparametric Methods for SAR Patch Scene Categorization*, IEEE JSTARS, 8 (4), pp. 1623-1634, 2015.

[296] **Grossi, M.**, **Valks, P.**, **Loyola, D.**, **Aberle, B.**, **Slijkhuis, S.**, Wagner, T., Beirle, S., Lang, R.: *Total column water vapour measurements from GOME-2 MetOp-A and MetOp-B*, Atmospheric Measurement Techniques, 8, pp. 1111-1133, 2015.

[297] Guanter, L., Kaufmann, H., Segl, K., Förster, S., Rogass, C., Chabrillat, S., Küster, T., Hollstein, A., Rossner, G., Chlebek, C., Straif, C., Fischer, S., Schrader, S., **Storch, T.**, Heiden, U., Müller, A., Bachmann, M., Mühle, H., **Müller, R.**, Habermeyer, M., Ohndorf, A., Hill, J., Buddenbaum, H., Hostert, P., van der Linden, S., Leitao, P. J., Rabe, A., Doerffer, R., Krasemann, H., Xi, H., Mauser, W., Hank, T., Locherer, M., Rast, M., Staenz, K., Sang, B.: *The EnMAP Spaceborne Imaging Spectroscopy Mission for Earth Observation*, Remote Sensing, pp. 8830-8857, 2015.

[298] Hamilton, B., Dean, C., Kurata, N., Vella, K., Soloviev, A., Tatar, A., Shivji, M., Matt, S. C., Perrie, W., **Lehner, S.**: *Surfactant associated bacteria in the sea surface microlayer: Case studies in the Straits of Florida and the Gulf of Mexico*, Canadian Journal of Remote Sensing, 41 (2), pp. 135-143, 2015.

[299] Hillen, F., **Meynberg, O.**, Höfle, B.: *Routing in Dense Human Crowds Using Smartphone Movement Data and Optical Aerial Imagery*, ISPRS International Journal of Geo-Information, 4 (2), pp. 974-988, 2015.

[300] Ilardo, M., **Meringer, M.**, Freeland, S. J., Rasulev, B., Cleaves, H. J.: *Extraordinarily adaptive properties of the genetically encoded amino acids*, Scientific Reports, 5, pp. 1-6, 2015.

[301] Jehle, M., Hueni, A., **Lenhard, K.**, **Baumgartner, A.**, Schaepman, M. E.: *Detection and Correction of Radiance Variations During Spectral Calibration in APEX*, IEEE Geoscience and Remote Sensing Letters, 12 (5), pp. 1023-1027, 2015.

[302] Klügel, T., Höppner, K., Falk, R., Kühmstedt, E., Plötz, C., Reinhold, A., Rülke, A., Wojdziak, R., **Balss, U.**, Diedrich, E., **Eineder, M.**, Henniger, H., Metzig, R., Steigenberger, P., Gisinger, C., Schuh, H., Böhm, J., Ojha, R., Kadler, M., Humbert, A., Braun, M., Sun, J.: *Earth and space observation at the German Antarctic Receiving Station O'Higgins*, Polar Record, 51 (6), pp. 590-610, 2015.

[303] Koepke, P., Gasteiger, J., Hess, M.: *Technical Note: Optical properties of desert aerosol with non-spherical mineral particles: data incorporated to OPAC*, Atmospheric Chemistry and Physics, 15 (10), pp. 5947-5956, 2015.

[304] Kuzmic, M., Grisogono, B., **Li, X.-M.**, **Lehner, S.**: *Examining deep and shallow Adriatic bora events*, Quarterly Journal of the Royal Meteorological Society, 141 (693), pp. 3434-3438, 2015.

[305] Lee, G. H., Li, B., Pollefeys, M., **Fraundorfer, F.**: *Minimal solutions for the multi-camera pose estimation problem*, The International Journal of Robotics Research, 34 (7), pp. 837-848, 2015.

[306] **Lenhard, K.**, **Baumgartner, A.**, **Gege, P.**, Nevas, S., Nowy, S., Sperling, A.: *Impact of improved calibration of a NEO HySpex VNIR-1600 sensor on remote sensing of water depth*, IEEE Transactions on Geoscience and Remote Sensing, 53 (11), pp. 6085-6098, 2015.

[307] **Lenhard, K.**, **Baumgartner, A.**, **Schwarzmaier, T.**: *Independent Laboratory Characterization of NEO HySpex Imaging Spectrometers VNIR-1600 and SWIR-320m-e*, IEEE Transactions on Geoscience and Remote Sensing, 53 (4), pp. 1828-1841, 2015.

[308] Letu, H., Bao, Y., **Xu, J.**, Qing, S., Bao, G.: *Radiative properties of cirrus clouds based on hexagonal and spherical ice crystals models*, Spectroscopy and Spectral Analysis, 35 (5), pp. 1165-1168, 2015.

[309] Liu, K., **Mattyus, G.**: *Fast Multiclass Vehicle Detection on Aerial Images*, IEEE Geoscience and Remote Sensing Letters, 12 (9), pp. 1938-1942, 2015.

[310] **Loos, J.**, **Birk, M.**, **Wagner, G.**: *Pressure broadening, -shift, speed dependence and line mixing in the v3 rovibrational band of N2O*, Journal of Quantitative Spectroscopy and Radiative Transfer, 151, pp. 300-309, 2015.

[311] Mahmoudi, F. T., **Samadzadegan, F.**, **Reinartz, P.**: *Context Aware Modification on the Object Based Image Analysis*, Journal of the Indian Society of Remote Sensing, 43 (4), pp. 709-717, 2015.

[312] Mahmoudi, F. T., **Samadzadegan, F.**, **Reinartz, P.**: *Object Recognition Based on the Context Aware Decision-Level Fusion in Multiviews Imagery*, IEEE JSTARS, 8 (1), pp. 12-21, 2015.

[313] Moreira, A., Krieger, G., Hajnsek, I., Papathanassiou, K., Younis, M., Lopez-Dekker, P., Huber, S., Villano, M., Pardini, M., **Eineder, M.**, **De Zan, F.**, **Parizzi, A.**: *Tandem-L: A Highly Innovative Bistatic SAR Mission for Global Observation of Dynamic Processes on the Earth's Surface*, IEEE Geoscience and Remote Sensing Magazine (GRSM), 3 (2), pp. 8-23, 2015.

[314] **Palubinskas, G.**: *Joint Quality Measure for Evaluation of Pansharpening Accuracy*, Remote Sensing, 7 (7), pp. 9292-9310, 2015.

[315] Prats, P., Rodriguez-Cassola, M., **De Zan, F.**, Scheiber, R., Lopez-Dekker, P., Barat, I., Geudtner, D.: *Role of the Orbital Tube in Interferometric Spaceborne SAR Missions*, IEEE Geoscience and Remote Sensing Letters, 12 (7), pp. 1486-1490, 2015.

[316] **Radoi, A.**, **Datcu, M.**: *Automatic Change Analysis in Satellite Images Using Binary Descriptors and Lloyd–Max Quantization*, IEEE Geoscience and Remote Sensing Letters, 12 (6), pp. 1223-1227, 2015.

[317] **Ressel, R.**, **Frost, A.**, **Lehner, S.**: *A Neural Network Based Classification for Sea Ice Types on X-Band SAR Images*, IEEE JSTARS, 8 (7), pp. 3672-3680, 2015.

[318] Román, R., Antón, M., Cachorro, V. E., **Loyola, D.**, Ortiz de Galisteo, J. P., de Frutos, A., Romero-Campos, P. M.: *Comparison of total water vapor column from GOME-2 on MetOp-A against ground-based GPS measurements at the Iberian Peninsula*, Science of the Total Environment, 533, pp. 317-328, 2015.

[319] **Rossi, C.**, **Eineder, M.**: *High-Resolution InSAR Building Layovers Detection and Exploitation*, IEEE Transactions on Geoscience and Remote Sensing, 53 (12), pp. 6457-6468, 2015.

[320] **Rossi, C.**, Erten, E.: *Paddy Rice Monitoring Using TanDEM-X*, IEEE Transactions on Geoscience and Remote Sensing, 53 (2), pp. 900-910, 2015.

[321] Schaepman, M. E., Jehle, M., Hueni, A., D'Odorico, P., Damm, A., Weyermann, J., Schneider, F. D., Laurent, V., Popp, C., Seidel, F., **Lenhard, K.**, **Gege, P.**, Küchler, C., Brazile, J., Kohler, P., De Vos, L., Meuleman, K., Meynart, R., Schläpfer, D., Kneubühler, M., Itten, K. I.: *Advanced radiometry measurements and Earth science applications with the Airborne Prism Experiment (APEX)*, Remote Sensing of Environment, 158, pp. 207-219, 2015.

[322] Schläpfer, D., **Richter, R.**, Feingersh, T.: *Operational BRDF Effects Correction for Wide-Field-of-View Optical Scanners (BREFCOR)*, IEEE Transactions on Geoscience and Remote Sensing, 53 (4), pp. 1855-1864, 2015.

[323] ***Schmitt, M.***, ***Shahzad, M.***, **Zhu, X. X.**: *Reconstruction of Individual Trees from Multi-Aspect TomoSAR Data*, Remote Sensing of Environment, 165, pp. 175-185, 2015.

[324] **Schreier, F.**, ***Gimeno Garcia, S.***, **Vasquez, M.**, **Xu, J.**: *Algorithmic vs. finite difference Jacobians for infrared atmospheric radiative transfer*, Journal of Quantitative Spectroscopy and Radiative Transfer, 164, pp. 147-160, 2015.

[325] **Schwind, P.**, **d'Angelo, P.**: *Evaluating the applicability of BRISK for the geometric registration of remote sensing images*, Remote Sensing Letters, 6 (9), pp. 677-686, 2015.

[326] ***Shahzad, M.***, **Zhu, X. X.**: *Robust Reconstruction of Building Façades for Large Areas Using Spaceborne TomoSAR Point Clouds*, IEEE Transactions on Geoscience and Remote Sensing, 53 (2), pp. 752-769, 2015.

[327] **Suchandt, S.**, **Runge, H.**: *Ocean Surface Observations Using the TanDEM-X Satellite Formation*, IEEE JSTARS, 8 (11), pp. 5096-5105, 2015.

[328] **Tian, J.**, Nielsen, A., **Reinartz, P.**: *Building damage assessment after the earthquake in Haiti using two postevent satellite stereo imagery and DSMs*, International Journal of Image and Data Fusion, 6 (2), pp. 155-169, 2015.

[329] **Tings, B.**, **Bentes da Silva, C. A.**, **Lehner, S.**: *Dynamically adapted ship parameter estimation on TerraSAR-X images*, International Journal of Remote Sensing, 37, pp. 1990-2015, 2015.

[330] **Ulmer, F.-G.**, **Adam, N.**: *A Synergy Method to Improve Ensemble Weather Predictions and Differential SAR Interferograms*, ISPRS Journal of Photogrammetry and Remote Sensing, pp. 98-107, 2015.

[331] **Wang, Y.**, **Zhu, X. X.**: *Automatic feature-based geometric fusion of multi-view TomoSAR point clouds in urban area*, IEEE JSTARS, 8 (3), pp. 953-965, 2015.

[332] Wetzel, G., Oelhaf, H., **Birk, M.**, de Lange, A., Engel, A., Friedl-Vallon, F., Kirner, O., Kleinert, A., Maucher, G., Nordmeyer, H., Orphal, J., Ruhnke, R., Sinnhuber, B.-M., **Vogt, P.**: *Partitioning and budget of inorganic and organic chlorine species observed by MIPAS-B and TELIS in the Arctic in March 2011*, Atmospheric Chemistry and Physics, 15 (14), pp. 8065-8076, 2015.

[333] **Wiehle, S.**, **Lehner, S.**: *Automated waterline detection in the German Wadden Sea using high-resolution TerraSAR-X images*, Journal of Sensors, 2015, pp. 1-6, 2015.

[334] Wuite, J., Rott, H., Hetzenecker, M., **Floricioiu, D.**, De Rydt, J., Gudmundsson, G. H., Nagler, T., Kern, M.: *Evolution of surface velocities and ice discharge of Larsen B outlet glaciers from 1995 to 2013*, The Cryosphere, 9, pp. 957-969, 2015.

[335] Xie, C., Xu, J., Shao, Y., Cui, B., **Goel, K.**, Zhang, Y., Yuan, M.: *Long term detection of water depth changes of coastal wetlands in the Yellow River Delta based on distributed scatterer interferometry*, Remote Sensing of Environment, 164, pp. 238-253, 2015.

[336] **Yang, J.**, Zhang, J.: *Parallel Performance of Typical Algorithms in Remote Sensing-based Mapping on a Multi-Core Computer*, Photogrammetric Engineering and Remote Sensing (PE&RS), 81 (5), pp. 373-385, 2015.

[337] **Zhu, X. X.**, ***Ge, N.***, ***Shahzad, M.***: *Joint Sparsity in SAR Tomography for Urban Mapping*, IEEE Journal of Selected Topics in Signal Processing, 9 (8), pp. 1498-1509, 2015.

2014

[338] Alam, K., **Trautmann, T.**, Blaschke, T., Subhan, F.: *Changes in aerosol optical properties due to dust storms in the Middle East and Southwest Asia*, Remote Sensing of Environment, 143, pp. 216-227, 2014.

[339] **Andreou, C.**, Karathanassi, V.: *Estimation of the Number of Endmembers Using Robust Outlier Detection Method*, IEEE JSTARS, 7 (1), pp. 247-256, 2014.

[340] ***Auer, S.***, ***Gernhardt, S.***: *Linear Signatures in Urban SAR Images — Partly Misinterpreted?*, IEEE Geoscience and Remote Sensing Letters, 11 (10), pp. 1762-1766, 2014.

[341] Bigdeli, B., **Samadzadegan, F.**, **Reinartz, P.**: *A decision fusion method based on multiple support vector machine system for fusion of hyperspectral and LIDAR data*, International Journal of Image and Data Fusion, 5 (3), pp. 196-209, 2014.

[342] Bigdeli, B., **Samadzadegan, F.**, **Reinartz, P.**: *Feature grouping-based multiple fuzzy classifier system for fusion of hyperspectral and LIDAR data*, Journal of Applied Remote Sensing, 8 (1), pp. 1-16, 2014.

[343] Blanchart, P., Ferecatu, M., **Cui, S.**, **Datcu, M.**: *Pattern Retrieval in Large Image Databases Using Multiscale Coarse-to-Fine Cascaded Active Learning*, IEEE JSTARS, 7 (4), pp. 1127-1141, 2014.

[344] Brenot, H., Theys, N., Clarisse, L., van Geffen, J., van Gent, J., Van Roozendael, M., van der A, R., Hurtmans, D., Coheur, P.-F., Clerbaux, C., **Valks, P.**, **Hedelt, P.**, Prata, A. J., Rasson, O., Sievers, K., Zehner, C.: *Support to Aviation Control Service (SACS): an online service for near real-time satellite monitoring of volcanic plumes*, Natural Hazards and Earth System Sciences (NHESS), 14, pp. 1099-1123, 2014.

[345] **Cerra, D.**, **Müller, R.**, **Reinartz, P.**: *Noise Reduction in Hyperspectral Images through Spectral Unmixing*, IEEE Geoscience and Remote Sensing Letters, 11 (1), pp. 109-113, 2014.

[346] **Cerra, D.**, **Reinartz, P.**, **Datcu, M.**: *Authorship analysis based on data compression*, Pattern Recognition Letters, 42, pp. 79-84, 2014.

[347] Chiou, E., Bhartia, P., McPeters, R. D., **Loyola, D.**, Coldewey-Egbers, M., Fioletov, V. E., Van Roozendael, M., Spurr, R., Lerot, C., Frith, S.: *Comparison of profile total ozone from SBUV (v8.6) with GOME-type and ground-based total ozone for a 16-year period (1996 to 2011)*, Atmospheric Measurement Techniques, 7 (6), pp. 1681-1692, 2014.

[348] Coldewey-Egbers, M., **Loyola, D.**, Braesicke, P., Dameris, M., van Roozendael, M., Lerot, C., **Zimmer, W.**: *A new health check of the ozone layer at global and regional scales*, Geophysical Research Letters, 41, pp. 4363-4372, 2014.

[349] **Cui, S.**, **Schwarz, G.**, **Datcu, M.**: *A Comparative Study of Statistical Models for Multilook SAR Images*, IEEE Geoscience and Remote Sensing Letters, 11 (10), pp. 1752-1756, 2014.

[350] **De Zan, F.**, **Parizzi, A.**, Prats, P., López-Dekker, P.: *A SAR interferometric model for soil moisture*, IEEE Transactions on Geoscience and Remote Sensing, 52 (1), pp. 418-425, 2014.

[351] **Doicu, A.**, **Efremenko, D.**, **Loyola, D.**, **Trautmann, T.**: *Approximate models for broken clouds in stochastic radiative transfer theory*, Journal of Quantitative Spectroscopy and Radiative Transfer, 145, pp. 74-87, 2014.

[352] **Doicu, A.**, **Efremenko, D.**, **Loyola, D.**, **Trautmann, T.**: *Discrete ordinate method with matrix exponential for stochastic radiative transfer in broken clouds*, Journal of Quantitative Spectroscopy and Radiative Transfer, 138, pp. 1-16, 2014.

[353] Doitsidis, L., ***Fraundorfer, F.***, Kosmatopoulos, E. B., Martinelli, A., Achtelik, M. W., Chli, M., Chatzichristos, S. A., Kneip, L., Gurdan, D., Heng, L., Lee, G. H., Lynen, S., Meier, L., Pollefeys, M., Renzaglia, A., Siegwart, R., SMünchen (TU)pf, J. C., Tanskanen, P., Troiani, C., Weiss, S., Scaramuzza, D., Achtelik, M. C.: *Vision-controlled micro flying robots: from system design to autonomous navigation and mapping in gps-denied environments*, IEEE Robotics & Automation Magazine, 21 (3), pp. 26-40, 2014.

[354] **Efremenko, D.**, **Doicu, A.**, **Loyola, D.**, **Trautmann, T.**: *Optical property dimensionality reduction techniques for accelerated radiative transfer performance: Application to remote sensing total ozone retrievals*, Journal of Quantitative Spectroscopy and Radiative Transfer, 133, pp. 128-135, 2014.

[355] **Efremenko, D.**, **Loyola, D.**, **Doicu, A.**, Spurr, R.: *Multi-core-CPU and GPU-accelerated radiative transfer models based on the discrete ordinate method*, Computer Physics Communications, 185 (12), pp. 3079-3089, 2014.

[356] **Efremenko, D.**, **Loyola, D.**, Spurr, R., **Doicu, A.**: *Acceleration of radiative transfer model calculations for the retrieval of trace gases under cloudy conditions*, Journal of Quantitative Spectroscopy and Radiative Transfer, 135, pp. 58-65, 2014.

[357] **Gege, P.**: *WASI-2D - A software tool for regionally optimized analysis of imaging spectrometer data from deep and shallow waters*, Computers & Geosciences, 62, pp. 208-215, 2014.

[358] Gleich, D., **Datcu, M.**: *Despeckling and Information Extraction From SLC SAR Images*, IEEE Transactions on Geoscience and Remote Sensing, 52 (8), pp. 4633-4649, 2014.

[359] **Goel, K.**, **Adam, N.**: *A distributed scatterer interferometry approach for precision monitoring of known surface deformation phenomena*, IEEE Transactions on Geoscience and Remote Sensing, 52 (9), pp. 5454-5468, 2014.

[360] Groh, A., Ewert, H., Rosenau, R., **Fagiolini, E.**, Gruber, C., **Floricioiu, D.**, **Abdel Jaber, W.**, Linow, S., Flechtner, F., **Eineder, M.**, Dierking, W., Dietrich, R.: *Mass, volume and velocity of the Antarctic Ice Sheet: present-day changes and error effects*, Surveys in Geophysics, 35 (6), pp. 1481-1505, 2014.

[361] **Hao, N.**, Koukouli, M., Inness, A., **Valks, P.**, **Loyola, D.**, **Zimmer, W.**, Balis, D., Zyrichidou, I., Van Roozendael, M., Lerot, C., Spurr, R.: *GOME-2 total ozone columns from MetOp-A/MetOp-B and assimilation in the MACC system*, Atmospheric Measurement Techniques, 7, pp. 2937-2951, 2014.

[362] Heng, L.., Honegger, D., Lee, G. H., Meier, L., Tanskanen, P., ***Fraundorfer, F.***, Pollefeys, M.: *Autonomous visual mapping and exploration with a micro aerial vehicle*, Journal of Field Robotics, 31 (4), pp. 654-675, 2014.

[363] Hillen, F., Höfle, B., Ehlers, M., **Reinartz, P.**: *Information fusion infrastructure for remote-sensing and in-situ sensor data to model people dynamics*, International Journal of Image and Data Fusion, 5 (1), pp. 54-69, 2014.

[364] Joughin, I., Smith, B., Shean, D., **Floricioiu, D.**: *Brief Communication: Further summer speedup of Jakobshavn Isbræ*, The Cryosphere, 8, pp. 209-214, 2014.

[365] Kahle, R., **Runge, H.**, Ardaens, J.-S., **Suchandt, S.**, Romeiser, R.: *Formation Flying for Along-Track Interferometric Oceanography - First In-Flight Demonstration with TanDEM-X*, Acta Astronautica, 99 (C), pp. 130-142, 2014.

[366] **Krauß, T.**: *Six Years Operational Processing of Satellite data using CATENA at DLR: Experiences and Recommendations*, Kartographische Nachrichten, 64 (2), pp. 74-80, 2014.

[367] Lambrecht, A., Mayer, C., Aizen, V., **Floricioiu, D.**, Surazarov, A.: *The evolution of Fedchenko glacier in the Pamir, Tajikistan, during the past eight decades*, Journal of Glaciology, 60 (220), pp. 233-244, 2014.

[368] **Leitloff, J.**, **Rosenbaum, D.**, **Kurz, F.**, **Meynberg, O.**, **Reinartz, P.**: *An Operational System for Estimating Road Traffic Information from Aerial Images*, Remote Sensing, 6 (11), pp. 11315-11341, 2014.

[369] Lerot, C., Van Roozendael, M., Spurr, R., **Loyola, D.**, Coldewey-Egbers, M., Kochenova, S., van Gent, J., Koukouli, M., Balis, D., Lambert, J.-C., Granville, J., Zehner, C.: *Homogenized total ozone data records from the European sensors GOME/ERS-2, SCIAMACHY/Envisat, and GOME-2/MetOp-A*, Journal of Geophysical Research: Atmospheres, 119 (3), pp. 1639-1662, 2014.

[370] **Li, X.-M.**, Chi, L., Chen, X., Ren, Y., **Lehner, S.**: *SAR observation and numerical modeling of tidal current wakes at the East China Sea offshore wind farm*, Journal of Geophysical Research - Oceans, 119 (8), pp. 4958-4971, 2014.

[371] **Li, X.-M.**, **Lehner, S.**: *Algorithm for sea surface wind retrieval from TerraSAR-X and TanDEM-X data*, IEEE Transactions on Geoscience and Remote Sensing, 52 (5), pp. 2928-2939, 2014.

[372] **Li, X.-M.**, **Lehner, S.**, Bruns, T.: *Simultaneous Measurements by Advanced SAR and Radar Altimeter on Potential Improvement of Ocean Wave Model Assimilation*, IEEE Transactions on Geoscience and Remote Sensing, 52 (5), pp. 2508-2518, 2014.

[373] Mahmoudi, F., **Samadzadegan, F.**, **Reinartz, P.**: *Multi-Agent Recognition System based on Object Based Image Analysis Using WorldView-2*, Photogrammetric Engineering and Remote Sensing (PE&RS), 80 (2), pp. 161-170, 2014.

[374] **Makarau, A.**, Richter, R., **Müller, R.**, **Reinartz, P.**: *Haze detection and removal in remotely sensed multispectral imagery*, IEEE Transactions on Geoscience and Remote Sensing, 52 (9), pp. 5895-5905, 2014.

[375] Mannschatz, T., **Pflug, B.**, Borg, E., Feger, K.-H., Dietrich, P.: *Uncertainties of LAI estimation from satellite imaging due to atmospheric correction*, Remote Sensing of Environment, 153, pp. 24-39, 2014.

[376] Marsh, O. J., Rack, W., Golledge, N. R., Lawson, W., **Floricioiu, D.**: *Grounding-zone ice thickness from InSAR: inverse modelling of tidal elastic bending*, Journal of Glaciology, 60 (221), pp. 526-536, 2014.

[377] **Murillo Montes de Oca, A.**, Nistor, N.: *Non-significant intention–behavior effects in educational technology acceptance: A case of competing cognitive scripts?*, Computers in Human Behavior, 34, pp. 333-338, 2014.

[378] Planinsic, P., **Singh, J.**, Dusan, G.: *SAR Image Categorization Using Parametric and Nonparametric Approaches Within a Dual Tree CWT*, IEEE Geoscience and Remote Sensing Letters, 11 (10), pp. 1757-1761, 2014.

[379] Ramzi, P., **Samadzadegan, F.**, **Reinartz, P.**: *Classification of Hyperspectral Data Using an AdaBoostSVM Technique Applied on Band Clusters*, IEEE JSTARS, 7 (6), pp. 2066-2079, 2014.

[380] Ramzi, P., **Samadzadegan, F.**, **Reinartz, P.**: *An AdaBoost Ensemble Classifier System for Classifying Hyperspectral Data*, Photogrammetrie Fernerkundung Geoinformation, 2014 (1), pp. 27-39, 2014.

[381] Raspini, F., Loupasakis, C., Rozos, D., **Adam, N.**, Moretti, S.: *Ground subsidence phenomena in the Delta municipality region (Northern Greece): Geotechnical modeling and validation with Persistent Scatterer Interferometry*, International Journal of Applied Earth Observation and Geoinformation, 28, pp. 78-89, 2014.

[382] Richter, R., Heege, T., Kiselev, V., Schläpfer, D.: *Correction of ozone influence on TOA radiance*, International Journal of Remote Sensing, 35, pp. 8044-8056, 2014.

[383] Romeiser, R., **Runge, H.**, **Suchandt, S.**, Kahle, R., **Rossi, C.**, Bell, P.: *Quality Assessment of Surface Current Fields From TerraSAR-X and TanDEM-X Along-Track Interferometry and Doppler Centroid Analysis*, IEEE Transactions on Geoscience and Remote Sensing, 52 (5), pp. 2759-2772, 2014.

[384] Rott, H., **Floricioiu, D.**, Wuite, J., Scheiblauer, S., Nagler, T., Kern, M.: *Mass changes of outlet glaciers along the Nordensjköld Coast, northern Antarctic Peninsula, based on TanDEM-X satellite measurements*, Geophysical Research Letters, 41, pp. 1-7, 2014.

[385] **Schreier, F.**, ***Gimeno-Garcia, S.***, **Hedelt, P.**, Hess, M., Mendrok, J., **Vasquez, M.**, **Xu, J.**: *GARLIC - A General Purpose Atmospheric Radiative Transfer Line-by-Line Infrared Code: Implementation and Evaluation*, Journal of Quantitative Spectroscopy and Radiative Transfer, 137, pp. 29-50, 2014.

[386] **Schüssler, O.**, **Loyola, D.**, **Doicu, A.**, Spurr, R.: *Information Content in the Oxygen A-Band for the Retrieval of Macrophysical Cloud Parameters*, IEEE Transactions on Geoscience and Remote Sensing, 52 (6), pp. 3246-3255, 2014.

[387] Shao, W., **Li, X.-M.**, **Lehner, S.**, Guan, C.: *Development of polarization ratio model for sea surface wind field retrieval from TerraSAR-X HH polarization data*, International Journal of Remote Sensing, 35 (11-12), pp. 4046-4063, 2014.

[388] **Singha, S.**, **Velotto, D.**, **Lehner, S.**: *Near real time monitoring of platform sourced pollution using TerraSAR-X over the North Sea*, Marine Pollution Bulletin, 86 (1-2), pp. 379-390, 2014.

[389] Spinetti, C., Salerno, G., Caltabiano, T., Carboni, E., Clarisse, L., Corradini, S., Grainger, R., **Hedelt, P.**, Koukouli, M., Merucci, L., Siddans, R., Tampellini, L., Theys, N., **Valks, P.**, Zehner, C.: *Volcanic SO2 by UV-TIR satellite retrievals: validation by using ground-based network at Mt. Etna*, Annals of Geophysics, 57, pp. 1-6, 2014.

[390] ***Szottka, I. Butenuth, M.***: *Advanced Particle Filtering for Airborne Vehicle Tracking in Urban Areas*, IEEE Geoscience and Remote Sensing Letters, 11 (3), pp. 686-690, 2014.

[391] **Tao, J.**, ***Auer, S.***, **Palubinskas, G.**, **Reinartz, P.**, **Bamler, R.**: *Automatic SAR simulation techniques for object identification in complex urban scenarios*, IEEE JSTARS, 7 (3), pp. 994-1003, 2014.

[392] **Tian, J.**, **Cui, S.**, **Reinartz, P.**: *Building change detection based on satellite stereo imagery and digital surface models*, IEEE Transactions on Geoscience and Remote Sensing, 52 (1), pp. 406-417, 2014.

[393] **Tian, J.**, Nielsen, A., **Reinartz, P.**: *Improving Change Detection in Forest Areas Based on Stereo Panchromatic Imagery using Kernel MNF*, IEEE Transactions on Geoscience and Remote Sensing, 52 (11), pp. 7130-7139, 2014.

[394] **Valks, P.**, **Hao, N.**, **Gimeno Garcia, S.**, **Loyola, D.**, Dameris, M., Jöckel, P., Delcloo, A.: *Tropical tropospheric ozone column retrieval for GOME-2*, Atmospheric Measurement Techniques, 7 (8), pp. 2513-2530, 2014.

[395] **Velotto, D.**, **Soccorsi, M.**, **Lehner, S.**: *Azimuth Ambiguities Removal for Ship Detection Using Full Polarimetric X-Band SAR Data*, IEEE Transactions on Geoscience and Remote Sensing, 52 (1), pp. 76-88, 2014.

[396] **Wang, Y.**, **Zhu, X. X.**, **Bamler, R.**: *An Efficient Tomographic Inversion Approach for Urban Mapping using Meter Resolution SAR Image Stacks*, IEEE Geoscience and Remote Sensing Letters, 11 (7), pp. 1250-1254, 2014.

[397] Wurm, M., **d'Angelo, P.**, **Reinartz, P.**, Taubenböck, H.: *Investigating the Applicability of Cartosat-1 DEMs and Topographic Maps to Localize Large-Area Urban Mass concentrations*, IEEE JSTARS, 7 (10), pp. 4138-4152, 2014.

[398] **Zhu, X. X.**, **Bamler, R.**: *Superresolving SAR Tomography for Multidimensional Imaging of Urban Areas*, IEEE Signal Processing Magazine, 31 (4), pp. 51-58, 2014.

[399] **Zhu, X. X.**, ***Shahzad, M.***: *Facade Reconstruction Using Multiview Spaceborne TomoSAR Point Clouds*, IEEE Transactions on Geoscience and Remote Sensing, 52 (6), pp. 3541-3552, 2014.

[400] Zink, M., Bachmann, M., Bräutigam, B., **Fritz, T.**, Hajnsek, I., Krieger, G., Moreira, A., Wessel, B.: *TanDEM-X: The New Global DEM Takes Shape*, IEEE Geoscience and Remote Sensing Magazine (GRSM), 2 (2), pp. 8-23, 2014.

2013

[401] Afanas'ev, V., **Efremenko, D.**, Ivanov, D., Kaplya, P., Lubenchenko, A.: *Photoelectron emission for layers of finite thickness*, Surface Investigation X-Ray, Synchrotron and Neutron Techniques, 7 (2), pp. 382-387, 2013.

[402] Afanas'ev, V., **Efremenko, D.**, Lubenchenko, A.: *Experimental verification of the technique for calculating light scattering in turbid media and determination of the single-scattering albedo based on the spectroscopy of elastically reflected electrons*, Surface Investigation X-Ray, Synchrotron and Neutron Techniques, 7 (2), pp. 285-289, 2013.

[403] Alam, K., **Trautmann, T.**, Blaschke, T., Majid, H.: *Aerosol optical and radiative properties during summer and winter seasons over Lahore and Karachi*, Atmospheric Environment, 50, pp. 234-245, 2013.

[404] **Arefi, H.**, **Reinartz, P.**: *Building Reconstruction Using DSM and Orthorectified Images*, Remote Sensing, 5 (4), pp. 1681-1703, 2013.

[405] Berger, C., Voltersen, M., Eckardt, R., Eberle, J., Heyer, T., Salepci, N., Hese, S., Schmullius, C., **Tao, J.**, ***Auer, S.***, **Bamler, R.**, Ewald, K., Gartley, M., Jacobson, J., Buswell, A., Du, Q., Pacifici, F.: *Multi-Modal and Multi-Temporal Data Fusion: Outcome of the 2012 GRSS Data Fusion Contest*, IEEE JSTARS, 6 (3), pp. 1324-1340, 2013.

[406] Bigdeli, B., **Samadzadegan, F.**, **Reinartz, P.**: *Band Grouping versus Band Clustering in SVM Ensemble Classification of Hyperspectral Imagery*, Photogrammetric Engineering and Remote Sensing (PE&RS), 79 (6), pp. 523-534, 2013.

[407] Bigdeli, B., **Samadzadegan, F.**, **Reinartz, P.**: *A Multiple SVM System for Classification of Hyperspectral Remote Sensing Data*, Journal of the Indian Society of Remote Sensing, 41 (4), pp. 763-776, 2013.

[408] **Bruck, M., Lehner, S.**: *Coastal wave field extraction using TerraSAR-X data*, Journal of Applied Remote Sensing, 7 (1), pp. 1-19, 2013.

[409] **Cerra, D.**, **Datcu, M.**: *Expanding the Algorithmic Information Theory Frame for Applications to Earth Observation*, Entropy, 15 (1), pp. 407-415, 2013.

[410] **Cerra, D.**, **Müller, R.**, **Reinartz, P.**: *A Classification Algorithm for Hyperspectral Images based on Synergetics Theory*, IEEE Transactions on Geoscience and Remote Sensing, 51 (5), pp. 2887-2898, 2013.

[411] **Chaabouni-Chouayakh, H.**, Rodes, I., **Reinartz, P.**: *Towards automatic 3-D change detection through multi-spectral and digital elevation model information fusion*, International Journal of Image and Data Fusion, 4 (1), pp. 89-101, 2013.

[412] **Cui, S.**, **Dumitru, C. O.**, **Datcu, M.**: *Ratio-Detector-Based Feature Extraction for Very High Resolution SAR Image Patch Indexing*, IEEE Geoscience and Remote Sensing Letters, 10 (5), pp. 1175-1179, 2013.

[413] **Cui, S.**, **Dumitru, C.**, **Datcu, M.**: *Semantic Annotation in Earth Observation Based on Active Learning*, International Journal of Image and Data Fusion, 5 (1), pp. 1-23, 2013.

[414] Dadras Javan, F., **Samadzadegan, F.**, **Reinartz, P.**: *Spatial Quality Assessment of Pan-sharpened High Resolution Satellite Imagery Based on an Automatically Estimated Edge Based Metric*, Remote Sensing, 5, pp. 6539-6559, 2013.

[415] **Doicu, A.**, **Efremenko, D.**, **Trautmann, T.**: *A multi-dimensional vector spherical harmonics discrete ordinate method for atmospheric radiative transfer*, Journal of Quantitative Spectroscopy and Radiative Transfer, 118, pp. 121-131, 2013.

[416] **Doicu, A.**, **Efremenko, D.**, **Trautmann, T.**: *An analysis of the short-characteristic method for the spherical harmonic discrete ordinate method (SHDOM)*, Journal of Quantitative Spectroscopy and Radiative Transfer, pp. 114-127, 2013.

[417] **Dumitru, O.**, **Datcu, M.**: *Information Content of Very High Resolution SAR Images: Study of Feature Extraction and Imaging Parameters*, IEEE Transactions on Geoscience and Remote Sensing, 51 (8), pp. 4591-4610, 2013.

[418] **Efremenko, D.**, **Doicu, A.**, **Loyola, D.**, **Trautmann, T.**: *Acceleration techniques for the discrete ordinate method*, Journal of Quantitative Spectroscopy and Radiative Transfer, 114, pp. 73-81, 2013.

[419] **Efremenko, D.**, **Doicu, A.**, **Loyola, D.**, **Trautmann, T.**: *Small-angle modification of the radiative transfer equation for a pseudo-spherical atmosphere*, Journal of Quantitative Spectroscopy and Radiative Transfer, 114, pp. 82-90, 2013.

[420] **Eineder, M.**, **Bamler, R.**, ***Cong, X.***, ***Gernhardt, S.***, **Fritz, T.**, **Zhu, X. X.**, **Balss, U.**, **Breit, H.**, **Adam, N.**, **Floricioiu, D.**: *Globale Kartierung und lokale Deformationsmessungen mit den Satelliten TerraSAR-X und TanDEM-X*, ZFV - Zeitschrift für Geodasie, Geoinformation und Landmanagement, 1/2013, pp. 75-84, 2013.

[421] **Espinoza-Molina, D.**, **Datcu, M.**: *Earth-Observation Image Retrieval Based on Content, Semantics, and Metadata*, IEEE Transactions on Geoscience and Remote Sensing, 51 (11), pp. 5145-5159, 2013.

[422] Fioletov, V. E., McLinden, C. A., Krotkov, N., Yang, K., **Loyola, D.**, **Valks, P.**, Theys, N., Van Roozendael, M., Nowlan, C., Chance, K., Liu, X., Lee, C., Martin, R. V.: *Application of OMI, SCIAMACHY and GOME-2 satellite SO2 retrievals for detection of large emission sources*, Journal of Geophysical Research: Atmospheres, 118 (19), pp. 11399-11418, 2013.

[423] **Goel, K.**, **Adam, N.**: *Fusion of monostatic/bistatic InSAR stacks for urban area analysis via distributed scatterers*, IEEE Geoscience and Remote Sensing Letters, 11 (4), pp. 733-737, 2013.

[424] **Hedelt, P.**, von Paris, P., Godolt, M., Gebauer, S., Grenfell, J. L., Rauer, H., **Schreier, F.**, Selsis, F., **Trautmann, T.**: *Spectral features of Earth-like planets and their detectability at different orbital distances around F, G, and K-type stars*, Astronomy & Astrophysics, 553, pp. 1-14, 2013.

[425] Hueni, A., **Lenhard, K.**, **Baumgartner, A.**, Schaepman, M.: *Airborne Prism Experiment Calibration Information System*, IEEE Transactions on Geoscience and Remote Sensing, 51 (11), pp. 5169-5180, 2013.

[426] Kasai, Y., Sagawa, H., Kreyling, D., Suzuki, K., Dupuy, E., Sato, T. O., Mendrok, J., Baron, P., Nishibori, T., Mizobuchi, S., Kikuchi, K., Manabe, T., Ozeki, H., Sugita, T., Fujiwara, M., Irimajiri, Y., Walker, K. A., Bernath, P. F., Boone, C., Stiller, G., von Clarmann, T., Orphal, J., Urban, J., Murtagh, D., Llewellyn, E. J., Degenstein, D., Bourassa, A. E., Lloyd, N. D., Froidevaux, L., **Birk, M.**, **Wagner, G.**, **Schreier, F.**, **Xu, J.**, **Vogt, P.**, **Trautmann, T.**, Yasui, M.: *Validation of stratospheric and mesospheric ozone observed by SMILES from International Space Station*, Atmospheric Measurement Techniques, 6 (9), pp. 2311-2338, 2013.

[427] Kuzmic, M., **Li, X.-M.**, Grisogono, B., Tomazic, I., **Lehner, S.**: *TerraSAR-X observations of the Senj bora wind: Early results*, Acta Adriatica, 54 (1), pp. 13-26, 2013.

[428] **Lehner, S., Pleskatchevsky, A., Velotto, D., Jacobsen, S.**: *Meteo-Marine Parameters and Their Variability Observed by High Resolution Satellite Radar Images*, Oceanography, pp. 80-91, 2013.

[429] **Li, X.**, **Lehner, S.**: *Observation of TerraSAR-X for studies on offshore wind turbine wake in near and far fields*, IEEE JSTARS, 6 (3), pp. 1757-1768, 2013.

[430] Mahmoudi, F., **Samadzadegan, F.**, **Reinartz, P.**: *Object oriented image analysis based on multi-agent recognition system*, Computers & Geosciences, 54 (1), pp. 219-230, 2013.

[431] **Makarau, A.**, **Palubinskas, G.**, **Reinartz, P.**: *Alphabet-based Multisensory Data Fusion and Classification using Factor Graphs*, IEEE JSTARS, 6 (2), pp. 969-990, 2013.

[432] Marsh, O. J., Rack, W., **Floricioiu, D.**, Golledge, N. R., Lawson, W.: *Tidally induced velocity variations of the Beardmore Glacier, Antarctica, and their representation in satellite measurements of ice velocity*, The Cryosphere, 7, pp. 1375-1384, 2013.

[433] **Meringer, M.**, Cleaves, H. J., Freeland, S. J.: *Beyond Terrestrial Biology: Charting the Chemical Universe of α-Amino Acid Structures*, Journal of Chemical Information and Modeling, 53 (11), pp. 2851-2862, 2013.

[434] **Meringer, M.**, Schymanski, E. L.: *Small Molecule Identification with MOLGEN and Mass Spectrometry*, Metabolites, 3 (2), pp. 440-462, 2013.

[435] **Palubinskas, G.**: *Fast, simple and good pan-sharpening method*, Journal of Applied Remote Sensing, 7 (1), pp. 1-12, 2013.

[436] Rastiveis, H., **Samadzadegan, F.**, **Reinartz, P.**: *A fuzzy decision making system for building damage map creation using high resolution satellite imagery*, Natural Hazards and Earth System Sciences (NHESS), 13 (1), pp. 455-472, 2013.

[437] **Rossi, C.**, ***Gernhardt, S.***: *Urban DEM generation, analysis and enhancements using TanDEM-X*, ISPRS Journal of Photogrammetry and Remote Sensing, 85C, pp. 120-131, 2013.

[438] Rothman, L. S., Gordon, I. E., Babikov, Y., Barbe, A., Benner, D. C., Bernath, P. F., **Birk, M.**, Bizzocchi, L., Boudon, V., Brown, L. R., Campargue, A., Chance, K., Coudert, L. H., Devi, V. M., Drouin, B. J., Fayt, A., Flaud, J.-M., Gamache, R. R., Harrison, J., Hartmann, J.-M., Hill, C., Hodges, J. T., Jacquemart, D., Jolly, A., Lamouroux, J., LeRoy, R. J., Li, G., Long, D., Mackie, C. J., Massie, S. T., Mikhailenko, S., Müller, H. S.P., Naumenko, O. V., Nikitin, A. V., Orphal, J., Perevalov, V. I., Perrin, A., Polovtseva, E. R., Richard, C., Smith, M. A.H., Starikova, E., Sung, K., Tashkun, S. A., Tennyson, J., Toon, G. C., Tyuterev, V., **Wagner, G.**: *The HITRAN 2012 Molecular Spectroscopic Database*, Journal of Quantitative Spectroscopy and Radiative Transfer, 130, pp. 4-50, 2013.

[439] Safieddine, S., Clerbaux, C., George, M., Hadji-Lazaro, J., Hurtmans, D., Coheur, P.-F., Wespes, C., **Loyola, D.**, **Valks, P.**, **Hao, N.**: *Tropospheric ozone and nitrogen dioxide measurements in urban and rural regions as seen by IASI and GOME-2*, Journal of Geophysical Research: Atmospheres, 118 (18), pp. 10555-10566, 2013.

[440] Shi, Y., **Zhu, X. X.**, Ellero, M., Adams, N. A.: *Analysis of interpolation schemes for the accurate estimation of energy spectrum in Lagrangian methods*, Computers & Fluids, 82 (8), pp. 122-131, 2013.

[441] **Singh, J.**, **Datcu, M.**: *SAR Image Categorization With Log Cumulants of the Fractional Fourier Transform Coefficients*, IEEE Transactions on Geoscience and Remote Sensing, 51 (12), pp. 5273-5282, 2013.

[442] **Sirmacek, B.**, **Reinartz, P.**: *Feature analysis for detecting people from remotely sensed images*, Journal of Applied Remote Sensing, 7 (1), pp. 1-13, 2013.

[443] Spurr, R., Natraj, V., Lerot, C., Roozendael, M. V., **Loyola, D.**: *Linearization of the Principal Component Analysis method for radiative transfer acceleration: Application to retrieval algorithms and sensitivity studies*, Journal of Quantitative Spectroscopy and Radiative Transfer, 125, pp. 1-17, 2013.

[444] **Storch, T.**, Habermeyer, M., Eberle, S., Mühle, H., **Müller, R.**: *Towards a Critical Design of an Operational Ground Segment for an Earth Observation Mission*, Journal of Applied Remote Sensing, 7 (1), pp. 1-12, 2013.

[445] Straub, C., **Tian, J.**, Seitz, R., **Reinartz, P.**: *Assessment of Cartosat-1 and WorldView-2 stereo imagery in combination with a LiDAR-DTM for timber volume estimation in a highly structured forest in Germany*, Forestry, 86 (4), pp. 463-473, 2013.

[446] **Tian, J.**, **Reinartz, P.**, **d'Angelo, P.**, Ehlers, M.: *Region-based automatic building and forest change detection on Cartosat-1 stereo imagery*, ISPRS Journal of Photogrammetry and Remote Sensing, 79, pp. 226-239, 2013.

[447] **Türmer, S.**, **Kurz, F.**, **Reinartz, P.**, Stilla, U.: *Airborne vehicle detection in dense urban areas using HoG features and disparity maps*, IEEE JSTARS, 6 (6), pp. 2327-2337, 2013.

[448] **Vaduva, C.**, Costachioiu, T., Patrascu, C., Gavat, I., Lazarescu, V., **Datcu, M.**: *A Latent Analysis of Earth Surface Dynamic Evolution Using Change Map Time Series*, in Proc. EUSIPCO 2012, 51 (4), pp. 2105-2117, 2013.

[449] **Vaduva, C.**, Gavat, I., **Datcu, M.**: *Latent Dirichlet Allocation for Spatial Analysis of Satellite Images*, in Proc. EUSIPCO 2012, 51 (5), pp. 2770-2786, 2013.

[450] **Vasquez, M.**, **Gottwald, M.**, ***Gimeno Garcia, S.***, Krieg, E., **Lichtenberg, G.**, **Schreier, F.**, **Slijkhuis, S.**, Snel, R., **Trautmann, T.**: *Venus observations from ENVISAT–SCIAMACHY: Measurements and modeling*, Advances in Space Research, 51, pp. 835-848, 2013.

[451] **Vasquez, M.**, **Schreier, F.**, ***Gimeno Garcia, S.***, Kitzmann, D., Patzer, B., Rauer, H., **Trautmann, T.**: *Infrared radiative transfer in atmospheres of Earth-like planets around F, G, K, and M stars. II. Thermal emission spectra influenced by clouds*, Astronomy and Astrophysics, 557 (A46), pp. 1-14, 2013.

[452] **Vasquez, M.**, **Schreier, F.**, ***Gimeno Garcia, S.***, Kitzmann, D., Patzer, B., Rauer, H., **Trautmann, T.**: *Infrared radiative transfer in atmospheres of Earth-like planets around F, G, K, and M stars - I. Clear-sky thermal emission spectra and weighting functions*, Astronomy and Astrophysics, 549 (A26), pp. 1-13, 2013.

[453] **Velotto, D.**, Nunziata, F., Migliaccio, M., **Lehner, S.**: *Dual-Polarimetric TerraSAR-X SAR Data for Target at Sea Observation*, IEEE Geoscience and Remote Sensing Letters, 10 (5), pp. 1114-1118, 2013.

[454] Venganzones, M., **Datcu, M.**, Graa, M.: *Further results on dissimilarity spaces for hyperspectral images RF-CBIR*, Pattern Recognition Letters, 34 (14), pp. 1659-1668, 2013.

[455] von Paris, P., **Hedelt, P.**, Selsis, F., **Schreier, F.**, **Trautmann, T.**: *Characterization of potentially habitable planets: Retrieval of atmospheric and planetary properties from emission spectra*, Astronomy & Astrophysics, 551, pp. 1-14, 2013.

[456] Zhou, D. R., Ding, A. J., Mao, H. T., Fu, C. B., *Wang*, T., Chan, L. Y., Ding, K., **Zhang, Y.**, Liu, J., Lu, A., **Hao, N.**: *Impacts of the East Asian monsoon on lower tropospheric ozone over coastal South China*, Environmental Research Letters, 8 (044011), pp. 1-7, 2013.

[457] **Zhu, X. X.**, **Bamler, R.**: *A Sparse Image Fusion Algorithm with Application to Pan-sharpening*, IEEE Transactions on Geoscience and Remote Sensing, 51 (5), pp. 2827-2836, 2013.

Other Publications with Full Paper Review

2018 under review[1]

[458] **Adam, N. A.**: *The Development of a High Precision Troposphere Effect Mitigation Processor for SAR Interferometry*, in Proc. IGARSS 2018, accepted, 2018.

[459] **Auer, S.**, ***Schmitt, M.***, **Reinartz, P.**: *Object-related alignment of heterogeneous image data in remote sensing*, in Proc. FUSION 2018, accepted, 2018.

[460] ***Bagheri, H.***, ***Schmitt, M.***, **Zhu, X. X.**: *Urban TanDEM-X raw DEM fusion based on TV-L1 and Huber models*, in Proc. IGARSS 2018, accepted, 2018.

[461] **Cerra, D.**, **Figueiredo Vaz Pato, M.**, **Carmona, E.**, **Azimi, S.**, **Tian, J.**, **Bahmanyar, R.**, **Kurz, F.**, **Vig, E.**, **Bittner, K.**, **Henry, C.**, **d'Angelo, P.**, **Müller, R.**, **Alonso, K.**, **Fischer, P.**, **Reinartz, P.**: *Combining Deep and Shallow Neural Networks with ad hoc Detectors for the Classification of Complex Multi-modal Urban Scenes*, in Proc. IGARSS 2018, accepted, 2018.

[462] Dabboor, M., **Singha, S.**, Montpetit, B., Deschamps, B., Flett, D.: *Assessment of simulated compact polarimetry of the RCM medium Resolution SAR modes for oil spill detection*, in Proc. IGARSS 2018, accepted, 2018.

[463] de Macedo, C. R., Buono, A., Nunziata, F., **Velotto, D.**, Migliaccio, M.: *Sea Oil Seep Monitoring Using a Time Series of Co-Polarized Coherent SAR Measurements*, in Proc. IGARSS 2018, accepted, 2018.

[464] **Dumitru, C. O.**, **Schwarz, G.**, **Datcu, M.**: *Evaluation of Retrieved Categories from a TerraSAR-X Benchmarking Data Set*, in Proc. IGARSS 2018, accepted, 2018.

[465] **Frost, A.**, **Wiehle, S.**, **Singha, S.**, Krause, D.: *Sea Ice Motion Tracking from Near Real Time SAR-data acquired during Antarctic circumnavigation expedition*, in Proc. IGARSS 2018, accepted, 2018.

[466] **Gisinger, C.**, **Balss, U.**, **Breit, H.**, Schubert, A., Garthwaite, M., Small, D., Gruber, T., **Eineder, M.**, **Fritz, T.**, Miranda, N.: *Recent Findings on the Sentinel-1 Geolocation Accuracy using the Australian Corner Reflector Array*, in Proc. 2018 IEEE International Geoscience and Remote Sensing Symposium (IGARSS), accepted, 2018.

[467] ***Grohnfeldt, C.***, ***Schmitt, M.***, **Zhu, X. X.**: *A conditional generative adversarial network to fuse SAR and multispectral optical data for cloud removal from Sentinel-2 images*, in Proc. IGARSS 2018, accepted, 2018.

[468] **Hong, D.**, **Yokoya, N.**, **Xu, J.**, **Zhu, X. X.**: *Joint & Progressive Learning from High-Dimensional Data for Multi-Label Classification*, in Proc. European Conference on Computer Vision (ECCV) 2018, accepted, 2018.

[469] **Hu, J.**, **Zhu, X.**: *Exploring Sentinel-1 Data For Local Climate Zone Classification*, in Proc. IGARSS 2018, accepted, 2018.

[470] ***Hughes, L.***, ***Schmitt, M.***, **Zhu, X. X.**: *Generative Adversarial Networks for Hard Negative Mining In CNN-based SAR-Optical Image Matching*, in Proc. IGARSS 2018, accepted, 2018.

[471] ***Kang, J.***, ***Wang, Y.***, **Zhu, X. X.**: *Multi-pass SAR interferometry for 3D reconstruction of complex mountainous areas based on robust low rank tensor decomposition*, in Proc. IGARSS 2018, accepted, 2018.

[472] **Lachaise, M.**, **Schättler, B.**: *Production Simulator for Tandem-L higher Level products*, in Proc. IGARSS 2018, accepted, 2018.

[1] Since 2017 the IGARSS conference requests full paper submissions. Therefore IGARSS papers of 2017 and 2018 are listed in this category.

[473] Louis, J., **Pflug, B.**, **Main-Knorn, M.**, Debaecker, V., Müller-Wilm, U., Gascon, F.: *Integration and Assimilation of Meteological (ECMWF) Aerosol Estimates into Sen2Cor Atmospheric Correction*, in Proc. IGARSS 2018, accepted, 2018.

[474] Nunziata, F., de Macedo, C. R., Buono, A., **Velotto, D.**, Migliaccio, M.: *On the Effects of Acquisition Parameters and Surface Properties in Sea Oil Seep Observation by Means of High–Resolution SAR*, in Proc. IGARSS 2018, accepted, 2018.

[475] ***Qiu, C.***, ***Schmitt, M.***, **Ghamisi, P.**, ***Mou, L.***, **Zhu, X. X.**: *Feature importance analysis of Sentinel-2 imagery for large-scale Urban Local Climate Zone classification*, in Proc. IGARSS 2018, accepted, 2018.

[476] ***Schmitt, M.***, **Zhu, X. X.**: *The SEN1-2 dataset for deep learning in SAR-optical data fusion*, in Proc. ISPRS TCI Symposium 2018, accepted, 2018.

[477] Sheu, C.-Y., **Kurz, F.**, **d'Angelo, P.**: *Automatic 3D lane marking reconstruction using multi-view aerial imagery*, in Proc. ISPRS TC I Midterm Symposium 2018, accepted, 2018.

[478] **Singha, S.**: *Potential of compact polarimetry for operational sea ice monitoring over Arctic and Antarctic Region*, in Proc. IGARSS 2018, accepted, 2018.

[479] **Storch, T.**, Honold, H.-P., Guanter, L., **Schwind, P.**, Mücke, M., Segl, K., Fischer, S.: *The Imaging Spectroscopy Mission EnMAP – Its Status and Expected Products*, in Proc. WHISPERS 2018, accepted, 2018.

[480] **Storch, T.**, Honold, H.-P., **Krawczyk, H.**, Wachter, R., **de los Reyes, R.**, **Langheinrich, M.**, Mücke, M., Fischer, S.: *Spectral Characterization and Smile Correction for the Imaging Spectroscopy Mission EnMAP*, in Proc. IGARSS 2018, accepted, 2018.

[481] **Storch, T.**, Reck, C., Holzwarth, S., Keuck, V.: *CODE-DE – The Germany Operational Environment for Accessing and Processing Copernicus Sentinel Products*, in Proc. IGARSS 2018, accepted, 2018.

[482] **Tian, J.**, Dezert, J., Qina, R.: *Time-series 3D Building Change Detection Based on Belief Functions*, in Proc. 21st International Conference on Information Fusion (FUSION), accepted, 2018.

[483] **Velotto, D.**, **Tings, B.**: *Performance analysis of time-frequency technique for the detection of small ships in SAR imagery at large grazing angle and moderate metocean conditions*, in Proc. IGARSS 2018, accepted, 2018.

[484] ***Wang, Y.***, ***Kang, J.***, **Zhu, X. X.**: *Fusion of SAR interferometry and social media images for 4D urban modeling*, in Proc. FUSION 2018, accepted, 2018.

[485] ***Wang, Y.***, **Zhu, X. X.**: *The SARptical dataset for joint analysis of SAR and optical image in dense urban area*, in Proc. IGARSS 2018, accepted, 2018.

[486] **Yao, W.**, **Datcu, M.**: *Deep neural networks based semantic segmentation for optical time series*, in Proc. IGARSS 2018, accepted, 2018.

2018

[487] **Ansari, H.**, **De Zan, F.**, **Bamler, R.**: *Distributed scatterer interferometry tailored to the analysis of big InSAR data*, in Proc. EUSAR 2018, pp. 1-5, 2018.

[488] Ao, D., **Datcu, M.**: *Ship Azimuth Velocity Estimation in TerraSAR-X data based on Minimum-Entropy Criterion*, in Proc. EUSAR 2018, pp. 1-4, 2018.

[489] Buckreuss, S., **Fritz, T.**, Bachmann, M., Zink, M.: *TerraSAR-X and TanDEM-X Mission Status*, in Proc. EUSAR 2018, pp. 47-51, 2018.

[490] **De Zan, F.**, **Gomba, G.**, **Yokoya, N.**: *The Ambiguities related to Closure-Phase Model Inversion*, in Proc. EUSAR 2018, pp. 1-4, 2018.

[491] **De Zan, F.**, Prats, P., Rodriguez Cassola, M.: *The theoretical performance of different algorithms for shift estimation between SAR images*, in Proc. 12th European Conference on Synthetic Aperture Radar (EUSAR), pp. 1-4, 2018.

[492] Dekker, A., Pinnel, N., **Gege, P.**, Briottet, X., Court, A., Peters, S., Turpie, K., Sterckx, S., Costa, M., Giardino, C., Brando, V., Braga, F., Bergeron, M., Heege, T., **Pflug, B.**: *Feasibility Study of an Aquatic Ecosystem Earth Observing System*, pp. 197, 2018.

[493] **Dumitru, C. O.**, **Schwarz, G.**, **Datcu, M.**: *Monitoring of Coastal Environments Using Data Mining*, in Proc. IARIA 2018: The International Workshop on Knowledge Extraction and Semantic Annotation, KESA, pp. 1-6, 2018.

[494] **Fischer, P.**, Schuegraf, P., **Merkle, N. M.**, **Storch, T.**: *An Evolutionary Algorithm for fast intensity based image matching between optical and SAR imagery*, in Proc. ISPRS TC III Mid-term Symposium, IV (3), pp. 83-90, 2018.

[495] Guan, B., Vasseur, P., Demonceaux, C., **Fraundorfer, F.**: *Visual odometry using a homography formulation with decoupled rotation and translation estimation using minimal solutions*, in Proc. International Conference on Robotics and Automation (ICRA) 2018, pp. 1-9, 2018.

[496] Hashemi, M., Rabus, B., **Lehner, S.**: *Ocean feature extraction from SAR Quicklook Imagery using Convolutional Neural Networks*, in Proc. EUSAR 2018, pp. 1-5, 2018.

[497] ***Hughes, L.***, **Auer, S.**, ***Schmitt, M.***: *Investigation of Joint Visibility Between SAR and Optical Images of Urban Environments*, in Proc. ISPRS technical Commission II Symposium 2018, IV (2), pp. 129-136, 2018.

[498] **Jacobsen, S.**, **Pleskachevsky, A.**, **Velotto, D.**: *Reducing the antenna beam pattern impact on Sentinel-1 wind fields*, in Proc. EUSAR 2018, pp. 736-740, 2018.

[499] ***Kang, J.***, ***Wang, Y.***, **Zhu, X. X.**: *Low rank modeling-based multipass InSAR technique*, in Proc. EUSAR 2018, pp. 1-6, 2018.

[500] Kjærgaard, M. B., **Werner, M.**, Sangogboye, F. C., Arendt, K.: *DCount-A Probabilistic Algorithm for Accurately Disaggregating Building Occupant Counts into Room Counts*, in Proc. 19th International Conference on Mobile Data Management, pp. 1-10, 2018.

[501] **Lachaise, M.**, **Schättler, B.**, **Fritz, T.**, **Parizzi, A.**: *Systematic generation concepts for Tandem-L products*, in Proc. EUSAR 2018, pp. 185-190, 2018.

[502] **Lehner, S.**, Schwarz, E., Soloviev, A., Dean, C.: *The Interaction of Crude Oil on the Sea Surface with Ocean Fronts observed by SAR*, in Proc. EUSAR 2018, pp. 1-5, 2018.

[503] **Parizzi, A.**, **Abdel Jaber, W.**: *Exploiting the information of the interferometric phase gradients. Examples and error characterization*, in Proc. EUSAR 2018, pp. 1-4, 2018.

[504] **Pleskachevsky, A.**, Schwarz, E., **Jacobsen, S.**, **Tings, B.**, Krause, D.: *Sea State Retrieval from Sentinel-1 Imagery as Support of Maritime Situation Awareness*, in Proc. EUSAR 2018, pp. 961-966, 2018.

[505] Reimann, J., Steinbrecher, U., **Breit, H.**, Klenk, P., Tous Ramon, N., Schwerdt, M.: *Precise SAR Antenna Pointing Determination using Phase Coherent Difference Images*, in Proc. EUSAR 2018, pp. 1-3, 2018.

[506] **Rodriguez Gonzalez, F.**, **Parizzi, A.**, **Brcic, R.**: *Evaluating the impact of geodetic corrections on interferometric deformation measurements*, in Proc. EUSAR 2018, pp. 377-381, 2018.

[507] ***Shi, Y.***, ***Wang, Y.***, ***Kang, J.***, **Lachaise, M.**, **Zhu, X. X.**, **Bamler, R.**: *3D reconstruction from very small TanDEM-X stacks*, in Proc. EUSAR 2018, pp. 257-260, 2018.

[508] **Singha, S.**, Jäger, M.: *Characterization of Arctic Sea Ice using L, S and X-Band Fully Polarimetric Airborne F-SAR System*, in Proc. European Conference on Synthetic Aperture Radar (EUSAR), pp. 441-445, 2018.

[509] **Suchandt, S.**, **Pleskachevsky, A.**, Borla Tridon, D.: *Oceanographic Data Retrieval with Tandem-L*, in Proc. EUSAR 2018, pp. 1322-1325, 2018.

[510] **Tings, B.**, **Velotto, D.**: *Ship Wake Detectability and Classification on TerraSAR-X high resolution data*, in Proc. EUSAR 2018, pp. 1307-1310, 2018.

[511] **Velotto, D.**, **Tings, B.**: *Detecting small ships in TerraSAR-X/TanDEM-X acquisitions at large grazing angle and moderate metocean conditions*, in Proc. EUSAR 2018, pp. 925-928, 2018.

[512] ***Wang, Y.***, **Zhu, X. X.**: *Robust nonlinear blind SAR tomography in urban areas*, in Proc. EUSAR 2018, pp. 594-599, 2018.

[513] **Werner, M.**: *Topology Extraction from Occupancy Grids*, in Proc. 14th International Conference on Location Based Services, pp. 133-149, 2018.

[514] **Wiehle, S.**, **Pleskachevsky, A.**: *Bathymetry derived from Sentinel-1 Synthetic Aperture Radar*, in Proc. EUSAR 2018, pp. 747-750, 2018.

[515] **Xia, Y.**, **Tian, J.**, **Angelo, P.**, **Reinartz, P.**: *Dense matching comparison between census and a convolutional neural network algorithm for plant reconstruction*, in Proc. ISPRS TC II Mid-term Symposium "Towards Photogrammetry 2020", IV (2), pp. 303-309, 2018.

[516] **Zhu, X. X.**, **Sun, Y.**, **Ge, N.**, ***Shi, Y.***, ***Wang, Y.***: *Towards Global 3D/4D Urban Modeling Using TanDEM-X Data*, in Proc. EUSAR 2018, pp. 165-170, 2018.

2017

[517] **Abdel Jaber, W.**, **Floricioiu, D.**, **Johnson, E**., Rott, H.: *Recent surface elevation changes of patagonian glaciers derived with TanDEM-X*, in Proc. 2017 IEEE International Geoscience and Remote Sensing Symposium (IGARSS), pp. 2821-2824, 2017.

[518] Anghel, A., Cacoveanu, R., **Datcu, M.**: *Phase sensitivity analysis of spaceborne transmitter - stationary ground-based receiver bistatic SAR interferometry with one imaging channel*, in Proc. IGARSS 2017, pp. 1051-1054, 2017.

[519] **Ansari, H.**, **De Zan, F.**, **Bamler, R.**: *Sequential Estimator: a Novel Approach for Efficient High-Precision Analysis of Interferometric Time Series*, in Proc. IGARSS 2017, pp. 980-983, 2017.

[520] Ao, D., **Dumitru, C. O.**, **Schwarz, G.**, **Datcu, M.**: *Coastline Detection with Time Series of SAR Images*, in Proc. SPIE Remote Sensing, pp. 1-9, 2017.

[521] **Auer, S.**, **Balss, U.**: *Simulation-based Evaluation of Light Posts and Street Signs as 3-D Geolocation Targets in SAR Images*, in Proc. HRIGI17 - High-Resolution Earth Imaging for Geospatial Information, IV-1 (W1), pp. 11-18, 2017.

[522] **Auer, S.**, ***Schmitt, M.***, **Reinartz, P.**: *Automatic Alignment of High Resolution Optical and SAR Images for Urban Areas*, in Proc. IGARSS 2017, pp. 1-4, 2017.

[523] ***Bagheri, H.***, ***Schmitt, M.***, **Zhu, X. X.**: *Fusion of TanDEM-X and Cartosat-1 DEMs using TV-Norm Regularization and ANN-Predicted Weights*, in Proc. IGARSS 2017, pp. 1-4, 2017.

[524] **Baier, G.**, **Rossi, C.**, **Lachaise, M.**, **Zhu, X. X.**, **Bamler, R.**: *Nonlocal InSAR filtering for high resolution DEM generation from TanDEM-X interferograms*, in Proc. IGARSS 2017, pp. 1-5, 2017.

[525] Borla Tridon, D., Bachmann, M., **De Zan, F.**, Krieger, G., Zink, M., Schulze, D., Moreira, A.: *Tandem-L Observation Concept - Contributions and Challenges of Systematic Monitoring of Earth System Dynamics*, in Proc. International Radar Symposium (IRS), pp. 1-9, 2017.

[526] **Cui, S.**, **Meynberg, O.**, **Reinartz, P.**: *Bayesian Linear Regression for Crowd Density Estimation in Aerial Images*, in Proc. JURSE 2017, pp. 1-4, 2017.

[527] Dabboor, M., **Singha, S.**, Topouzelis, K., Flett, D.: *Oil spill detection using simulated RADARSAT constellation mission compact polarimetric SAR data*, in Proc. IGARSS 2017, pp. 4582-4585, 2017.

[528] Damian, C., Coltuc, D., Garoi, F., **Datcu, M.**: *Improvement of submillimeter spectrometric measurement via deconvolution*, in Proc. International Symposium on Signals, Circuits and Systems (ISSCS 2017), pp. 1-4, 2017.

[529] Danisor, C., Fornaro, G., **Datcu, M.**: *Non-Linear Least Squares Algorithm for Detection of Simple and Double Persistent Scatterers*, in Proc. IGARSS 2017, pp. 6020-6023, 2017.

[530] Danisor, C., Pauciullo, A., Fornaro, G., **Datcu, M.**: *Optimization of NLLS Algorithm Using Matrix Algebra: Application on SAR Tomography*, in Proc. 25th Telecommunications Forum (TELFOR 2017), pp. 1-4, 2017.

[531] Du, P., Xia, J., **Ghamisi, P.**, Iwasaki, A., Benediktsson, J. A.: *Multiple composite kernel learning for hyperspectral image classification*, in Proc. IGARSS 2017, pp. 2223-2226, 2017.

[532] **Espinoza-Molina, D.**, **Bahmanyar, R.**, Diaz-Delgado, R., Bustamante, J., **Datcu, M.**: *Land-Cover Change Detection Using Local Feature Descriptors Extracted From Spectral Indices*, in Proc. IGARSS 2017, pp. 1938-1941, 2017.

[533] **Fischer, P.**, Plaß, B., **Kurz, F.**, **Krauß, T.**, **Runge, H.**: *Validation of HD maps for autonomous driving*, in Proc. International Conference on Intelligent Transport Systems in Theory and Practice, mobil.TUM, pp. 1-8, 2017.

[534] Focsa, A., Toma, S.-A., **Datcu, M.**: *Maximium Entropy Image Reconstruction Applied to C-Band Ground Based Synthetic Aperture Radar*, in Proc. IGARSS 2017, pp. 3437-3440, 2017.

[535] **Frost, A.**, **Jacobsen, S.**, **Singha, S.**: *High Resolution Sea Ice Drift Estimation using Combined TerraSAR-X and RADARSAT-2 Data: First Tests*, in Proc. IGARSS 2017, pp. 342-345, 2017.

[536] Geudtner, D., Prats, P., ***Yague-Martinez, N.***, **De Zan, F.**, **Breit, H.**, Larsen, Y., Monti-Guarnieri, A., Barat, I., Navas Traver, I., Torres, R.: *Sentinel-1 Constellation SAR Interferometry Performance Verification*, in Proc. ESA FRINGE Workshop, 2017.

[537] **Ghamisi, P.**, Rasti, B., **Zhu, X.**: *Feature fusion of hyperspectral and lidar data using extinction profiles and total variation*, in Proc. IGARSS 2017, pp. 2621-2624, 2017.

[538] Griparis, A., Faur, D., **Datcu, M.**: *Evaluation of Dimensionality Reduction Methods for Remote Sensing Images Using Classification and 3D Visualization*, in Proc. 18th International Conference, ACIVS 2017, pp. 203-211, 2017.

[539] Griparis, A., Georgescu, F.-A., **Datcu, M.**: *Visual Data Mining applied on Earth Observation datasets*, in Proc. IGARSS 2017, pp. 566-569, 2017.

[540] He, N., Fang, L., Li, S., **Ghamisi, P.**, Benediktsson, J. A.: *Hyperspectral images classification by fusing extinction profiles feature*, in Proc. IGARSS 2017, pp. 2267-2270, 2017.

[541] Holzmann, T., **Fraundorfer, F.**, Bischof, H.: *A Detailed Description of Direct Stereo Visual Odometry Based on Lines*, in Proc. International Joint Conference on Computer Vision, Imaging and Computer Graphics, pp. 353-373, 2017.

[542] Holzmann, T., Oswald, M., Poliefeys, M., **Fraundorfer, F.**, Bischof, H.: *Plane-based surface regularization for urban 3d construction*, in Proc. 28th British Machine Vision Conference, pp. 1-9, 2017.

[543] ***Hong, D.***, **Yokoya, N.**, Chanussot, J., **Zhu, X.**: *Learning A Low-Coherence Dictionary to Address Spectral Variability for Hyperspectral Unmixing*, in Proc. International Conference on Image Processing (ICIP 2017), pp. 1-5, 2017.

[544] ***Hu, J.***, **Mou, L.**, Schmitt, A., **Zhu, X. X.**: *FusioNet: A Two-Stream Convolutional Neural Network for Urban Scene Classification using PolSAR and Hyperspectral Data*, in Proc. JURSE 2017, pp. 1-4, 2017.

[545] ***Hu, J.***, **Wang, Y.**, **Ghamisi, P.**, **Zhu, X.**: *Evaluation of Polsar Similarity Measures with Spectral Clustering*, in Proc. IGARSS 2017, pp. 1-4, 2017.

[546] **Israel, M.**, Reinhard, A.: *Detecting nests of lapwing birds with the aid of a small unmanned aerial vehicle with thermal camera*, in Proc. International Conference on Unmanned Aircraft Systems, pp. 1-9, 2017.

[547] **Jacobsen, S.**, **Pleskachevsky, A.**, **Singha, S.**, **Velotto, D.**, **Frost, A.**: *SAR-based wind fields over offshore wind farms - a valuable tool for planning, monitoring and optimization*, in Proc. IGARSS 2017, pp. 1611-1613, 2017.

[548] ***Kang, J.***, **Wang, Y.**, ***Körner, M.***, **Zhu, X. X.**: *Improve multi-baseline InSAR parameter retrieval by semantic information from optical images*, in Proc. IGARSS 2017, pp. 1-4, 2017.

[549] Klotz, M., Wurm, M., **Zhu, X. X.**, Taubenböck, H.: *Digital deserts on the ground and from space An experimental spatial analysis combining social network and earth observation data in megacity Mumbai*, in Proc. JURSE 2017, pp. 1-4, 2017.

[550] **Langheinrich, M.**, **Fischer, P.**, **Krauß, T.**: *Modeling wind flow over complex urban terrain*, in Proc. JURSE 2017, pp. 1-4, 2017.

[551] Maccarone, M. C., Parsons, D. R., Gaug, M., **de los Reyes, R.**, et al., e. a.: *Tools and Procedures for the CTA Array Calibration*, in Proc. 35th International Cosmic Ray Conference (ICRC2017), pp. 1-8, 2017.

[552] **Main-Knorn, M.**, **Pflug, B.**, Louis, J., Debaecker, V., Gascon, F., Müller-Wilms, U.: *Sen2Cor for Sentinel-2*, in Proc. SPIE Remote Sensing, 10427, pp. 1-13, 2017.

[553] **Marmanis, D.**, Schindler, K., Wegner, J. D., **Datcu, M.**, Stilla, U.: *Semantic Segmentation of Aerial Images with Explicit Class-Boundary Modeling*, in Proc. IGARSS 2017, pp. 5165-5168, 2017.

[554] Maurer, M., Hofer, M., **Fraundorfer, F.**, Bischof, H.: *Automated Inspection of Power Line Corridors to measure Vegetation Undercut using UAV-based Images*, in Proc. ISPRS conference, pp. 33-40, 2017.

[555] **Merkle, N.**, **Fischer, P.**, **Auer, S.**, **Müller, R.**: *On the Possibility of Conditional Adversarial Networks for Multi-Sensor Image Matching*, in Proc. IGARSS 2017, pp. 1-4, 2017.

[556] Moacă, O.-M., Anghel, A., **Datcu, M.**: *Investigation of displacement measurements performed with a ground-based fixed receiver bistatic SAR simulator*, in Proc. IGARSS 2017, pp. 3814-3817, 2017.

[557] ***Montazeri, S.***, **Gisinger, C.**, **Zhu, X. X.**, **Eineder, M.**, **Bamler, R.**: *Automatic Positioning of SAR Ground Control Points from Multi-Aspect TerraSAR-X Acquisitions*, in Proc. IGARSS 2017, pp. 961-964, 2017.

[558] Moreira, A., Krieger, G., Hajnsek, I., Papathanassiou, K., Younis, M., Huber, S., Villano, M., Pardini, M., Zink, M., Zonno, M., Sanjuan Ferrer, M. J., Borla Tridon, D., Rizzoli, P., **Eineder, M.**, **De Zan, F.**, **Parizzi, A.**: *Tandem-L: Global Observation of the Earth's Surface with DinSAR, PolinSAR ans Tomography*, in Proc. ESA FRINGE Workshop, 2017.

[559] Mostegel, C., Prettenthaler, R., **Fraundorfer, F.**, Bischof, H.: *Scalable Surface Reconstruction from Point Clouds with Extreme Scale and Density Diversity*, in Proc. CVPR 2017, pp. 904-913, 2017.

[560] **Mou, L.**, **Ghamisi, P.**, **Zhu, X.**: *Fully conv-deconv network for unsupervised spectral-spatial feature extraction of hyperspectral imagery via residual learning*, in Proc. IGARSS 2017, pp. 1-4, 2017.

[561] **Mou, L.**, ***Schmitt, M.***, **Wang, Y.**, **Zhu, X. X.**: *A CNN for the identification of corresponding patches in SAR and optical imagery of urban scenes*, in Proc. JURSE 2017, pp. 1-4, 2017.

[562] **Mou, L.**, ***Schmitt, M.***, **Wang, Y.**, **Zhu, X.**: *Identifying corresponding patches in SAR and optical imagery with a convolutional neural network*, in Proc. IGARSS 2017, pp. 1-4, 2017.

[563] Prats, P., Lopez-Dekker, P., **De Zan, F.**, ***Yague-Martinez, N.***, Zonno, M., Rodriguez-Cassola, M.: *3-D Surface Deformation Performance for Simultaneous Squinted SAR Acquisitions*, in Proc. ESA FRINGE Workshop, pp. 1-4, 2017.

[564] ***Qiu, C.***, ***Schmitt, M.***, **Zhu, X. X.**: *Comparative evaluation of signal-based and descriptor-based similarity measures for SAR-optical image matching*, in Proc. IGARSS 2017, pp. 1-4, 2017.

[565] **Riedel, S.**, **Janas, J.**, **Gege, P.**, Oppelt, N.: *Deriving Aerosol Parameters from in–situ Spectrometer Measurements for Validation of Remote Sensing Products*, in Proc. SPIE Remote Sensing: Remote Sensing of Clouds and the Atmosphere XXII, 10424 (1), pp. 1-11, 2017.

[566] Rikka, S., **Pleskachevsky, A.**, Uiboupin, R., **Jacobsen, S.**: *Sea state parameters in highly variable environment of Baltic Sea from satellite radar images*, in Proc. IGARSS 2017, pp. 2965-2968, 2017.

[567] **Rossi, C.**, **Baier, G.**, Rizzoli, P., Bueso Bello, J.: *Topographical changes caused by the 2016 central Italy earthquake series*, in Proc. IGARSS 2017, pp. 5689-5692, 2017.

[568] Rott, H., Wuite, J., Nagler, T., **Floricioiu, D.**, Rizzoli, P., Helm, V.: *InSAR Scattering Phase Centre of Antarctic Snow - An Experimental Study*, in Proc. Fringe 2017, 2017.

[569] ***Rußwurm, M., Körner, M.***: Temporal Vegetation Modelling Using Long Short-Term Memory Networks for Crop Identification From Medium-Resolution Multi-Spectral Satellite Images, CVPR 2017, pp. 1496-1504, 2017.

[570] Schenk, F., **Fraundorfer, F.**: *Combining Edge Images and Depth Maps for Robust Visual Odometry*, in Proc. 28th British Machine Vision Conference, pp. 1-12, 2017.

[571] Schenk, F., **Fraundorfer, F.**: *Robust Edge-based Visual Odometry using Machine-Learned Edges*, in Proc. International Conference on Intelligent Robots and Systems (IROS) 2017, pp. 1-8, 2017.

[572] ***Schmitt, M.***, Tupin, F., **Zhu, X. X.**: *Fusion of SAR and optical remote sensing data - challenges and recent trends*, in Proc. IGARSS 2017, pp. 1-4, 2017.

[573] **Singha, S.**: *Evaluation of polarimetric features for sea ice characterization at X, C and L- band SAR*, in Proc. IGARSS 2017, pp. 338-341, 2017.

[574] Stefanik, S., **de los Reyes, R.**, Nosek, D.: *Atmospheric monitoring and array calibration in CTA using the Cherenkov Transparency Coefficient*, in Proc. 35th International Cosmic Ray Conference (ICRC2017), pp. 1-8, 2017.

[575] **Sun, Y.**, ***Shahzad, M.***, **Zhu, X.**: *Building height estimation in single SAR image using OSM building footprints*, in Proc. JURSE2017, pp. 1-4, 2017.

[576] Tanase, R., Cazacu, C., Faur, D., Sacaleanu, D. I., **Datcu, M.**: *Potential of polarimetric SAR data use for ecosystems monitoring*, in Proc. International Symposium on Signals, Circuits and Systems (ISSCS 2017), pp. 1-4, 2017.

[577] **Velotto, D.**, Marino, A., Nunziata, F.: *Backscattering analysis of offshore platforms in Gulf of Mexico via multi-polarization TerraSAR-X/TanDEM-X data*, in Proc. IGARSS 2017, pp. 3890-3893, 2017.

[578] **Velotto, D.**, **Tings, B.**, **Bentes da Silva, C. A.**: *Comparison of ship detectability between TerraSAR-X and Sentinel-1*, in Proc. 3rd International Forum on Research and Technologies for Society and Industry (RTSI), pp. 1-5, 2017.

[579] **Wang, Y.**, **Zhu, X. X.**: *Earth observation using SAR and social media images*, in Proc. CVPR 2017 EarthVision Workshop, pp. 95-103, 2017.

[580] **Wang, Y.**, **Zhu, X. X.**: *Robust blind scatterer separation in multibaseline InSAR*, in Proc. IGARSS 2017, pp. 1-4, 2017.

[581] **Yao, W.**, **Marmanis, D.**, **Datcu, M.**: *Semantic segmentation using the fully convolutional networks for SAR and optical image pairs*, in Proc. Big Data from Space (BiDS'17), pp. 289-292, 2017.

[582] **Yokoya, N.**, **Ghamisi, P.**, Xia, J.: *Multimodal, multitemporal, and multisource global data fusion for local climate zones classification based on ensemble learning*, in Proc. IGARSS, pp. 1197-1200, 2017.

2016

[583] Afanas'ev, V. P., Gryazev, A. S., Kaplya, P. S., **Efremenko, D.**, Ridzel, O. Y.: *Software tools for profile analysis of multi-layered systems by using the Elastic Peak Electron Spectroscopy*, Proc. Atomic Layer Deposition (BALD), pp. 34-37, 2016.

[584] **Andreou, C.**, **Halbritter, F.**, Rogge, D., **Müller, R.**: *Effects of the multiscaled-band partitioning on the abundance estimation*, in Proc. WHISPERS 2016, pp. 1-4, 2016.

[585] Babaee, M., Rigoll, G., **Datcu, M.**: *Position-Aware Non-negative Matrix Factorization for Satellite Image Representation*, in Proc. EUSAR 2016, pp. 410-413, 2016.

[586] Bachmann, M., Borla Tridon, D., **De Zan, F.**, Krieger, G., Zink, M.: *Tandem-L Observation Concept - An Acquisition Scenario for the Global Scientific Mapping Machine*, in Proc. EUSAR 2016, pp. 1150-1154, 2016.

[587] ***Baier, G.***, **Zhu, X. X.**, **Lachaise, M.**, **Breit, H.**, **Bamler, R.**: *Nonlocal InSAR Filtering for DEM generation and Addressing the Staircasing Effect*, in Proc. EUSAR 2016, pp. 997-1000, 2016.

[588] **Bentes da Silva, C. A.**, **Frost, A.**, **Velotto, D.**, **Tings, B.**: *Ship-Iceberg Discrimination with Convolutional Neural Networks in High Resolution SAR Images*, in Proc. EUSAR 2016, pp. 491-494, 2016.

[589] Bi, H., Zhang, B. C., **Zhu, X. X.**, Hong, W., Wu, Y.: *CFAR Detection for the Complex Approximated Message Passing Reconstructed SAR Image*, in Proc. 4th Int. Workshop on Compressed Sensing Theory and its Applications to Radar, Sonar and Remote Sensing (CoSeRa 2016), pp. 133-137, 2016.

[590] Bi, H., Zhang, B. C., **Zhu, X. X.**, Jiang, C., Wei, Z., Hong, W.: *lq Regularization Method for Spaceborne SCANSAR and TOPSAR Imaging*, in Proc. EUSAR 2016, pp. 953-956, 2016.

[591] **Brachmann, J.**, **Baumgartner, A.**, **Lenhard, K.**, **Schwarzmaier, T.**: *Calibration Procedures for Imaging Spectrometers: Improving Data Quality from Satellite Missions to UAV Campaigns*, in Proc. SPIE Remote Sensing 2016, pp. 1-12, 2016.

[592] **Cagatay, N. D.**, **Datcu, M.**: *Bag-of-visual-words model for classification of interferometric SAR images*, in Proc. EUSAR 2016, pp. 243-246, 2016.

[593] **Cagatay, N. D.**, **Datcu, M.**: *Multi-scale feature extraction approaches for classification of InSAR and phase gradient InSAR images*, in Proc. IEEE International Conference on Image Processing (ICIP), pp. 1359-1363, 2016.

[594] Chan, J.-W., **Yokoya, N.**: *Mapping land covers of Brussels capital region using spatially enhanced hyperspectral images*, in Proc. WHISPERS 2016, pp. 1-5, 2016.

[595] **Davydova, K.**, **Cui, S.**, **Reinartz, P.**: *Building footprint extraction from Digital Surface Models using Neural Networks*, in Proc. SPIE Remote Sensing 2016, 10004, pp. 1-10, 2016.

[596] de Souza, C. R., Gaidon, A., **Vig, E.**, López, A. M.: *Sympathy for the Details: Dense Trajectories and Hybrid Classification Architectures for Action Recognition*, in Proc. 14th European Conference on Computer Vision (ECCV), 9911 (P VII), pp. 697-716, 2016.

[597] **Dumitru, C. O.**, **Schwarz, G.**, **Cui, S.**, **Datcu, M.**: *Improved Image Classification by Proper Patch Size Selection: TerraSAR-X vs. Sentinel-1A*, in Proc. The 23rd International Conference on Systems, Signals and Image Processing (IWSSIP 2016), pp. 1-4, 2016.

[598] **Dumitru, C. O.**, **Schwarz, G.**, **Cui, S.**, **Espinoza Molina, D.**, **Datcu, M.**: *Semi-Automated Semantic Annotation of Big Archives of High Resolution SAR Images*, in Proc. EUSAR 2016, pp. 1-4, 2016.

[599] **Duque Biarge, S.**, **Parizzi, A.**, **De Zan, F.**, **Rodriguez Gonzalez, F.**: *Novel Approach and Analysis to Determine Absolute Heights Using a Single Long Aperture SAR Acquisition*, in Proc. EUSAR 2016, pp. 665-668, 2016.

[600] **Efremenko, D.**, **Loyola, D.**, **Doicu, A.**, **Trautmann, T.**: *Data-intensive computing in radiative transfer modelling*, in Proc. Big Data from Space (BiDS'16), pp. 188-191, 2016.

[601] **Espinoza-Molina, D.**, **Datcu, M.**: *Data mining tools for Sentinel 1 and Sentinel 2 data exploitation*, in Proc. SPIE Remote Sensing, 10004, pp. 1-9, 2016.

[602] **Espinoza-Molina, D.**, Manilici, V., **Dumitru, C.**, Reck, C., **Cui, S.**, Rotzoll, H., Hofmann, M., **Schwarz, G.**, **Datcu, M.**: *The Earth Observation Image Librarian (EOLIB): The Data Mining Component of the TerraSAR-X Payload Ground Segment*, in Proc. Big Data from Space (BidS'16), pp. 228-231, 2016.

[603] ***Fürsich, B.***, **Bamler, R.**, Augustin, S., Hübers, H.-W., **Zhu, X. X.**: *Towards single-pixel FMCW radar reconstruction*, in Proc. 4th Int. Workshop on Compressed Sensing Theory and its Applications to Radar, Sonar and Remote Sensing (CoSeRa 2016), pp. 95-99, 2016.

[604] Gaidon, A., Wang, Q., Cabon, Y., **Vig, E.**: *Virtual Worlds as Proxy for Multi-Object Tracking Analysis*, in Proc. Conference on Computer Vision and Pattern Recognition 2016, pp. 4340-4349, 2016.

[605] **Ghamisi, P.**, Souza, R., Benediktsson, J. A., **Zhu, X. X.**, Rittner, L., Lotufo, R.: *Extended Extinction Profile for the Classification of Hyperspectral Images*, in Proc. WHISPERS 2016, pp. 1-4, 2016.

[606] **Gharib Bafghi, Z.**, **Tian, J.**, **d'Angelo, P.**, **Reinartz, P.**: *A New Algorithm for Void Filling in a DSM from Stereo Satellite Images in Urban Areas*, in Proc. ISPRS Congress, III-1, pp. 55-61, 2016.

[607] **Gomba, G.**, **De Zan, F.**, **Parizzi, A.**: *Ionospheric Phase Screen and Ionospheric Azimuth Shift Estimation Combining the Split-Spectrum and Multi-Squint Methods*, in Proc. EUSAR 2016, pp. 1-4, 2016.

[608] **Gottwald, M.**, **Floricioiu, D.**: *Kryosphäre im Wandel. Polarforschung mit Radarsatelliten*, Physik in unserer Zeit, 47 (2), pp. 66-74, 2016.

[609] Griparis, A., Faur, D., **Datcu, M.**: *A dimensionality reduction approach to support visual data mining: Co-ranking-based evaluation*, in Proc. COMM 2016, pp. 391-394, 2016.

[610] Grivei, A.-C., **Radoi, A.**, **Vaduva, C.**, **Datcu, M.**: *An Active-Learning approach to the query by example retrieval in remote sensing images*, in Proc. COMM 2016, pp. 377-380, 2016.

[611] Holzmann, T., **Fraundorfer, F.**, Bischof, H.: *Regularized 3d modeling from noisy building reconstructions*, in Proc. International Conference on 3D Vision 2016, pp. 1-9, 2016.

[612] Holzmann, T., **Fraundorfer, F.**, Bischof, H.: *Direct stereo visual odometry based on lines*, in Proc. VISAPP 2016, pp. 1-11, 2016.

[613] ***Hong, D.***, **Yokoya, N.**, **Zhu, X. X.**: *The K-LLE Algorithm for Nonlinear Dimensionality Reduction of Large-Scale Hyperspectral Data*, in Proc. WHISPERS 2016, pp. 1-5, 2016.

[614] ***Hu, J.***, **Ghamisi, P.**, Schmitt, A., **Zhu, X. X.**: *Object Based Fusion of Polarimetric SAR and Hyperspectral Imaging for Land Use Classification*, in Proc. WHISPERS 2016, pp. 1-5, 2016.

[615] ***Hu, J.***, Schmitt, A., **Zhu, X. X.**: *Dual-Channel PolSAR Speckle Reduction Using Non-Local Means Filter*, in Proc. EUSAR 2016, pp. 235-238, 2016.

[616] Isop, W. A., Pestana Puerta, J., Ermacora, G., **Fraundorfer, F.**, Schmalstieg, D.: *Micro Aerial Projector - stabilizing projected images of an airborne robotics projection platform*, in Proc. IROS 2016, pp. 5618-5625, 2016.

[617] Jetley, S., Murray, N., **Vig, E.**: *End-to-End Saliency Mapping via Probability Distribution Prediction*, in Proc. Conference on Computer Vision and Pattern Recognition 2016, pp. 5753-5761, 2016.

[618] ***Koch, T.***, **d'Angelo, P.**, **Kurz, F.**, **Fraundorfer, F.**, **Reinartz, P.**, ***Körner, M.***: *The TUM-DLR Multimodal Earth Observation Evaluation Benchmark*, in Proc. Conference on Computer Vision and Pattern Recognition, pp. 19-26, 2016.

[619] ***Koch, T.***, ***Körner, M.***, **Fraundorfer, F.**: *Automatic Alignment of Indoor and Outdoor Building Models using 3D Line Segments*, in Proc. Conference on Computer Vision and Pattern Recognition, pp. 10-18, 2016.

[620] ***Koch, T.***, **Zhuo, X.**, **Reinartz, P.**, **Fraundorfer, F.**: *A New Paradigm for Matching UAV- and Aerial Images*, in Proc. ISPRS Congress, III-3, pp. 83-90, 2016.

[621] **Köhler, C.**: *Optical Properties of Mineral Dust Aerosol in the Thermal Infrared*, in Proc. International Radiation Symposium 2016, pp. 050001_1-050001_4, 2016.

[622] Krieger, G., Moreira, A., Zink, M., Hajnsek, I., Huber, S., Villano, M., Papathanassiou, K., Younis, M., López Dekker, F., Pardini, M., Schulze, D., Bachmann, M., Borla Tridon, D., Reimann, J., Bräutigam, B., Steinbrecher, U., Tienda Herrero, C., Sanjuan-Ferrer, M. J., Zonno, M., **Eineder, M.**, **De Zan, F.**, **Parizzi, A.**, **Fritz, T.**, Diedrich, E., Maurer, E., Münzenmayer, R., Grafmüller, B., Wolters, R., te Hennepe, F., Ernst, R., Bewick, C.: *Tandem-L: Main Results of the Phase A Feasibility Study*, in Proc. IEEE International Geoscience and Remote Sensing Symposium (IGARSS), pp. 1-4, 2016.

[623] **Lachaise, M.**, **Fritz, T.**: *Update of the Interferometric Processing Algorithms for the TanDEM-X High Resolution DEMs*, in Proc. EUSAR, pp. 550-553, 2016.

[624] Lonjou, V., Desjardins, C., Hagolle, O., Petrucci, B., Tremas, T., Dejus, M., **Makarau, A.**, **Auer, S.**: *MACCS-ATCOR joint algorithm (MAJA)*, in Proc. SPIE Remote Sensing, 10001, pp. 1-13, 2016.

[625] **Makarau, A.**, **Richter, R.**, **Zekoll, V.**, **Reinartz, P.**: *Cirrus Removal in Multispectral Data without 1.38 µm Spectral Data*, in Proc. XXIII ISPRS Congress, III-7, pp. 41-44, 2016.

[626] **Marmanis, D.**, Wegner, J. D., Galliani, S., Schindler, K., **Datcu, M.**, Stilla, U.: *Semantic Segmentation of Aerial Images with an Ensemble of CNSS*, in Proc. ISPRS Congress, III-3, pp. 473-480, 2016.

[627] **Mattyus, G.**, Wang, S., Fidler, S., Urtasun, R.: *HD Maps: Fine-grained Road Segmentation by Parsing Ground and Aerial Images*, in Proc. Conference on Computer Vision and Pattern Recognition, pp. 1-9, 2016.

[628] Mostegel, C., Rumpler, M., **Fraundorfer, F.**, Bischof, H.: *UAV-based Autonomous Image Acquisition with Multi-View Stereo Quality Assurance by Confidence Prediction*, in Proc. 7th International Workshop on Computer Vision in Vehicle Technology (CVVT 2016), pp. 1-17, 2016.

[629] Mostegel, C., Rumpler, M., **Fraundorfer, F.**, Bischof, H.: *Using Self-Contradiction to Learn Confidence Measures in Stereo Vision*, in Proc. Conference on Computer Vision and Pattern Recognition 2016, pp. 4067-4076, 2016.

[630] **Parizzi, A.**, **De Zan, F.**, **Rodriguez Gonzalez, F.**, **Eineder, M.**: *Study of the impact of Polarization for Distributed Targets Interferometry*, in Proc. EUSAR 2016, pp. 134-136, 2016.

[631] Quan, X., Zhang, B. C., **Zhu, X. X.**, Hong, W., Wu, Y.: *DPCA Imaging from Nonuniform Sampling: an lq Regularization Based Approach*, in Proc. EUSAR 2016, pp. 1-4, 2016.

[632] **Ressel, R.**, **Singha, S.**, **Lehner, S.**: *Investigations into the X and C band Quad-Pol features for sea ice classification*, in Proc. EUSAR 2016, pp. 590-593, 2016.

[633] Schenk, F., Mohr, L., Rüther, M., **Fraundorfer, F.**, Bischof, H.: *Guided sparse camera pose estimation*, in Proc. OAGM Workshop 2016, pp. 139-146, 2016.

[634] ***Schmitt, M.***, **Zhu, X. X.**: *Forest Analysis by Single-Pass Millimeterwave SAR Tomography*, in Proc. EUSAR 2016, pp. 40-43, 2016.

[635] **Singha, S.**, **Ressel, R.**, **Lehner, S.**: *Offshore pollution monitoring using fully-polarimetric X- and C-band synthetic aperture radar: a near-real-time perspective*, in Proc. SPIE Asia-Pacific Remote Sensing Symposium, 9878, pp. 1-13, 2016.

[636] **Singha, S.**, **Ressel, R.**, **Lehner, S.**: *Investigations into the X and C band Quad-Pol features for oil slick characterization*, in Proc. EUSAR 2016, pp. 583-586, 2016.

[637] Stancalie, G., Craciunescu, V., Dana Negula, I., Nedelcu, I., Serban, F., Teleaga, D., Tomas, S., Faur, D., **Datcu, M.**, Virsta, A.: *Development of a downstream emergency response service for disaster hazard management based on Earth observation data*, AgroLife Scientific Journal, 5 (1), pp. 199-208, 2016.

[638] **Storch, T.**, **Fischer, P.**, **Fast, S.**, Philipp, S., **Krauß, T.**, **Müller, R.**: *Towards Fast Morphological Mosaicking of High-Resolution Multi-Spectral Products – On Improvements of Seamlines*, in Proc. ISPRS 2016, III-1, pp. 91-98, 2016.

[639] **Tian, J.**, Qinb, R., **Cerra, D.**, **Reinartz, P.**: *Building Change Detection in Very High Resolution Satellite Stereo Image Time Series*, in Proc. ISPRS Congress, III-7, pp. 149-155, 2016.

[640] **Wang, Y.**, **Zhu, X. X.**: *Practical demonstration of robust InSAR optimization for multipass InSAR*, in Proc. EUSAR 2016, pp. 879-883, 2016.

[641] Wessel, B., Breunig, M., Bachmann, M., Huber, M., Martone, M., **Lachaise, M.**, **Fritz, T.**, Zink, M.: *Concept and first example of TanDEM-X high-resolution DEM*, in Proc. EUSAR 2016, pp. 554-557, 2016.

[642] **Yokoya, N.**, **Ghamisi, P.**: *Land-cover monitoring using time-series hyperspectral data via fractional-order Darwinian particle swarm optimization*, in Proc. WHISPERS 2016, pp. 1-5, 2016.

[643] **Yokoya, N.**, **Zhu, X. X.**, Plaza, A.: *Graph-regularized coupled spectral unmixing for multisensor time-series analysis*, in Proc. WHISPERS 2016, pp. 1-5, 2016.

2015

[644] **Andreou, C.**, Rogge, D., Rivard, B., **Müller, R.**: *A novel approach for endmember bundle extraction using spectral space splitting*, in Proc. WHISPERS 2015, pp. 1-4, 2015.

[645] **Auer, S.**, Donaubauer, A.: *Buildings in High Resolution SAR Images - Identification based on CityGML Data*, in Proc. Photogrammetric Image Analysis (PIA) 2015, pp. 9-16, 2015.

[646] **Bahmanyar, R.**, Murillo, A.: *Evaluating the Sensory Gap for Earth Observation Images Using Human Perception and an LDA-Based Computational Model*, in Proc. IEEE International Conference on Image Processing (ICIP), pp. 566-570, 2015.

[647] **Bieniarz, J.**, **Cerra, D.**, **Zhu, X. X.**, **Müller, R.**, **Reinartz, P.**: *Hyperspectral Resolution Enhancement Using Multisensor Image Data*, in Proc. WHISPERS 2015, pp. 1-4, 2015.

[648] Boerner, W., Krieger, G., Reigber, A., Hajnsek, I., Schmullius, C., Moreira, A., **Eineder, M.**, **Bamler, R.**, Meyer, F.-J., Hensley, S., van Zyl, J. J., Neumann, M., Shimada, M., Ohki, M., Sumantyo, J., Hattori, K., Ocampo-Torres, F., Ponce, O., Moreira, J., Campos, J., Lu, Y.-L., Dubois-Fernandez, P., Pottier, E., Le Toan, T., Surussavadee, C., Koo, V.-C., Lim, V.-C., Triharjanto, R., Hasbi, W., Mohan, S., Singh, G.,: *Development of new multi-band equatorially orbiting POLinSAR satellite sensors system configurations for varying latitudinal coverage within total tropical belt (Invited Group presentation for establishing an associated Consortium)*, in: Proc. Asian Pacific Conference on Synthetic Aperture Radar (APSAR), pp. 1-4, 2015.

[649] Buckreuss, S., Steinbrecher, U., **Schättler, B.**: *The TerraSAR-X Mission*, in Proc. Asia-Pacific Conference on Synthetic Aperture Radar (APSAR), 2015.

[650] **Cagatay, N. D.**, **Datcu, M.**: *Classification of Interferometric SAR Images Based on Parametric Modeling in the Fractional Fourier Transform Domain*, in Proc. IEEE International Conference on Image Processing (ICIP), pp. 1364-1368, 2015.

[651] **Cerra, D.**, **Bieniarz, J.**, **Storch, T.**, **Müller, R.**, **Reinartz, P.**: *Restoration of EnMAP Data through Sparse Reconstruction*, in Proc. Whispers 2015, pp. 1-4, 2015.

[652] **Cui, S.**, **Schwarz, G.**, **Datcu, M.**: *Image Classification: No Features, no Clustering*, in Proc. ICIP 2015, pp. 1960-1964, 2015.

[653] **Davydova, K.**, **Kuschk, G.**, Hoegner, L., **Reinartz, P.**, Stilla, U.: *Consistent Multi-View Texturing of Detailed 3D Surface Models*, in Proc. Photogrammetric Image Analysis (PIA) 2015, pp. 25-31, 2015.

[654] **Dumitru, C.**, **Cui, S.**, **Datcu, M.**: *A Study of Multi-Sensor Satellite Image Indexing*, in Proc. JURSE 2015, pp. 1-4, 2015.

[655] **Fraundorfer, F.**: *Building and site reconstruction from small scale unmanned aerial vehicles (UAV's)*, in Proc. JURSE 2015, pp. 1-4, 2015.

[656] ***Grohnfeldt, C.***, Burns, T. M., **Zhu, X. X.**: *Dynamic Dictionary Learning Strategies for Sparse Representation Based Hyperspectral Image Enhancement*, in Proc. WHISPERS 2015, pp. 1-4, 2015.

[657] ***Grohnfeldt, C.***, **Zhu, X. X.**, **Bamler, R.**: *Splitting the Hyperspectral-Multispectral Image Fusion Problem into Weighted Pan-sharpening Problems - The Spectral Grouping Concept*, in Proc. WHISPERS 2015, pp. 1-4, 2015.

[658] Holzmann, T., Prettenthaler, R., Pestana, J., Muschick, D., Mostengel, C., **Fraundorfer, F.**, Bischof, H., Graber, G.: *Performance Evaluation of Vision-Based Algorithms for MAVs*, in Proc. OAGM Workshop 2015, pp. 1-8, 2015.

[659] ***Hu, J.***, **Guo, R.**, **Zhu, X.**, ***Baier, G.***, **Wang, Y.**: *Non-Local Means Filter for Polarimetric SAR Speckle Reduction-Experiments Using Terrasar-X Data*, in Proc. PIA15+HRIGI15, II-3 (W4), pp. 71-77, 2015.

[660] **Krauß, T.**: *Preprocessing of Satellite Data for Urban Object Extraction*, in Proc. Photogrammetric Image Analysis (PIA) 2015, pp. 115-120, 2015.

[661] Martone, M., Gonzalez, C., Bräutigam, B., **Duque, S.**, **Fritz, T.**: *Bandwidth Considerations in Range and Azimuth for Interferometric Applications*, Bandwidth Considerations in Range and Azimuth for Interferometric Applications, pp. 43, 2015.

[662] **Mattyus, G.**, **Fraundorfer, F.**: *Aerial image mosaicking with online calibration - A feasibility study*, in Proc. Conference of the Hungarian Association for Image Processing and Pattern Recognition, pp. 1-8, 2015.

[663] **Mattyus, G.**, Wang, S., Fidler, S., Urtasun, R.: *Enhancing Road Maps by Parsing Aerial Images Around the World*, in Proc. International Conference on Computer Vision, pp. 1689-1697, 2015.

[664] **Merkle, N.**, **Müller, R.**, **Schwind, P.**, **Palubinskas, G.**, **Reinartz, P.**: *A New Approach for Optical and SAR Satellite Image Registration*, in Proc. PIA15+HRIGI15, II-3/W, pp. 119-126, 2015.

[665] Moreira, A., Krieger, G., Hajnsek, I., Papathanassiou, K., Younis, M., Lopez-Dekker, P., Huber, S., **Eineder, M.**, Shimada, M., Motohka, T., Watanabe, M., Ohki, M., Uematsu, A., Ozawa, S.: *ALOS-Next/Tandem-L: A Highly Innovative SAR Mission for Global Observation of Dynamic Processes on the Earth's Surface*, in Proc. IGARSS 2015, pp. 1253-1256, 2015.

[666] Orthuber, E., **Avbelj, J.**: *3D Building Reconstruction from LIDAR Point Clouds by Adaptive Dual Contouring*, in Proc. PIA15+HRIGI15 – Joint ISPRS conference, II-3 (W4), pp. 157-164, 2015.

[667] Özcan, A. H., Ünsalan, C., **Reinartz, P.**: *Sparse People Group and Crowd Detection using Spatial Point Statistics in Airborne Images*, in Proc. 7th International Conference on Recent Advances in Space Technologies (RAST) 2015, pp. 307-310, 2015.

[668] Özcan, A. H., Ünsalan, C., **Reinartz, P.**: *Crowd Detection in Airborne Images using Spatial Point Statistics*, in Proc. 23th Signal Processing and Communications Applications Conference (SIU), 2015, pp. 419-422, 2015.

[669] **Palubinskas, G.**, **Reinartz, P.**: *Template based matching of optical and SAR Imagery*, in Proc. JURSE 2015, pp. 1-4, 2015.

[670] **Partovi, T.**, Huang, H., **Krauß, T.**, Mayer, H., **Reinartz, P.**: *Statistical Building Proof Reconstruction from Worldview-2 Stereo Imagery*, in Proc. Photogrammetric Image Analysis (PIA) 2015, 43 (W2), pp. 161-167, 2015.

[671] Rahimi, S., **Arefi, H.**, **Bahmanyar, R.**: *Automatic Road Extraction Based on Integration of High Resolution LiDar and Aerial Imagery*, in Proc. 3rd International Conference on Geoinformation Modeling and Environmental Monitoring (SMPR), pp. 1-5, 2015.

[672] ***Schmitt, M.***: *Three-dimensional Reconstruction of Urban Areas by Multi-aspect TomoSAR Data Fusion*, in Proc. JURSE 2015, pp. 1-4, 2015.

[673] ***Schmitt, M.***, Stilla, U.: *Möglichkeiten der Erzeugung städtischer Oberflächenmodelle mit interferometrischer SAR-Fernerkundung*, gis.SCIENCE, 28 (2), pp. 62-70, 2015.

[674] ***Shahzad, M.***, ***Schmitt, M.***, **Zhu, X. X.**: *Segmentation and crown parameter extraction of indiviudal trees in an airborne TomoSAR point cloud*, in Proc. PIA15+HRIGI15 – Joint ISPRS conference, XL-3/W, pp. 205-209, 2015.

[675] ***Shahzad, M.***, **Zhu, X. X.**: *Detection of Buildings in Spaceborne TomoSAR Point Clouds via Hybrid Region Growing and Energy Minimization Technique*, in Proc. JURSE 2015, pp. 1-4, 2015.

[676] ***Shahzad, M.***, **Zhu, X. X.**: *Reconstruction of Building Footprints using Spaceborne TOMOSAR Point Clouds*, in Proc. CMRT 2015, pp. 385-392, 2015.

[677] ***Shi, Y.***, **Zhu, X.**, **Bamler, R.**: *Optimized parallelization of non-local means filter for image noise reduction of InSAR image*, in Proc. 2015 IEEE International Conference on Information and Automation, pp. 1515-1518, 2015.

[678] Tanase, R., **Vaduva, C.**, **Datcu, M.**, Raducanu, D.: *A Validation of ICA Decomposition for PolSAR Images by Using Measures of Normalized Compression Distance*, in Proc. IEEE International Conference on Image Processing (ICIP) 2015, pp. 2369-2373, 2015.

[679] **Tian, J.**, Dezert, J., **Reinartz, P.**: *Refined Building Change Detection in Satellite Stereo Imagery Based on Belief Functions and Reliabilities*, in Proc. IEEE 2015 International Conference on Multisensor Fusion and Integration for Intelligent Systems, pp. 160-165, 2015.

[680] **Tian, J.**, **Reinartz, P.**, Dezert, J.: *Building change detection in satellite stereo imagery based on belief functions*, in Proc. JURSE 2015, pp. 1-4, 2015.

[681] Tscharf, A., Rumpler, M., **Fraundorfer, F.**, Mayer, G., Bischof, H.: *On the use of uavs in mining and archaeology - geo-accurate 3d reconstructions using various platforms and terrestrial views*, in Proc. International Conference on Unmanned Aerial Vehicles in Geomatics, II-1/ (W1), pp. 15-22, 2015.

[682] Ulmer, F.-G.: *Cinderella: Method Generalisation of the Elimination Process to Filter Repeating Patterns*, in Proc. IEEE International Conference on Digital Signal Processing 2015, pp. 1001-1005, 2015.

[683] Wang, Y., **Zhu, X. X.**: *Semantic interpretation of InSAR estimates using optical images with application to urban infrastructure monitoring*, in Proc. CMRT 2015, pp. 1-8, 2015.

[684] Wang, Y., **Zhu, X. X.**: *The robust InSAR optimization framework with application to monitoring cities on volcanoes*, in Proc. JURSE 2015, pp. 1-4, 2015.

[685] Yokoya, N., **Zhu, X. X.**: *Graph Regularized Coupled Spectral Unmixing for Change Detection*, in Proc. WHISPERS 2015, pp. 1-4, 2015.

2014

[686] Adam, N.: *Algorithmic PSI Improvement in Mountainous Areas by Atmosphere Mitigation*, Terrafirma (ESA) Technical Note, pp. 98, 2014.

[687] Alonso Gonzalez, K., **Datcu, M.**: *Accelerated Knowledge-Driven Image Mining System for Data Fusion in Big Data*, in Proc. ESA-EUSC-JRC 2014, pp. 97-100, 2014.

[688] Babaee, M., **Bahmanyar, R.**, **Datcu, M.**, Rigoll, G.: *Interactive clustering for SAR image understanding*, in Proc. EUSAR 2014, pp. 634-637, 2014.

[689] Babaee, M., **Bahmanyar, R.**, Rigoll, G., **Datcu, M.**: *Farness Preserving Non-Negative Matrix Factorization*, in Proc. ICIP 2014, pp. 1-5, 2014.

[690] Babaee, M., Rigoll, G., **Bahmanyar, R.**, **Datcu, M.**: *Locally Linear Salient Coding for image classification*, in Proc. 12th International Workshop on Content-Based Multimedia Indexing (CBMI), pp. 1-4, 2014.

[691] Babaee, M., Rigoll, G., **Datcu, M.**: *Visualization of Image Collection in 3D: Application to Immersive Information Mining*, in Proc. ESA-EUSC-JRC 2014, pp. 107-111, 2014.

[692] Babaee, M., Tsoukalas, S., Babaee, M., Rigoll, G., **Datcu, M.**: *Dimensionality Reduction using Relative Attributes*, in Proc. European Conference on Computer Vision (ECCV) 2014, pp. 1-5, 2014.

[693] Babaee, M., Tsoukalas, S., Rigoll, G., **Datcu, M.**: *Discriminative Feature Learning from SAR Images for Data Clustering*, in Proc. Big Data from Space - BiDS'14, pp. 283-286, 2014.

[694] Babaee, M., Tsoukalas, S., Rigoll, G., **Datcu, M.**: *Interactive Visualization based Active Learning*, in Proc. European Conference on Computer Vision (ECCV) 2014, pp. 1-4, 2014.

[695] Babaee, M., Tsoukalas, S., Schenk, S., Rigoll, G., **Datcu, M.**: *Immersive Visualization of SAR Images Using Nonnegative Matrix Factorization*, in Proc. Big Data from Space - BiDS'14, pp. 385-388, 2014.

[696] Babaee, M., Yu, X., **Datcu, M.**: *Immersive Visual Analytic of Earth Observation Data*, in Proc. Big Data from Space - BiDS'14, pp. 381-384, 2014.

[697] Bahmanyar, R., **Datcu, M.**, Rigoll, G.: *Comparing the information extracted by feature descriptors from EO images using Huffman coding*, in Proc. 12th International Workshop on Content-Based Multimedia Indexing (CBMI), pp. 1-6, 2014.

[698] Bahmanyar, R., Yao, W., **Cui, S.**, Loffeld, O., **Datcu, M.**: *Exploring high Resolution Satellite Image Collections Using their High-Level Features*, in Proc. ESA-EUSC-JRC 2014, pp. 77-80, 2014.

[699] Balss, U., Gisinger, C., ***Cong, X.***, **Brcic, R.**, **Hackel, S.**, **Eineder, M.**: *Precise Measurements on the Absolute Localization Accuracy of TerraSAR-X on the Base of Far-Distributed Test Sites*, in Proc. EUSAR 2014, pp. 993-996, 2014.

[700] Bentes da Silva, C. A., **Tings, B.**, **Lehner, S.**: *Ship Detection on Wide ScanSAR TerraSAR-X Images*, in Proc. EUSAR 2014, pp. 708-711, 2014.

[701] Bieniarz, J., Aguilera, E., **Zhu, X. X.**, **Müller, R.**, **Reinartz, P.**: *Spectral-Spatial Joint Sparsity Unmixing of Hyperspectral Data using Overcomplete Dictionaries*, in Proc. WHISPERS 2014, pp. 1-4, 2014.

[702] Breit, H., Fischer, M., **Balss, U.**, **Fritz, T.**: *TerraSAR-X Staring Spotlight Processing and Products*, in Proc. EUSAR 2014, pp. 193-196, 2014.

[703] Cagatay, N. D., **Datcu, M.**: *Scene Recognition Based on Phase Gradient InSAR Images*, in Proc. ICIP 2014, pp. 1-5, 2014.

[704] Cagatay, N. D., **Datcu, M.**: *Complex-valued Markov Random Field Based Feature Extraction for InSAR Images*, in Proc. EUSAR 2014, pp. 620-623, 2014.

[705] ***Cong, X.***, **Eineder, M.**: *Monitoring Active Volcanoes Using Advanced SAR Interferometric Methods*, in Proc. EUSAR 2014, pp. 838-841, 2014.

[706] Costăchioiu, T., Constantinescu, R., **Datcu, M.**: *Multitemporal Satellite Image Time Series Analysis of Urban Development in Bucharest and Ilfov Areas*, in Proc. 10th International Conference on Communications (COMM), 2014, pp. 1-4, 2014.

[707] Cui, S., **Datcu, M.**: *A Comparative Study of Sample Selection Strategies Based on Optimum Experimental Design for SAR Image Classification*, in Proc. ESA-EUSC-JRC 2014, pp. 1-4, 2014.

[708] Cui, S., **Datcu, M.**: *Supervised Incremental Feature Coding for SAR Image Classification*, in Proc. ESA-EUSC-JRC 2014, pp. 85-88, 2014.

[709] Datcu, M., **Singh, J.**: *Phase-Scale Analysis of Complex-Valued SAR Images*, in Proc. EUSAR 2014, pp. 1121-1124, 2014.

[710] Dumitru, O., **Cui, S.**, **Schwarz, G.**, **Datcu, M.**: *A Taxonomy for High Resolution SAR Images*, in Proc. ESA-EUSC-JRC 2014, pp. 89-92, 2014.

[711] Duque Biarge, S., **Balss, U.**, ***Cong, X.***, **Yague-Martinez, N.**, **Fritz, T.**: *Absolute Ranging for Maritime Applications using TerraSAR-X and TanDEM-X Data*, in Proc. EUSAR 2014, pp. 1405-1408, 2014.

[712] Efremenko, D., **Loyola, D.**, **Doicu, A.**, Spurr, R.: *Multi-core-CPU and GPU-accelerated radiative transfer models used for trace gas retrieval*, in Proc. Big Data From Space (BiDS'14), pp. 259-262, 2014.

[713] Erten, E., **Rossi, C.**, Yuzugullu, O., Hajnsek, I.: *Phenological growth stages of paddy rice according to the BBCH scale and SAR images*, in Proc. IEEE International Geoscience and Remote Sensing Symposium (IGARSS), pp. 1017-1020, 2014.

[714] Espinoza-Molina, D., Chadalawada, J., **Datcu, M.**: *SAR image content retrieval by speckle robust compression based methods*, in Proc. EUSAR 2014, pp. 650-653, 2014.

[715] Espinoza-Molina, D., **Datcu, M.**, Teleaga, D., Balint, C.: *Application of Visual Data Mining for Earth Observation Use Cases*, in Proc. ESA-EUSC-JRC 2014, pp. 111-114, 2014.

[716] Fritz, T., **Breit, H.**, **Lachaise, M.**, **Rossi, C.**, **Yague-Martinez, N.**: *Processing Strategies for Global Interferometric TanDEM-X DEM Generation*, in Proc. EUSAR 2014, pp. 1-4, 2014.

[717] Gege, P.: *A case study at Starnberger See for hyperspectral bathymetry mapping using inverse modeling*, in Proc. WHISPERS 2014, pp. 1-4, 2014.

[718] Georgescu, F.-A., **Vaduva, C.**, **Datcu, M.**, Răducanu, D.: *A Framework for Benchmarking of Feature Extraction Methods in Earth Observation image Analysis*, in Proc. ESA-EUSC-JRC 2014, pp. 81-84, 2014.

[719] Gisinger, C., **Balss, U.**, **Eineder, M.**, Hugentobler, U.: *Atmosphärische Korrekturen für TerraSAR-X basierend auf GNSS Beobachtungen*, in Proc. 34. Wissenschaftlich Technische Jahrestagung der DGPF, 23, pp. 161-1-161-6, 2014.

[720] Gleich, D., **Singh, J.**: *Wavelet-Fourier Descriptors for SAR Patch Scene Categorization*, in Proc. ESA-EUSC-JRC 2014, pp. 17-20, 2014.

[721] **Grohnfeldt, C.**, **Zhu, X. X.**, **Bamler, R.**: *The J-SparseFI-HM Hyperspectral Resolution Enhancement Method - Now Fully Automated.*, in Proc. WHISPERS 2014, pp. 1-4, 2014.

[722] **Guo, R.**, **Zhu, X. X.**: *High-rise building feature extraction using high resolution spotlight TanDEM-X data*, in Proc. EUSAR 2014, pp. 55-58, 2014.

[723] Hajnsek, I., Shimada, M., **Eineder, M.**, Papathanassiou, K., Motooka, T., Watanabe, M., Ohki, M., **De Zan, F.**, López Dekker, F., Krieger, G., Moreira, A.: *Tandem-L: Science Requirements and Mission Concept*, in Proc. European Conference on Synthetic Aperture Radar (EUSAR), pp. 1-4, 2014.

[724] Kevin, A., **Datcu, M.**: *Image Information Mining: an Accelerated Bayesian Algorithm for Data Fusion of SAR Big Data*, in Proc. EUSAR 2014, pp. 604-607, 2014.

[725] Koukouli, M., Zyrichidou, I., Balis, D., Lerot, C., Van Roozendael, M., **Loyola, D.**, Coldewey-Egbers, M., Zehner, C.: *Validation of an improved European long-term multi-sensor total ozone record as part of the ESA Climate Change Initiative*, in: Proc. 12th International Conference on Meteorology, Climate and Atmospheric Physics (COMECAP), pp. 60-64, 2014.

[726] **Lachaise, M.**, **Fritz, T.**, **Eineder, M.**: *Dual-Baseline Phase Unwrapping Challenges in the TanDEM-X Mission*, in Proc. EUSAR 2014, pp. 1129-1132, 2014.

[727] Lee, G. H., Pollefeys, M., ***Fraundorfer, F.***: *Relative pose estimation for a multicamera system with known vertical direction*, in; Proc. IEEE Conference on Computer Vision and Pattern Recognition (CVPR), pp. 540-547, 2014.

[728] Murillo, A., Nistor, N., **Datcu, M.**: *A Case Study for User Evaluation of a CBIR Tool: an Application of Open-Ended Feedback with Comment Clustering and Inductive Categorization*, in Proc. ESA-EUSC-JRC 2014, pp. 93-96, 2014.

[729] Murillo, A., Nistor, N., **Datcu, M.**: *Creating a Reference Data Set for Satellite Image Content Based Retrieval*, in Proc. Big Data from Space - BiDS'14, pp. 71-75, 2014.

[730] Nikolaou, C., Kyzirakos, K., Bereta, K., Dogani, K., Giannakopoulou, S., Smeros, P., Garbis, G., Koubarakis, M., **Espinoza-Molina, D.**, **Dumitru, C.**, **Schwarz, G.**, **Datcu, M.**: *Big, Linked and Open Data: Applications in the German Aerospace Center*, in Proc. 11th Extended Semantic Web Conference (ESWC) 2014, pp. 444-449, 2014.

[731] Nikolaou, C., Kyzirakos, K., Bereta, K., Dogani, K., Giannakopoulou, S., Smeros, P., Garbis, G., Koubarakis, M., **Espinoza-Molina, D.**, **Dumitru, C.**, **Schwarz, G.**, **Datcu, M.**: *Improving Knowledge Discovery from Synthetic Aperture Radar Images Using the Linked Open Data Cloud and Sextant*, in Proc. ESA-EUSC-JRC 2014, pp. 63-66, 2014.

[732] Özcan, A. H., Cem, Ü., **Reinartz, P.**: *A Probabilistic Approach to Building Change Detection*, in Proc. 2014 IEEE 22nd Signal Processing and Communications Applications Conference (SIU 2014), pp. 489-492, 2014.

[733] Özcan, A. H., Cem, Ü., **Reinartz, P.**: *A Systematic Approach for Building Change Detection using Multi-Source Data*, in Proc. 2014 IEEE 22nd Signal Processing and Communications Applications Conference (SIU 2014), pp. 477-480, 2014.

[734] **Palubinskas, G.**: *Mystery behind Similarity Measures MSE and SSIM*, in Proc. ICIP 2014, pp. 575-579, 2014.

[735] **Parizzi, A.**, Papathanassiou, K., **Eineder, M.**: *Study of the impact of Polarizations for DInSAR Displacement Measures*, in Proc. EUSAR 2014, pp. 1-4, 2014.

[736] Patrascu, C., Faur, D., Popescu, A., **Datcu, M.**: *A - Class Evolution Data Analytics from SAR Image Time Series Using Information Theory Measures*, in Proc. ICIP 2014, pp. 1-5, 2014.

[737] Pătrașcu, C., Popescu, A., **Datcu, M.**: *Adaptive Multilooking for Long Term Monitoring of Critical Infrastructure*, in Proc. EUSAR 2014, pp. 552-555, 2014.

[738] **Radoi, A.**, **Datcu, M.**: *A L2-Norm Regularized Pseudo-Code for Change Analysis in Satellite Image Time Series*, in Proc. First International Workshop on Learning over Multiple Contexts (LMCE 2014), pp. 1-13, 2014.

[739] **Radoi, A.**, **Datcu, M.**: *Learned Atoms from Multispectral Satellite Image Time Series*, in Proc. ESA-EUSC-JRC 2014, pp. 71-75, 2014.

[740] **Radoi, A.**, Tanase, R., **Datcu, M.**: *Change Maps for Pairs of Images Extracted from Satellite Image Time Series*, in Proc. Big Data from Space - BiDS'14, pp. 132-135, 2014.

[741] **Ressel, R.**, **Lehner, S.**: *Texture-based sea ice classification on TerraSAR-X imagery*, in Proc. IAHR-ICE 2014, pp. 503-509, 2014.

[742] Romeiser, R., **Runge, H.**: *Measuring the Temporal Autocorrelation Function of Backscattered X-Band Signals From the Ocean With TanDEM-X*, in Proc. EUSAR 2014, pp. 1299-1301, 2014.

[743] **Rossi, C.**, **Eineder, M.**, **Fritz, T.**: *Detecting Building Layovers in a SAR Interferometric Processor Without External References*, in Proc. EUSAR 2014, pp. 59-62, 2014.

[744] Saurer, O., Vasseur, P., Demonceaux, C., ***Fraundorfer, F.***: *A homography formulation to the 3pt plus a common direction relative pose problem*, in: Proc. 12th Asian Conference on Computer Vision, pp. 1-14, 2014.

[745] Stilla, U., Schmitt, M., Maksymiuk, O., ***Auer, S.***: *Towards the Recognition of Individual Trees in Decimeter-Resolution Airborne Millimeterwave SAR*, in: Proc. International Workshop on Pattern Recognition in Remote Sensing, pp. 1-4, 2014.

[746] **Suchandt, S.**, **Runge, H.**: *High-Resolution Surface Current Mapping Using TanDEM-X ATI*, in Proc. EUSAR 2014, pp. 1310-1313, 2014.

[747] Tanase, R., **Radoi, A.**, Georgescu, F.-A., **Datcu, M.**, Raducani, D.: *Using Biquarternions Algebra and Joint Time Frequency Aanalysis Towards a New PolSAR Data Indexing Method*, in Proc. Big Data from Space - BiDS'14, pp. 59-62, 2014.

[748] **Tian, J.**, **Reinartz, P.**: *Dempster-Shafer fusion based building change detection from satellite stereo imagery*, in Proc. 17th International Conference on Information Fusion (FUSION2014), pp. 1-7, 2014.

[749] **Velotto, D.**, **Lehner, S.**: *On the use of full polarimetric SAR data to remove azimuth ambiguity: Application ship detection*, in Proc. EUSAR 2014, pp. 712-715, 2014.

[750] **Wang, Y.**, **Zhu, X. X.**, **Bamler, R.**: *Robust covariance matrix estimation with application to volcano monitoring using SAR image stacks*, in Proc. EUSAR 2014, pp. 938-941, 2014.

[751] **Yague-Martinez, N.**, **Rodriguez-Gonzalez, F.**, **Balss, U.**, **Breit, H.**, **Fritz, T.**: *TerraSAR-X TOPS, ScanSAR and WideScanSAR interferometric processing*, in Proc. EUSAR 2014, pp. 945-948, 2014.

[752] Yao, W., **Cui, S.**, Nies, H., Loffeld, O.: *Classification of Land Cover Types in TerraSAR-X Images Using Copula and Speckle Statistics*, in Proc. EUSAR 2014, pp. 1-4, 2014.

[753] **Zhu, X. X.**, **Bamler, R.**, **Lachaise, M.**, ***Adam, F.***, Shi, Y., **Eineder, M.**: *Improving TanDEM-X DEMs by Non-local InSAR Filtering*, in Proc. EUSAR 2014, pp. 1-4, 2014.

[754] **Zhu, X. X.**, **Li, X. M.**, **Guo, R.**: *Compressive Sensing for Super-resolving SAR Imaging to Support Target Detection in Coastal Zone*, in Proc. EUSAR 2014, pp. 1223-1226, 2014.

[755] **Zhu, X. X.**, **Wang, Y.**, ***Shahzad, M.***, **Bamler, R.**: *Spaceborne TomoSAR and beyond: from SAR image stacks to objects*, in Proc. EUSAR 2014, pp. 1-4, 2014.

2013

[756] **Arefi, H.**, Alizadeh, A., Ghafouri, A.: *Building Extraction Using Surface Model Classification*, in Proc. GIS Ostrava 2013 - Geoinformatics for City Transformations, pp. 1-10, 2013.

[757] **Avbelj, J.**, **Müller, R.**, **Reinartz, P.**: *Fusion of Hyperspectral Images and Height Models Using Edge Probability*, in Proc. WHISPERS 2013, pp. 1-4, 2013.

[758] Babaee, M., Rigoll, G., **Datcu, M.**: *Immersive Interactive Information Mining with Application to Earth Observation Data Retrieval*, in Proc. International Cross Domain Conference and Workshop (CD-ARES 2013), 8127, pp. 376-386, 2013.

[759] **Bahmanyar, R.**, **Datcu, M.**: *Measuring the Semantic Gap Based on a Communication Channel Model*, in Proc. ICIP 2013, pp. 4377-4381, 2013.

[760] **Baumgartner, A.**: *Characterization of Integrating Sphere Homogeneity with an Uncalibrated Imaging Spectrometer*, in Proc. WHISPERS 2013, pp. 1-4, 2013.

[761] **Bieniarz, J.**, **Zhu, X. X.**, **Müller, R.**, **Reinartz, P.**: *Sparse spectral unmixing with endmember groups pre-selection*, in Proc. WHISPERS 2013, pp. 1-4, 2013.

[762] **Cerra, D.**, **Müller, R.**, **Bieniarz, J.**, **Reinartz, P.**: *On the Application of Spectral Unmixing for Noise Reduction*, in Proc. WHISPERS 2013, 5, pp. 1-4, 2013.

[763] Costachioiu, T., Constantinescu, R., Lăzărescu, V., **Datcu, M.**: *Semantic Analysis of EO-1 Hyperion Hyperspectral Data*, in Proc. WHISPERS 2013, pp. 1-4, 2013.

[764] Costachioiu, T., **Vaduva, C.**, Lazarescu, V., **Datcu, M.**: *Content extraction of long-term Satellite Image Time Series: spatiotemporal analysis of Bucharest metropolitan area*, in Proc. MultiTemp 2013, pp. 1-4, 2013.

[765] **Cui, S.**, **Datcu, M.**: *Cascade Active Learning for Evolution Pattern Extraction from SAR Image Time Series*, in Proc. MultiTemp 2013, pp. 1-4, 2013.

[766] **Dumitru, O.**, **Datcu, M.**: *Diversity of Settlement Categories in Very High Resolution SAR Images*, in Proc. JURSE 2013, pp. 87-90, 2013.

[767] **Efremenko, D.**, **Doicu, A.**, **Loyola, D.**, **Trautmann, T.**: *Accelerations of the Discrete Ordinate Method for Nadir Viewing Geometries*, AIP Conference Proceedings, 1531, pp. 55-58, 2013.

[768] **Efremenko, D., Doicu, A., Loyola, D., Trautmann, T.**: *Analysis of acceleration techniques for linearized radiative transfer codes*, in 7th International Symposium on Radiative Transfer, pp. 38-49, 2013.

[769] **Espinoza-Molina, D.**, **Datcu, M.**: *Urban Area Understanding Based on Compression Methods*, in Proc. JURSE 2013, pp. 174-177, 2013.

[770] Faur, D., **Espinoza-Molina, D.**, Gavat, I., **Datcu, M.**: *Multi Temporal Analysis of Floods and Tsunami Effects: Annotation and Quantitative Analysis*, in Proc. MultiTemp 2013, pp. 1-4, 2013.

[771] **Gege, P.**: *A model of underwater spectral irradiance accounting for wave focusing*, AIP Conference Proceedings, 1531, pp. 931-934, 2013.

[772] **Goel, K.**, **Adam, N.**: *Advanced Stacking of TerraSAR-X and TanDEM-X Data in Complex Urban Areas*, in Proc. JURSE 2013, pp. 115-118, 2013.

[773] Hillen, F., Höfle, B., Ehlers, M., **Reinartz, P.**: *The Potential of Agent-Based Modelling for Verification of People Trajectories Based on Smartphone Sensor Data*, in Proc. ISDE 2013, pp. 1-6, 2013.

[774] **Kuschk, G.**, Cremers, D.: *Fast and Accurate Large-scale Stereo Reconstruction using Variational Methods*, in Proc. ICCV Workshop on Big Data in 3D Computer Vision, pp. 1-8, 2013.

[775] **Kuschk, G.**: *Model-free Dense Stereo Reconstruction Creating Realistic 3D City Models*, in Proc. JURSE 2013, pp. 202-205, 2013.

[776] **Kuschk, G.**: *Large Scale Urban Reconstruction from Remote Sensing Imagery*, in Proc. 5th International Workshop 3D-ARCH'2013, XL-5/W1, pp. 139-146, 2013.

[777] **Lenhard, K.**: *Monte-Carlo based determination of measurement uncertainty for imaging spectrometers*, in Proc. WHISPERS 2013, pp. 1-4, 2013.

[778] Linnemann, K., **Gege, P.**, Rößler, S., Schneider, T., Melzer, A.: *CDOM retrieval using measurements of downwelling irradiance*, in Proc. SPIE Remote Sensing 2013, 8888, pp. 1-10, 2013.

[779] **Mattyus, G.**, **Kurz, F.**, **Rosenbaum, D.**, **Meynberg, O.**: *A real-time optical airborne road traffic monitoring system*, in Proc. KEPAF 2013, pp. 645-656, 2013.

[780] **Meynberg, O.**, **Kuschk, G.**: *Airborne Crowd Density Estimation*, in Proc. CMRT13 - City Models, Roads and Traffic 2013, II-3/W, pp. 49-54, 2013.

[781] **Pflug, B.**: *Ground based measurements of aerosol properties using Microtops instruments*, AIP Conference Proceedings, 1531, pp. 588-591, 2013.

[782] **Reinartz, P.**, **Tian, J.**, Nielsen, A. A.: *Building damage assessment after the earthquake in Haiti using two post-event satellite stereo imagery and DSM*, in Proc. JURSE 2013, pp. 57-60, 2013.

[783] **Schreier, F.**, ***Gimeno Garcia, S.***, Milz, M., Kottayil, A., Höpfner, M., Clarmann von, T., Stiller, G.: *Intercomparison of three microwave/infrared high resolution line-by-line radiative transfer codes*, AIP Conference Proceedings, 1531, pp. 119-122, 2013.

[784] **Schreier, F.**, ***Gimeno Garcia, S.***: *Py4CAtS - Python Tools for Line-by-Line Modelling of Infrared Atmospheric Radiative Transfer*, AIP Conference Proceedings, 1531, pp. 123-126, 2013.

[785] **Schreier, F.**, **Xu, J.**, **Doicu, A.**, **Vogt, P.**, **Trautmann, T.**: *Deriving Stratospheric Trace Gases From Balloon-borne Infrared/Microwave Limb Sounding Measurements*, in Proc. International Radiation Symposium IRS 2012, 1531, pp. 392-395, 2013.

[786] **Schwarzmaier, T.**, **Baumgartner, A.**, **Gege, P.**, **Lenhard, K.**: *Calibration of a monochromator using a lambdameter*, in Proc. SPIE Remote Sensing 2013, 8889, pp. 1-6, 2013.

[787] ***Shahzad, M.***, **Zhu, X. X.**: *Building façades reconstruction using multi-view TomoSAR point clouds*, in Proc. JURSE 2013, pp. 163-166, 2013.

[788] ***Shahzad, M.***, **Zhu, X. X.**: *Robust Building Facade Reconstruction from Spaceborne Tomosar Points*, in Proc. CMRT13 – City Models, Roads and Traffic 2013, II-3/W, pp. 85-90, 2013.

[789] **Singh, J.**, **Datcu, M.**: *Parametric modeling of the fractional Fourier transform coefficients for complex-valued SAR image categorization*, in Proc. ICIP 2013, pp. 2882-2886, 2013.

[790] **Storch, T.**, Bachmann, M., Eberle, S., Habermeyer, M., **Makasy, C.**, **de Miguel, A.**, Mühle, H., **Müller, R.**: *EnMAP Ground Segment Design: An Overview and its Hyperspectral Image Processing Chain*, in Proc. Earth Observation of Global Changes 2011 (EOGC 2011), pp. 49-62, 2013.

[791] Taubert, D. R., Hollandt, J., Sperfeld, P., Höpe, A., Hauer, K.-O., **Gege, P.**, **Schwarzmaier, T.**, **Lenhard, K.**, **Baumgartner, A.**: *Providing Radiometric Traceability for the Calibration Home Base of DLR by PTB*, AIP Conference Proceedings, 1531, pp. 376-379, 2013.

[792] **Tian, J.**, **Reinartz, P.**: *Fusion of multi-spectral bands and DSM from Worldview-2 Stereo imagery for building extraction*, in Proc. JURSE 2013, pp. 135-138, 2013.

[793] **Wang, Y.**, **Zhu, X. X.**, **Bamler, R.**, ***Gernhardt, S.***: *Towards TerraSAR-X street view: creating city point cloud from multi-aspect data stacks*, in Proc. JURSE 2013, pp. 198-201, 2013.

[794] **Xu, J.**, **Schreier, F.**, **Vogt, P.**, **Doicu, A.**, **Trautmann, T.**: *A sensitivity study for far infrared balloon-borne limb emission sounding of stratospheric trace gases*, Geoscientific Instrumentation, Methods and Data Systems Discussions (GID), 3, pp. 251-303, 2013.

[795] ***Zhu, K.***, Neilson, D., **d'Angelo, P.**: *Confidence-Based Surface Prior for Energy-Minimization Stereo Matching*, in Proc. German Conference on Pattern Recognition 2013, 8142, pp. 91-100, 2013.

[796] **Zhu, X. X.**, **Bamler, R.**: *Sparse Reconstruction techniques for Tomographic SAR Inversion*, in Proc. 2013 European Signal Processing Conference (EUSIPCO-2013), pp. 1-5, 2013.

[797] **Zhu, X. X.**, **Grohnfeldt, C.**, **Bamler, R.**: *Collabrative sparse image fusion with application to pan-sharpening*, in Proc. 18th International Conference on Digital Signal Processing (DSP), pp. 1-6, 2013.

[798] **Zhu, X. X.**, **Wang, Y.**, ***Gernhardt, S.***, **Bamler, R.**: *Tomo-GENESIS: DLR's tomographic SAR processing system*, in Proc. JURSE 2013, pp. 159-162, 2013.

Books

2017

[799] **Rother, T.**: *Green's Functions in Classical Physics*, Lecture Notes in Physics, Springer International Publishing, pp. 1-267, ISBN 978-3-319-52436-8, 2017.

2015

[800] **Rother, T.**: *Greenfunktionen Klassischer Teilchen und Felder*, BoD Verlag Norderstedt, pp. 1-308, ISBN 978-3-7386-1338-4, 2015.

2013

[801] Kerber, A., Laue, R., **Meringer, M.**, Rücker, C., Schymanski, E. L.: *Mathematical Chemistry and Chemoinformatics*, De Gruyter, pp. 1-491, ISBN 978-3-11-025407-5, 2013.

[802] **Rother, T.**, Kahnert, M.: *Electromagnetic Wave Scattering on Nonspherical Particles: Basic Methodology and Simulations*, Springer Series in Optical Sciences, 2. Auflage, Springer, pp. 1-287, ISBN 978-3-642-00703-3, 2013.

Book Contributions

2018

[803] **Dumitru, C. O.**, **Schwarz, G.**, **Datcu, M.**, Hummel, H., Hummel, C.: *Analysis of Coastal Areas Using SAR Images: A Case Study of the Dutch Wadden Sea Region*, in: Topics in Radar Signal Processing, InTech Publishing, pp. 115-136, 2018.

[804] **Efremenko, D.**, **Doicu, A.**, **Loyola, D.**, **Trautmann, T.**: *Fast Stochastic Radiative Transfer Models for Trace Gas and Cloud Property Retrievals Under Cloudy Conditions*, in: Springer Series in Light Scattering: Volume 1: Multiple Light Scattering, Radiative Transfer and Remote Sensing, Springer Series in Light Scattering, Springer International Publishing, pp. 231-277, ISBN 978-3-319-70796-9, 2018.

[805] Hieronymi, M., **Gege, P.**, König, M., Macke, A., Oppelt, N., Ruhtz, T.: *Ocean colour remote sensing: measurements of water-leaving reflectance and water constituents*, in: The Expeditions PS106/1 and 2 of the Research Vessel POLARSTERN to the Arctic Ocean in 2017, Berichte zur Polar- und Meeresforschung, Alfred-Wegener-Institut, pp. 39-44, 2018.

[806] Oppelt, N., Birnbaum, G., **Gege, P.**, König, M., Fuchs, N.: *Physical characteristics of melt ponds*, in: The Expeditions PS106/1 and 2 of the Research Vessel POLARSTERN to the Arctic Ocean in 2017, Berichte zur Polar- und Meeresforschung, Alfred-Wegener-Institut, pp. 48-56, 2018.

2017

[807] ***Bagheri, H.***, ***Schmitt, M.***, **Zhu, X. X.**: *Uncertainty assessment and weight map generation for efficient fusion of TanDEM-X and Cartosat-1 DEMs*, in: International Archives of the Photogrammetry, Remote Sensing and Spatial Information Sciences, (1/W1), pp. 433-439, 2017.

[808] **Fraundorfer, F.**: *Computer Vision for MAVs*, in: Computer Vision in Vehicle Technology: Land, Sea & Air, John Wiley & Sons Ltd, pp. 55-74, ISBN 9781118868072, 2017.

[809] **Gege, P.**: *Radiative transfer theory for inland waters*, in: Bio-Optical Modelling and Remote Sensing of Inland Waters, Elsevier, pp. 25-67, ISBN 9780128046449, 2017.

[810] Li, X., **Lehner, S.**: *Hurricane Monitoring With Spaceborne Synthetic Aperture Radar*, in: Natural Hazards, Springer Nature Singapore Pte Ltd. 2017, pp. 99-119, ISBN 978-981-10-2892-2, 2017.

[811] **Rossi, C.**: *Rice Plant Height Monitoring from Space with Bistatic Interferometry*, in: Advances in International Rice Research, Agricultural and biological sciences, Intech, pp. 287-313, ISBN 978-953-51-3010-9, 2017.

[812] Topouzelis, K., **Singha, S.**: *Oil Spill Detection Using Space-Borne Sentinel-1 SAR Imagery*, in: Oil Spill Science and Technology, Elsevier, pp. 387-394, ISBN 9780128094136, 2017.

[813] Weber, M., Steinbrecht, W., Frith, S., Tweedy, O., **Coldewey-Egbers, M.**, Davis, S., Degenstein, D., Fioletov, V. E., Froidevaux, L., de Laat, J., Long, C., **Loyola, D.**, Roth, C., Wild, J.: *Stratospheric Ozone*, in: BAMS State of the Climate in 2016, 8, American Meteorological Society, pp. S49-S51, 2017.

2016

[814] **Bamler, R.**, **Eineder, M.**: *Grenzen der Vermessung der Erde aus dem All mit Synthetischem Apertur Radar*, in: Handbuch der Geodäsie, Band "Photogrammetrie und Fernerkundung", Springer Berlin Heidelberg, pp. 1-42, ISBN 3-642-54138-0, 978-3-642-54138-4, 2016.

[815] Hadjimitsis, D., Agapiou, A., Lysandrou, V., Themistocleous, K., Cuca, B., Nisantzi, A., Lasaponara, R., Masini, N., Biscione, M., Nolè, G., **Brcic, R.**, **Cerra, D.**, **Eineder, M.**, Gessner, U., **Krauß, T.**, Schreier, G.: *Establishing a Remote Sensing Science Center in Cyprus: First Year of Activities of ATHENA Project*, in: Digital Heritage. Progress in Cultural Heritage: Documentation, Preservation, and Protection, Lecture Notes in Computer Science, Springer International Publishing, pp. 275-282, ISBN 978-3-319-48973-5, 978-3-319-48974-2, 2016.

[816] Kaufmann, H., Sang, B., **Storch, T.**, Segl, K., Förster, S., Guanter, L., Erhard, M., Heider, B., Hofer, S., Honold, H.-P., Penné, B., Bachmann, M., Habermeyer, M., Müller, A., **Müller, R.**, Rast, M., Staenz, K., Straif, C., Chlebek, C.: *Environmental Mapping and Analysis Program – A German Hyperspectral Mission*, in: Optical Payloads for Space Missions, John Wiley & Sons, pp. 161-182, ISBN 978-1-118-94514-8 (P) 9781118945179 (E), 2016.

[817] Weber, M., Steinbrecht, W., Roth, C., Coldewey-Egbers, M., Degenstein, D., Fioletov, V. E., Frith, S., Froidevaux, L., de Laat, J., Long, C., **Loyola, D.**, Wild, J.: *Stratospheric Ozone*, in: BAMS State of the Climate in 2015, 8, American Meteorological Society, pp. S49-S51, 2016.

[818] Zink, M., Bachmann, M., Bräutigam, B., **Fritz, T.**, Hajnsek, I., Krieger, G., Moreira, A., Wessel, B.: *TanDEM-X: Das neue globale Höhenmodell der Erde*, in: Handbuch der Geodäsie, Springer Reference Naturwissenschaften, Springer-Verlag Berlin Heidelberg, pp. 1-30, ISBN 978-3-662-46900-2 (Online), 2016.

2015

[819] **Bamler, R.**: *Die Vermessung der Stadt aus dem Orbit*, in: Globale Urbanisierung, Perspektive aus dem All, Springer Spektrum, Springer Berlin Heidelberg, 2015, pp. 265-266, ISBN 3662448408, 9783662448403, 2015.

[820] **Gottwald, M.**, Thomas, F., **Breit, H.**, **Schättler, B.**, Harris, A.: *Mapping terrestrial impact craters with the TanDEM-X digital elevation model*, in: Special Paper 518: Large Meteorite Impacts and Planetary Evolution V, GSA Special Papers, Geological Society of America, pp. 177-211, ISBN 978-0-8137-2518-5, 2015.

[821] **Lehner, S.**, Schwarz, E., Nyenhuis, M.: *Satellite based maritime surveillance to increase safety, security and efficiency of ship traffic*, in: Applications of Satellite Earth Obeservations: Serving Society, Science & Industry - Full Report, pp. 128-130, 2015.

[822] Oppelt, N., Scheiber, R., **Gege, P.**, Wegmann, M., Taubenböck, H., Berger, M.: *Fundamentals of remote sensing for terrestrial applications: Evolution, current state of the art, and future possibilities*, in: Remote Sensing Handbook, Vol. I: Remotely Sensed Data Characterization, Classification, and Accuracies, CRC Press, pp. 61-86, ISBN 9781482218015, 2015.

[823] Orphal, J., Barbe, A., **Birk, M.**, Burkholder, J. B., De Backer, M. R., Flaud, J.-M., Gorshelev, V., Gratien, A., Janssen, C., Moussay, P., Petersen, M., Picquet-Varrault, N., Rotger-Languereau, M., Serdyuchenko, A., Viallon, J., Viatte, C., **Wagner, G.**, Weber, M., Wielgosz, R. I.: *Laboratory Measurements and Evaluations of Ozone Absorption Cross-Sections in the Ultraviolet-Visible and Infrared (2009-2011)*, in: Absorption Cross-Sections of Ozone (ACSO) Status Report as of December 2015, GAW Report No. 218, GAW Report, 218, World Meteorological Organization, pp. 3-8, 2015.

[824] **Vaduva, C.**, Georgescu, F.-A., **Datcu, M.**: *Dictionary-Based Compact Data Representation for Very High Resolution Earth Observation Image Classification*, in: Advanced Concepts for Intelligent Vision Systems, Lecture Notes in Computer Vision, Springer Link, pp. 816-825, ISBN 978-3-319-25902-4, 2015.

[825] Weber, M., Steinbrecht, W., Roth, C., Coldewey-Egbers, M., van der A, R., Degenstein, D., Fioletov, V. E., Frith, S., Froidevaux, L., Long, C., **Loyola, D.**, Wild, J.: *Stratospheric Ozone*, in: State of the Climate in 2014, Bulletin of the American Meteorological Society, 7, American Meteorological Society, pp. S44-S46, 2015.

2014

[826] Ferrucci, F., Theys, N., Clarisse, L., Hirn, B., Laneve, G., **Valks, P.**, Van Der A, R., Tait, S., Di Bartola, C., Brenot, H.: *Operational integration of space borne measurements of Lava discharge rates and Sulphur Dioxide concentrations for Global Volcano Monitoring*, in: Early Warning for Geological Disasters: Scientific Methods and Current Practice, Advanced Technologies in Earth Sciences, Springer, pp. 307-331, ISBN 978-3-642-12232-3, 2014.

[827] Gugisch, R., Kerber, A., Laue, R., Kohnert, A., **Meringer, M.**, Rücker, C., Wassermann, A.: *MOLGEN 5.0, A Molecular Structure Generator*, in: Advances in Mathematical Chemistry and Applications, Bentham Science Publishers Ltd., pp. 113-138. ISBN 978-1-60805-929-4, 2014.

[828] **Lehner, S.**, **Pleskachevsky, A.**, **Brusch, S.**, **Bruck, M.**, **Soccorsi, M.**, **Velotto, D.**: *Ship Surveillance with High Resolution TerraSAR-X Satellite in African Waters*, in: Remote Sensing of the African Seas, Springer Netherlands, pp. 285-313, ISBN 978-94-017-8007-0 (P) 978-94-017-8008-7 (E), 2014.

[829] Taubenböck, H., Geiß, C., Wieland, M., Pittore, M., Saito, K., So, E., **Eineder, M.**: *The Capabilities of Earth Observation to Contribute along the Risk Cycle*, in: Earthquake Hazard, Risk and Disasters, Hazards and Disasters Series, Elsevier, pp. 25-53, ISBN 978-0-12-394848-9, 2014.

[830] Weber, M., Steinbrecht, W., van der A, R., Coldewey-Egbers, M., Fioletov, V. E., Frith, S., Long, C., **Loyola, D.**, Wild, J.: *Stratospheric Ozone*, in: State of the climate in 2013, Bulletin of the American Meteorological Society, American Meteorological Society, pp. 538-540, 2014.

2013

[831] Afanas'ev, V., **Efremenko, D.**, Lubenchenko, A.: *On the application of the invariant embedding method and the radiative transfer equation codes for surface state analysis*, in: Light Scattering Reviews, Springer-Verlag Berlin Heidelberg, pp. 363-423, ISBN 978-3-642-32105-4, 2013.

[832] **Hoja, D.**, **Krauß, T.**, **Reinartz, P.**: *Detailed Damage Assessment after the Haiti Earthquake*, in: Earth Observation of Global Changes (EOGC), Lecture Notes in Geoinformation and Cartography, Springer, pp. 193-204, ISBN 978-3-642-32713-1, 2013.

[833] Koukouli, M. **Valks, P.**, Poupkou, A., Zyrichidou, I., **Rix, M.**, **Hao, N.**, Katragkou, E., Balis, D., **Loyola, D.**, Melas, D., *Investigating the GOME-2/Metop-A Total Sulphur Dioxide Load with the Aid of Chemical Transport Modelling over the Balkan Region,* in: Advances in Meteorology, Climatology and Atmospheric Physics, Springer, pp. 1075-1080. ISBN 978-3-642-29171-5, 2013.

Other Publications

2018

[834] ***Bagheri, H.***, ***Schmitt, M.***, **d'Angelo, P.**, **Zhu, X.**: *Exploring the applicability of semi-global matching for SAR-optical stereogrammetry of urban scenes*, in Proc. ISPRS TC II Mid-term Symposium 2018, XLII-2, pp. 43-48, 2018.

[835] **Bittner, K.**, **d'Angelo, P.**, ***Körner, M.***, **Reinartz, P.**: *Automatic Large-Scale 3D Building Shape Refinement Using Conditional Generative Adversarial Networks*, in Proc. ISPRS TC II Mid-term Symposium "Towards Photogrammetry 2020", XLII-2, pp. 1-6, 2018.

[836] ***Qiu, C.***, ***Schmitt, M.***, **Ghamisi, P.**, **Zhu, X. X.**: *Effect of the training set configuration on Sentinel-2-based urban Local Climate Zone Classification*, in Proc. ISPRS TC II Mid-term Symposium 2018, XLII-2, pp. 931-936, 2018.

[837] ***Schmitt, M.***, ***Hughes, L.***, ***Körner, M.***, **Zhu, X. X.**: *Colorizing Sentinel-1 SAR Images using a variational Autoencoder conditioned on Sentinel-2 imagery*, in Proc. ISPRS Technical Commission Symposium 2018, XLII-2, pp. 1045-1051, 2018.

[838] **Xu, J.**, **Heue, K.-P.**, Coldewey-Egbers, M., **Romahn, F.**, **Doicu, A.**, **Loyola, D.**: *Full-Physics Inverse Learning Machine for satellite remote sensing of ozone profile shapes and tropospheric columns*, in Proc. ISPRS Technical Commission III Symposium 2018, XLII-3, pp. 1995-1998, 2018.

2017

[839] Afanas'ev, V. P., Gryazev, A. S., **Efremenko, D.**, Kaplya, P. S., Kuznecova, A. V.: *X-ray photoelectron spectra of Wolfram, determination of differential inelastic scattering cross-sections in Wolfram*, in Proc. XX Conference: Plasma Surface Interaction, pp. 22-25, 2017.

[840] Anghel, A., Cacoveanu, R., Moldovan, A.-S., Savlovschi, C., Rommen, B., **Datcu, M.**: *Bistatic SAR Imaging with Sentinel-1 Operating in TOPSAR Mode*, in Proc. Radar Conference (RadarConf), 2017, pp. 601-605, 2017.

[841] **Bittner, K.**, **Cui, S.**, **Reinartz, P.**: *Building Extraction from Remote Sensing Data using fully convolutional Networks*, in Proc. ISPRS Hannover Workshop: HRIGI 17, XLII-1 (W1), pp. 481-486, 2017.

[842] **Carmona, E.**, **Avbelj, J.**, **Alonso, K.**, Bachmann, M., **Cerra, D.**, Eckardt, A., **Gerasch, B.**, Graham, L., Günther, B., Heiden, U., Kerr, G., Knodt, U., Krutz, D., **Krawczyk, H.**, **Makarau, A.**, Miller, R., **Müller, R.**, Perkins, R., Walter, I.: *Data Processing for the space-based DESIS Hyperspectral Sensor*, in Proc. ISPRS Hannover Workshop 2017, XLII (1/W1), pp. 271-277, 2017.

[843] **Cerra, D.**, **Traganos, D.**, **Gege, P.**, **Reinartz, P.**: *Unmixing-based Denoising as a pre-processing step for Coral Reef Analysis*, in Proc. ISPRS Hannover Workshop: HRIGI 17, XLII-1 (W1), pp. 279-282, 2017.

[844] de Macedo, C. R., Nunziata, F., **Velotto, D.**, Migliaccio, M.: *Oil seepage polarimetric contrast analysis in a time series of TerraSAR-X images*, in Proc. POLinSAR 2017, pp. 1-6, 2017.

[845] **Dumitru, C. O.**, **Schwarz, G.**, **Datcu, M.**: *Image Representation Alternatives for the Analysis of Satellite Image Time Series*, in Proc. MultiTemp 2017, pp. 1-4, 2017.

[846] Estevam Schmiedt, J., **Cerra, D.**, Dahlke, D., Dill, S., **Ge, N.**, Göttsche, J., Haas, A., Heiden, U., **Israel, M.**, **Kurz, F.**, Linkiewicz, M., Patel, D., Peichl, M., **Plattner, S.**, Pless, S., Schiricke, B., Schorn, C., Tiddens, A., **Zhu, X. X.**: *Remote sensing techniques for building models and energy performance studies of buildings*, in Proc. EBC Annex 71: Building energy performance assessment based on in-situ measurements, pp. 1-9, 2017.

[847] Fuchs, C., Schmidt, C., Rödiger, B., Shrestha, A., Brechtelsbauer, M., Ramírez, J., Pacheco, J., **Gstaiger, V.**: *DLR's Free Space Experimental Laser Terminal for Optical Aircraft Downlinks*, in Proc. Photonics West, 10096, pp. 1-12, 2017.

[848] Grivei, A., **Radoi, A.**, **Datcu, M.**: *Land Cover Change Detection in Satellite Image Time Series Using an Active Learning Method*, in Proc. 9th International Workshop (Multitemp), pp. 1-4, 2017.

[849] **Ilehag, R.**, **Auer, S.**, **Angelo, P.**: *Exploitation of Digital Surface Models Generated from WorldView-2 Data for SAR Simulation Techniques*, in Proc. HRIGI17 - High-Resolution Earth Imaging for Geospatial Information, pp. 55-61, 2017.

[850] **Israel, M.**: *UAV-gestützte Detektion von Kiebitznestern in Agrarflächen*, in Proc. 23. CBA-Workshop – Leibniz-Institut für Agrartechnik und Bioökonomie e.V. (ATB), pp. 1-8, 2017.

[851] ***Kang, J.***, **Wang, Y.**, ***Körner, M.***, **Zhu, X. X.**: *Robust object-based multi-baseline InSAR*, in Proc. FRINGE 2017, pp. 1-9, 2017.

[852] **Krauß, T.**, **Fischer, P.**: *Endangerment of Cultural Heritage Sites by Strong Rain*, in Proc. Fifth International Conference on Remote Sensing and Geoinformation of the Environment (RSCy2017), 10444, pp. 1-9, 2017.

[853] **Marmanis, D.**, **Yao, W.**, ***Adam, F.***, **Datcu, M.**, **Reinartz, P.**, Schindler, K., Wegner, J. D., Stilla, U.: *Artificial generation of big data for improving image classification: a generative adversarial network approach on SAR data*, in Proc. Big data from space 2017, pp. 1-4, 2017.

[854] Mu, J., **Cui, S.**, **Reinartz, P.**: *Building Detection using Aerial Images and Digital Surface Models*, in Proc. ISPRS Hannover Workshop: HRIGI 17, XLII-1 (W1), pp. 159-165, 2017.

[855] Nunziata, F., Migliaccio, M., **Velotto, D.**: *Tandem-X bistatic polarimetric mode for maritime applications*, in Proc. OCEANS '17, pp. 1-4, 2017.

[856] **Palubinskas, G.**, Bachmann, M., **Carmona, E.**, **Gerasch, B.**, **Krawczyk, H.**, **Makarau, A.**, **Schneider, M.**, **Schwind, P.**: *Image Products from a new German Hyperspectral Mission EnMAP*, in Proc. IGTF 2017, pp. 1-12, 2017.

[857] **Partovi, T.**, **Fraundorfer, F.**, **Azimi, S.**, **Marmanis, D.**, **Reinartz, P.**: *Roof Type Selection based on patch-based classsification using deep learning for high Resolution Satellite Imagery*, in Proc. ISPRS Hannover Workshop: HRIGI 17, XLII-1 (W1), pp. 653-657, 2017.

[858] **Piñuela Garcia, F.**, **Cerra, D.**, **Müller, R.**: *Enabling Searches on Wavelengths in a Hyperspectral Indices Database*, in Proc. ISPRS Spec3D, XLII-3 (W3), pp. 161-164, 2017.

[859] ***Qiu, C.***, ***Schmitt, M.***, **Zhu, X. X.**: *A tie point matching strategy for very high resolution SAR-optical stereogrammetry over urban areas*, in Proc. ISPRS Hannover Workshop 2017, pp. 1-7, 2017.

[860] ***Rußwurm, M., Körner, M.***: *Multitemporal Crop Identification from Medium-Resolution Multi-Spectral Satellite Images based on Long Short-Term Memory Neural Networks*, in Proc. ISPRS Hannover Workshop 2017, XLII-1 (W1), pp. 551-558, 2017.

[861] **Singha, S.**, Jäger, M.: *Arctic Sea Ice Characterization using Multi-frequency Fully Polarimetric Airborne DLR-FSAR system*, in Proc. ESA POLinSAR Workshop, pp. 1-4, 2017.

[862] **Storch, T.**, **Müller, R.**: *Processing Chains for DESIS and EnMAP Imaging Spectroscopy Data: Similarities and Differences*, in Proc. ISPRS SPEC3D 2017, XLII-3, pp. 177-180, 2017.

[863] **Tian, J.**, **Krauß, T.**, **d'Angelo, P.**: *Automatic Rooftop Extraction in Stereo Imagery Using Distance and Building Shape Regularized Level Set Evolution*, in Proc. ISPRS Hannover Workshop 2017, XLII-1 (W1), pp. 393-397, 2017.

[864] Tian, J., **Metzlaff, L.**, **d'Angelo, P.**, **Reinartz, P.**: *Region-based Building Rooftop Extraction and Change Detection*, in Proc. ISPRS Geospatial Week 2017, XLII-2, pp. 903-908, 2017.

[865] Traganos, D., **Cerra, D.**, **Reinartz, P.**: *Cubesat-derived Detection of Seagrasses using Planet Imagery following unmixing-based Denoising: Is small the next big?*, in Proc. ISPRS Hannover Workshop: HRIGI 17, XLII-1 (W1), pp. 283-287, 2017.

[866] Vaduva, C., Danisor, C., **Datcu, M.**: *Temporal analysis of SAR imagery for permanent and evolving Earth land cover behavior assessment*, in Proc. 9th International Workshop (Multitemp), pp. 1-4, 2017.

[867] Velotto, D., Marino, A., Nunziata, F.: *On the backscattering of offshore platforms via single and dual-polarization TerraSAR-X data*, in Proc. POLinSAR 2017, pp. 1-6, 2017.

[868] Wang, Y., **Zhu, X. X.**, ***Montazeri, S.***, ***Kang, J.***, **Mou, L.**, ***Schmitt, M.***: *Potential of the "SARptical" system*, in Proc. FRINGE 2017, pp. 1-6, 2017.

[869] Wiehle, S., Martinez, B., Hartmann, K., Verlaan, M., Thornton, T., Lewis, S., Schaap, D.: *The BASE-platform project: Deriving the bathymetry from combined satellite data*, in Proc. Hydro17, pp. 1-6, 2017.

[870] Yao, W., **Marmanis, D.**, **Datcu, M.**: *Semantic segmentation using deep neural networks for SAR and optical image pairs*, in Proc. Big data from space 2017, pp. 1-4, 2017.

[871] Zhao, J., **Floricioiu, D.**: *The penetration effects on TanDEM-X elevation using the GNSS and laser altimetry measurements in Antarctica*, in Proc. ISPRS Geospatial Week 2017, XLII-2 (W7), pp. 1593-1600, 2017.

2016

[872] Abdel Jaber, W., **Floricioiu, D.**, Rott, H.: *Geodetic mass balance of the Patagonian Icefields derived from SRTM and TanDEM-X data.*, in Proc. IGARSS 2016, pp. 342-345, 2016.

[873] Abdi, G., **Samadzadegan, F.**, **Kurz, F.**: *Pose Estimation of Unmanned Aerial Vehicles Based on a Vision-Aided Multi-Sensor Fusion*, in Proc. ISPRS Congress, XLI-B6, pp. 193-199, 2016.

[874] Agapiou, A., Lysandrou, V., Themistocleous, K., Lasaponara, R., Masini, N., **Krauß, T.**, **Cerra, D.**, Gessner, U., Schreier, G., Hadjimitsis, D. G.: *Searching data for supporting archaeolandscapes in Cyprus: an overview of aerial, satellite and cartographic datasets of the island*, in Proc. 4th International Conference on Remote Sensing and Geoinformation of the Environment (RSCy2016), pp. 1-10, 2016.

[875] Anghel, A., Cacoveanu, R., Moldovan, A.-S., Popescu, A., **Datcu, M.**, Serban, F.: *Simplified bistatic SAR imaging with a fixed receiver and TerraSAR-X as transmitter of opportunity - first results*, in Proc. IGARSS 2016, pp. 2094-2097, 2016.

[876] Ansari, H., **De Zan, F.**, **Goel, K.**, **Adam, N.**, **Bamler, R.**: *Sequential Estimator for Distributed Scatterer Interferometry*, in Proc. IGARSS 2016, pp. 6859-6862, 2016.

[877] Auer, S., **Bamler, R.**, **Reinartz, P.**: *RaySAR - 3D SAR Simulator: Now Open Source*, in Proc. IGARSS 2016, pp. 6730-6733, 2016.

[878] ***Baier, G.***, **Zhu, X. X.**: *GPU-based nonlocal filtering for large scale SAR processing*, in Proc. IGARSS 2016, pp. 7608-7611, 2016.

[879] Balss, U., **Runge, H.**, **Suchandt, S.**, ***Cong, X.***: *Automated Extraction of 3-D Ground Control Points from SAR Images - An Upcoming Novel Data Product*, in Proc. IGARSS 2016, pp. 5023-5026, 2016.

[880] Brachmann, J. F., **Baumgartner, A.**, **Lenhard, K.**: *The Calibration Home Base for Imaging Spectrometers: Present Activities in an Overview*, in Proc. Onera-DLR ODAS Symposium 2016, pp. 1-8, 2016.

[881] Brachmann, J., **Baumgartner, A.**, **Gege, P.**: *The Calibration Home Base for Imaging Spectrometers*, Journal of Large-Scale Research Facilities JLSRF, 2 (A82), pp. 1-9, 2016.

[882] Cerra, D., **Bieniarz, J.**, **Müller, R.**, **Reinartz, P.**: *Cloud Removal from Sentinel-2 Image Time Series through Sparse Reconstruction from Random Samples*, in Proc. ISPRS 2016, pp. 469-473, 2016.

[883] Cerra, D., **Tian, J.**, Lysandrou, V., Plank, S.: *Automatic Damage Detection for Sensitive Cultural Heritage Sites*, in Proc. ISPRS 2016, pp. 215-219, 2016.

[884] ***Cong, X.***, **Balss, U.**, **Suchandt, S.**, **Eineder, M.**, **Runge, H.**: *SAR Absolute Ranging - Validation and Application of SAR Geodesy Processor using ECMWF Reanalysis and Operational Data*, in Proc. IGARSS 2016, pp. 3246-3249, 2016.

[885] d'Angelo, P.: *Improving Semi-Global Matching: Cost aggregation and confidence measure*, in Proc. ISPRS Congress 2016, XLI-B1, pp. 299-304, 2016.

[886] Danisor, C., Fornaro, G., **Datcu, M.**: *Applications of SAR Tomography on Persistent Scatterers detection, based on Beam-Forming filtering*, in Proc. IGARSS 2016, pp. 1428-1431, 2016.

[887] Dörnhöfer, K., **Gege, P.**, **Pflug, B.**, Oppelt, N.: *Mapping indicators of lake ecology at Lake Starnberg, Germany – First results of Sentinel-2A*, in Proc. Living Planet Symposium 2016, SP-740, pp. 1-8, 2016.

[888] Duque Biarge, S., **Parizzi, A.**, **De Zan, F.**, **Eineder, M.**: *Precise and automatic 3D absolute geolocation of targets using only two long-aperture SAR acquisitions*, in Proc. IGARSS 2016, pp. 715-7418, 2016.

[889] Eder, E., Dörnhöfer, K., **Gege, P.**, Schenk, K., Klinger, P., Wenzel, J., Oppelt, N., Gruber, N.: *Analysis of mineral-rich suspended matter in glacial lakes using simulations and satellite data*, in Proc. Living Planet Symposium 2016, pp. 1-6, 2016.

[890] Espinoza-Molina, D., **Alonso, K.**, **Datcu, M.**: *Visual Data Mining for Feature Space Exploration using In-situ Data*, in Proc. IGARSS 2016, pp. 5905-5908, 2016.

[891] Fernandez Arguedas, V., **Velotto, D.**, **Tings, B.**, Greidanus, H., **Bentes da Silva, C. A.**: *Ship classification in high and very high resolution satellite SAR imagery*, in Proc. 11. Future Security, pp. 347-354, 2016.

[892] Fischer, P., **Ehrensperger, S.**, **Krauß, T.**: *A New Method to Detect Regions Endangered by High Wind Speeds*, in Proc. ISPRS Congress 2016, XLI-B8, pp. 59-63, 2016.

[893] Fischer, P.: *When Rainfall Threatens*, DLR Magazin, pp. 34-35, 2016.

[894] Gebhardt, C. P., Bidlot, J.-R., **Pleskachevsky, A.**, **Ressel, R.**, Rosenthal, W., **Lehner, S.**, **Gemmrich, J.**: *Sea state events in the marginal ice zone with TerraSAR-X satellite images as observational basis*, in Proc. EGU General Assembly 2016, 18, pp. EGU2016-2305, 2016.

[895] Gege, P., **Grötsch, P.**: *A spectral model for correcting sunglint and skyglint*, in Proc. Ocean Optics XXIII, pp. 1-10, 2016.

[896] Ghamisi, P., Souza, R., Rittner, L., Benediktsson, J. A., Lotufo, R., **Zhu, X. X.**: *Extinction Profiles: A Novel Approach for the Analysis of Remote Sensing Data*, in Proc. IGARSS 2016, pp. 1-4, 2016.

[897] Goel, K., **Adam, N. A.**, **Shau, R.**, **Rodriguez-Gonzalez, F.**: *Improving the reference network in wide-area Persistent Scatterer Interferometry for non-urban areas*, in Proc. IGARSS 2016, pp. 1448-1451, 2016.

[898] Gottwald, M.: *184 crateres d'impact sur la Terre*, Pour la Science, 90, pp. 26-31, 2016.

[899] Gretschany, S., **Lichtenberg, G.**, **Meringer, M.**, Theys, N., Lerot, C., Liebing, P., Noel, S., Dehn, A., Fehr, T.: *New Developments in the SCIAMACHY L2 Ground Processor*, in Proc. Living Planet Symposium 2016, SP-740, pp. 1-3, 2016.

[900] Griparis, A., Faur, D., **Datcu, M.**: *A dimensionality reduction approach for the visualization of the cluster space: A trustworthiness evaluation*, in Proc. IGARSS 2016, pp. 2917-2920, 2016.

[901] **Gstaiger, V.**, Nippold, R., Kiefl, R.: *Forschungsprojekt VABENE++: Verkehrsmanagement bei Großereignissen und Katastrophen*, Im Einsatz, pp. 34-36, 2016.

[902] Guanter, L., Segl, K., Foerster, S., Hollstein, A., Rossner, G., Chlebek, C., **Storch, T.**, Heiden, U., Müller, A., **Müller, R.**, Sang, B.: *Overview of the EnMAP Imaging Spectroscopy Mission*, in Proc. IGARSS 2016, pp. 261-263, 2016.

[903] **Hamidouche, M.**, ***Gimeno Garcia, S.***, **Schreier, F.**, **Meringer, M.**, **Lichtenberg, G.**, **Hochstaffl, P.**, **Trautmann, T.**: *Atmospheric methane with SCIAMACHY: Operational Level 2 data analysis and verification*, in Proc. Living Planet Symposium 2016, pp. 1-3, 2016.

[904] ***Hong, D.***, **Yokoya, N.**, **Zhu, X. X.**: *Local Manifold Learning with Robust Neighbors Selection for Hyperspectral Dimensionality Reduction*, in Proc. IGARSS 2016, pp. 40-43, 2016.

[905] ***Kang, J.***, **Wang, Y.**, ***Körner, M.***, **Zhu, X. X.**: *Object-based InSAR deformation reconstruction with application to bridge monitoring*, in Proc. IGARSS 2016, pp. 6871-6874, 2016.

[906] Kerr, G. H., **Avbelj, J.**, **Carmona, E.**, Eckardt, A., **Gerasch, B.**, Graham, L., Günther, B., Heiden, U., Krutz, D., **Krawczyk, H.**, **Makarau, A.**, Miller, R., **Müller, R.**, Perkins, R., Walter, I.: *The Hyperspectral Hyperspectral sensor DESIS on MUSES: processing and application*, in Proc. IGARSS 2016, pp. 268-271, 2016.

[907] **Köhler, C. H.**: *Airborne Imaging Spectrometer HySpex*, Journal of Large-Scale Research Facilities JLSRF, 2 (A93), pp. 1-6, 2016.

[908] **Köhn, A.**, **Tian, J.**, **Kurz, F.**: *Automatic Building Extraction and Roof Reconstruction in 3K Imagery based on line Segments*, in Proc. XXIII ISPRS Congress, XLI (B3), pp. 625-631, 2016.

[909] **Krauß, T.**: *Extraction and modelling of three-dimensional Urban Objects from VHR Satellite Stereo Imagery*, in Proc. RSCy2016, 9688, pp. 96880E-1, 2016.

[910] **Kurz, F.**, **Rosenbaum, D.**, **Runge, H.**, **Cerra, D.**, **Mattyus, G. S.**, **Reinartz, P.**: *Long-Term Tracking of a Specific Vehicle Using Airborne Optical Camera Systems*, in Proc. ISPRS Congress, XLI-B2, pp. 521-525, 2016.

[911] **Lachaise, M.**, **Fritz, T.**: *Phase unwrapping strategy and assessment for the high resolution DEMs of the TanDEM-X mission*, in Proc. IGARSS 2016, pp. 3223-3226, 2016.

[912] **Lehner, S.**, **Gemmrich, J.**: *Sea State Events in the Mariginal Ice Zone with TerraSAR-X Satellite Images*, in Proc. IGARSS 2016, pp. 2220-2222, 2016.

[913] ***Liebel, L.***, ***Körner, M.***: Single-Image Super Resolution for Multispectral Remote Sensing Data Using Convolutional Neural Networks, in Proc. ISPRS Prague, Volume XLI-B3, pp. 883-890, 2016.

[914] **Liu, S.**, **Valks, P.**, Pinardi, G., Smedt, I. D., Yu, H., Beirle, S.: *An improved total and tropospheric NO2 column retrieval for GOME-2*, in Proc. Living Planet Symposium 2016 - ESA, SP-740, pp. 1-6, 2016.

[915] Louis, J., Debaecker, V., **Pflug, B.**, **Main-Knorn, M.**, **Bieniarz, J.**, Mueller-Wilm, U., Cadau, E., Gascon, F.: *SENTINEL-2 SEN2COR: L2A Processor for Users*, in Proc. ESA Living Planet Symposium 2016, SP-740, pp. 1-8, 2016.

[916] Moacă, O.-m., Popescu, A., Anghel, A., **Datcu, M.**: *A bistatic SAR simulator for ground-based fixed-receiver geometry*, in Proc. IGARSS 2016, pp. 6098 -6101, 2016.

[917] ***Montazeri, S.***, **Zhu, X. X.**, **Balss, U.**, Gisinger, C., **Wang, Y.**, **Eineder, M.**, **Bamler, R.**: *SAR Ground Control Point Identification with the Aid of High Resolution Optical Data*, in Proc. IGARSS 2016, pp. 3205-3208, 2016.

[918] **Mou, L.**, **Zhu, X. X.**: *Spatiotemporal Scene Interpretation of Space Videos via Deep Neural Network and Tracklet Analysis*, in Proc. IGARSS 2016, pp. 1823-1826, 2016.

[919] Mrowka, F., Göttfert, T., Wörle, M. T., **Schättler, B.**, Stathopoulos, F.: *The TerraSAR-X/TanDEM-X Mission Planning System: Realizing new Customer Visions by Applying new Upgrade Strategies*, in Proc. SpaceOps 2016 - 12th International Conference on Space Operations, pp. 1-10, 2016.

[920] **Müller, R.**, **Avbelj, J.**, **Carmona, E.**, **Gerasch, B.**, Graham, L., Günther, B., Heiden, U., Kerr, G., Knodt, U., Krutz, D., **Krawczyk, H.**, **Makarau, A.**, Miller, R., Perkins, R., Walter, I.: *The New Hyperspectral Sensor DESIS on the Multi-Payload Platform MUSES Installed on the ISS*, in Proc. XXIII ISPRS CONGRESS, XLI-B1, pp. 461-467, 2016.

[921] **Palubinskas, G.**: *Image fusion methods based on a linear mixing model of multispectral remote sensing data*, in Proc. IGTF 2016, pp. 1-11, 2016.

[922] **Palubinskas, G.**: *Pan-Sharpening Approaches Based on Unmixing of Multispectral Remote Sensing Imagery*, in Proc. ISPRS 2016, XLI-B7, pp. 693-702, 2016.

[923] **Pflug, B.**, **Main-Knorn, M.**, **Bieniarz, J.**, Debaecker, V., Louis, J.: *Early Validation of Sentinel-2 L2A Processor and Products*, in Proc. Living Planet Symposium 2016, SP-740, pp. 1-6, 2016.

[924] **Pleskachevsky, A.**, **Lehner, S.**, Rosenthal, W.: *Meteo-marine parameters from the TS-X satellite on a near-real time basis and wave model forecast validation*, in Proc. EGU General Assembly 2016, 18, pp. EGU2016-17333, 2016.

[925] **Pleskachevsky, A.**, **Wiehle, S.**, **Gebhardt, C. P.**, Schwarz, E., Krause, D., Bruns, T., Kieser, J.: *Sea State from High Resolution Satellite-borne Synthetic Aperture Radar Imagery*, in Proc. HYDRO 2016, pp. 1-10, 2016.

[926] **Ressel, R.**, **Singha, S.**, **Lehner, S.**: *Neural Network based automatic Sea Ice Classification for CL-pol RISAT-1 Imagery*, in Proc. IGARSS 2016, pp. 4835-4838, 2016.

[927] **Ressel, R.**, **Singha, S.**, **Lehner, S.**: *Comparing the behavior of polarimetric SAR imagery (TerraSAR-X, Radarsat-2, Sentinel-1) for automated sea ice classification*, in Proc. ESA Living Planet Symposium, SP-740, pp. 1-7, 2016.

[928] **Ressel, R.**, **Singha, S.**, **Lehner, S.**: *Evaluating suitability of Pol-SAR (TerraSAR-X, Radarsat-2, Sentinel) for automated sea ice classification*, in Proc. SPIE Asia-Pacific Remote Sensing Symposium, 9877, pp. 1-14, 2016.

[929] **Rossi, C.**, **Minet, C.**, Magnusson, E.: *Surface Changes at the Northwest Vatnajökull Glacier, Iceland, during the 2014-2015 Bardarbunga Eruption*, in Proc. IGARSS 2016, pp. 7101-7104, 2016.

[930] **Runge, H.**, **Balss, U.**, **Suchandt, S.**, Klarner, R., ***Cong, X.***: *DriveMark – Generation of High Resolution Road Maps with Radar Satellites*, in Proc. 11th ITS European Congress, pp. 1-6, 2016.

[931] **Schättler, B.**, Mrowka, F., Schwarz, E., **Lachaise, M.**: *The TerraSAR-X Ground Segment in service for nine years: current status and recent extensions*, in Proc. IGARSS 2016, pp. 1400-1403, 2016.

[932] ***Schmitt, M.***, ***Shahzad, M.***, **Zhu, X. X.**: *Forest remote sensing on the individual tree level by airborne millimeterwave SAR*, in Proc. IGARSS 2016, pp. 151-154, 2016.

[933] ***Schmitt, M.***, **Zhu, X. X.**: *On the challenges in stereogrammetric fusion of SAR and optical imagery for urban areas*, in Proc. ISPRS Congress 2016, XLI (B7), pp. 719-722, 2016.

[934] **Singha, S.**, **Ressel, R.**, **Lehner, S.**: *Multi-Frequency and Multi-Polarization Analysis of Oil Slicks using TerraSAR-X and RADARSAT-2 Data*, in Proc. IGARSS 2016, pp. 4035-4038, 2016.

[935] **Singha, S.**, **Ressel, R.**, **Lehner, S.**: *Oil Spill Detection and Characterization using Fully-Polarimetric X and C band SAR Imagery: A Near Real Time Perspective*, in Proc. ESA Living Planet Symposium, SP-740, pp. 1-5, 2016.

[936] **Sun, Y.**, ***Shahzad, M.***, **Zhu, X. X.**: *First Prismatic Building Model Reconstruction from TomoSAR Points Clouds*, in Proc. ISPRS Congress 2016, XLI-B3, pp. 381-386, 2016.

[937] Tanase, R., **Datcu, M.**, Raducanu, D.: *A convolutional deep belief network for polarimetric SAR data feature extraction*, in Proc. IGARSS 2016, pp. 2917-2920, 2016.

[938] Tavri, A., **Singha, S.**, **Lehner, S.**, Topouzelis, K.: *Observation of sub-mesoscale eddies over Baltic Sea using TerraSAR-X and Oceanographic data*, in Proc. ESA Living Planet Symposium, SP-740, pp. 1-5, 2016.

[939] Tong, J., **Li, X.-M.**, **Velotto, D.**: *Study on oil spills in the North Sea Forties field observed in TerraSAR-X and TanDEM-X imagery*, in Proc. IGARSS 2016, pp. 7708-7710, 2016.

[940] Topouzelis, K., **Singha, S.**: *Oil spill detection: past and future trends*, in Proc. ESA Living Planet Symposium, SP-740, pp. 1-4, 2016.

[941] Tscharf, A., Markus, R., Mayer, G., **Fraundorfer, F.**, Bischof, H.: *UAV Vermessung im Bergbau – Stand der Forschung und Ausblick*, in Proc. 17. GEOKINEMATISCHER TAG Freiberg 2016, 1, pp. 250-265, 2016.

[942] Udelhoven, T., Bossung, C., **Rock, G.**, **Fischer, P.**, Müller, A., **Storch, T.**, Segl, K., Eisele, A., Schlerf, M., Knigge, T.: *High Resolution Temperature and Spectral Emissivity Mapping (HITESEM)*, in Proc. IGARSS 2016, pp. 272-275, 2016.

[943] **Vaduva, C.**, Georgescu, F.-A., **Datcu, M.**: *Compound and configurable framework for exploratory earth observation data analysis*, in Proc. IGARSS 2016, pp. 5492-5495, 2016.

[944] **Velotto, D.**, Nunziata, F., **Bentes da Silva, C. A.**, Migliaccio, M., **Lehner, S.**: *Investigation of the experimental Tandem-X pursuit monostatic mode for oil and ship detection*, in Proc. IGARSS 2016, pp. 4023-4026, 2016.

[945] **Wang, Y.**, **Zhu, X. X.**: *Robust multibaseline InSAR optimization*, in Proc. IGARSS 2016, pp. 1464-1467, 2016.

[946] **Wiehle, S.**, Martinez, B., Hartmann, K., Verlaan, M., Thornton, T., Lewis, S., Schaap, D.: *The BASE-platform project: Deriving the bathymetry from combined satellite data*, in Proc. HYDRO 2016, pp. 1-8, 2016.

[947] **Willberg, M.**, Gisinger, C., **Balss, U.**, **Fritz, T.**, **Eineder, M.**: *Geodetic Stereo SAR With Small Multi-Directional Radar Reflectors*, in Proc. IGARSS 2016, pp. 5011-5014, 2016.

[948] **Xu, J.**, **Schreier, F.**, **Doicu, A.**, **Trautmann, T.**, **Birk, M.**, **Wagner, G.**: *Stratospheric Profiling of HDO from Far Infrared Limb Measurements by TELIS*, in Proc. Living Planet Symposium 2016, pp. 1-4, 2016.

[949] **Xu, J.**, **Schreier, F.**, Kenntner, M., Szajkowski, M., Fix, A., **Trautmann, T.**: *Towards the Temperature Retrieval by Using Airborne Microwave Radiometer Data*, in Proc. Living Planet Symposium 2016, pp. 1-5, 2016.

[950] **Xu, J.**, **Schreier, F.**, **Loyola, D.**, ***Schüssler, O.***, **Doicu, A.**, **Trautmann, T.**: *Monitoring ozone in different spectral regimes from space and balloon (Sentinel-4/-5P, TELIS)*, in Proc. IGARSS 2016, pp. 360-363, 2016.

[951] Zhang, J. X., Yang, J. H., **Reinartz, P.**: *the optimized block-regression-based fusion algorithm for pansharpening of very high resolution satellite imagery*, in Proc. ISPRS 2016, pp. 739-746, 2016.

[952] Zhao, J., Guo, W., **Cui, S.**, Zhang, Z., Yu, W.: *Convolutional neural Network for SAR Image Classification at Patch Level*, in Proc. IGARSS 2016, pp. 945-948, 2016.

[953] **Zhuo, X.**, **Cui, S.**, **Kurz, F.**, **Reinartz, P.**: *Fusion and classification of aerial images from MAVS and airplanes for local information enrichment*, in Proc. IGARSS 2016, pp. 3567-3570, 2016.

2015

[954] **Alonso, K.**, **Espinoza-Molina, D.**, **Datcu, M.**: *LUCAS Visual Browser: A Tool for Land Cover Visual Analytics*, in Proc. IGARSS 2015, pp. 1484-1487, 2015.

[955] **Ansari, H.**, **Goel, K.**, **Parizzi, A.**, **De Zan, F.**, **Adam, N.**, **Eineder, M.**: *Tandem-L Performance for Three Dimensional Earth Deformation Monitoring*, in Proc. IGARSS 2015, pp. 1-4, 2015.

[956] **Ansari, H.**, **Goel, K.**, **Parizzi, A.**, Sudhaus, H., **Adam, N.**, **Eineder, M.**: *InSAR Sensitivity Analysis of Tandem-L Mission for Modeling Volcanic and Seismic Deformation Sources*, in Proc. FRINGE 2015, pp. 1-8, 2015.

[957] **Auer, S.**, ***Gernhardt, S.***, Eder, K., Gisinger, C.: *Simulation of Facade Reference Data for 3D SAR Algorithms*, in Proc. IGARSS 2015, pp. 2927-2930, 2015.

[958] Babaee, M., Tsoukalas, S., Babaee, M., **Datcu, M.**: *Active Learning Using a Low-Rank Classifier*, in Proc. 23rd Iranian Conference on Electrical Engineering (ICEE) 2015, pp. 561-566, 2015.

[959] Babaee, M., Yu, X., Merget, D., Babaeian, A., Rigoll, G., **Datcu, M.**: *Interactive feature learning from SAR image patches*, in Proc. IGARSS 2015, pp. 541-544, 2015.

[960] ***Baier, G.***, **Zhu, X. X.**: *Region Growing Based Nonlocal Filtering for InSAR*, in Proc. IGARSS 2015, pp. 1-4, 2015.

[961] **Bamler, R.**: *Satellite InSAR Data – Reservoir Monitoring from Space*, IEEE Geoscience and Remote Sensing Magazine (GRSM), 3 (1), pp. 53-54, 2015.

[962] **Bamler, R.**: *TerraSAR-X, TanDEM-X and beyond*, in Proc. PIA15/HRIGI2015, XL-3 (W2), pp. 295-296, 2015.

[963] **Bentes da Silva, C. A.**, **Velotto, D.**, **Lehner, S.**: *Target Classification in Oceanographic SAR Images with Deep Neural Networks: Architecture and Initial Results*, in Proc. IGARSS 2015, pp. 3703-3706, 2015.

[964] Beyer, F., Jarmer, T., Siegmann, B., **Fischer, P.**: *Improved crop classification using multitemporal RapidEye data*, in Proc. Analysis of Multitemporal Remote Sensing Images (Multi-Temp), 2015 8th International Workshop on the, pp. 1-4, 2015.

[965] **Bieniarz, J.**, **Zhu, X. X.**, **Müller, R.**, **Reinartz, P.**: *Sparse Pixel-wise spectral Unmixing - which Algorithm to use and how to improve the Results*, in Proc. IGARSS 2015, pp. 2860-2863, 2015.

[966] Braun, A. C., Weinmann, M., Keller, S., **Müller, R.**, **Reinartz, P.**, Hinz, S.: *The EnMAP Contest: Developing and Comparing Classification Approaches for the Environmental Mapping and Analysis Programme - Dataset and First results*, in Proc. ISPRS Geospatial Week 2015, XL-3/ (W3), pp. 169-175, 2015.

[967] **Cerra, D.**, **Müller, R.**, **Reinartz, P.**: *Cloud removal in image time series through unmixing*, in Proc. Analysis of Multitemporal Remote Sensing Images (Multi-Temp) 2015, pp. 1-4, 2015.

[968] **Cui, S.**, **Datcu, M.**: *A Comparison of Bag-of-Words method and Normalized Compression Distance for Satellite Image Retrieval*, in Proc. IGARSS 2015, pp. 4392-4395, 2015.

[969] **Cui, S.**, **Datcu, M.**: *Comparison of Kullback-Leibler Divergence Approximation Methods Between Gaussian Mixture Models for Satellite Image Retrieval*, in Proc. IGARSS 2015, pp. 3719-3722, 2015.

[970] **Eineder, M.**, **Balss, U.**, **Suchandt, S.**, Gisinger, C., ***Cong, X.***, **Runge, H.**: *A Definition of Next-Generation SAR Products for Geodetic Applications*, in Proc. IGARSS 2015, pp. 1638-1641, 2015.

[971] Erten, E., **Rossi, C.**, Yuzugullu, O.: *Comparison of the TanDEM-X response between vertical and horizontal oriented vegetation*, in Proc. IGARSS 2015, pp. 2899-2902, 2015.

[972] **Espinoza Molina, D.**, **Alonso Gonzales, K.**, **Datcu, M.**: *Semantic Indexing of TERRASAR-X and in situ data for urban analytics*, in Proc. SMPR 2015, XL-1-W, pp. 185-188, 2015.

[973] **Espinoza Molina, D.**, **Datcu, M.**: *Data Mining and Knowledge Discovery Tools for Exploiting Big Earth Observation Data*, in Proc. 36th International Symposium on Remote Sensing of Environment (ISRSE), XL-7 (W3), pp. 627-633, 2015.

[974] **Espinoza-Molina, D.**, **Alonso, K.**, **Datcu, M.**: *Visual Analytics for Semantic Queries of TerraSAR-X Image Content*, in Proc. SPIE Remote Sensing Conference, pp. 1-10, 2015.

[975] Faur, D., **Datcu, M.**: *A rapid mapping approach to quantify damages caused by the 2003 Bam earthquake using high resolution multitemporal optical images*, in Proc. MULTITEMP 2015, pp. 1-4, 2015.

[976] **Fischer, P.**, Etienne, C., **Tian, J.**, **Krauß, T.**: *Prediction of Wind Speeds based on Digital Elevation Models using Boosted Regression Trees*, in Proc. 3rd International Conference on Sensors and Models in Photogrammetry and Remote Sensing, pp. 1-6, 2015.

[977] Florea, B.-F., Grigore, O., **Datcu, M.**: *Ant based exploration algorithms - A brief survey*, in Proc. 9th International Symposium on Advanced Topics in Electrical Engineering (ATEE) 2015, pp. 889-892, 2015.

[978] Florea, B.-F., Grigore, O., **Datcu, M.**: *Pheromone averaging exploration algorithm*, in Proc. International Conference on Advanced Robotics (ICAR) 2015, pp. 617-622, 2015.

[979] **Floricioiu, D.**, **Abdel Jaber, W.**, **Minet, C.**, **Rossi, C.**, **Eineder, M.**: *TanDEM-X for mass balance of glaciers and subglacial volcanic activities*, in Proc. Geoscience and Remote Sensing Symposium (IGARSS), 2015 IEEE International, pp. 2903-2906, 2015.

[980] ***Ge, N.***, **Zhu, X. X.**: *SAR tomography using staring and high-resolution spotlight data from the TanDEM-X pursuit monostatic mode*, in Proc. IGARSS 2015, pp. 1-4, 2015.

[981] ***Ge, N.***, **Zhu, X. X.**: *Sparse Reconstruction Automaton for Synthetic Aperture Radar Tomography*, in Proc. European Radar Conference 2015, pp. 1-4, 2015.

[982] Gemmrich, J., **Pleskachevsky, A.**, **Lehner, S.**, Rogers, E.: *Surface waves in arctic seas, observed from TerraSAR-X*, in Proc. IGARSS 2015, pp. 3442-3445, 2015.

[983] Georgescu, F.-A., **Datcu, M.**, Raducanu, D.: *Gabor and Weber Local Descriptors performance in multispectral Earth Observation image data analysis*, in Proc. AFASES 2015, pp. 1-5, 2015.

[984] Gisinger, C., ***Gernhardt, S.***, **Auer, S.**, **Balss, U.**, **Hackel, S.**, Pail, R., **Eineder, M.**: *Absolute 4-D Positioning of Persistent Scatterers with TerraSAR-X by Applying Geodetic Stereo SAR*, in Proc. IGARSS 2015, pp. 2991-2994, 2015.

[985] **Gomba, G.**, ***Cong, X.***, **Eineder, M.**: *Correction of ionospheric and tropospheric path delay for L-band interferograms*, in Proc. IGARSS 2015, pp. 310-313, 2015.

[986] **Gomba, G.**, **De Zan, F.**: *Estimation of ionospheric height variations during an aurora event using multiple semi-focusing levels*, in Proc. IGARSS 2015, pp. 4065 -4068, 2015.

[987] **Gottwald, M.**, Krieg, E., **Lichtenberg, G.**, **Reissig, K.**, Noel, S., Bramstedt, K., Bovensmann, H.: *SCIAMACHY Operations History and the New Level 1b Product - an Approach for Long-term Data Preservation*, in Proc. ATMOS 2015, pp. 87-88, 2015.

[988] **Gottwald, M.**: *Irdische Einschlagkrater im Radarbild*, Sterne und Weltraum, 4, pp. 26-37, 2015.

[989] Griparis, A., Faur, D., **Datcu, M.**: *Feature space dimensionality reduction for the optimization of visualization methods*, in Proc. IGARSS 2015, pp. 1120-1123, 2015.

[990] ***Grohnfeldt, C.***, **Zhu, X. X.**: *Towards a Combined Sparse Representation and Unmixing Based Hyperspectral Resolution Enhancement Method*, in Proc. IGARSS 2015, pp. 1-4, 2015.

[991] **Gstaiger, V.**, Nippold, R., Gullotta, G., Hamacher, U.: *Ad hoc Sensorverbund? Der Traum vom „plug and play" –Wie ein Experiment Begehrlichkeiten weckt(e) …*, Bevölkerungsschutz, 2015 (2), pp. 25-30, 2015.

[992] **Gstaiger, V.**, Römer, H., **Rosenbaum, D.**, Henkel, F.: *Airborne Camera System for Real-Time Applications - Support of a National Civil Protection Exercise*, in Proc. 36th International Symposium on Remote Sensing of Environment (ISRSE), XL-7 (W3), pp. 1189-1194, 2015.

[993] ***Heublein, M.***, **Zhu, X. X.**, Alshawaf, F., Mayer, M., **Bamler, R.**, Hinz, S.: *Compressive sensing for neutrospheric water vapor tomography using GNSS and InSAR observations*, in Proc. IGARSS 2015, pp. 5268-5271, 2015.

[994] Hollstein, A., Rogass, C., Segl, K., Guanter, L., Bachmann, M., **Storch, T.**, **Müller, R.**, **Krawczyk, H.**: *EnMAP Radiometric Inflight Calibration, Post-Launch Product Validation, and Instrument Characterization Activities*, in Proc. IGARSS 2015, pp. 1-4, 2015.

[995] Huber, K. C., Loeser, T., Looye, G., Liersch, C. M., **Lindermeir, E.**, Kemptner, E., Klimmek, T., Koch, S., Kuchar, R., Nauroz, M., Paul, M., Rein, M., Rode, G., Rohlf, D., Rütten, M., Schütte, A., Schwithal, J., Siggel, M., Voss, A., Zimper, D.: *Bewertung und Entwurf von agilen und hoch gepfeilten Flugzeugkonfigurationen*, pp. 120, 2015.

[996] **Israel, M.**, **Mende, M.**, Keim, S.: *UAVRC, a generic MAV flight assistance software*, International Archives of Photogrammetry and Remote Sensing, XL-1/W, pp. 287-291, 2015.

[997] **Israel, M.**, **Mende, M.**, Keim, S.: *UAVRC, a generic MAV flight assistance software*, in Proc. 15th ONERA-DLR Aerospace Symposium, pp. 1-5, 2015.

[998] **Jacobsen, S.**, **Lehner, S.**, **Hieronimus, J.**, Schneemann, J., Kühn, M.: *Joint offshore wind turbine wake monitoring with spaceborne SAR and in-situ Lidar measurements*, in Proc. 36th International Symposium on Remote Sensing of Environment (ISRSE), XL-7 (W3), pp. 959-966, 2015.

[999] **Krauß, T.**, **d'Angelo, P.**, **Kuschk, G.**, **Tian, J.**, **Partovi, T.**: *3D-Information Fusion from Very High Resolution Satellite Sensors*, in Proc. 36th International Symposium on Remote Sensing of Environment (ISRSE), pp. 1-6, 2015.

[1000] **Kurz, F.**, **Rosenbaum, D.**, **Runge, H.**, **Reinartz, P.**: *Validation of advanced driver assistance systems by airborne optical imagery*, in Proc. Mobil.TUM 2015 – International Scientific Conference on Mobility and Transport, pp. 1-11, 2015.

[1001] **Lehner, S.**, **Pleskachevsky, A.**, Gebhardt, C. P., Rosenthal, W., Bruns, T., Kieser, J., Hoffmann, P.: *High resolution wind and wave measurements from TS-X in comparison to marine forecast*, in Proc. IGARSS 2015, pp. 2519-2522, 2015.

[1002] **Lehner, S.**, **Tings, B.**: *Maritime NRT products using TerraSAR-X imagery*, in Proc. 36th International Symposium on Remote Sensing of Environment (ISRSE), XL-7 (W3), pp. 967-973, 2015.

[1003] **Lindermeir, E.**, Rütten, M.: *Infrarotsignaturbewertung von agilen und hoch gepfeilten Flugzeugkonfigurationen*, in Proc. Deutscher Luft- und Raumfahrtkongress 2015, pp. 1-8, 2015.

[1004] **Loos, J.**, **Birk, M.**, **Wagner, G.**, Campargue, A., Mondelain, D., Hase, F., Orphal, J., Tran, H., Perrin, A., Daumont, L., Rotger, M., Bigazzi, A., Zehner, C., Coudert, L., Dufour, G., Eremenko, M., Cuesta, J.: *Spectroscopic database for TROPOMI/Sentinel 5 precursor*, in Proc. ATMOS 2015, pp. 1-15, 2015.

[1005] Lukac, N., Zalik, B., **Cui, S.**, **Datcu, M.**: *GPU-based Kernelized Locality-Sensitive Hashing for Satellite Image Retrieval*, in Proc. IGARSS 2015, pp. 1468-1471, 2015.

[1006] Main-Knorn, M., **Pflug, B.**, Louis, J., Debaecker, V.: *Calibration and Validation plan for the L2A processor and products of the Sentinel-2 mission*, in Proc. 36th International Symposium on Remote Sensing of Environment (ISRSE), XL-7 (W3), pp. 1249-1255, 2015.

[1007] Makarau, A., **Richter, R.**, **Storch, T.**, **Reinartz, P.**: *SENTINEL-2 Level 2A Product Prototype Processor: Research and Design Aspects*, in Proc. Information Technologies and Systems 2015 (ITS 2015), pp. 262-263, 2015.

[1008] Meringer, M., **Hrechanyy, S.**, **Lichtenberg, G.**, Hilboll, A., Richter, A., Burrows, J. P.: *Limb-Nadir Matching for Tropospheric NO2: A New Algorithm in the SCIAMACHY Operational Level 2 Processor*, in Proc. ATMOS 2015, SP-735, pp. 1-4, 2015.

[1009] Montazeri, S., Zhu, X. X., Eineder, M., Hanssen, R., **Bamler R.**: *Deformation monitoring of urban infrastructure by tomographic SAR using multi-view TerraSAR-X data stacks*, in Proc. ESA FRINGE Workshop, SP-731, pp. 1-8, 2015.

[1010] Merkle, N., **Müller, R.**, **Reinartz, P.**: *Registration of Optical and SAR Satellite Images based on Geometric Feature Templates*, in Proc. SMPR 2015, XL-1-W, pp. 447-452, 2015.

[1011] Palubinskas, G.: *Framework for Multi-Sensor Data Fusion using Template Based Matching*, in Proc. IGARSS 2015, pp. 621-624, 2015.

[1012] Palubinskas, G.: *Joint Quality Measure for Accuracy Assessment of Pansharpening Methods*, in Proc. IGARSS 2015, pp. 601-604, 2015.

[1013] Pertovici, M.-A., Coltuc, D., **Datcu, M.**, Vasile, T.: *Rate-Distortion Performance of Compressive Sensing in Single Pixel Camera*, in Proc. ICIT 2015, pp. 1747-1751, 2015.

[1014] Pestana, J., Prettenthaler, R., Holzmann, T., Muschick, D., Mostengel, C., **Fraundorfer, F.**, Bischof, H.: *Graz Griffins' Solution to the European Robotics Challenges 2014*, in Proc. OAGM Workshop 2015, pp. 11-12, 2015.

[1015] Peters, S., Alikas, K., Hommersom, A., Latt, S., Reinart, A., Giardino, C., Bresciani, M., Philipson, P., Ruescas, A., Stelzer, K., Schenk, K., Heege, T., **Gege, P.**, Koponen, S., Kallio, K., Zhang, Y.: *Global Lakes Sentinel Services: Water quality parameters retrieval in lakes using the MERIS and S3-OLCI band sets*, in Proc. SENTINEL-3 for Science Workshop, SP-734, pp. 1-5, 2015.

[1016] Pflug, B., **Main-Knorn, M.**, **Makarau, A.**, **Richter, R.**: *Validation of aerosol estimation in atmospheric correction algorithm ATCOR*, in Proc. 36th International Symposium on Remote Sensing of Environment (ISRSE), XL-7 (W3), pp. 677-683, 2015.

[1017] Pleskachevsky, A., **Lehner, S.**, Hoffmann, P., Kieser, J., Bruns, T., Lindenthal, A., Janssen, F., Behrens, A.: *Satellite-based radar measurements for validation of high-resolution sea state forecast models in German Bight*, in Proc. 36th International Symposium on Remote Sensing of Environment (ISRSE), XL-7 (W3), pp. 983-990, 2015.

[1018] Radoi, A., **Datcu, M.**: *Spatio-Temporal Characterization in Satellite Image Time Series*, in Proc. MULTITEMP 2015, pp. 1-4, 2015.

[1019] Radoi, A., Tanase, R., **Datcu, M.**: *Semantic interpretation of multi-level change detection in multi-temporal satellite images*, in Proc. MULTITEMP 2015, pp. 4157-4160, 2015.

[1020] Ressel, R., **Frost, A.**, **Lehner, S.**: *Investigating the potential of different polarimetric features based on dual polarimetric TerraSAR-X data for automated sea ice classification*, in Proc. ESA POLinSAR 2015, SP-729, pp. 1-6, 2015.

[1021] Ressel, R., **Frost, A.**, **Lehner, S.**: *Comparing automated sea ice classification on single-pol and dual-pol TerraSAR-X data*, in Proc. IGARSS 2015, pp. 3442-3445, 2015.

[1022] Ressel, R., **Frost, A.**, **Lehner, S.**: *Navigation assistance for ice-infested waters through automatic iceberg detection and ice classification based on TerraSAR-X imagery*, in Proc. 36th International Symposium on Remote Sensing of Environment (ISRSE), XL-7 (W3), pp. 1049-1056, 2015.

[1023] Rodriguez Gonzalez, F., **Brcic, R.**, ***Yague-Martinez, N.***, **Shau, R.**, **Parizzi, A.**, **Adam, N.**: *Demonstration of TerraSAR-X ScanSAR Persistent Scatterer Interferometry*, in Proc. ESA FRINGE Workshop, SP-731, pp. 1-6, 2015.

[1024] Rossi, C., **Fritz, T.**, **Eineder, M.**: *TanDEM-X DSM uncertainty measures and demonstrations*, in Proc. IGARSS 2015, pp. 3830-3833, 2015.

[1025] Sakar, N., **Brcic, R.**, **Rodriguez Gonzalez, F.**, ***Yague-Martinez, N.***: *An Advanced Co-Registration Method for TOPSAR Interferometry*, in Proc. IGARSS 2015, pp. 5240-5243, 2015.

[1026] Sakkas, V., Lagios, E., Vassilopoulou, S., **Adam, N.**: *Ground Deformation in the Broader Area of the Atalanti Fault Zone (Central Greece) Based on GPS & PSI-WAP*, in Proc. IGARSS 2015, pp. 4676-4679, 2015.

[1027] ***Schmitt, M.***, Wei, L., **Zhu, X. X.**: *Automatic Coastline Detection in Non-locally Filtered TanDEM-X Data*, in Proc. IGARSS 2015, pp. 1036-1039, 2015.

[1028] Schneemann, J., **Hieronimus, J.**, **Jacobsen, S.**, **Lehner, S.**, Kühn, M.: *Offshore wind farm flow measured by complementary remote sensing techniques: radar satellite TerraSAR-X and lidar windscanners*, in Proc. Wake Conference 2015, 625 (1), pp. 1-8, 2015.

[1029] Singha, S., **Velotto, D.**, **Lehner, S.**: *Towards operational near real time oil spill detection service using polarimetric TerraSAR-X images*, in Proc. ESA PolinSAR 2015, SP-729, pp. 1-6, 2015.

[1030] Singha, S., **Velotto, D.**, **Lehner, S.**: *Dual-Polarimetric Feature Extraction and Evaluation for Oil Spill Detection: A Near Real Time Perspective*, in Proc. IEEE International Geoscience and Remote Sensing Symposium (IGARSS) 2015, pp. 3235-3238, 2015.

[1031] Stan, M., Popescu, A., **Datcu, M.**, Stoichescu, D. A.: *An assessment of feature extraction methods for SENTINEL-1 images on urban areas*, in Proc. IGARSS 2015, pp. 369-372, 2015.

[1032] Tanase, R., **Radoi, A.**, **Datcu, M.**, Raducanu, D.: *Polarimetric SAR Data Feature Selection Using Measures of Mutual Information*, in Proc. IGARSS 2015, pp. 1140-1143, 2015.

[1033] Velotto, D., **Bentes da Silva, C. A.**, **Lehner, S.**: *Ships and maritime targets observation campaigns using avialable C- and X-band SAR satellite*, in Proc. ESA POLinSAR 2015, SP-729, pp. 1-6, 2015.

[1034] Velotto, D., **Bentes da Silva, C. A.**, **Tings, B.**, **Lehner, S.**: *Comparison of Sentinel-1 und TerraSAR-X for ship detection*, in Proc. IGARSS 2015, pp. 3282-3285, 2015.

[1035] Wang, Y., **Zhu, X. X.**: *Semantic interpretation of InSAR point cloud*, in Proc. IGARSS 2015, pp. 5019-5022, 2015.

[1036] Wang, Y., **Zhu, X. X.**: *InSAR forensics: tracing InSAR scatterers in high resolution optical image*, in Proc. FRINGE 2015, SP-731, pp. 1-8, 2015.

[1037] Wiehle, S., **Lehner, S.**, **Pleskachevsky, A.**: *Waterline detection and monitoring in the German Wadden Sea using high resolution satellite-based radar measurements*, in Proc. 36th International Symposium on Remote Sensing of Environment (ISRSE), XL-7 (W3), pp. 1029-1033, 2015.

[1038] Xu, J., **Schreier, F.**, **Doicu, A.**, **Birk, M.**, **Wagner, G.**, **Trautmann, T.**: *Remote Sensing of Stratospheric Trace Gases by TELIS*, in Proc. ATMOS 2015, 735, pp. 1-6, 2015.

[1039] Xu, J., **Schreier, F.**, Kenntner, M., Fix, A., **Trautmann, T.**: *Retrieval of Atmospheric Temperature from Airborne Microwave Radiometer Observations*, in Proc. ATMOS 2015, 735, pp. 1-4, 2015.

[1040] Yao, W., Loffeld, O., **Datcu, M.**: *A hierarchical Patch Clustering Method for High Resolution TerraSAR-X Images*, in Proc. IEEE International Geoscience and Remote Sensing Symposium (IGARSS) 2015, pp. 2370-2373, 2015.

[1041] Zhang, L., Du, Q., **Datcu, M.**: *Special Section Guest Editorial: Management and Analytics of Remotely Sensed Big Data*, Journal of Applied Remote Sensing, 9 (1), pp. 1-2, 2015.

[1042] Zhu, X. X., **Bamler, R.**: *Exploiting sparsity in remote sensing and earth observation: theory, applications and future trends*, in Proc. IGARSS 2015, pp. 2840 -2843, 2015.

[1043] Zhu, X. X., ***Ge, N.***, ***Shahzad, M.***: *Exploiting Group Sparsity in SAR Tomography*, in Proc. CoSeRa 2015, pp. 1-5, 2015.

[1044] Zhu, X. X., ***Ge, N.***, ***Shahzad, M.***: *Group Sparsity in SAR Tomography – Experiments on TanDEM-X Data Stacks*, in Proc. International Radar Symposium 2015, pp. 386-391, 2015.

[1045] Zhuo, X., **Kurz, F.**, **Reinartz, P.**: *Fusion of Multi-View and Multi-Scale Aerial Imagery for Real-Time Situation Awareness Applications*, in Proc. UAV-g 2015, pp. 201-206, 2015.

[1046] Zink, M., Bachmann, M., Bräutigam, B., **Fritz, T.**, Hajnsek, I., Krieger, G., Moreira, A., Wessel, B.: *TanDEM-X: A Single-Pass SAR Interferometer for global DEM Generation and Demonstration of new SAR Techniques*, in Proc. IGARSS 2015, pp. 1-4, 2015.

2014

[1047] Abdel Jaber, W., Floricioiu, D., Rott, H.: *Glacier dynamics of the Northern Patagonia Icefield derived from SRTM, TanDEM-X and TerraSAR-X data*, in Proc. IGARSS 2014, pp. 4018-4021, 2014.

[1048] Alonso, K., **Datcu, M.**: *Knowledge-driven image mining system for Big Earth Observation data fusion: GIS maps inclusion in active learning stage*, in Proc. IGARSS 2014, pp. 3538-3541, 2014.

[1049] Ansari, H., **Adam, N.**, **Brcic, R.**: *Amplitude Time Series Analysis in Detection of persistent and temporal coherent Scatterers*, in Proc. IGARSS 2014, pp. 2213-2216, 2014.

[1050] Avbelj, J., **Müller, R.**: *Quality Assessment of Building Extraction from Remote Sensing Imagery*, in Proc. IGARSS 2014, pp. 3184-3187, 2014.

[1051] Bachmann, M., **Müller, R.**, **Schneider, M.**, **Walzel, T.**, Habermeyer, M., **Storch, T.**, Kaufmann, H., Segl, K., Rogass, C.: *Data Quality Assurance for hyperspectral L1 and L2 products - Cal/Val/Mon procedures within the EnMAP Ground Segment*, in Proc. ESA Ipve - Land Product Validation and Evolution Workshop, pp. 1-35, 2014.

[1052] Balss, U., **Breit, H.**, **Fritz, T.**, Steinbrecher, U., Gisinger, C., **Eineder, M.**: *Analysis of Internal Timings and Clock Rates of TerraSAR-X*, in Proc. IGARSS 2014, pp. 2671-2674, 2014.

[1053] Bentes da Silva, C. A., **Velotto, D.**, **Lehner, S.**: *Analysis of ship size detectability over different Terrasar-X Modes*, in Proc. IGARSS 2014, pp. 5137-5140, 2014.

[1054] Bieniarz, J., **Müller, R.**, **Zhu, X. X.**, **Reinartz, P.**: *Hyperspectral Image Resolution Enhancement Based on Joint Sparsity Spectral Unmixing*, in Proc. IGARSS 2014, pp. 2645-2648, 2014.

[1055] Cerra, D., **Müller, R.**, **Reinartz, P.**: *Unmixing-based Denoising for Destriping and Inpainting of Hyperspectral Images*, in Proc. IGARSS 2014, pp. 4620-4623, 2014.

[1056] ***Cong, X.***, **Eineder, M.**, **Fritz, T.**: *Retrieving Reliable Deformation Signal from Active Volcanic Areas Using VHR SAR Images Combined with a Tandem-X DEM – Test Site El Hierro Island*, in Proc. IGARSS 2014, pp. 1-5, 2014.

[1057] d'Angelo, P., **Kuschk, G.**, **Reinartz, P.**: *Evaluation of Skybox Video and Still Image products*, in Proc. PECORA 19, XL-1, pp. 95-99, 2014.

[1058] d'Angelo, P., **Rossi, C.**, **Minet, C.**, **Eineder, M.**, Flory, M., Niemeyer, I.: *High Resolution 3D Earth Observation Data Analysis for Safeguards Activities*, in Proc. Symposium on International Safeguards, pp. 1-8, 2014.

[1059] Datcu, M.: *Big Data Challenge: Mining Heterogeneous Data*, in Proc. Copernicus Big Data workshop, pp. 1-22, 2014.

[1060] Deo, R., **Rossi, C.**, **Fritz, T.**, **Eineder, M.**, **Lachaise, M.**: *Fusion of ascending and descending pass raw TanDEM-X DEM*, in Proc. IGARSS 2014, pp. 21-24, 2014.

[1061] Dumitru, C., **Cui, S.**, **Datcu, M.**: *Quantitative flood assessment: Case study of floods in Germany*, in Proc. IGARSS 2014, pp. 3506-3509, 2014.

[1062] Eineder, M., **Balss, U.**, **Duque Biarge, S.**: *Water level measurement by controlled radar reflection and TerraSAR-X imaging geodesy*, in Proc. IGARSS 2014, pp. 5141-5143, 2014.

[1063] Eineder, M., **Balss, U.**, Gisinger, C., **Hackel, S.**, ***Cong, X.***, **Ulmer, F.-G.**, **Fritz, T.**: *TerraSAR-X pixel localization accuracy: Approaching the centimeter level*, in Proc. IGARSS 2014, pp. 2669-2670, 2014.

[1064] Fischer, P., **Krauß, T.**, Peters, T.: *Automatic Surface Classification for retrieving areas which are highly endangered by extreme rain*, in Proc. ISPRS Technical Commission VII Symposium, XL (7), pp. 93-100, 2014.

[1065] Floricioiu, D., **Abdel Jaber, W.**, Jezek, K.: *TerraSAR-X and TanDEM-X observations of the Recovery Glacier system, Antarctica*, in Proc. IGARSS 2014, pp. 4852-4855, 2014.

[1066] Goel, K., **Adam, N.**: *Recent advances in high resolution SAR interferometric stacking techniques exploiting distributed scatterers*, in Proc. IGARSS 2014, pp. 29-32, 2014.

[1067] Goel, K., **Rodriguez Gonzalez, F.**, **Adam, N.**, Duro, J., Gaset, M.: *Thermal dilation monitoring of complex urban infrastructure using high resolution SAR data*, in Proc. IGARSS 2014, pp. 954-957, 2014.

[1068] Gomba, G., **Eineder, M.**, **Parizzi, A.**, **Bamler, R.**: *High-resolution estimation of ionospheric phase screens through semi-focusing processing*, in Proc. IGARSS 2014, pp. 17-20, 2014.

[1069] Gstaiger, V., **Kurz, F.**, Hohloch, M.: *VABENE++ multi-sensor approach to support crisis management*, in Proc. 5th International Disaster and Risk Conference IDRC 2014, pp. 283-286, 2014.

[1070] Gstaiger, V., **Rosenbaum, D.**: *Automatische Verkehrserfassung aus der Luft – Unterstützung für das Katastrophenmanagement*, in Proc. Deutscher Luft- und Raumfahrtkongress 2014, pp. 1-5, 2014.

[1071] Jaenicke, J., Münzer, U., Mayer, C., **Minet, C.**, Franke, J., Siegert, F., Guðmundsson, Á.: *Überwachung isländischer Vulkane mit innovativen Fernerkundungs-Technologien und 3D Visualisierung*, in Proc. 34. Wissenschaftlich-Technische Jahrestagung der DGPF, 23, pp. 1-14, 2014.

[1072] Krauß, T.: *Exploiting Satellite Focal Plane Geometry for automatic Extraction of Traffic Flow from single optical Satellite Imagery*, in Proc. PECORA 19, XL-1, pp. 179-187, 2014.

[1073] Krawczyk, H., **Gerasch, B.**, **Walzel, T.**, **Storch, T.**, **Müller, R.**, Sang, B., Chlebek, C.: *EnMAP Radiometric Inflight Calibration*, in Proc. IGARSS 2014, pp. 1-5, 2014.

[1074] Kurz, F., **Rosenbaum, D.**, **Meynberg, O.**, **Mattyus, G.**, **Reinartz, P.**: *Performance of a real-time sensor and processing system on a helicopter*, in Proc. Pecora 19 Symposium in conjunction with the Joint Symposium of ISPRS Technical Commission I and IAG Commission 4, pp. 189-193, 2014.

[1075] Kurz, F., **Rosenbaum, D.**, **Meynberg, O.**, **Mattyus, G.**: *Real-time mapping from a helicopter with a new optical sensor system*, in Proc. 34. Wissenschaftlich-Technische Jahrestagung der DGPF, 23, pp. 1-8, 2014.

[1076] Kuschk, G., **d'Angelo, P.**, Qin, R., Poli, D., **Reinartz, P.**, Cremers, D.: *DSM Accuracy Evaluation for the ISPRS Commission I Image matching Benchmark*, in Proc. ISPRS Technical Commission I Symposium, XL-1, pp. 195-200, 2014.

[1077] Lachaise, M., **Fritz, T.**, **Breit, H.**: *InSAR Processing and Dual-Baseline Phase Unwrapping for global TanDEM-X DEM Generation*, in Proc. IGARSS 2014, pp. 2229-2232, 2014.

[1078] Lehner, S., Krumpen, T., **Frost, A.**, **Ressel, R.**, Busche, T., Schwarz, E.: *First Tests on Near Real Time Ice Type Classification in Antarctica*, in Proc. IGARSS 2014, pp. 4876-4879, 2014.

[1079] Li, X.-M., **Lehner, S.**, **Jacobsen, S.**: *Sea surface wakes observed by spaceborne SAR in the offshore wind farms*, in Proc. 2014 DRAGON 3 MID Term Results Symposium, SP-724, pp. 1-4, 2014.

[1080] Lindermeir, E., Rütten, M.: *MIRA: An IR Signature Model for Unmanned Aerial Vehicles (UAV)*, in Proc. Optro 2014 - International Symposium on Optronics in Defence and Security, pp. 1-9, 2014.

[1081] Lindermeir, E.: *MIRA - Ein Infrarot-Signaturmodell für Flugzeuge*, Wehrwissenschaftliche Forschung, pp. 44-45, 2014.

[1082] Makarau, A., Richter, R., **Müller, R.**, **Reinartz, P.**: *Spectrally consistent haze removal in multispectral data*, in Proc. SPIE Remote sensing Europe, 9244, pp. 1-7, 2014.

[1083] Maksymiuk, O., Schmitt, M., ***Auer, S.***, Stilla, U., *Single Tree Detection in Millimeterwave SAR Data by Morphological Attribute Filters*, in: Proc. 34. Wissenschaftliche Jahrestagung der DGPF, pp. 1-9, 2014.

[1084] Metz, A., Marconcini, M., Esch, T., **Reinartz, P.**, Ehlers, M.: *Classification of grassland types by combining multi-seasonal TerraSAR-X and Radarsat-2 imagery*, in Proc. IGARSS 2014 / 35th CSRS, pp. 1202-1205, 2014.

[1085] Meynberg, O., Hillen, F., Höfle, B.: *Navigation in Dense Human Crowds Using Smartphone Trajectories and Optical Aerial Imagery*, in Proc. Photogrammetric Computer Vision - PCV 2014, pp. 1-4, 2014.

[1086] Nevas, S., Nowy, S., Sperling, A., **Lenhard, K.**, **Baumgartner, A.**: *Stray light characterisation of a hyperspectral spectrometer for airborne remote sensing applications*, in Proc. NEWRAD 2014, pp. 53-54, 2014.

[1087] Palubinskas, G.: *Quality Assessment of Pan-sharpening Methods*, in Proc. IGARSS 2014, pp. 2526-2529, 2014.

[1088] Partovi, T., **Bahmanyar, R.**, **Krauß, T.**, **Reinartz, P.**: *Building Roof Component Extraction from Panchromatic Satellite Images Using a Clustering-Based Method*, in Proc. PCV 2014, XL-3, pp. 247-252, 2014.

[1089] Partovi, T., **Krauß, T.**, **Arefi, H.**, Mohammad, O., **Reinartz, P.**: *Model-driven 3D building reconstruction based on integration of DSM and spectral information of satellite images*, in Proc. IGARSS 2014, pp. 3168-3171, 2014.

[1090] Pătrașcu, C., Popescu, A., **Datcu, M.**: *Multi-set analysis of platform influence on density and quality of Persistent Scatterers: A case study for Bucharest area*, in Proc. 2014 IEE Radar Conference, pp. 1233-1236, 2014.

[1091] Pflug, B., **Main-Knorn, M.**: *Validation of atmospheric correction algorithm ATCOR*, in Proc. SPIE Remote Sensing 2014, 9242 (92420W), pp. 1-8, 2014.

[1092] Reinartz, P., **Tian, J.**, **Arefi, H.**, **Krauß, T.**, **Kuschk, G.**, **Partovi, T.**, **d'Angelo, P.**: *Advances in DSM Generation and Higher Level Information Extraction from High Resolution Optical Stereo Satellite Data*, in Proc. Earsel 2014, 34, pp. 1-9, 2014.

[1093] Rossi, C., **Eineder, M.**, **Duque Biarge, S.**, **Fritz, T.**, **Parizzi, A.**: *Principal slope estimation at SAR building layovers*, in Proc. IGARSS 2014, pp. 1-4, 2014.

[1094] Rossi, C., Erten, E.: *Generation of rice crops temporal change maps with differential TanDEM-X interferometry*, in Proc. IGARSS 2014, pp. 1-4, 2014.

[1095] Rütten, M., Karl, S., **Lindermeir, E.**: *Numerical Investigation of Engine Exhaust Plume Characteristics of Unmanned Combat Air Vehicles*, in Proc. AIAA AVIATION Conference, pp. 1-18, 2014.

[1096] Schönberger, J. L., ***Fraundorfer, F.***, Frahm, J. M.: *Structure-from-motion for mav image sequence analysis with photogrammetric applications*, in Proc. PCV 2014, XL-3, pp. 305-312, 2014.

[1097] Schwind, P., **Schneider, M.**, **Müller, R.**: *Improving HySpex Sensor Co-Registration Accuracy using BRISK and Sensor-model based RANSAC*, in Proc. Pecora 19 Symposium in conjunction with the Joint Symposium of ISPRS Technical Commission I and IAG Commission 4, XL-1, pp. 371-376, 2014.

[1098] ***Shahzad, M.***, **Zhu, X. X.**: *Automatic large Area Reconstruction of Building Facades from Spaceborne TomoSAR Point Clouds*, in Proc. IGARSS 2014, pp. 1548-1551, 2014.

[1099] ***Shahzad, M.***, **Zhu, X. X.**: *Reconstructing 2-D/3-D Building Shapes From Spaceborne Tomographic SAR Point Clouds*, in Proc. Photogrammetric Computer Vision PCV 2014, XL-3, pp. 313-320, 2014.

[1100] Singh, J., **Espinoza-Molina, D.**, **Schwarz, G.**, **Datcu, M.**: *On the statistical similarity of synthetic aperture radar images from COSMO-SKYMED and TerraSAR-X*, in Proc. IGARSS 2014, pp. 4726-4729, 2014.

[1101] Singha, S., **Velotto, D.**, **Lehner, S.**: *Near real time operational oil spill detection service using a classification tree*, in Proc. IEEE GOLD Remote Sensing Conference, pp. 1-3, 2014.

[1102] Storch, T., Bachmann, M., Honold, H.-P., Kaufmann, H., **Krawczyk, H.**, **Müller, R.**, Sang, B., **Schneider, M.**, Segl, K., Chlebek, C.: *EnMAP Data Product Standards*, in Proc. IGARSS 2014, pp. 2586-2589, 2014.

[1103] Suchandt, S., Lehmann, A.: *Analysis of ocean surface currents with TanDEM-X ATI: A case study in the Baltic Sea*, in Proc. IGARSS 2014, pp. 3918-3921, 2014.

[1104] Tanase, R., **Datcu, M.**, Raducanu, D.: *PolSAR Data Indexing Using Biquarternions Algebra and Joint Time-Frequency Analysis*, in Proc. 1st ESA SAOCOM Companion Satellite Workshop, pp. 1-17, 2014.

[1105] Tian, J., **Krauß, T.**, **Reinartz, P.**: *DTM Generation in Forest Regions From Satellite Stereo Imagery*, in Proc. ISPRS Technical Commission I Symposium 2014, XL-1, pp. 401-405, 2014.

[1106] Vaduva, C., **Datcu, M.**: *A new comprehensive approach for Earth observation scene classification using joint image and text analysis*, in Proc. IGARSS 2014, pp. 1658-1661, 2014.

[1107] Yague-Martinez, N., Fielding, E., Haghshenas Haghighi, M., ***Cong, X.***, Motagh, M., Steinbrecher, U., **Eineder, M.**, **Fritz, T.**: *Ground displacement measurement of the 2013 M7.7 and M6.8 Balochistan Earthquake with TerraSAR-X ScanSAR data*, in Proc. IGARSS 2014, pp. 950-953, 2014.

[1108] Zhu, X. X., **Lachaise, M.**, ***Adam, F.***, Shi, Y., **Eineder, M.**, **Bamler, R.**: *Beyond the 12m TanDEM-X DEM*, in Proc. IGARSS 2014, pp. 1-4, 2014.

[1109] Zhu, X. X., **Montazeri, S.**, Gisinger, C., Hanssen, R., **Bamler, R.**: *Geodetic TomoSAR – Fusion of SAR Imaging Geodesy and TomoSAR for 3D absolute Scatterer Positioning*, in Proc. IGARSS 2014, pp. 1-4, 2014.

2013

[1110] Abdel Jaber, W., **Floricioiu, D.**, Rott, H., **Eineder, M.**: *Surface elevation changes of glaciers derived from SRTM and TanDEM-X DEM differences*, in Proc. IGARSS 2013, pp. 1893-1896, 2013.

[1111] Adam, N., **Rodriguez Gonzalez, F.**, **Parizzi, A.**, **Brcic, R.**: *Wide Area Persistent Scatterer Interferometry: Current Developments, algorithms and Examples*, in Proc. IGARSS 2013, pp. 1-4, 2013.

[1112] ***Auer, S.***, ***Gernhardt, S.***, Eder K.: *Evaluation of Persistent Scatterer Patterns at Building Facades by Simulation Techniques*, in Proc. ISPRS Hannover Workshop, XL-1/W1, pp. 7-12, 2013.

[1113] Avbelj, J., Iwaszczuk, D., **Müller, R.**, **Reinartz, P.**, Stilla, U.: *Line-Based Registration of DSM and Hyperspectral Images*, in Proc. ISPRS Hannover Workshop, XL-1/W, pp. 13-18, 2013.

[1114] Babaee, M., **Datcu, M.**, Rigoll, G.: *Assessment of dimensionality reduction based on communication channel model; application to immersive information visualization*, in Proc. Big Data 2013, pp. 1-6, 2013.

[1115] Babaee, M., Rigoll, G., **Bahmanyar, R.**, **Datcu, M.**: *Immersive Visual Information Mining for Exploring the Content of TerraSAR-X Archives*, in Proc. 5th TerraSAR-X Science Team Meeting, pp. 1-3, 2013.

[1116] Babaee, M., Rigoll, G., **Datcu, M.**: *Immersive Visualization of the Quality of Dimensionality Reduction*, in Proc. SMPR 2013, XL-1 (W3), pp. 67-71, 2013.

[1117] Bahmanyar, R., Rigoll, G., **Datcu, M.**: *A Clustering-Based Approach for Evaluation of EO Image Indexing, Sensors and Models in Photogrammetry and Remote Sensing*, in Proc. SMPR 2013, XL-1 (W3), pp. 79-84, 2013.

[1118] Balss, U., Gisinger, C., ***Cong, X.***, **Brcic, R.**, Steigenberger, P., **Eineder, M.**, Pail, R., Hugentobler, U.: *High Resolution Geodetic Earth Observation with TerraSAR-X: Correction Schemes and Validation*, in Proc. IGARSS 2013, pp. 4499-4502, 2013.

[1119] Balss, U., Gisinger, C., ***Cong, X.***, **Eineder, M.**, **Brcic, R.**: *Precise 2-D and 3-D Ground Target Localization with TerraSAR-X*, in Proc. ISPRS Hannover Workshop, XL-1/W, pp. 23-28, 2013.

[1120] Balss, U., Gisinger, C., ***Cong, X.***, **Eineder, M.**, **Fritz, T.**, **Breit, H.**, **Brcic, R.**: *GNSS Based Signal Path Delay and Geodynamic Corrections for Centimeter Level Pixel Localization with TerraSAR-X*, in Proc. 5th TerraSAR-X Science Team Meeting, pp. 1-4, 2013.

[1121] Bigdeli, B., **Samadzadegan, F.**, **Reinartz, P.**: *Classifier Fusion of Hyperspectral and Lidar Remote Sensing Data For Improvement of Land Cover Classification*, in Proc. SMPR 2013, XL-1/W, pp. 97-102, 2013.

[1122] Brcic, R., **Adam, N.**: *Detecting Changes in Persistent Scatterers*, in Proc. IGARSS 2013, pp. 1-4, 2013.

[1123] Cagatay, D., **Datcu, M.**: *2D Phase Unwrapping using Markov Random Field Based Phase Locked Loops*, in Proc. SPIE Remote Sensing 2013, 8891, pp. 1-8, 2013.

[1124] Carl, S., Bärisch, S., Lang, F., **d'Angelo, P.**, **Arefi, H.**, **Reinartz, P.**: *Operational Generation of High-Resolution Digital Surface Models from Commercial Tri-Stereo Satellite Data*, in Proc. Photogrammetric Week 2013, pp. 261-269, 2013.

[1125] Cerra, D., **Gege, P.**, **Müller, R.**, **Reinartz, P.**: *Exploiting noisy hyperspectral bands for water analysis*, in Proc. 33th EARSeL Symposium, pp. 43-48, 2013.

[1126] Cerra, D., **Müller, R.**, **Reinartz, P.**: *About the Applications of Unmixing-Based Denoising for Hyperspectral Data*, in Proc. SMPR 2013, pp. 103-106, 2013.

[1127] Costachioiu, T., Alzenk, B., Constantinescu, R., **Datcu, M.**: *Unsupervised classification of EO-1 Hyperion hyperspectral data using Latent Dirichlet Allocation*, in Proc. ISSCS 2013, pp. 1-4, 2013.

[1128] d'Angelo, P.: *Automatic Orientation of large multitemporal Satellite Image Blocks*, in Proc. International Symposium on Satellite Mapping Technology and Application, pp. 1-6, 2013.

[1129] d'Angelo, P.: *Evaluation of ZY-3 for DSM and Ortho Image Generation*, in Proc. ISPRS Hannover Workshop 2013, XL-1/W, pp. 57-61, 2013.

[1130] Dumitru, O., **Datcu, M.**: *How Many Categories Are in Very High Resolution SAR Images?*, in Proc. IGARSS 2013, pp. 4257-4260, 2013.

[1131] Eichmann, K.-U., Bovensmann, H., Noel, S., Richter, A., Wittrock, F., Buchwitz, M., Rozanov, A., Kokhanovsky, A. A., Burrows, J. P., Lerot, C., Van Roozendael, M., Tilstra, L. G., Snel, R., Krijger, M., **Lichtenberg, G.**, **Doicu, A.**, **Schreier, F.**, **Hrechanyy, S.**, ***Gimeno-Garcia, S.***, **Kretschel, K.**, **Meringer, M.**, Hess, M., **Gottwald, M.**, Dehn, A., Fehr, T., Brizzi, G.: *Development of SCIAMACHY Operational ESA Level 2 Version 6 Products*, in Proc. ESA Living Planet Symposium, pp. 1-7, 2013.

[1132] Espinoza-Molina, D., **Datcu, M.**: *Architecture Concept for Earth Observation Data Mining System*, in Proc. IGARSS 2013, pp. 1729-1732, 2013.

[1133] Gleich, D., Planinsic, P., **Singh, J.**: *SAR Scene Characterization Using Complex Wavelets*, in Proc. IGARSS 2013, pp. 1737-1740, 2013.

[1134] Goel, K., **Adam, N.**: *Integration of TerraSAR-X and TanDEM-X InSAR stacks for complex urban area analysis using distributed scatterers*, in Proc. IGARSS 2013, pp. 4178-4181, 2013.

[1135] Goel, K., **Adam, N.**: *Persistent scatterer interferometry in complex urban environments exploiting Terrasar-x and Tandem-X data*, in Proc. IGARSS 2013, pp. 4182-4185, 2013.

[1136] Gomba, G., Eineder, M., Fritz, T., Parizzi, A.: *Simulation of ionospheric effects on L-band Synthetic Aperture Radar images*, in Proc. IGARSS 2013, pp. 4463-4466, 2013.

[1137] Gottwald, M., **Fritz, T.**, **Breit, H.**, **Schättler, B.**, Harris, A.: *Mapping Terrestrial Impact Craters with the TanDEM-X Digital Elevation Model*, in Proc. 4. TanDEM-X Science Team Meeting, pp. 1-4, 2013.

[1138] Gottwald, M., Krieg, E., **Reissig, K.**, How, J., Brizzi, G., Dehn, A., Fehr, T.: *The SCIAMACHY Consolidated Level 0 Dataset*, in Proc. ESA Living Planet Symposium, pp. 1-7, 2013.

[1139] Grohnfeldt, C., **Zhu, X. X.**, **Bamler, R.**: *Jointly Sparse Fusion of Hyperspectral and Multispectral Imagery*, in Proc. IGARSS 2013, pp. 1-4, 2013.

[1140] Gstaiger, V., **d'Angelo, P.**, Schneiderhan, T., **Krauß, T.**: *Crisis DSM Generation to Support Refugee Camp Management*, in Proc. ESA Living Planet Symposium 2013, SP 722, pp. 1-4, 2013.

[1141] Hujebri, B., **Samadzadegan, F.**, **Arefi, H.**: *Fusion of ALS Point Cloud and Optical Imagery for 3D Reconstruction of Building's Roof*, in Proc. SMPR 2013 Conference, XL-1/W, pp. 197-201, 2013.

[1142] Kleinschrodt, A., Bangert, P., Schmidt, M., Schilling, K., Boie, E., Frank, S., Mohnhaupt, D., Haunschild, M., **Minet, C.**, **Eineder, M.**: *Space Based Automatic Identification and Monitoring System for the Large-Scale Railway Transportation, GP-AIMS*, in Proc. 19th IFAC Symposium on Automatic Control in Aerospace, pp. 1-6, 2013.

[1143] Krauß, T., **d'Angelo, P.**, **Schneider, M.**, **Gstaiger, V.**: *The Fully Automatic Optical Processing System CATENA at DLR*, in Proc. ISPRS Hannover Workshop 2013, XL-1/W, pp. 177-181, 2013.

[1144] Krauß, T., **d'Angelo, P.**, **Tian, J.**, **Reinartz, P.**: *Automatic DEM Generation and 3D Change Detection from Satellite Imagery*, in Proc. ESA Living Planet Symposium 2013, pp. 1-7, 2013.

[1145] Krauß, T., Stätter, R., Philipp, R., Bräuninger, S.: *Traffic Flow Estimation from Single Satellite Images*, in Proc. SMPR Conference 2013, XL-1/W (WG I/4), pp. 241-246, 2013.

[1146] Kuschk, G., **d'Angelo, P.**: *Fusion of Multi-Resolution Digital Surface Models*, in Proc. SMPR Conference 2013, XL-1/W (WG I/4), pp. 247-251, 2013.

[1147] Lachaise, M., Fritz, T., Yague-Martinez, N., Breit, H.,: *Dual-baseline phase unwrapping correction for the TanDEM-X mission: After one year experience*, in Proc. IGARSS 2013, pp. 2966-2969, 2013.

[1148] Laka-Inurrategi, M., Alberdi, I., **Alonso-Gonzalez, K.**, Quartulli, M.: *Cloud Based N-Dimensional Weather Forecast Visualization Tool with Image Analysis Capabilities*, in Proc. ISPRS Conference on Serving Society with Geoinformation, XL-7/W, pp. 133-137, 2013.

[1149] Lehner, S., **Li, X.-M.**, Ren, Y., He, M.-X.: *Sea surface wind field by X-band TerraSAR-X and Tandem-X*, in Proc. Dragon 2 final results and Dragon 3 kickoff symposium, pp. 10, 2013.

[1150] Lehner, S., **Pleskachevsky, A.**, **Li, X.-M.**, **Brusch, S.**, **Bruck, M.**, **Velotto, D.**: *SAR Oceanography: Wind, Waves, Currents and Oil detection*, in Proc. Education TOOL, pp. 1-150, 2013.

[1151] Leister, W., **Türmer, S.**, **Reinartz, P.**, Hoffmann, K. H., Stilla, U.: *Validation of Vehicle Candidate Areas in Aerial Images Using Color Co-Occurrence Histograms*, in Proc. ISPRS2013-SSG, XL-7/W, pp. 139-144, 2013.

[1152] Mahmoudi, F., **Samadzadegan, F.**, **Reinartz, P.**: *A Decision Level Fusion Method for Object Recognition Using Multi-Angular Imagery*, in Proc. SMPR 2013, XL-1/W, pp. 409-414, 2013.

[1153] Mattyus, G.: *Near real-time automatic vessel detection on optical satellite images*, in Proc. ISPRS Hannover Workshop 2013, pp. 233-237, 2013.

[1154] Müller, R., **Cerra, D.**, **Reinartz, P.**: *Synergetics Framework for Hyperspectral Image Classification*, in Proc. ISPRS Hannover Workshop 2013, pp. 257-262, 2013.

[1155] Oezcan, A. H., Uensalan, C., **Reinartz, P.**: *Building Detection Using Local Features and DSM Data*, in Proc. 6th International Conference on Recent Advances in Space Technologies (RAST), pp. 139-143, 2013.

[1156] Partovi, T., **Arefi, H.**, **Krauß, T.**, **Reinartz, P.**: *Automatic Model Selection for 3D Reconstruction of Buildings from Satellite Imagary*, in Proc. SMPR 2013 Conference, XL-1/W, pp. 315-320, 2013.

[1157] Patrascu, C., **Datcu, M.**: *Analysis of PS Detection and Parameter Optimization*, in Proc. IGARSS 2013, pp. 1-4, 2013.

[1158] Reize, T., **Müller, R.**, Kiefl, R.: *An Interative Graphical User Interface for Maritime Security Services*, in Proc. ISPRS Conference on Serving Society with Geoinformatics, pp. 201-206, 2013.

[1159] Riha, S., **Krawczyk, H.**: *Remote Sensing of Cyanobacteria and Green Algae in the Baltic Sea*, in Proc. ASPRS 2013 Annual Conference, pp. 1-8, 2013.

[1160] Rossi, C., **Eineder, M.**, **Fritz, T.**, **d'Angelo, P.**, **Reinartz, P.**: *Quality assessment of TanDEM-X Raw DEMs oriented to a fusion with CartoSAT-1 DEMs*, in Proc. 33rd EARSeL Symposium, pp. 1-9, 2013.

[1161] Schwarz, G., **Datcu, M.**: *Image Information Mining for the Exploration of Earth Observation Data: The Sentinel Challenge*, in Proc. European Data Forum 2013, pp. 1-15, 2013.

[1162] Schwarz, G., **Datcu, M.**: *Preparation of Scenarios for the Performance Optimization of a Content-Based Remote Sensing Image Mining System*, in Proc. IGARSS 2013, pp. 4352-4355, 2013.

[1163] Schwarz, G., **Datcu, M.**: *The impact of rain, frost, seasonal cycle, and wind on sequences of high resolution urban SAR images*, in Proc. IGARSS 2013, pp. 4367-4370, 2013.

[1164] ***Shahzad, M.***, **Zhu, X. X.**: *Reconstruction of building façades using spaceborne multiview TomoSAR point clouds*, in Proc. IGARSS 2013, pp. 1-4, 2013.

[1165] Storch, T., **Schwind, P.**, **Palubinskas, G.**, **Müller, R.**, **Schneider, M.**, **Reinartz, P.**, Chlebek, C., Gascon, F.: *Image Processing Chains for ALOS and EnMAP Data: Similarities and Differences*, in Proc. ESA Living Planet Symposium 2013, SP-722, pp. 1-5, 2013.

[1166] Talebi, S., Zarea, A., Sadeghian, S., **Arefi, H.**: *Detection of Tree Crowns Based on Reclassification Using Aerial Images and Lidar Data*, in Proc. SMPR 2013 Conference, XL-1/W, pp. 415-420, 2013.

[1167] Tao, J., ***Auer, S.***, **Reinartz, P.**, **Bamler, R.**: *Object-based change detection for individual buildings in SAR images captured with different incidence angles*, in Proc. IGARSS 2013, pp. 1238-1241, 2013.

[1168] Tian, J., **Reinartz, P.**: *Comparison of two fusion based building change detection methods using satellite stereo imagery and DSMs*, in Proc. IWIDF2013, XL-7/W1, pp. 103-108, 2013.

[1169] Velotto, D., Nunziata, F., Migliaccio, M., **Lehner, S.**: *A Robust Symmetry-Based Approach to Exploit TERRASAR-X Dual-Pol Data for Targets at Sea Observation*, in Proc. POLinSAR 2013, pp. 1-6, 2013.

[1170] Wang, Y., **Zhu, X. X.**: *Feature-based fusion of TomoSAR point clouds from multi-view TerraSAR-X data stacks*, in Proc. IGARSS 2013, pp. 85-88, 2013.

[1171] Wimmer, T., **Israel, M.**, **Haschberger, P.**, Weimann, A.: *Rehkitzrettung mit dem Fliegenden Wildretter: Erfahrungen der ersten Feldeinsätze*, in Proc. 19. Workshop Computer-Bildanalyse in der Landwirtschaft und 2. Workshop Unbemannte autonom fliegende Systeme (UAS) in der Landwirtschaft, pp. 85-95, 2013.

[1172] Wimmer, T., **Israel, M.**, **Haschberger, P.**, Weimann, A.: *Der Fliegende Wildretter in Aktion: DLR und BJV nutzen ferngesteuerte Flugplattform zur Rehkitzrettung*, in Proc. Symposium des Landesjagdverbandes Bayern - Hege und Bejagung des Rehwildes, 20, pp. 71-77, 2013.

[1173] Yague-Martinez, N., **Balss, U.**, **Breit, H.**, **Rodriguez Gonzalez, F.**, **Fritz, T.**, **Lachaise, M.**, **Adam, N.**: *Operational Stacking of TerraSAR-X ScanSAR and TOPS Data*, in Proc. IGARSS 2013, pp. 888-890, 2013.

[1174] Zhu, X. X., **Grohnfeldt, C.**, **Bamler, R.**: *Collaborative Sparse Reconstruction for Pan-Sharpening*, in Proc. IGARSS 2013, pp. 1-4, 2013.

Acronyms and Abbreviations

3K	System of three Canon EOS1Ds Mark II digital cameras developed by IMF
AC-SAF	Satellite Application Facility on Atmospheric Composition
ADM-Aeolus	Atmospheric Dynamics Mission (ESA)
Aeolus	Atmospheric Dynamics Mission (ESA)
AI	Artificial Intelligence
AI4EO	Artificial Intelligence for Earth Observation
ALADIN	Doppler Lidar instrument (onboard ADM-Aeolus)
ALOS	Advanced Land Observing Satellite (Japan)
APEX	Airborne Prism Experiment (imaging spectrometer, ESA)
AWI	Alfred-Wegener-Institut für Polar- und Meeresforschung (Alfred Wegener Institute for Polar and Marine Research)
BGR	Bundesanstalt für Geowissenschaften und Rohstoffe (Federal Institute for Geosciences and Natural Resources)
BMBF	Bundesministerium für Bildung und Forschung (German Ministry for Education and Research)
BRDF	Bidirectional Reflectance Distribution Function
CATENA	Automatic processing system (developed at IMF)
CDOP	Continuous Development and Operations Phase
CFC	Chlorofluorocarbon
CHB	Calibration Home Base (established by IMF under ESA contract)
CNES	Centre National d'Etudes Spatiales (French Space Agency)
CNN	Convolutional neural network
CODE-DE	Copernicus Data and Exploitation Platform – Deutschland
Copernicus	European (ESA, EU) Program for Global Monitoring for Environment and Security, former GMES
COTS	Commercial off-the-shelf
DEM	Digital Elevation Model
DESIS	DLR Earth Sensing Imaging Spectrometer (on ISS)
DFD	Deutsches Fernerkundungsdatenzentrum (German Remote Sensing Data Center)
DFG	Deutsche Forschungsgemeinschaft (German Research Foundation)
DIMS	Data and Information Management System of DFD
DLR	Deutsches Zentrum für Luft- und Raumfahrt e.V. (German Aerospace Center)
DOM	Discrete Ordinate Method
DRACULA	aDvanced Retrieval of the Atmosphere with Constrained and Unconstrained Least squares Algorithms (develop at IMF)
DSI	Distributed Scatterer Interferometry
DSM	Digital Surface Model
DTM	Digital Terrain Model
E2S	end-to-end simulator
EADS Astrium	European Aeronautic Defence and Space company
ECMWF	European Centre for Medium-Range Weather Forecasts
ECSS	European Cooperation for Space Standardization
ECV	Essential Climate Variables
EnMAP	Environmental Mapping and Analysis Program (German hyperspectral satellite)
ENVISAT	Environmental Satellite (ESA)
EO	Earth Observation
EOC	Earth Observation Center
EOLib	Earth Observation Image Librarian (ESA project)
ERS	European Remote Sensing Satellite (ESA)
ESA	European Space Agency
ESRIN	European Space Research Institute (ESA)
EU	European Union
EUMETSAT	European Organisation for the Exploitation of Meteorological Satellites
FAU	
FCN	Fully convolutional networks
FP-ILM	Full-Physics Inverse Learning Machine
GAF AG	geo-spatial service provider (Munich)
GAN	generative adversarial network

GARLIC	Generic Atmospheric Radiation Line-by-Line Infrared Code (developed at IMF)
GCAPS	Generic Calibration Processing System (developed at IMF)
GCOS	Global Climate Observing System
GENESIS	DLR's Generic System for Interferometric SAR Processing
GEOMAR	Helmholtz-Zentrum für Ozeanforschung Kiel
GFZ	Geoforschungszentrum Potsdam (Germany's National Research Centre for Geosciences)
GNSS	Global Navigation Satellite System
GOME	Global Ozone Monitoring Experiment (onboard ERS-2)
GOME2	Global Ozone Monitoring Experiment-2 (on MetOp Satellite)
GSD	Ground Sampling Distance
GSOC	German Space Operations Center
GTO	GOME-type total ozone
GUF	Global Urban Footprint (developed at DFD)
HD	High definition
HGF	Helmholtz-Gemeinschaft Deutscher Forschungszentren (Helmholtz Association of German Research Centres)
HITRAN	High-Resolution Transmission Molecular Absorption Data Base
HPC	High Power Computing
HRWS	High Resolution Wide Swath (commercial X-band SAR mission concept)
HTM	Haze Thickness Map
HySpex	Imaging spectrometer (Norsk Elektro Optikk)
IASI	Infrared Atmospheric Sounding Interferometer (onboard MetOp)
IMF	Institut für Methodik der Fernerkundung (Remote Sensing Technology Institute)
InSAR	Interferometric SAR
IPA	DLR's Institute of Atmospheric Physics
IR	Infrared (spectral range)
ISRO	Indian Space Research Organization
ISS	International Space Station
ITP	Integrated TanDEM-X Processor
JAXA	Japan Aerospace Exploration Agency
KIT	Karlsruher Institut für Technologie
KNMI	Koninklijk Nederlands Meteorologisch Instituut (Royal Netherlands Meteorological Institute)
LBL	Line-by-line
LCZ	Local Climate Zone
LMF	Lehrstuhl für Methodik der Fernerkundung, TU München (Remote Sensing Technology)
LMU	Ludwig-Maximilians-Universität München
LTM	Long-term Monitoring
MAV	Micro Air Vehicle
MAJA	MACCS-ATCOR Joined Atmospheric Correction (ESA project)
MERLIN	Methane Remote Sensing Lidar Mission (Franco-German cooperative mission)
MetOp	Meteorological Operational Satellites (EUMETSAT)
MIRA	Model for IR Scene Analysis
MPC	Mission Performance Center
MSI	Multispectral Imager
MTG	Meteosat Third Generation satellite (EUMETSAT)
MUSES	Multi-User System for Earth Sensing (platform on ISS)
NASA	National Aeronautics and Space Administration (USA)
NDACC	Network for the Detection of Atmospheric Composition Change
NIR	Near infrared (spectral range)
NISAR	NASA-ISRO Synthetic Aperture Radar
NL-LRTC	Non-Local Low-Rank Tensor Completion
NOAA	National Oceanic and Atmospheric Administration (USA)
NRT	Near real-time
OCRA	Optical Cloud Recognition Algorithm (developed at IMF)
OMI	Ozone Monitoring Instrument
OpAiRS	Optical Airborne Remote Sensing Facility and Calibration Home Base (EOC user service)
PACO	Python Atmospheric Correction
PAZ	Spanish X-Band SAR satellite based on TerraSAR-X

PDGS	Payload Data Ground Segment
PDR	Preliminary Design Review
PGS	Payload Ground Segment
PILS	Profile Inversion for Limb Sounding (developed at IMF)
PolInSAR	polarimetric SAR interferometry
PS	Persistent scatterer
PSI	Persistent scatterer interferometry
PTB	Physikalisch-Technische Bundesanstalt
Py4CatS	Python scripts for Computational Atmospheric Spectroscopy
RoMIO	Robust Multi-pass InSAR technique via Object-based low-rank tensor decomposition (developed at IMF)
SAINT	(developed at IMF)
SAOCOM-CS	Argentinian L-band SAR system with passive companion satellite
SAR	Synthetic Aperture Radar
SAR-Lab	IMF's research and development environment for SAR processing
SCIAMACHY	Scanning Imaging Absorption Spectrometer for Atmospheric Cartography (onboard ENVISAT)
SGM	Semi-global matching
SiPEO	Signal Processing in Earth Observation (research team at TUM)
SIR-C/XSAR	Spaceborne Imaging Radar-C/X-band Synthetic Aperture (Space Shuttle mission)
SRON	Netherlands Institute for Space Research
SRTM	Shuttle Radar Topography Mission (2000)
SSU	Sparse Spectral Unmixing
SVM	Support Vector Machine
SWIR	Shortwave infrared spectral region
TanDEM-X	German TerraSAR-X add-on for Digital Elevation Measurement
Tandem-L	Mission proposal based on two L-Band SARs
TCCON	Total Carbon Column Observing Network
TELIS	Terahertz and Submillimeter-Wave Limb Sounder (developed at IMF)
TerraSAR-X	German high-resolution X-band SAR satellite
TMSP	TerraSAR-X Multi-Mode SAR Processor (developed at IMF)
TOA	Top of atmosphere
TOPS	Terrain Observation with Progressive Scan (SAR scan mode)
TROPOMI	Tropospheric Ozone Monitoring Instrument
TUM	Technical University of Munich
UAV	Unmanned aerial vehicle
UPAS	Universal Processor for UV/VIS/NIR Atmospheric Sensors (developed at IMF)
UV	Ultra-violet (spectral range)
VHR	Very high resolution
VirES	Virtual workspace for Earth Observation scientists (web-based service of ESA)
VIS	Visible (spectral range)
VNIR	Visible and near infrared spectral region
WDC-RSAT	World Data Center for Remote Sensing of the Atmosphere (at DFD)
XDibias	IMF's image processing system
ZKI	Center for Satellite-based Crisis Information at DFD

DLR at a glance

DLR is the national aeronautics and space research center of the Federal Republic of Germany. Its extensive research and development work in aeronautics, space, energy, transport and security is integrated into national and international cooperative ventures. In addition to its own research, as Germany's space agency, DLR has been given responsibility by the federal government for the planning and implementation of the German space programme. DLR is also the umbrella organisation for the nation's largest project management agency.

DLR has approximately 8000 employees at 20 locations in Germany: Cologne (headquarters), Augsburg, Berlin, Bonn, Braunschweig, Bremen, Bremerhaven, Dresden, Goettingen, Hamburg, Jena, Juelich, Lampoldshausen, Neustrelitz, Oberpfaffenhofen, Oldenburg, Stade, Stuttgart, Trauen, and Weilheim. DLR also has offices in Brussels, Paris, Tokyo and Washington D.C.

Remote Sensing Technology Institute

DLR's Remote Sensing Technology Institute (Institut für Methodik der Fernerkundung – IMF) is located in Oberpfaffenhofen, Berlin-Adlershof, Bremen and Neustrelitz.
IMF carries out research and development for retrieving geoinformation from remote sensing data. It conducts basic research on physical principles of remote sensing and develops algorithms, techniques, and operational processing systems. The processing systems are in operational use for national, European, and international Earth observation missions. The institute focuses on the remote sensing technologies synthetic aperture radar, optical remote sensing and spectrometric sounding of the atmosphere, and develops data science and artificial intelligence algorithms for Earth observation data analysis. For preparation and in support of space missions, IMF operates optical airborne sensors and laboratories. The institute contributes its expertise to novel sensor and mission concepts.

The German Remote Sensing Data Center (DFD) and IMF form DLR's Earth Observation Center (EOC).

Imprint

Publisher:
German Aerospace Center (DLR)
Remote Sensing Technology Institute

Address:
Oberpfaffenhofen
82234 Weßling

Phone +49 8153 28-2673
e-mail richard.bamler@dlr.de

DLR.de

Deutsches Zentrum
für Luft- und Raumfahrt
German Aerospace Center

Supported by:

Federal Ministry
for Economic Affairs
and Energy

on the basis of a decision
by the German Bundestag